Aus dem Institut für Virologie
des Fachbereichs Veterinärmedizin
der Freien Universität Berlin

Molecular characterization and pathogenesis of equine and elephant herpesviruses

Inaugural-Dissertation
zur Erlangung des Grades eines
PhD.of Biomedical Sciences
an der
Freien Universität Berlin

vorgelegt von
Pavulraj Selvaraj

Tierarzt
aus Villupuram, India

Berlin 2019

Journal- Nr: 4180

Gedruckt mit Genehmigung
des Fachbereichs Veterinärmedizin
der Freien Universität Berlin

Dekan: Univ.-Prof. Dr. Jürgen Zentek
Erster Gutachter: Univ.-Prof. Dr. Klaus Osterrieder
Zweiter Gutachter: Prof. Dr. Benedikt Kaufer
Dritter Gutachter: Univ.-Prof. Dr. Robert Klopfleisch

Deskriptoren (nach CAB-Thesaurus):

equid herpesvirus 1; equid herpesvirus 4; elephantid herpesvirus 1; pathogenesis; peripheral blood mononuclear cells; endothelium, outbreaks; ELISA; polymerase chain reaction

Tag der Promotion: 10.12.2019

“If I have a thousand ideas and only one turns out to be good, I am satisfied”.

- ***Alfred Nobel***

“Ask the right questions, and nature will open the doors to her secrets”.

- ***C V Raman***

“Dream is not that you see in sleep, dream is something that does not let you sleep”.

- ***Dr A P J Abdul kalam***

“The greatness of a nation and its moral progress can be judged by the way its animals are treated”.

- ***Mahatma Gandhi***

“One, remember to look up at the stars and not down at your feet. Two, never give up work. Work gives you meaning and purpose and life is empty without it. Three, if you are lucky enough to find love, remember it is there and don't throw it away”.

- ***Dr Stephen Hawking***

“Institute is bigger than individuals. Always work in team. Don’t fly in sky when you achieve great things, always have your feet on ground. Don’t forget where you come from”.

- ***Dr Nitin Virmani***

Dedicated to……

My beloved

Parents, sisters

and pets

List of contents

Page

2 List of figures and tables

List of figures

List of tables

3 List of Abbreviations

Abbreviations	Refers to
Δ	Deletion
%	Percentage
-	Negative
µg	Microgram
µl	Microliter
µm	Micron/micrometer
2D	Two dimensional
293T	Human embryonic kidney cells
293T ND10	Human embryonic kidney nuclear domain 10 deletion mutant
3D	Three dimensional
ANOVA	Analysis of variance
Arg	Arginine
BAC	Bacterial artificial chromosome
BD	Bovine dermal
BoHV-1	Bovine herpesvirus type 1
BoHV-2	Bovine herpesvirus type 2
BoHV-4	Bovine herpesvirus type 4
BoHV-6	Bovine herpesvirus type 6
BoHV-5	Bovine herpesvirus type 5
ºC	Degree Celsius
C3	Complement component 3
CCL	Chemokine (C-C motiff) ligand
CD	Cluster of differentiation
CO_2	Carbon dioxide
CPE	Cytopathic effect
CrFK	Crandell-Rees feline kidney
CSPG	Chondroitin sulfate proteoglycans
C_T	cycle threshold
CTL	Cytotoxic T lymphocytes
DE17	Deutschland 2017
DMEM	Dulbecco’s modified Eagle’s medium
DNA	Deoxyribonucleic acid
E	Early

EBV	Epstein-Barr virus
EC	Endothelial cells
ED	Equine dermal cells
EDTA	Ethylenediaminetetraacetic acid
EEHV	Elephant endotheliotropic herpesvirus
EEHV-1	Elephant endotheliotropic herpesvirus type 1
EEHV-2	Elephant endotheliotropic herpesvirus type 2
EEHV-3	Elephant endotheliotropic herpesvirus type 3
EEHV-4	Elephant endotheliotropic herpesvirus type 4
EEHV-5	Elephant endotheliotropic herpesvirus type 5
EEHV-6	Elephant endotheliotropic herpesvirus type 6
EEHV-7	Elephant endotheliotropic herpesvirus type 7
EHV	Equine herpesvirus
EHV-1	Equine herpesvirus type 1
EHV-2	Equine herpesvirus type 2
EHV-3	Equine herpesvirus type 3
EHV-4	Equine herpesvirus type 4
EHV-5	Equine herpesvirus type 5
EHV-6	Equine herpesvirus type 6
EHV-7	Equine herpesvirus type 7
EHV-8	Equine herpesvirus type 8
EHV-9	Equine herpesvirus type 9
ELISA	Enzyme linked immunosorbent assay
EREC	Equine respiratory epithelial cells
FACS	Fluorescence-activated cell sorting
FASP	Filter-aided sample preparation
FBS	Foetal bovine serum
FDR	False discovery rate
FGF-2	Fibroblast growth factor 2
FHV-1	Feline herpesvirus type 1
Fwd	Forward primer
g	Relative centrifugal force
gB	Glycoprotein B
gC	Glycoprotein C
G+C	Guanine and cytosine
G-CSF	Granulocyte-colony stimulating factor

gD	Glycoprotein D
gE	Glycoprotein E
GFP	Green fluorescent protein
gG	Glycoprotein G
gH	Glycoprotein H
gI	Glycoprotein I
gK	Glycoprotein K
gL	Glycoprotein L
gM	Glycoprotein M
gN	Glycoprotein N
GO	Gene ontology
gp2	Glycoprotein 2
GRO	Growth related oncogene
GTPase	Guanosine triphosphate hydrolase
H_2O	Water
HCMV	Human cytomegalovirus
HHV-6	Human herpesvirus type 6
HHV-7	Human herpesvirus type 7
hpi	Hours post infection
h/hr/hrs	Hour/hours
HrT-18G	Human rectal tumor 18G cells
HSPG	Heparan sulfate proteoglycans
HSV-1	Herpes simplex type 1
HSV-2	Herpes simplex type 2
ICAM-1	Intercellular adhesion molecule 1
ICP	Infected cell protein
IE	Immediate early
IFNα	Interferon alpha
IFNγ	Interferon gamma
IL-1α	Interleukin 1 alpha
IL-1β	Interleukin 1 beta
IL-2	Interleukin 2
IL-8	Interleukin 8
IL-10	Interleukin 10
ILTV	Infectious laryngotracheitis virus
IM	Intermediate BAC clone

IMDM	Iscove's modified Dulbecco's medium
Indirect IF	Indirect immunofluorescence
IP-10	IFNγ-inducible protein CXCL10
IR2	Internal repeat 2
IR3	Internal repeat 3
ISCOM	Immune stimulating complexes
JNK	c-Jun amino-terminal kinases
Kan^r	Kanamycin resistance
Kb/kbp	Kilobase pair
KDa	Kilodaltons
KEGG	Kyoto encyclopedia of genes and genomes
KSHV	Kaposi's sarcoma-associated herpesvirus
L	Late
LAT	Latency associated transcripts
LFA-1	Leukocyte function-associated antigen 1
LFQ	Label-free quantification
LN	Lymph node
Lys	Lysine
M	Molar
Mac-1	Macrophage 1 antigen
MAP	Mitogen-activated protein
MAPK	Mitogen activated protein kinase
MCMV	Mouse cytomegalovirus
MDCK II	Madin-Darby canine kidney II
MDV-1	Marek's disease virus type 1
MDV-2	Marek's disease virus type 2
MEM	Minimum essential medium Eagle
MHC-I	Major histocompatibility complex I
MHC-II	Major histocompatibility complex II
ml	Milliliter
MLV	Modified-live virus
MOI	Multiplicity of infection
MS	Mass spectrometry
n	Number
n/a	Not tested
NF-κB	Nuclear factor-kappa B

ng	Nanogram
NK	Natural killer
nM	Nanomolar
OD	Optical density
OHV-2	Ovine herpesvirus type 2
OIE	Office international des epizooties
Oligo	Oligonucleotides
ORF	Open reading frame
PBMC	Peripheral blood mononuclear cells
PBS	Phosphate buffered saline
PCR	Polymerase chain reaction
PFA	Paraformaldehyde
PFU	Plaque forming units
pM	Picomolar
PRV	Pseudorabies virus
P-S	Penicillin/streptomycin
qPCR	Quantitative-polymerase chain reaction
RBPJ	Recombination signal binding protein for immunoglobulin kappa J region
RE	Restriction enzyme
Rev	Reverse primer
RFLP	Restriction fragment length polymorphism
RK-13	Rabbit kidney 13
ROCK1	Rho-associated coiled-coil containing protein kinase-1
RT	Room temperature
s	Seconds
SD	Standard deviation
SDS-PAGE	Sodium dodecyl sulfate-polyacrylamide gel electrophoresis
SHV-3	Suid herpesvirus type 3
SHV-4	Suid herpesvirus type 4
SHV-5	Suid herpesvirus type 5
STAT	Signal transducer and activator of transcription
TEM	Transmission electron microscopy
TID	‘ter in die‘ – three times a day
TK	Thymidine kinase
TM	Transmembrane
TNFα	Tumor necrosis factor alpha

TRADD	TNFRSF1A associated via death domain
UL	Unique-long
US	Unique-short
VCAM-1	Vascular cell adhesion molecule 1
Vero	African green monkey kidney
VLA-4	Very late antigen 4
VNT	Virus neutralization test
V/V	Volume/volume
VZV	Varicella-zoster virus
WB	Western blot
wt	Wild type
W/V	Weight/volume

4 Introduction

Virus infections are generally recognized only when they cause or suspected to cause disease in the host. Most of the viral activity in host may not display any clinical signs and the infection goes sub-clinical (1-3). Host immune response is usually highly successful in combating most of the viral infections (4, 5). Viruses in general have co-evolved with their host species. As these viruses are solely relying on host for their replication, the evolution has been favoured to run this interaction smoothly. One successful example is herpesviruses, which are large virus family characterized by lifelong persistence in their hosts. Herpesviruses most likely have a long evolutionary history of co-evolution with the host species (6-8). At the end, the viruses have reached a fine-tuned balance with their corresponding host, which allowing them to persist and spread successfully to new hosts, of the same species, without being lethal (9). Primary herpesvirus infection usually results in productive infection, which is subsequently limited by host immune responses, leaving behind lifelong latent infection. Latency is the state in which virus genome is carried within the cells in the absence of virus production but with ability to reactivate and re-enter the lytic cycle (10-16). The delicate balance between herpesviruses and hosts results from interaction of variety of viral and cellular factors, which together shape the tropism for particular host (17, 18). Understanding these interactions will provide insights into the viral life cycle and cell biology in general. Further, it will facilitate comprehension of herpesvirus pathogenesis and enable the development of new strategies to combat disease-causing herpesviruses. Successful development of therapeutic vaccines and anti-herpesviral drugs are dependent on understanding interactions between virus and host cell factors. In the current study, I have investigated herpesvirus host-pathogen interaction, and characterized equine (equine herpesvirus type 1 and 4) and elephant herpesviruses (elephant endotheliotropic herpesvirus).

4.1 Taxonomy and phylogeny of herpesviruses

4.1.1 Classification of the order *Herpesvirales*

The new taxonomic order *Herpesvirales* comprises more than 100 large DNA viruses which infect variety of host species including mammals, fishes and molluscs. The order *Herpesvirales* have been classified into three distinct families: (i) *Herpesviridae*, (ii) *Alloherpesviridae* and (iii) *Malacoherpesviridae* (19). The family *Alloherpesviridae* include herpesviruses of fish (Ictalurid herpesvirus 1) (20) and other unassigned genus viruses of fishes (Cyprinid herpesvirus1 & 2, Acipenserid herpesvirus 1 & 2, Anguillid herpesvirus 1, Esocid herpesvirus 1, Percid herpesvirus 1, Pleuronecid herpesvirus 1 and Salmonid

herpesvirus 1 & 2) and frogs (Ranid herpesvirus 1 & 2 (21-24)). Ostreid herpesvirus 1 is the solely member of *Malacoherpesviridae* family infecting oysters (25).

Herpesviridae is the largest family in the order *Herpesvirales*, which has been further divided into three different subfamilies: (i) *alphaherpesvirinae*, (ii) *beteherpesvirinae* and (iii) *Gammaherpesvirinae*; based on genetic diversity, host specificity, tissue tropism, disease severity and virus replication properties. Members within each subfamily share several characters including conserved nature of genome, colinear arrangement of their genes and antigenic relatedness of important viral proteins as demonstrated by immunological assays (26-28). Especially, homologs of glycoprotein (g)B or glycoprotein H (gH) are conserved among members of different subfamilies. In addition, nucleic acid and protein sequence homologies are also considered for classification of closely related viruses (29-32).

4.1.1.1 Subfamily *Alphaherpesvirinae*

The members of the subfamily *alphaherpesvirinae* are classified and grouped based on broad host range, short replication cycle, rapid spread between cells and efficient destruction of infected cells with capacity to establish latency mostly but not limited to sensory ganglion. They employ multiple strategies to evade host immune antiviral responses in order to maintain their persistence in the host for successful replication and spread. This subfamily contains four genera: (i) *Simplexvirus* (herpes simplex virus type 1 [HSV-1], HSV-2 and Bovine herpesvirus type 2 [BoHV-2]), (ii) *Varicellovirus* (equine herpesvirus type 1 [EHV-1], EHV-3, EHV-4, EHV-8, EHV-9, varicella-zoster virus [VZV], pseudorabies virus [PRV], feline herpesvirus type 1 [FHV-1], BoHV-1 and BoHV-5), (iii) *Mardivirus* (Marek's disease virus type 1 [MDV-1] and MDV-2) and (iv) *Iltovirus* (infectious laryngotracheitis virus [ILTV]) (19, 28).

4.1.1.2 Subfamily *Betaherpesvirinae*

The subfamily *beteherpesvirinae* members have common characteristic features like narrow host range, long reproductive cycle, slow virus spread in culture condition and enlargement of infected cells (cytomegalia). The virus establishes latency in glands, kidney, lymphoreticular cells and other tissues. This subfamily has been divided into four genera: (i) *Cytomegalovirus* (human cytomegalovirus [HCMV]), (ii) *Muromegalovirus* (mouse cytomegalovirus [MCMV]), (iii) *Roseolovirus* (human herpesvirus type 6 [HHV-6] and HHV-7) and (iv) *Proboscivirus* (elephant endotheliotropic herpesvirus type 1 [EEHV-1]) (19, 28).

4.1.1.2 Subfamily *Gammaherpesvirinae*

Gammaherpesvirinae subfamily members have restricted host range, replicates mainly in lymphoblastoid cells and occasionally causes lytic infection in fibroblastic and epithelioid cells. Few member viruses of this subfamily are very specific to either T or B lymphocytes. In infected lymphocytes, the virus may remain in a pre-lytic or in a lytic stage with production of progeny viruses. Latency predominantly established in lymphoid cells. Genera in this subfamily are (i) *Lymphocryptovirus* (Epstein-Barr virus [EBV]), (ii) *Rhadinovirus* (Kaposi's sarcoma-associated herpesvirus [KSHV], BoHV-4), (iii) *Macavirus* (BoHV-6, ovine herpesvirus type 2 [OHV-2], suid herpesvirus type 3 [SHV-3], SHV-4 and SHV-5) and (iv) *Percavirus* (EHV-2, EHV-5, EHV-7) (19, 28). The phylogenetic tree of the order *Herpesvirales* is shown in Figure 1.

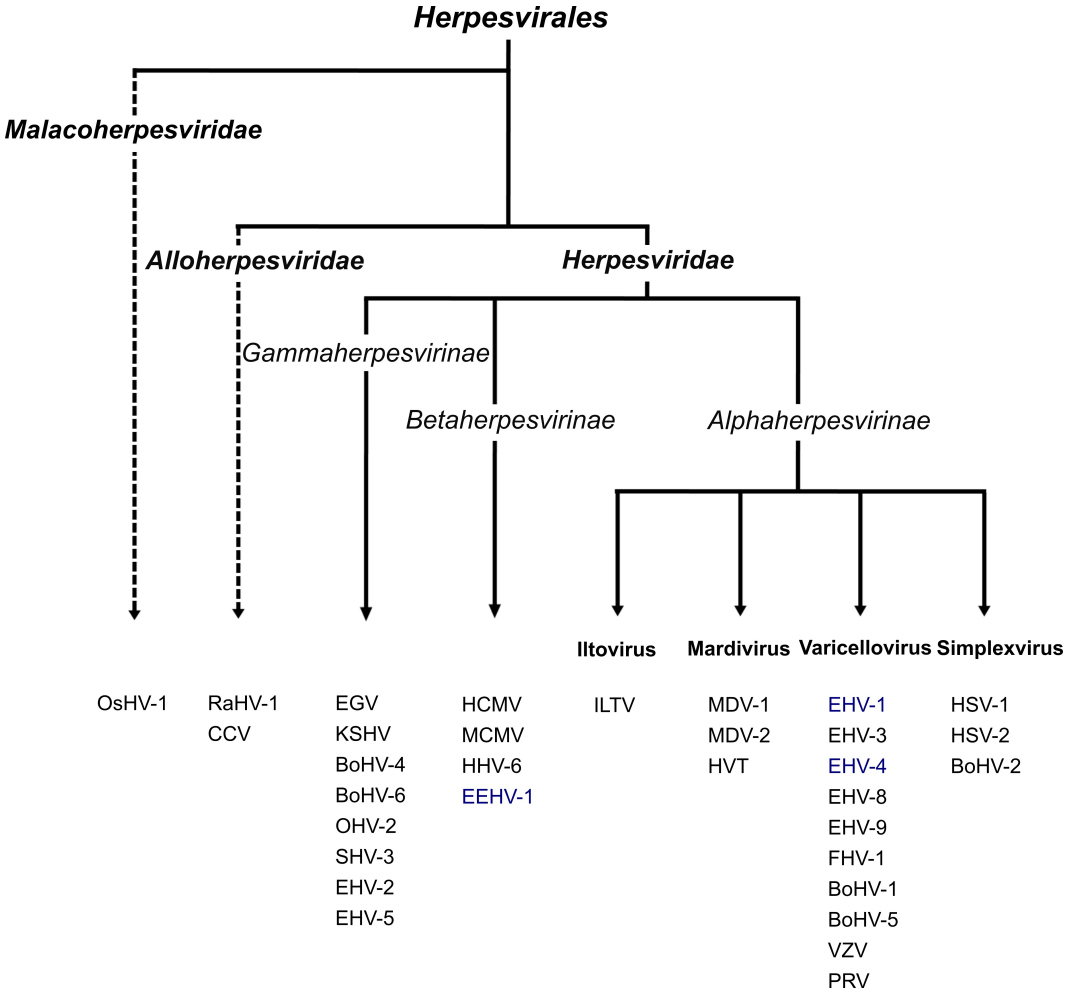

Figure 1: Phylogenetic tree of the order Herpesvirales (according to Davison, 2009 (19)

4.1.2 Equid and elephant herpesviruses

The current study focused on herpesviruses of equine (EHV-1 and EHV-4) and elephant (EEHV-1) herpesviruses. EHVs are highly successful pathogens of all members of the *Equidae* family worldwide. Of the nine EHVs characterized so far, five types (EHV-1 to EHV-5) infect domestic horses, and EHV-6 to EHV-9 are associated with wild equids, donkeys and giraffe (33-35). As EHVs are ubiquitous in both domestic and wild equid population, it is likely enduring the success of the EHV as pathogens results from ancient co-evolution with the *Equidae* family and adaptation of the virus life cycle to ensure efficient spread within their host population (36). Herpesvirus of elephant is a cause of rapid death of young Asian elephants (*Elephas maximus*) with signs of acute hemorrhagic disease. Young Asian elephants of 1 to 8 years of age are highly susceptible to fatal infection; infection is asymptomatic in adult elephants (37, 38). Details regarding virus species, host specificity and disease manifestations for reported herpesviruses of horses and elephants were given in Table 1 and 2, respectively.

4.1.2.1 Classification of known equine herpesviruses, host range and disease manifestations

S. No:	Virus	Host	Disease manifestations	References
1	Equine herpesvirus 1 (equine abortion virus)	Horse	Respiratory infection, abortion, neurological illness	(33, 39)
2	Equine herpesvirus 2 (equine cytomegalovirus)	Horse	Respiratory infection, immunosuppression	(40, 41)
3	Equine herpesvirus 3 (equine coital exanthema)	Horse	Coital exanthema	(42)
4	Equine herpesvirus 4 (equine rhinopneumonitis virus)	Horse	Respiratory infection	(43)
5	Equine herpesvirus 5	Horse	Multinodular pulmonary fibrosis	(44)
6	Equine herpesvirus 6 (asinine herpesvirus 1)	Donkey	Coital exanthema	(45)
7	Equine herpesvirus 7 (asinine herpesvirus 2)	Donkey	Not known	(46)
8	Equine herpesvirus 8	Horse and	Respiratory disease	(47, 48)

	(asinine herpesvirus 3)	donkey		
9	Equine herpesvirus 9 (gazelle herpesvirus)	Gazelles, giraffe and rhinoceros	Non-suppurative encephalitis	(49-51)

Table 1: Known species of equine herpesviruses, host species and disease manifestations in infected animals.

4.1.2.2 Classification of elephant endotheliotropic herpesviruses, host and disease manifestations

S.No:	Virus	Host	Disease manifestations	References
1	EEHV-1A	Asian elephant	Haemorrhagic disease	(52)
2	EEHV-1B	Asian elephant	Haemorrhagic disease	(53)
3	EEHV-2	African elephant	Haemorrhagic disease and skin nodules	(53)
4	EEHV-3A	African elephant	Haemorrhagic disease, skin nodules and lung nodules	(54)
5	EEHV-3B	African elephant	Skin nodules	(55)
6	EEHV-4A	Asian elephant	Haemorrhagic disease	(56)
7	EEHV-4B	Asian elephant	Mild clinical signs with anorexia and viremia	(38, 56, 57)
8	EEHV-5A	Asian elephant	Haemorrhagic disease	(58)
9	EEHV-5B	Asian elephant	Subclinical infection with viremia	(59)
10	EEHV-6	African elephant	Lung nodules	(55)
11	EEHV-7A and B	African elephant	Lung nodules and skin nodules	(60)

Table 2: Species of elephant endotheliotropic herpesviruses, host species and disease manifestations in infected elephants.

4.2 Important equine herpesviruses affecting equine population

Equine herpesvirus type 1 (EHV-1) and 4 (EHV-4) are important viral pathogens infecting horse population worldwide. The term ‘herpes’ is derived from a Greek word *herpein* means ‘to creep or crawl’ in reference to the spreading nature of the herpetic skin lesions. EHV-1 infection predominantly causes upper respiratory tract infection (61). Following infection and initial replication in the upper respiratory tract epithelium, EHV-1 infects migratory

mononuclear cells, pass through the basement membrane, enters general systemic circulation and results in cell associated viraemia (62, 63). Through cell associated viraemia in peripheral blood mononuclear cells (PBMC), EHV-1 reach throughout the body (64). Subsequent virus transfer from infected PBMC to endothelial cells (EC) in gravid uterus and brain, and replication in EC are responsible for disease outcomes; abortion during last trimester and neurological disorders including myeloencephalopathy (65-67). Although cell associated viraemia have been reported in other alphaherpesviruses like PRV and VZV, EHV-1 can spread through cell junctions between PBMC and EC without being neutralized by antibodies through a mechanism that requires coordination of several host and viral proteins (68-70). Initially EHV-1 was designated as equine abortion virus or equine rhino-pneumonitis virus, now termed as equine herpesvirus type 1. It shows a close relationship with EHV-4, a member of the same genus, *Varicellovirus*. EHV-1 and EHV-4 by far are the most relevant pathogens of herpesviruses affecting equids and were considered subtypes of one and the same virus species until 1981 (71). Both viruses are genetically and antigenically very similar to certain extent, but their pathogenic potentials are strikingly different. The degree of amino acid sequence homology between EHV-1 and EHV-4 proteins ranges from 55% (open reading frame [ORF] 76) to 96% (ORF42). The corresponding range of DNA sequence conservation is between 55 and 84%. EHV-1 is capable in propagating in many cell types of multiple species, while EHV-4 entry and replication appear to be restricted mainly to equine derived cells (72). Despite the fact that EHV-4 can infect upper respiratory tract cells and cause inefficient cell associated viremia in PBMC, no subsequent endothelial infection has been reported (73-75). Both EHV-1 and -4 were the subject of international research effort for the last five decades. EHV-1 can infect PBMC, however, virus replication is highly restricted (76, 77). The process of virus transfer between PBMC and endothelium is complex, and the viral and host factors responsible for cell-to-cell spread was not fully understood. It was considered that EC infection is established upon close contact of infected PBMC to EC without the virus being egressed out from PBMC, where cell-to-cell virus transfer can take place (78, 79). Factors favouring adhesion of two cells and establishing cell-to-cell contact are essential for viral spread (80, 81).

Like other members of the subfamily *Alphaherpesvirinae*, in the life cycle EHV-1 and -4, two general phases are found: the ‘lytic’ phase, which is followed by a persistent, ‘latent’ phase that usually lasts for the lifetime of the host. Latency usually established in trigeminal ganglia and in lymphoid cells. During latency, no infectious progeny is produced, normal expression of viral genes in the lytic state is repressed and only a very limited set of viral proteins are produced. Especially, single region is found to be transcriptionally active during latency, producing non-polyadenylated latency associated transcripts (LAT) (82-84). Establishment of

the latent carrier state gives potential to the virus to reactivate at any time during the stress condition in life of the infected individual, which result in severe economic losses in the form of abortion and may eliminate valuable offspring and threaten the breeding potential of affected studs (85). Most horses are exposed to the EHV-1 within 6 months to a year after birth and are frequently re-infected throughout their life time (33). EHV is an air-borne viral disease, which is contagious mainly in horses. However, infections with EHV-1 or closely related viruses have been identified in other equid species like zebras, donkeys and onagers, and in non-equid species including Indian tapir, polar bear, antelopes, rhinoceros, camels, Thomson's gazelle, llamas (86-95).

4.3 History of EHV

EHV-1 infection was reported for the first time in aborted foetus of a mare in Kentucky (96), but the virus was successfully isolated few decades later (97, 98). Initially this virus was isolated from the horse suffering from equine influenza so it was called by the name of Army 183 equine influenza strain but after a decade it was confirmed that Army 183 was not equine influenza but a virus having separate identity as equine abortion virus (99). Subsequently, histopathological descriptions of aborted foals were described and complement fixation based diagnostic assay was developed. Earlier studies proposed that major antigenic differences might exist among clinical isolates of equine abortion virus (100-102). In early 1980s, the virus has been given the name of equine herpesvirus (27). Till then, both EHV-1 and EHV-4 were considered as subtype of same virus. Viral genomic fingerprint based on restriction fragment length polymorphism (RFLP) analysis revealed genomic difference between both viruses (103), but official recognition of the distinction between these two viruses came later (104).

4.4 Equine herpesvirus type 1 and type 4: Structure and morphology

4.4.1 Equine herpesvirus Structure

In general, herpesvirus structure is complex in nature. Like other members of the subfamily *alphaherpesvirinae*, EHVs have a unique four-layered structure: (i) virus core containing large, double stranded deoxyribonucleic acid (DNA) genome which is enclosed by (ii) an icosapentahedral capsid made up of capsomers. The viral capsid is 100 – 110 nanometers (nm) in diameter. Viral capsid is protected by (iii) tightly adherent amorphous proteinaceous coat called tegument. Capsid and tegument are loosely surrounded by host (iv) cell membrane derived lipid bilayer envelope. The envelope is composed of lipids, polyamines and glycoproteins. These surface glycoproteins anchored on envelope membrane, confer

unique property to EHV-1 & -4 and determines pathogenicity (105-107). Schematic diagram for structure of EHV-1 is given in figure 2.

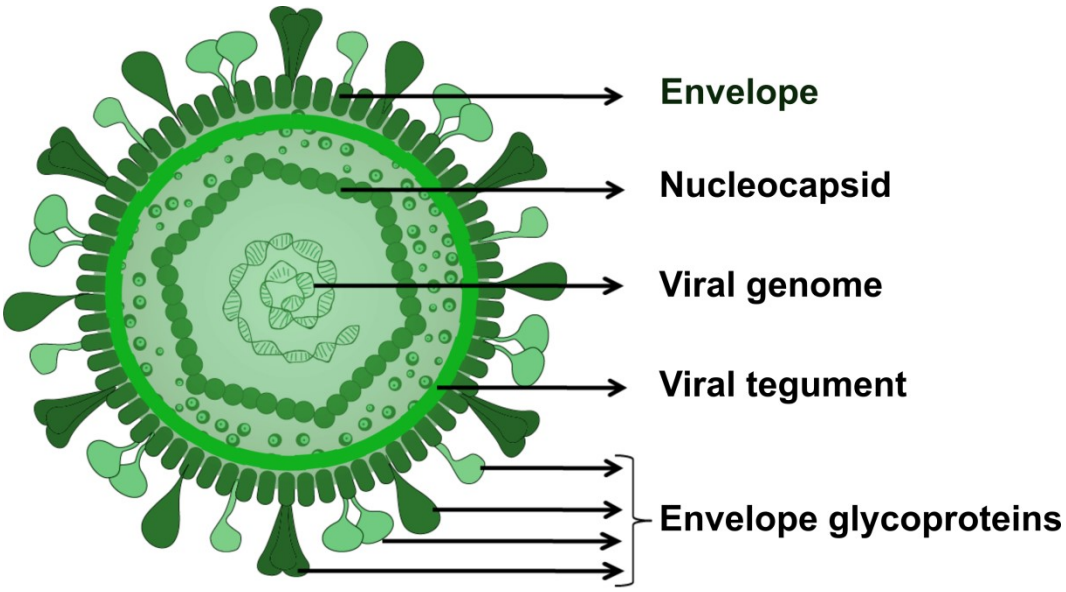

Figure 2: Schematic of structural components of EHV-1.

4.4.2 Equine herpesvirus genome

EHV-1 DNA molecule is approximately 150 kilobase pair (150 kbp) in size with 56.7% G+C composition and coding for at least 78 ORF. The linear 150 kbp DNA is divided into two segments as unique long (U_L) and unique short (U_S) regions that are flanked by identical pair of identical repeat regions, terminal repeat (TR) and internal repeat regions (IR). Genomic organization of EHV-1 is given in figure 3. In EHV-1, six genes are present in two copies (ORFs: 64, 65, 66, 67, 77 and 78) in IR and TR region (108). On the other hand, EHV-4 genome is slightly smaller, 145 kbp in length with 50.5% G+C content, in which only three genes are present in two copies (64, 65 and 66). Both EHV-1 and -4 possess five unique genes (ORF1, ORF2, ORF67, ORF71 and ORF75) that have no homologs in other known herpesviruses (109, 110). These unique genes are expected to play major role in virus pathogenesis.

Figure 3: Genomic organization of EHV-1. U_L – unique long region; IR – internal repeat region; U_S – unique short region; TR – terminal repeat region.

4.4.3 Viral proteins

EHV-1 genome encodes 76 viral proteins that consist of single immediate early (IE) gene, 55 early (E) genes and 20 late (L) genes (26, 111-113). Recently, two additional viral proteins have been identified, IR2 and IR3. IR2 is a truncated form of immediate-early protein and IR3 is a late 1.0 kb transcript, encoded by ORF77 and ORF78 genes, respectively (108, 114). Each of these viral proteins is involved in various functions altogether determining complexity of lifecycle and pathogenesis. Resolving the function of each viral protein would be the key step in understanding EHV pathogenesis and optimizing therapeutics. Till date, functions of most of the major viral proteins of EHV have been determined. In which, at least 30 proteins are associated with virion particles, in which 6 proteins are associated with capsid, 12 proteins forms tegument and 12 are surface glycoproteins attached to envelope (106). Other viral proteins are involved in virus replication, including regulation of sequential viral gene expression, viral DNA synthesis and egress from infected cells (109). In addition, several viral proteins are involved in modulation of host immune response and immune evasion.

4.4.3.1 Glycoproteins

Envelope anchored glycoproteins play key roles in pathogenesis by determining tissue tropism and host specificity. Glycoproteins are named as per nomenclature established for the prototype virus of the subfamily, HSV-1. Till date, 12 surface envelope glycoproteins homologues for HSV-1 have been described in EHV-1, namely gB, gC, gD, gE, gG, gH, gI, gK, gL, gM, gN and gp2. Viral glycoprotein 2 (gp2) is unique for EHV-1 and -4. These viral glycoproteins have three components: (i) external ectodomain, (ii) transmembrane domain and (iii) internal endodamain. Viral glycoproteins are essential for virus attachment, penetration, entry, egress and cell-to-cell spread (106, 109, 110). Known functions of each surface glycoproteins of EHV-1 were given in Table 3.

ORF	Protein	Functions	References
ORF33	gB	Attachment and penetration to target cells, membrane fusion, cell-to-cell virus spread, most immuno-dominant antigenic viral protein	(115-117)
ORF16	gC	Binds to heparin sulphate on cell surface and initiate virus entry, binds to third component of complement (C3) which allows the virus to avoid complement mediated inactivation of cell-free and cell-associated virus, role in virus release,	(118-120)

		immuno-dominant antigenic viral protein	
ORF72	gD	Key receptor binding protein, binds to host major histocompatibility complex I (MHC-I)receptor and facilitate virus entry via endocytosis and cell-to-cell fusion, immuno-dominant antigenic viral protein	(72, 121-123)
ORF74	gE	gE forms complex with gI, facilitates cell-to-cell and transsynaptic virus spread in nervous system, virulence factor of EHV-1	(124, 125)
ORF70	gG	Chemokine binding viral glycoprotein, blocks interaction of chemokines with specific receptors and glycosaminoglycans, interfere with leukocyte migration in tissues there by contributes to virus dissemination and virulence	(126-128)
ORF39	gH	Forms complex with gL, fusion regulator, determines virus entry pathway in the host cell	(129-131)
ORF73	gI	Associated with gE, role in cell-to-cell virus spread, determine virulence	(125, 132)
ORF6	gK	Present in virions and expressed on plasma membrane of the infected cells, facilitates cell-to-cell virus spread and virus egress	(133-135)
ORF62	gL	Forms complex with gH, role in virus attachment, virus entry, cell-to-cell fusion	(136-138)
ORF52	gM	Associated with gN, virus entry and cell-to-cell virus spread, production of progeny virus	(139-142)
ORF10	gN	Determine functional capacity of gM, interfere with transporter associated with antigen processing (TAP) in antigen processing and presentation function of MHC-I	(143, 144)
ORF71	gp2	Unique large glycoprotein of EHV-1 and -4, major virulence factor, role in cell-to-cell virus spread, secondary virus envelopment, signalling molecule	(141, 145)

Table 3: Function of EHV-1 surface glycoproteins.

4.4.3.2 ORF1 as an immunomodulatory protein

ORF1 of EHV-1 (a homolog to HSV-1 pUL56) is a recently identified immune evasion protein that plays a major role in MHC-I downregulation. ORF1 is a phosphorylated type II transmembrane (TM) protein, 21.6 kilodaltons (KDa) in size with 202 amino acids, expressed early during infection and localize in Golgi compartment. ORF1 protein has single TM domain, which is essential for correct localization within Golgi and function (146). Though this TM protein is dispensable for normal virus replication, it exists in all members of *Alpherpesvirinae* subfamily with exception of BHV-1 and -5. The conserved nature of the protein across the subfamily indicates that this encoded proteins may share similar functions. ORF1 protein co-ordinate with ORF17 protein and downregulates cell surface expression of MHC-I in the early stages of infection (147). On the surface of the EHV-1 infected cells, MHC-I molecules are internalized by dynamin-dependent endocytosis and degraded in the lysosomal compartment in ORF1 and ORF17-dependent fashion. ORF1-induced MHC-I endocytosis is independent of clathrin and caveolin-1 mediated endocytosis, and ubiquitination is essential for virus induced cell-surface MHC-I downregulation (148). In addition to MHC-I, ORF1 is involved in modulation of other surface proteins like cluster of differentiation (CD) 46 and CD63, which are involved in regulation of complement system and intracellular vesicles, respectively (149, 150). Deletion of EHV-1 ORF1 partially restored expression of MHC-I and MHC-II, and modulated mRNA expression of interferon alpha (IFNα) and interleukin 10 (IL-10) in equine respiratory epithelial cells (151). Further, deletion of EHV-1 ORF1 also significantly increased cytokine and chemokine expression in peripheral blood mononuclear cells (PBMC), chemotaxis of monocytes and neutrophils in equine respiratory epithelial culture (EREC) (148, 151).

Experimental infection study with EHV-1 ORF1/ORF2 deletion (∆) mutant in ponies showed altered course of disease with immunoregulatory effects compared to wild type (wt) EHV-1. The ∆ORF1/ORF2 virus caused significantly shorter pyrexia, reduced nasal virus shedding, attenuated PBMC IL-8 and increase T-box transcription factor (Tbet) response in comparison to wt-EHV-1(152). In another study, EHV-1 ORF1/ORF71 deletion mutant infected horses did not show pyrexia, had reduced virus shedding through nostrils and decreased cytokine release including IFNα, IL-10 and soluble CD14 (153). When the same (EHV-1∆ORF1/ORF71 infected) animals were challenaged with wt-EHV-1 after six months, 60% of the animals showed complete protection with no elevated body temperature and no virus shedding through nostrils (154).

ORF1 homolog in HSV-1 and -2 (UL56) also has similar expression kinetics and localization compartment (155). In addition, UL56 protein is incorporated into HSV-2 virions as tegument

protein (156, 157). However, whether ORF1 protein is getting incorporated in EHV-1/-4 virions yet to be understood.

Taken together, EHV-1 ORF1 is involved in protein sorting and trafficking thereby modulates virulence and immune response by regulating cytokine and chemokine expression, chemotaxis, antigen processing and presentation in both *in vitro* and *in vivo*. ORF1 gene is absent in both modified live virus vaccine strains RacH and Kentucky A (158)

4.4.3.3 ORF2 as a unique novel immunomodulatory protein

ORF2 is a unique gene present in EHV-1 and -4 which has no homolog or counterpart in any other members of *Alpherpesvirinae* subfamily (109). ORF2 also predicted to be a type II TM protein, 23.4 KDa in size with 205 amino acids and expressed early in infection like ORF1 (152). ORF2 is considered as one of the potential virulence factor along with ORF1 due to the fact that both genes are absent in RacL11 derived modified-live virus (MLV) vaccine strain RacH and the apathogenic strain Kentucky A (108, 109, 158, 159). Although ORF2 has been not characterized well, this gene could encode immunomodulatory protein, which involved in determining pathogenicity and virulence of the virus (152, 160). Role of ORF2 protein in relation to virus pathogenesis have been assessed mostly in *in vivo* experiments in horses. Deletion of ORF2 gene did not alter viremia, impacted in pyrexia and reduced virus shedding after primary infection (160). Subsequently, wt-EHV-1 challenge in the same (EHV-1ΔORF2 infected) animals after nine months, provided full protection against infection with absence of clinical signs, pyrexia, virus shedding and viremia (161). In another study, ponies infected with ORF1/ORF2 deletion mutant EHV-1 caused significant reduction in period of primary pyrexia, reduced virus shedding and modulated cytokine and chemokine response (152). In addition, it is well know that MLV vaccine strain RacH, devoid of ORF1, ORF2, ORF67 and other additional genes attenuated virus virulence and provided optimal proteins against virus challenge (67, 162, 163). This strain is used in commercially available MLV vaccines in Europe and United States (Prevaccinol® MSD tiergesunheit and Rhinomune® Boehinger Ingelheim, respectively). Experimental infections and vaccine efficacy studies confirmed ORF2 as a potential virulence determining and immunomodulating viral protein.

4.4.3.4 ORF17 as immunomodulatory protein

ORF17 of EHV-1 (a homolog to HSV-1 pUL43) is one of the less investigated and characterised viral protein. ORF17 is hydrophobic protein with ten TM domains, 43.2 KDa in size with 401 amino acids, expressed in early kinetics, predominantly localized in Golgi vesicles and degraded in lysosomes. ORF17 is involved in downregulation of surface MHC-I

in infected host cells. Interestingly, ORF17 cooperates with ORF1 in rerouting vesicles containing MHC-I to lysosomal compartment thereby reducing cell surface MHC-I expression. Intact N terminal region of ORF17, and TM domain of both ORF17 and ORF1 are necessary for proper localization within Golgi and MHC-I downregulation (147). Though ORF17 is nonessential for virus replication, ORF17 deletion mutant showed significant reduction in plaque size (around 20%) like homolog counterparts in HSV-1 and PRV (147, 164, 165). In PRV, ORF17 is present in vesicles and inhibits syncytium formation by affecting proteins involved in trafficking of vesicles and membranes (165). Further, EHV-1 ORF17 protein is getting incorporated into virion particles like PRV (147, 165). In addition to other genes deletion during passage in mice fibroblast L-M cells, ORF17 gene is also deleted in the MLV vaccine strain Kentucky A (108). However, ORF17-based experimental studies to determine its role in infection, disease course, virus shedding and viremia *in vivo* yet to be determined.

4.5 Epidemiology

Latently infected horses are reservoir for EHV infection. Environmental transmission plays an important role in virus spread during disease outbreak and minor role in maintenance of virus in horse population (166). Though the virus is labile and can easily be inactivated by heat and common disinfectants, EHV can persist in the environment under various climatic conditions for a period between 7 and 35 days (167, 168). Serological studies revealed that most of the adult horses have been exposed to EHV-1 and -4 (169-171). Epidemiological investigations suggest that EHV infection is acquired within first few weeks of life, mostly before or after weaning from silent shedding adult horses within the shed. Latently infected lactating mares act as important reservoirs of the virus, infecting their foals in the initial stage of life (71, 172). However, it is not very clear that maintenance of infection is due to either reactivation of endogenous latent viruses in individual horses or cycles of subclinical infection within the horse population. In general, EHV life cycle in horses share four major features (figure 4): (i) infection of young horses, (ii) establishment of latent stage, (iii) reactivation from latency due to stress and transmission of virus from adult horses to young populations and (iv) widespread ‘silent’ virus transmission between adult-adult, adult-foal and foal-foal cycles of endemic virus transmission (173). EHV latency, reactivation and virus transmission cycles are given in figure 4.

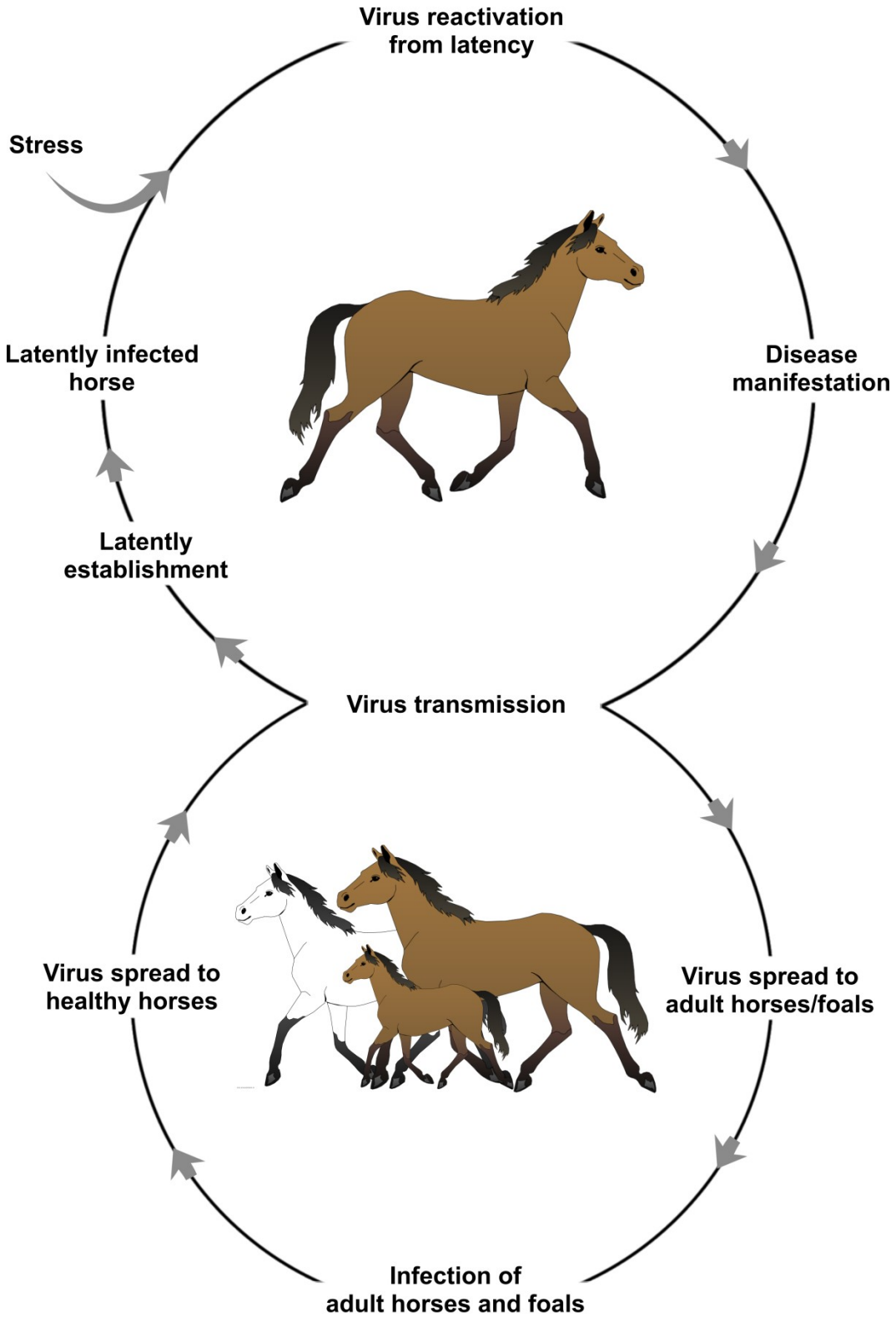

Figure 4: EHV latency, reactivation and transmission cycle in equine population. Images used in the figures were from IMGBIN® under non-commercial use (https://imgbin.com).

4.6 Pathogenesis and pathology of EHV

Though EHV infections have been reported in several host species, pathogenesis and pathology of EHV-1 and -4 following either natural or experimental infections have been well studied in horses (174, 175). After inhalation of virus particles-containing droplets or contact with infected fomites or virus reactivation from latency, both EHV-1 and EHV-4 primarily replicate in upper respiratory tract epithelium (63). Virus replication results in necrosis and erosion of the epithelium. The virus infects PBMC, quickly pass through underlying lamina propria and enter directly to general circulation or via draining lymph node. In the meanwhile the virus gets access to neurons of the trigeminal nerve within 48 hours (hrs) and may establish latency in trigeminal ganglion (176). In the general blood circulation, the virus establishes cell-free and cell associated viremia in PBMC. Infected horses shed viruses through nostrils for up to 14 days post infection and viremia persists up to 21 days. However, lower levels of virus shedding and viremia can occur transiently for long time after peak viremia, making it difficult to detect the virus in later stages (66, 177, 178). Unlike EHV-4, EHV-1 is unique in its ability to target and attack three separate organ systems of the horse (Respiratory, reproductive and central nervous systems) giving rise to large-scale outbreaks as respiratory tract disease, abortion, neonatal mortality and paralytic neurological disease (63, 67, 179). Schematic diagram of EHV-1 pathogenesis is given in figure 5. Though pathogenesis of EHV-4 is not completely understood, the virus initially replicates in respiratory mucosa and lymphoid associated tissues like EHV-1, and subsequently establishes latency in trigeminal ganglion. EHV-4 shows low endotheliotropism and do not establish viremia, therefore do not cause abortion or neurological disease. The duration of virus shedding for EHV-4 is transient than EHV-1 (74, 180, 181).

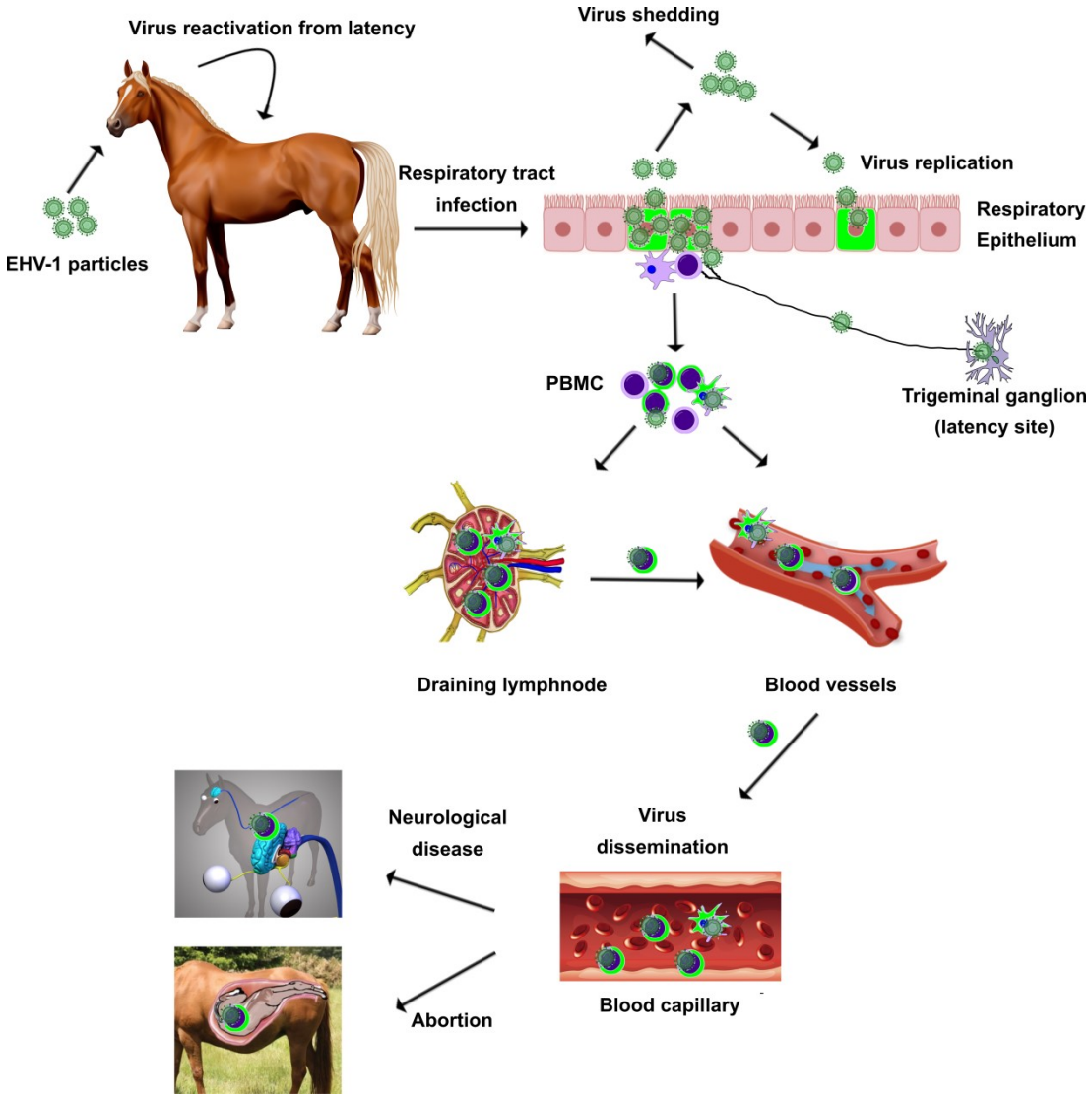

Figure 5: Pathogenesis of EHV-1. Images used in the figures were from IMGBIN® under non-commercial use (https://imgbin.com).

4.6.1 Epithelial infection

To get entry inside the body, herpesviruses first make contact with host cells by binding to cell surface heparan sulfate proteoglycans (HSPG) and chondroitin sulfate proteoglycans (CSPG) with the help of gC and/or gB (138, 182). After attachment, MHC-I act as an entry receptor and binds to gD of EHV-1 (123, 183). After binding, the virus enters host cells either by direct fusion of the virus envelope with the plasma membrane or via endocytosis followed by fusion between the virus envelope and an endosomal membrane. EHV-1 utilizes multiple endocytic pathways in different cell types to establish productive infection (184). Following penetration, cellular kinins, microtubules, dynein, and Rho-associated coiled-coil containing protein kinase-1 (ROCK1) help the virus in trafficking to the nucleus (185) where replication of the virus takes place and characterized by presence of intranuclear inclusion body. Within

the nucleus, viral DNA transcription and replication take place. Viral genome is transcribed in a cascade of events as IE gene, E genes, and finally L genes (186, 187). Translated capsid proteins are directed to the nucleus where newly formed DNA is assembled and forms nucleocapsid. The nucleocapsid leaves the nucleus via budding through inner nuclear membrane and acquire primary envelope. Subsequently, it fuses with the outer nuclear membrane and naked virus nucleocapsids is released into the cytoplasm. Subsequently, secondary envelopement takes place in Golgi, transported within secretory vesicles, reach cell surface via exocytosis and free virions egressed (188). In addition to gB, gC and gD, other viral proteins like gH-gL complex, gE-gI proteins play essential roles in membrane fusion, cell-to-cell virus spread and virus release (189).

4.6.2 Viremia, PBMC-EC interaction and endothelial infection

Viremia, either cell-associated and/or cell free, distributes the virus to endothelial lining of capillaries in uterus and central nervous system which results in abortion and neurological illness, respectively (71, 190). Though all viremic pregnant mares do not abort, viremia is a prerequisite for the disease in most of cases. Interestingly, EHV-1 infection of the PBMC during viremia is the critical step that decides EHV-1 pathogenesis; thereby the virus can spread from infected PBMC to EC without being neutralized by the host immune system (77). Though all three PBMC subsets namely T lymphocytes, B lymphocytes and monocytes can be infected with EHV-1 virus *in vivo* during cell-associated viremia, the virus will not undergo lytic replication and the virus can be recovered only by co-cultivation with suitable cells (‘restricted replication’) (64, 66, 76, 191).

The process of virus transfer between infected PBMC and EC is complex, requires co-ordinated action of viral proteins, adhesion molecules expressed by both cells, and cytokines and chemokines for the formation of inter-cellular adhesion, intra-cellular trafficking and cellular polarity (192, 193). Contact of PBMC to EC initiates the process of virus transfer and subsequent EC infection. Before making the initial contact to EC, PBMC approaches to and rolls over EC and finally makes firm adhesion (Figure 6). Margination and rolling of PBMC on EC is attributed by selectin molecules expressed on corresponding cells and their counter receptors (L-selectin – in PBMC; E-selectin – in endothelial cells; P-selectin – platelets and endothelial cells). PBMC makes firm adhesion to EC due to the endothelial presented chemokines/cytokines and other chemoattractnants that activates leukocyte α4β1 (also known as very late antigen 4[VLA-4]) and two other β2 integrins, namely leukocyte function-associated antigen 1 (LFA-1) and macrophage 1 antigen (Mac-1) which allows PBMC to bind to their cognate ligands, namely vascular cell adhesion molecule 1 (VCAM-1) and intercellular adhesion molecule 1 (ICAM-1), respectively (194). Several viral proteins are

also involved in mediating the process in infected PBMC. Previous studies revealed that EHV-1 gD, gB and US3 proteins play an essential role in PBMC and EC infection and transfer (72, 77). Further, EHV-1 infected PBMC still able to roll over EC efficiently than EHV-4 infected PBMC. EHV-4 infected PBMC show significant downregulation of adhesion molecules like LFA-1 and VLA-4 (195).

Cell-to-cell virus transfer considered to be a mechanism of immune evasion and immunomodulation properties of herpesviruses (196). Though all PBMC subsets can be infected with EHV-1, the subset of cells that transfer the virus to EC is not known. Virus transfer from PBMC to EC results in vasculitis, underlies both abortogenic and neurologic manifestations of the disease (179). EHV-1 induced abortions usually observed in the third trimester of the pregnancy, however, the main cause of abortion in late gestation is not clearly known (190). It is considered that there may be some undefined host factors (pregnancy or stress related), which activates latent EHV-1 and results in EC infection. Breach of the uteroplacental barrier and EHV-1 infection of the fetus have also been reported as factors of abortion and neonatal foal death (197). Vascular endothelium has been reported the site of replication for the virus which leads to vasculitis by two mechanisms, first by the direct damage to vascular endothelium and second by the deposition of immune complexes of EHV-1 virus and antibody like Arthus-type reaction. Arthus reaction is a type of localized type III hypersensitivity reaction due to deposition of antigen/antibody complexes in vascular walls, serosal layers and glomeruli (61). Vasculitis of microvasculature of the central nervous system caused microthrombosis in arterioles, leading to disseminated ischemic necrosis of the spinal cord and gray matter resulting in neurologic manifestation ranged from mild ataxia to paralysis due to EHV-1 infection in horses (198). Actual pathogenesis of the neurotropism is not known, however, it is suggested that the ability of EHV-1 to modulate IL-10 production might contribute to the increased inflammation and neuropathies (199). Exceptionally, reactivation of virus in neurological tissue and local neuronal tissue infection without viremia also possible, but difficult to assess.

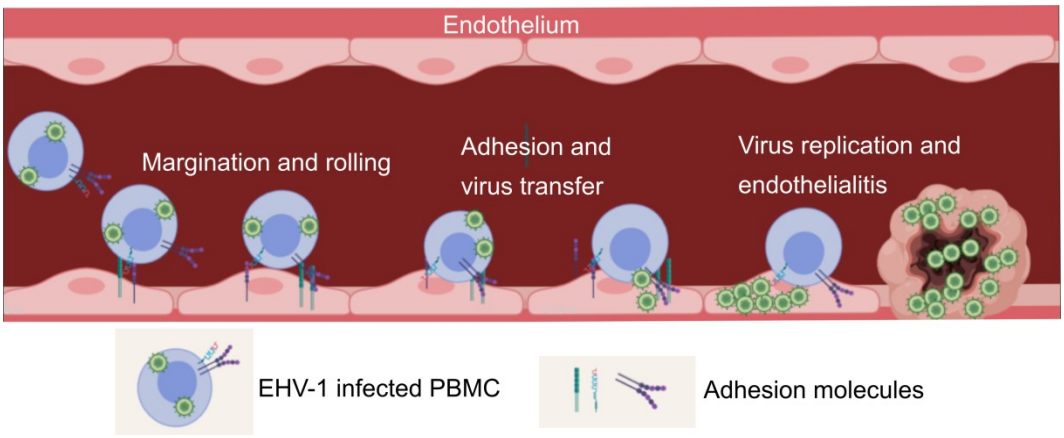

Figure 6: Virus transfer from infected PBMC to endothelial cells

4.7 Immune evasion strategies by EHV

In general, virus infected host cells are recognised and destroyed by three major host immune mechanisms: (i) antibody-dependent lysis, (ii) MHC-I dependent $CD8^+$ cytotoxic T lymphocyte mediated lysis and (iii) natural killer (NK) cell mediated lysis. However, herpesviruses modulate host immune responses, which have been well documented (200, 201). Herpesviruses evade host immune response by several strategies. Viral immune evasion genes can act by (i) decreasing the expression of molecules required for T-cell, or NK cell recognization; (ii) inhibiting antigen presentation; (iii) acting as a agonist or antagonist of cytokines and chemkines; (iv) blocking intracellular antivial or proinflammatory effects of interferons or other cytokines; and (v) modulating host signalling pathways (5). It is important to determine which viral immune evasion genes are critical, so that these genes can be specifically targeted for vaccines or therapeutic interventions. EHV-1 also developed an array of strategies to overcome immune-surveillance by minimizing recognition and destruction by immune cells, thereby the virus replicatess and spreads to new host to ensure its own survival. The mechanisms include MHC-I downregulation on the surface of infected cells (ORF1 and ORF17 of EHV-1), downregulation of adhesion molecules on the surface of infected PBMC (EHV-4), cell-to-cell virus spread in the presence of virus neutralizing antibodies (gB, gD and US3 of EHV-1), modulation of cytokines and chemokines production/expression by infected cells (various strains of EHV-1 and viral proteins namely ORF1 and ORF2 of EHV-1) (77, 146-148, 151-153, 160, 161, 195). Unlike other herpesviruses, immune evasion strategies employed by EHV has been explored only lately. Still several viral and host proteins, and various mechanisms of immune evasion strategies need to be studied.

4.8 Models to study equine herpesvirus pathogenesis

Horses are the gold standard animal model to study EHV; however, this model is very expensive and requires special biosafety animal facilities, trained personnel and ethical approvals. Due to difficulties associated with horse-based experimental infection, small animal model based-*in vivo* and -*in vitro* models were attractive alternative approaches to study EHV-1 pathogenesis and vaccine efficacy studies.

4.8.1 Small animal models

BALB/c mice were used as small animal models to study EHV-1 pathogenesis (202). Infected mice following intranasal virus inoculation developed clinical signs of disease like reduction in body weight, respiratory difficulties, hunched posture, depression, ruffled fur, crouching in the corners, neurological signs and cell associated viremia. Infection was limited to respiratory tract, and pulmonary lesions in BALB/c were almost similar to that of equines characterized by degeneration and necrosis of respiratory tract epithelium, and pneumonic changes with virus shedding through nostrils. In addition, EHV specific humoral and cell mediated immune response was observed in infected BALB/c mice (202). Subsequently several studies have been performed in mice to study virus pathogenesis, vaccine efficacy and therapeutics (203-206).

In addition, C57BL/6J and CBA strain mice also used to study EHV-1 pathogenesis and vaccine efficacy studies (207, 208). Although, both mice and equine showed similar tissue tropism, there is no documented evidence for transmission or spread of EHV-1 among mice (209). Clinical signs were only obsvered when mice were infected with high titer of EHV-1. The observation of clinical signs were considered to be subjective. As clinical signs were used to distinguish between pathogenic and non-pathogenic strains in mice (210), they were no reliable in distinguishing between intermediate and non-pathogenic strains. Further, the extent to which valid comparisons and extrapolations can be made of pathological and immunological parameters from mouse to horse is yet to be determined. With all given limitations of the mice with species difference, variation in placental type and unnatural host for EHV, these small animal models may not predict the success, but can predict the failure as mice provides a biological system to test vaccines/therapeutics efficiency, however ethical approval is still a major concern.

4.8.2 In vitro models

In vitro models provide less expensive alternative approaches to study virus pathogenesis. Currently available *in vitro* assays can be divided into two main categories. (i) Epithelium-

PBMC mimicking models, which include *ex vivo* nasal explants and equine respiratory epithelial cells (EREC) culture; (ii) PBMC-EC mimicking models, which include flow chamber assay and contact assay. These models are widely used to recapitulate *in vivo* architecture and investigate the host-pathogen interaction.

4.8.2.1 *Ex vivo* nasal explants

Epithelial cells of the respiratory mucosa are the primary target sites for EHV. Nasal explant model provides an attractive and alternative means to mimic the *in vivo* situation as a complex 3-dimentional tissue network keeping normal cell-to-cell contact nature. This model is readily accessible and is a powerful tool to overcome problems when using infection experiments in the natural host, including, but not restricted to, better standardization and the possibility to perform multiple replicates that are impossible in the horse infection model (36). Nasal explant cultures have been successfully used to study the pathogenesis, replication and invasion of EHV-1, EHV-3 and EHV-4, the response and migration of mononuclear cells during EHV-1 infection, basement membrane damage during infection, and EHV-induced cytokine response (62, 211-216). Confocal microscopy studies showed that EHV-1 crosses the basement membrane barrier through infected mononuclear cells "Trojan horse" that subsequently progresses to draining lymph nodes or blood vessel in lamina propria and results in cell-associated viremia (62, 215). Migration of mononuclear cells in response to virus infection or navigation of infected cells to blood vessels or lymph nodes is determined by complex network of cell signals and interactions of cytokines and chemokines.

Vaginal mucosal explant is a variant of mucosal explant culture, which is an alternate portal of entry for EHV-1 and EHV-3. Vaginal explants have been used to study replication kinetics, virus spread and invasion characteristics of EHV-1 and EHV-3. Though both viruses can replicate efficiently, EHV-3 showed replication advantage in vaginal mucosa in comparison to nasal explant due to virus tissue tropism under natural conditions (216).

4.8.2.2 EREC culture

Polarized epithelial cells differentially distribute proteins and lipids in the plasma membrane creating two distinct surfaces: the apical domain, which faces the external environment, and the basolateral domain, which contacts the underlying cells and systemic vasculature (217). Most studies on virus entry have been conducted with non-polarized cells that might not reflect the *in vivo* conditions. Epithelial cells grown on porous supports show evidence of increased differentiation in comparison with cells grown on conventional solid surfaces, which formed the base for EREC *in vitro* culture model (218, 219) (Figure 7A) and was

recently adopted to study EHV-1 pathogenesis (151, 220, 221). EREC were used to study replication kinetics and cytokine response after wild type and mutant EHV-1 infection. Further, an EREC-PBMC virus transfer system was developed and shown direct viral transfer from the epithelium to PBMC. Viral transfer through direct cell-to-cell contact resulted in pro-inflammatory, chemokine and antiviral responses that were strikingly different if each cell-type was infected independently. In addition, EREC system was successful to shed light on chemotaxis of monocytes and neutrophils in response to EHV-1 infection of respiratory epithelial cells (222). This unique primary equine epithelial cell system closely mimics *in vivo* conditions of primary infection. Further, most of the data related to EHV-1 obtained from this *in vitro* system mimics *in vivo* data obtained earlier or later (126, 146, 152). In conclusion, all data showed the importance of studying the cells representing different compartments of the body during infection with EHV-1 in relation to each other, rather than individually.

4.8.2.3 Contact assays

To mimic PBMC-EC interface and to investigate the interaction between PBMC and EC with subsequent virus transfer, an *in vitro* co-cultivation system was developed (67). The system involved either “contact” or “non-contact” setups where both PBMC and EC are sharing the same environment that contained neutralizing antibodies. In the contact model and under static conditions, EHV-1 infected PBMC were co-cultured with EC monolayers in the presence of neutralizing antibodies, and virus transfer from PBMC to EC was reported (Figure 7B). In the “non-contact” model, infected PBMC were placed into a transwell insert and were physically separated from EC monolayers by a porous membrane that prevents the migration of PBMC but allows the diffusion of cell-free virus (Figure 7B) (67, 77). Virus spread from infected PBMC to the underlying EC in the “contact” mode was reported and tracked using confocal microscopy and live cell imaging (77). The system proved to be flexible to study other aspects during virus spread, particularly the role of adhesion molecules in virus transmission (78).

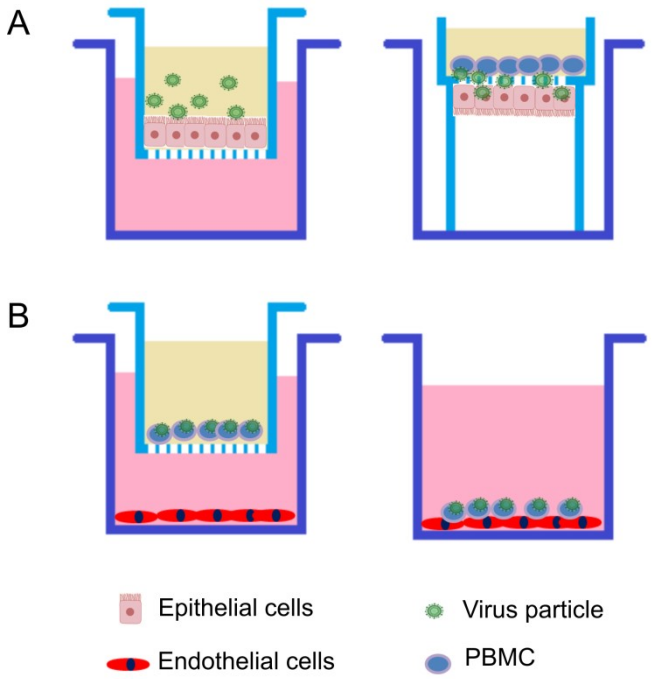

Figure 7: EREC and contact assay to determine cell-to-cell virus transfer in vitro. Schematic diagram of (A) EREC culture system and (B) contact assay are given.

4.8.2.4 Flow chamber system

To further address the more dynamic aspects of PBMC-EC interaction, a flow chamber setup was established, where infected PBMC are allowed to flow (0.5 mm/sec) over EC monolayers in the presence or absence of virus-neutralizing antibodies. The whole process was tracked by confocal live cell fluorescence imaging and automated cell tracking (Figure 8A-C). This system was able to document the differences between neuropathogenic and non-neuropathogenic EHV-1 strains as well as between EHV-1 and EHV-4. The role of different viral proteins in the process of virus spread from PBMC to EC was precisely addressed. The system was also able to document the kinetics of infected versus non-infected PBMC in terms of tethering, adhesion, and rolling (77). These experiments demonstrated the value of the flow chamber system for studying the dynamic events during EHV-1 transfer from infected PBMC to EC, role of adhesion molecules, effect of anti-inflammatory and anti-viral treatment on virus transmission.

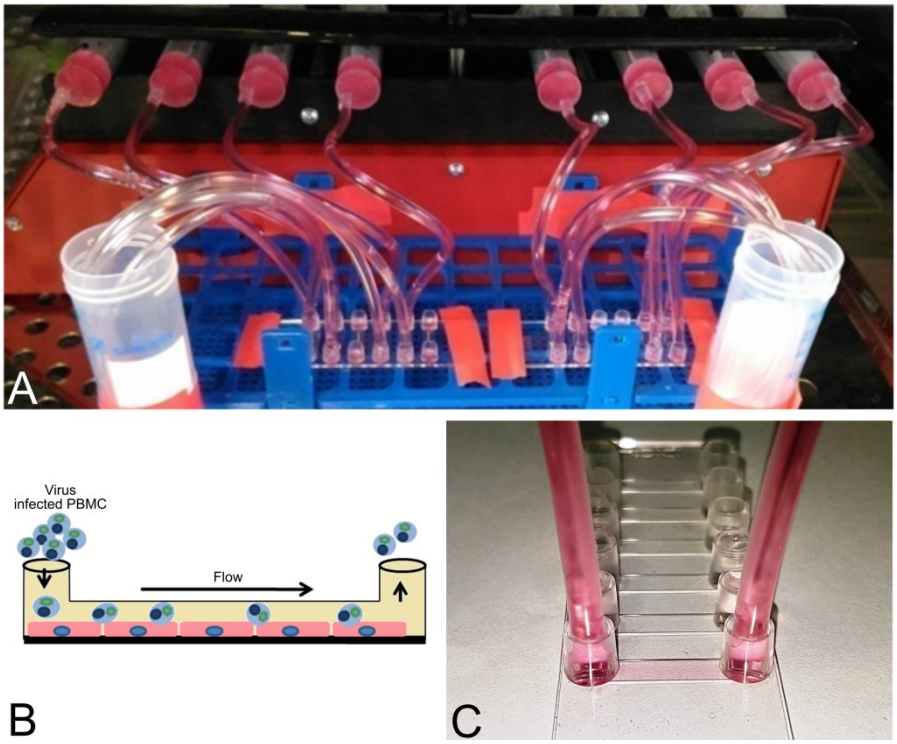

Figure 8: Flow chamber system to study cell-to-cell virus transfer from infected PBMC to endothelial cells under flow condition. (A) Flow chamber instrument, (B) schematic diagram of flow chamber model and (C) flow chamber slide.

Another aspect of EHV-1 pathogenesis targeting the role of EHV-1 in thrombus formation was studied using another flow microfluidic system. Through that system, it was possible to investigate the interaction between EHV-1 infected EC cells and platelets. The process of capturing un-activated platelets by infected EC and initiation of platelet aggregation was tracked in a dynamic mode using confocal microscopy (223, 224).

4.8.2.5 Other promising *in vitro* models

The development of *in vitro* models paved the way to fill in the gaps in our understanding of EHV-1 and EHV-4 pathogenesis. Conducting *in vivo* experiments on horses is always hampered by ethical approvals, costs, and presence of special facilities and manpower. Furthermore, suitable replicates of experiments is always a hurdle. Available *in vitro* experimental models added important insights into virus pathogenesis, virus-cell interaction, crosstalks between cells, and viral and cellular determinants during infection.

At animal welfare level, the currently available models were important steps toward reducing the suffering of horses during animal experiments, although some samples are still to be collected from horses at sacrifice. At technology level, these systems provided an important level of tissue complexity that allowed better understanding of virus pathogenesis; however,

upgrades are still need to be applied to mimic and recapitulate the complicated *in vivo* situation.

Horse-on-a-chip would be the suitable upgrade and future of these models. Three (3D) cell culture matrix is now widely accepted as highly complex and dynamic systems that promote many biological relevant functions through properly regulated cell-cell and cell-matrix interactions and the dynamic distribution of oxygen, nutrients and other molecules. Currently, there are several reports that have confirmed significant differences in the morphology, viability, response to stimuli, gene and protein expression, proliferation, migration, and functionality of cells between 3D and 2D cell cultures, which support the transition from 2D to 3D cell culture systems (225-227). The microfluidic technology can create controllable, reproducible and optimizable dynamic microenvironment that mimic the *in vivo* environment and provide efficient and high throughput cellular analysis and *in situ* monitoring of cellular events. The combination of microfluidic technology with 3D cell culture offers great potential for *in vivo*-like tissue-based applications. This system has been widely used to study cell biology for biomedical applications, genetic assays, protein studies, intracellular signaling, multidrug resistance, drug toxicity, and pathogen detection (226-230). Horse-on-a-chip microdevice will combine microfluidics and biotechnology techniques, represent alternatives to mimic the multicellular architectures, tissue-tissue interfaces, and physicochemical microenvironments. Such system will provide better levels of tissue and organ functionality compared with conventional cell culture systems, and have great potential to advance the study of disease etiology and drug discovery and development.

4.9 Vaccination

Vaccination against viral infection is the only mean of disease prevention. Optimal and potential vaccine should be safe and efficient delivery route, stimulate multilayered immune response including long-lived mucosal and systemic immune response with protective titre virus neutralizing antibodies and cytotoxic T lymphocytes (CTL) and memory B cells. EHV-1 vaccines were first introduced in late 1950s or early 1960s. (Patel and Heldens, 2005). First live hamster-adapted EHV-1 vaccine was first produced in Kentucky in 1961, which protected horses for 3 months against respiratory disease. Subsequently, commercial vaccine (Pneumabort-K) was developed and effectively used to control abortions in mares for next few decades (231). Along with vaccination, implementation of vigorous hygiene measures also impacted in reducing spread of virus and abortions. Recent randomized control study about assessing efficacy of commercial inactivated combined EHV-1/EHV-4 vaccine showed that the vaccination did not reduce the respiratory illness and viremia, but reduce virus shedding and abortion to certain extent (232, 233). No data is available

regarding efficacy on currently available vaccine in reducing EHV-1 induced neurological disease. Similarly, no data is available regarding efficacy of currently available vaccines in reducing or preventing outbreak of EHV disease.

There are at least 10 inactivated vaccines (8 in the United States and 2 in Europe) and 2 modified live virus vaccine (1 in the United States and 1 in Europe) is commercially available against EHV (Table 4) (173). These vaccines induce high titres of virus neutralizing antibodies and protects against respiratory tract infection. The vaccines reduced quantity and duration of nasal virus shedding upon virus challenge in vaccinated animals. Variable results are available regarding ability of inactivated virus and modified live virus in conferring protection against viremia and abortion as both vaccines claim protection (234, 235). However, sufficient field data is not available to make a conclusion.

These large numbers of commercially manufactured vaccines (both inactivated and live-attenuated) are currently available in market and used extensively by the animal owners. As described, each of the currently available EHV-1 vaccines induces some but not all of the desired components of the immune response against EHV-1, and none of the vaccines warrant complete protection. Further, it will be difficult to assess the impact of vaccination on the control of EHV disease because of the lack of randomized, controlled field studies. With all given facts, vaccination appears to be reducing clinical signs and abortion, but not appear to be effective in blocking the cycle of silent transmission of EHV-1 and EHV-4 in large equine studs.

Extensive research continues to develop improved vaccines against EHV-1 and -4. So far, the EHV vaccinology field gained only little attention because they are less commercially important in comparison to other herpesviruses. As described early, development of MLV-vaccine and recombinant based vaccines are current strategies of vaccine manufacturing. MLV- vaccines are constructed mainly by passaging in unnatural host/cell lines, and deleting essential / immunomodulatory / viral genes involved in specific pathways (158, 236, 237). On the other hand, recombinant vaccines using baculovirus and canary pox as vector to delivery EHV-1 gB, gC and gD along with immune modulating genes like CpG and CTL epitopes were developed (238). Subunit or inactivated virus vaccine based on immune stimulating complexes (ISCOM) and carbomer adjuvanted vaccines showed convincing serological response, but did not prevented virus shedding (239, 240). Recent advancement with bacterial artificial chromosome (BAC) based genetic recombineering technique enabled genetic manipulation for development of optimal vaccine candidates (241). Further, BAC technology helps in developing multivalent vaccines by incorporating immunodominant antigen from different pathogens in to BAC backbone (242, 243).

Inactivated vaccine		
Pneumabort K®+1B	Prevent respiratory disease, can be used in pregnant mares to prevent abortion	Zoetis
Duvaxyn® EHV-1/EHV-4	Reduce severity of respiratory disease, prevent abortion, reduce virus shedding through nostrils	Zoetis
Flu-Vac Innovator® 6	Protection against EHV-1/EHV-4, equine influenza Eastern and Venezuelan encephalomyelitis and tetanus toxoid. Protection against upper respiratory tract infection caused by EHV-1 and EHV-4	Zoetis
Equivac innovator® EHV-1/4	Protection against upper respiratory tract infection caused by EHV-1 and EHV-4	Zoetis
Vetera® 2^{XP}, Calvenza®-03 EIV/EHV	Protection against respiratory infection and equine influenza	Boehringer Ingelheim
Prestige®2, Prodigy® with Havlogen®	Prevent respiratory infection and abortion	Merck Animal health
Modified live virus vaccine		
Prevaccinol®	Contains RacH strain of EHV-1. Reduced severity of respiratory illness and duration of virus shedding through nostrils.	Intervet
Rhinomune	Prevent respiratory illness, pregnant mares can be vaccinated,	Pfizer animal health

Table 4: Details of commercially available inactivated and live EHV vaccines.

4.10 Elephant endotheliotropic herpesvirus

Asian elephants are an endangered animal species. Existence of the species is further threatened by the emergence of a lethal herpesvirus, elephant endotheliotropic herpesvirus (EEHV). Infection with this virus can cause a devastating haemorrhagic disease, mostly in

young Asian elephants between one and eight years of age, with up to 85% mortality. In older animals, the infection is predominantly inapparent (60, 244). The disease is characterized by sudden onset of illness, lethargy, edema, mild diarrhea, and sudden death with fatal haemorrhages in all visceral organs. Acute death of a young Asian elephant with haemorrhagic disease of unknown aetiology was first reported in 1988 (52); retrospectively, the cause of the reported disease was identified as EEHV (244). Since then, more than 100 confirmed cases of deaths of young elephants due to EEHVs have been reported in Asia, Europe, and North America (38, 245). EEHV infections have been reported mostly in Asian elephant calves in zoos. However, few deaths have also been documented in free-range Asian and African elephant calves (244). Tracking elephant health in the wild is difficult, which may contribute to the low number of documented EEHV cases of wild elephants.

As described early, EEHVs are members of the family *Herpesviridae*, and are allocated to genus *Proboscivirus* in the subfamily *Betaherpesvirinae*. Seven distinct genotypes and five major subtypes of EEHVs have been identified: EEHV-1A and -1B, EEHV-2, EEHV-3A and -3B, EEHV-4A and -4B, EEHV-5A and -5B, EEHV-6 and EEHV-7A, and -7B (38, 246). Although infection of elephants has been reported with all genotypes of EEHVs, mortalities were mainly associated with EEHV-1A and -1B (38).

Diagnosis of the disease largely relies on clinical signs as well as the age of the elephant, detection of viral nucleic acids in blood samples or trunk washes using quantitative PCR (qPCR), post-mortem lesions, histopathology, and immunohistochemistry (247). Despite decades of research, many aspects of disease pathogenesis, virus dissemination and transmission, predilection sites in host, sources of infection, and virus biology remain unclear. This may be partially attributable to the fact that the virus is not cultivable in vitro and that no small animal models are available. There is no vaccine or reliable therapeutic option available. Development of suitable cell culture systems and characterization of the virus remain the focus of current studies, with the hope to arrive at sustainable control measures in the future (53, 248).

4.11 Aims of the study and project summary

(i) EHV-1 can spread through cell junctions between PBMC and EC without being neutralized by antibodies through a mechanism that requires coordination of several host and viral proteins (68-70). Viral and host factors responsible for cell-to-cell virus spread are not fully identified. In previous studies, our group has revealed the essential role of glycoprotein B (gB) and unique-short region 3 (US3) protein in virus transfer between PBMC and EC *in vitro* (77). Further, our group identified two immune modulating proteins of EHV-1, i.e. ORF1 and ORF17 (151, 249), both viral proteins co-operate with each other and inhibit

MHC-I downregulation on the surface of infected PBMC (146-148). Adding to the list is ORF2, which is a unique protein in the *Alphaherpesvirinae* subfamily and has no counterpart among any of the members (109). *In vivo* studies have revealed the involvement of ORF1 and ORF2 in modulating cytokine and chemokine responses in infected horses and subsequently attenuated the course of the disease (152, 153, 160). With this background, I hypothesized that these three immune modulating viral genes (ORF1, ORF2, and ORF17) may affect the virus transfer between PBMC and EC. in one part of my thesis, I explored the role of these viral proteins of Ab4 strain of EHV-1 in determining virus transfer between PBMC and endothelial cells and virus induced changes in host cell pathways. Identifying viral proteins involved in virus transfer to EC and finding the underlying mechanisms would favor the development of optimal therapeutics against EHV-1.

(ii) EHV-4 causes only moderate respiratory infection in foals and horses of less than 2 years old. EHV-4 infections were mostly inapparent without any clinical signs and the infections in foals and horses may go unnoticed (75). As described earlier, EHV-4 is endemic in equine populations and serological surveys indicates sero-prevalence of more than 80% among horses, donkeys and mules in different geographical locations (250-255). The higher sero-prevalence shows the evidence of heavy exposure to the virus; however, epidemiological data regarding source and time of infection of naïve animal is not available. It is generally accepted that EHV-4 infection starts early in life, where foals and yearlings are the most clinically infected. Here, I report an outbreak of EHV-4 with clinical signs and rapid spread of infection within a stud with subsequent virus isolation and characterization. I aimed to investigate and describe clinical, virological, serological, and molecular findings of respiratory infection caused by EHV-4 in a equine breeding stud in Northern Germany.

(iii) Elephant endotheliotropic herpesvirus can cause an acute highly fatal hemorrhagic diease in young Asian elephants (38). Here, I report on the death of two young Asian elephants, which occurred within a period of eight days after suffering from acute haemorrhagic disease in Tierpark Hagenbeck, Hamburg, Germany. Molecular investigation revealed EEHV-1A as the cause of death. I performed pathological and virological investigations on infected tissues, including virus dissemination and viral load studies. I have further performed transmission electron microscopy (TEM) of negatively stained sections of liver, tongue, and spleen tissues to visualize virus particles. To isolate the virus, I attempted virus propagation on different cell lines and assessed virus replication by qPCR, indirect immunofluorescence (indirect IF), and western blot (WB) assays.

Despite of several decades of research, molecular mechanisms of several animal herepesviruses pathogenesis were less understood including EHV-1, EHV-4 and EEHV. This hampered the developement of fully protective vaccines and establishment of optimal therapeutics measures against these pathogenic animal viruses. My research can significantly contribute to this by unraveling the molecular mechanisms of PBMC infection and crucial step of subsequent virus transfer between PBMC and EC. In this regard, I have identified an essential role of ORF1, ORF2 and ORF17 viral proteins in endothelial infection. These (viral proteins targeted) virus mutants could be a potential candidates for development of live attenuated vaccine therapeutics against EHV-1 infection in equines. Regarding EHV-4 outbreak, though vaccination programs are regularly applied in studfarm, my study necessitates the importance of management practices, routine equestrian activities, exercise and seasonal changes as a multifactorial cause for stress in horses and which resulted in larger EHV-4 outbreak among foals, stallions and mares. In my study with EEHV-1 in young Asian elephants, I have showed the presence of EEHV particles in the infected tissues, observed limited viral replication in cell cultures, and provided evidence for the possibility of viral glycoprotein B (gB) cleavage similar to other members of the *Herpesviridae* family. The findings and facts of this EEHV study will be helpful for the development of suitable cell culture system and further characterization of EEHVs with respect to developing prophylactic strategies and implementing control measures in future. In general, my study makes a significant contribution to existing knowledge on herpesvirology which can also be applied to very relavent other human and animal herpesviruses.

5 Materials and Methods

5.1 Materials

The chemicals, enzymes, antibodies and commercial kits were used in this study as per manufacturer's instructions.

5.1.1 Chemicals, consumables and equipments

5.1.1.1 Chemicals

Name	Cat. No.	Manufacturer
Acetic acid	A3686.2500	Applichem, Darmstadt
Acetone	A160.2500	Applichem, Darmstadt
Acrylamide	UN 3624	Carl-Roth, Karlsruhe
Agar (Bacteriological)	2266.2	Carl-Roth, Karlsruhe
Agar 100	8619	Carl-Roth, Karlsruhe
Agarose-standard	3810.4	Carl-Roth, Karlsruhe
Ammonium acetate	131114.1210	Applichem, Darmstadt
Ammoniumpersulfate	K38297601	Merck, Darmstadt
Arabinose L (+)	A11921	Carl-Roth, Karlsruhe
Bromophenol blue	B1793	Alfa Aesar, Karlsruhe
BSA (albumin bovine fraction V)	A6588.0100	Applichem, Darmstadt
Cacodylic acid sodium salt trihydrate	5169.3	Carl-Roth, Karlsruhe
Calcium chloride	A1873.1000	Applichem, Darmstadt
Chloroform	411 K3944831	Merck, Darmstadt
Citric acid	131808.1210	Applichem, Darmstadt
Crystal violet	131762.1605	Applichem, Darmstadt
Dimethyl sulphoxide (DMSO)	1.02952.2500	Merck, Darmstadt
Dithiotheritol	3483-12-3	Sigma-Aldrich, St. Louis
DMP 30	AGR1063	Agar scientific, Essex
dNTP Mix (10mM total)	BIO-39053	Bioline, Luckenwalde
Dodecenylsuccinic anhydride	AGR1051	Agar scientific, Essex
Ethanol	A1613	Applichem, Darmstadt
Ethidium bromide 1%	2218.2	Carl-Roth, Karlsruhe
Ethylendiaminetetraacetic acid	A2937.1000	Applichem, Darmstadt
Famvir (Famciclovir)		Novartis Pharma, Vienna
Formaldehyde	4979.1	Carl-Roth, Karlsruhe

Glucose (α-D (+) glucose monohydrate)	303 K1468642	Merck, Darmstadt
Glutaraldehyde	G5882	Sigma-Aldrich, St. Louis
Glycerol	A2926.2500	Applichem, Darmstadt
Glycine	A1067.0500	Applichem, Darmstadt
Heparin	84020	Sigma-Aldrich, St. Louis
Hoechst	33342	Thermo Fischer Scientific, Kandel
Hydrogen peroxide	121076.1211	Applichem, Darmstadt
Hydrochloric acid	4625.2	Carl-Roth, Karlsruhe
Isoamyl alcohol	A2610.0500	Applichem, Darmstadt
Isopropyl alcohol	A0892	Applichem, Darmstadt
Magnesium chloride	5833.025	Merck, Darmstadt
β-mercaptoethanol	28625	Serva, Heidelberg
Methanol	A3493.1000	Applichem, Darmstadt
Methyl cellulose	M0262	Sigma-Aldrich, St. Louis
Methyl Nadic Anhydride	AGR1081	Agar scientific, Essex
Opti-MEM	31985062	Life Tech, Carlsbad
Osmium tetraoxide	E19120	Science services, Munich
Paraformaldehyde	P6148	Sigma-Aldrich, St. Louis
Peptone	A2210.0250	Applichem, Darmstadt
Phenol/Chloroform	A0889.0500	Applichem, Darmstadt
Phenol	0038.3	Roth, Karlsruhe
Phenylmethylsulfonyl fluoride	P7626	Sigma-Aldrich, St. Louis
PIPES	A1079.0100	Applichem, Darmstadt
Polyethyleneimine	23966-2	Polysciences, Hirschberg
Potassium acetate	A4279.0100	Applichem, Darmstadt
Potassium chloride	5346.2	Roth, Karlsruhe
Potassium dihydrogen phosphate	3904.1	Roth, Karlsruhe
Propylenoix	1280	VWR Life sciences, Dresden
Sodium chloride	A3597.5000	Applichem, Darmstadt
Sodium hydroxide	1.06462	Merck, Darmstadt
Sodium deoxycholate	A1531.0025	Applichem, Darmstadt

Sodium dodecyl sulphate	75746	Sigma-Aldrich, St Louis
Sodium phosphate, monobasic, monohydrate	S9638	Sigma-Aldrich, St Louis
di-Sodium hydrogenphosphate dodecahydrate	A3906	Applichem, Darmstadt
D(+)-Sucrose	A2211.1000	Applichem, Darmstadt
Sulfuric acid	131058.1611	Applichem, Darmstadt
Temed	2367.3	Roth, Karlsruhe
Tris	A1086.5000	Applichem, Darmstadt
Tris hydrochloride	A3452.0250	Applichem, Darmstadt
Triton X-100 detergent	8603	Merck, Darmstadt
Tween-20	9127.2	Roth, Karlsruhe
Uranyl acetate	AGR1260A	Agar scientific, Essex
Water, molecular biology grade	A7398	Applichem, Darmstadt

5.1.1.2 Consumables

Name	Manufacturer
15 µ-Slide VI 0.4	Ibidi, Martinsried
Cell culture dish: 6 and 24-well, 60 and 100 mm	Startsedt, Nümbrecht
Cell culture plate: 96 and 48-well	Startsedt, Nümbrecht
Cell culture flask: 25 and 75 ml	Startsedt, Nümbrecht
Cell scraper	Startsedt, Nümbrecht
Collagen type IV cellware 24-well plate	Corning, New York
Collagen type IV cellware 60 mm dish	Corning, New York
Conical test tubes 17 × 120 (15 ml)	Startsedt, Nümbrecht
Conical test tubes 30 × 115 (50 ml), with and without skirted base	Startsedt, Nümbrecht
Cryotubes 1.8 ml	Nunc, Kamstrupvej
BD Falcon Cell Strainers	BD Falcon, San Jose
Eppendorf tubes 1.5 and 2 ml	Sarstedt, Nümbrecht
Electroporation cuvettes	Biodeal, Markkleeberg
Falcon bacteria (13 ml)	Startsedt, Nümbrecht
Latex gloves	Unigloves, Troisdorf
Kimtech Science, Precision Wipes	Kimberly-Clark, Roswell
Nickel-grids	Agar scientific, Essex
Nitrile gloves	Hansa-Medical 24, Hamburg

Parafilm M	Bems, Neenah
PCR tubes - 0.2 ml	Applied biosystems, Berlin
Petri dishes for bacterial culture	Sarstedt, Nümbrecht
Pipettes: 5, 10, 25 ml	Sarstedt, Nümbrecht
Pipette tips: P1000, 200, 100 and 10	VWR International, West Chester
Polystyrene tubes with cell-strainer cap	Corning, New York
Infusion tube	Fresenius Kabi, Hamburg
Sterile syringe filters PVDF 0.45 µm	VWR International, West Chester
Syringe filters: 0.2 and 0.45 µm	Sarstedt, Nümbrecht
Transfection polypropylene tubes	TPP, Trasadingen
Transwell tissue culture insert – 0.4 and 3.0 µm	Sarstedt, Nümbrecht
Blotting paper – 0.35mm	Roth, Karlsruhe

5.1.1.3 Equipments

Name	Manufacturer
Bacterial incubator 07-26860	Binder, Turtlingen
Bacterial incubator shaker Innova 44	New Brunswick Scientific, New Jersey
Bunsen burner Type 1020	Usbeck, Radevormwald
Cell incubators Excella ECO-1	New Brunswick Scientific, New jersey
Centrifuge 5424, Rotor FA-45-24-11	Eppendorf, Hamburg
Centrifuge 5804R, Rotors A-4-44 and F45-30-11	Eppendorf, Hamburg
Covaris M220 focused-sonicator	Covaris, Woodingdean Brighton
CytoFLEX Flow Cytometer	Beckman Coulter Life Sciences, Krefeld
Electroporator Genepulser Xcell	Bio-Rad, Munich
Electrophoresis power supply Power Source 250 V	VWR International, West Chester
FACSAria	BD Bioscience, Heidelberg
Faster prep-24	MP Biomedicals, Irvine
Freezer -20°C	Liebherr, Bulle
Freezer -80°C	GFL, Burgwedel
Galaxy mini centrifuge	VWR International, West Chester
Gel electrophoresis chamber Mini Elektroforese System	VWR International, West Chester

Gel electrophoresis chamber SUB-Cell GT	Bio-Rad, Munich
HERAcell 240i CO_2 incubator	Thermo Fischer Scientific, Kandel
Ice machine AF100	Scotsman, Vernon Hills
Illumina MiSeq Machine	Illumina Inc., Hayward
INTEGRA Pipetboy	IBS Integrated Biosciences, Fernwald
Luminex MAGPIX system	Luminexcorp, Austin
Magnetic stirrer RH basic KT/C	IKA, Staufen
Microwave oven	Memmert, Buechenbach
Nanodrop 1000	Peqlab, Erlangen
Neubauer counting chamber	Assistant, Sondheim/Rhön
Nitrogen tank ARPEGE70	Air liquide, Düsseldorf
Orbital shaker 0S-10	PeqLab, Erlangen
Orbitrap Fusion Lumos	Thermo Fischer Scientific, Kandel
Perfusion system – Multi-syringe pump	World precision instruments, Friedberg
pH-meter RHBKT/C WTW pH level 1	Inolab, Weilheim
StepOnePlus real-timePCR system	Applied biosystems, Foster city
Sterile laminar flow chambers	Bleymehl, Inden
Reichert Ultracut S ultra-microtome	Fa. Leica, Wetzlar
Thermocycler Flexcycler	Analytik Jena, Jena
Transiluminator printer P93D	Mitsubishi, Rüsselsheim
Transiluminator VL-4C, 1x4W-254 nm	Vilber-Lourmat, Eberhardzell
Tristar LB 941 ELISA reader	Berthold technologies, Bad Wildbad
UV Transiluminator Bio-Vision-3026	PeqLab, Erlangen
Vortex Genie 2	Bender&Hobein AG, Zurich
Water baths TW2 and TW12	Julabo, Seelbach
Water bath shaker C76	New Brunswick Scientific, New Jersey

Microscope	
Axiovert.A1 fluorescence microscope equipped with Axiocam 503 camera	Carl Zeiss MicroImaging GmbH, Jena
Microscope AE20	Motic, Wetzlar
Olympus CX21	Olympus, Stuttgart
VisiScope scanning disk confocal laser microscope	Visitron systems, Puchheim
Zeiss EM 109 Electron microscope	Zeiss, Oberkochen

5.1.2 Softwares

Name	Version	Company/Source
Adobe photoshop	CC2017	Adobe Systems, Unterschleissheim
Axiovision software for Zeiss microscopes	4.8	Carl Zeiss MicroImaging, Jena
Burrows-Wheeler Alignment Tool	0.7.17	(256)
Chemi-Capt	-	Vilber-Lourmat, Eberhardzell
CytoFLEX CytExpert Software	1.2.11.0	Beckman Coulter Life Sciences, Krefeld
DNA copy numbers calculator		http://www.sciencelauncher.com/mwcalc.html
Endnote	X9	Clarivate Analytics, Philadelphia
Graphpad Prism 8	8.02	Graphpad Software, San Diego
Fiji-Image J	1.41	NIH, Bethesda
Inkscape	0.92.4	Software Freedom Conservancy, Brooklyn
Mapping assembler MIRA	4.9.6	(257)
MEGA	7.0.26	Pennsylvania State University, Pennsylvania
MikroWin 2000	4.41	Mikrotek Laborsysteme, Neunkirchen-Seelscheid
ND-1000	V.3.8.1	PeqLab, Erlangen
Perseus	1.6.1.3	Max Planck Institute of Biochemistry, Martinsried
Pilon	1.23	(258)
ProP 1.0 Server	1.0	Technical university of Denmark, Lyngby
Ragout	2.1.1	(259)
SPAdes assembler	3.13.0	(260)
Trimmomatic	0.36	RWTH Aachen University, Aachen
Vector NTI	9	Invitrogen Life Technologies, Grand Island
Vision-Capt	-	Vilber-Lourmat, Eberhardzel
xPONENT	4.2	Luminexcorp, Austin

5.1.3 Enzymes

Enzyme name	Cat. No.	Manufacturer
BamHI-HF	R3136	New England Biolabs, Ipswich
DpnI	ER1701	New England Biolabs, Ipswich
EcoRI-HF	R3101	New England Biolabs, Ipswich
KpnI	R0140S	New England Biolabs, Ipswich
Micrococcal nuclease	M0247S	New England Biolabs, Ipswich
Phusion High-Fidelity DNAPolymerase	M0530S	New England Biolabs, Ipswich
Proteinase K	7528.2	Carl-Roth, Karlsruhe
PstI	R0140S	New England Biolabs, Ipswich
Pvu1	R0150S	New England Biolabs, Ipswich
RNase A	A2760	Applichem, Darmstadt
Taq DNA Polymerase	01-1020	PeqLab, Erlangen
XbaI	R0145S	New England Biolabs, Ipswich
Makers		
Generuler 1 kb plus DANN ladder	SM0311	Fermentas, Mannheim
Page Ruler Plus Prestained	26619	Thermo Fischer Scientific, Kandel

5.1.4 Antibodies

Antibodies used various assays were diluted in suitable buffers and incubated for specified time as suggested by manufacturers.

Antibody	Cat. No.	Source
EEHV-1 anti-gB rabbit antibody (Ab7123 and Ab7125)		(247)
EHV-1 virus neutralizing serum		(67, 77)

EHV-4 anti-gD monoclonal antibody		Dr Jules Minke, Merial, Lyon (72)
Goat anti-mouse IgG Alexa Fluor 488 conjugated	A11001	Invitrogen, Karlsruhe
Goat anti-mouse IgG Alexa Fluor 568 conjugated	A11009	Invitrogen, Karlsruhe
Goat anti-rabbit IgG Alexa Fluor 488 conjugated	A11008	Invitrogen, Karlsruhe
Goat anti-rabbit IgG peroxidase conjugate	7074S	Cell signalling, Massachusetts
Mouse CD3 monoclonal antibody		Dr Bettina Wagner, Cornell University, New york (261)
Mouse CD14 monoclonal antibody		Dr Bettina Wagner, Cornell University, New York (261)
Mouse IgM monoclonal antibody		Dr Bettina Wagner, Cornell University, New York (261)

5.1.5 Commercial molecular biology kits

Name	Manufacturer
ECL Prime, Amersham	GE Healthcare, Chicaco
GF-1 AmbiClean PCR/Gel Purification kit	Vivantis, Malaysia
Hi Yield Gel/PCR DNA kit	SLG, Gauting
InnuPREP blood DNA mini kit	Analytik Jena, Überlingen
InnuPREP virus DNA/RNA kit	Analytik Jena, Überlingen
Milliplex MAP equine cytokine/chemokine magnetic bead based multiplex kit	EMD Millipore, Billerica
Monarch DNA Gel extraction kit	New England biolabs, Ipswich
NEBNext Library Quant Kit	New England biolabs, Ipswich
NEBNext Ultra II Library Prep kit	New England biolabs, Ipswich
RTP DNA-RNA virus mini kit	Stratec Molecular, Berlin
SeniFAST Probe Lo-ROX	Meridian Life Science, Memphis
Qiagen Plasmid mini kit	Qiagen, Hilden

5.1.6 Antibiotics

Antibiotics were either freshly made or prepared solutions were stored at -20 ºC till use.

Name (Cat. no.)	Working concentration	Manufacturer
Amphotericin B	2.5 µg/ml diluted in MEM	Biochrom, Berlin
Ampicillin (K0292)	100 µg/m diluted in ddH2O	Roth, Karlsruhe
Chloramphenicol (3886.3)	30 µg/ml diluted in 96% in ethanol	Roth, Karlsruhe
Gentamicin	40 µg/ml diluted in MEM	Alfa Aesar, Karlsruhe
Kanamycin sulphate (T832.3)	50 µg/ml diluted in ddH2O	Roth, Karlsruhe
Penicillin A1837)	100 U/ml diluted in MEM	Applichem, Darmstadt
Streptomycin (A1852)	100 U/ml diluted in MEM	Applichem, Darmstadt

5.1.7 Bacteria, cells, viruses and plasmids

5.1.7.1 Bacteria

Name	Feature	Source
DH10B	F^- endA1 recA1 galE15 galK16 nupG rpsL ΔlacX74 Φ80lacZΔM15 araD139 Δ(ara,leu)7697 mcrA Δ(mrr-hsdRMS-mcrBC) λ	Invitrogen, Norcross
GS1783	DH10B λcI857 ∆(cro-bioA)<>araC-$P_{BAD,}$ I-SceI	Greg Smith, Northwestern University, Chicaco

5.1.7.2 Cells

Cell name	Source
African green monkey kidney (Vero)	ATCC CCL-81
Bovine dermal (BD)	
Crandell–Rees feline kidney (CrFK)	ATCC CCL-94
Elephant fibroblast (ENL-2)	CCLV-RIE 856, Federal Research Institute for animal health, Greifswald
Elephant PBMC	Primary cells
Equine dermal (ED)	CCLV-RIE 1222, Federal Research Institute for animal health, Greifswald

Equine endothelial cells (EC)	(77)
Equine PBMC	Primary cells
Human embryonic kidney (293T)	ATCC CRL-11268
Human embryonic kidney nuclear domain 10 deletion mutant (293T ND10)	(262)
Human rectal tumour cells (HrT-18G)	(263)
Madin-Darby canine kidney II (MDCK II)	ATCC CCL-34
Rabbit kidney 13 (RK-13)	ATCC CCL-37

5.1.7.3 Viruses

Virus name	Feature	Reference
Ab4-wt EHV-1	Ab4 strain of EHV-1	(264)
RacL11 EHV-1	RacL11 strain of EHV-1	(158)
TH20P EHV-4	TH20p strain of EHV-4	(265)
T252 EHV-4	T252 strain of EHV-4	(266)

5.1.7.4 Plasmids

Name	Features	Source
pcDNA3.1	Mammalian expression vector (Cat. No.: V790-20)	Invitrogen, Norcross
pEPkan-S	pEP vector containing kanamycin resistance	(267)

5.1.8 Buffers, gel and bacterial culture media

5.1.8.1 Buffers

Buffer	Composition
Phosphate buffered saline (PBS)	1.8 mM KH_2PO_4 10 mM Na_2HPO_4 137 mM NaCl 2.7 mM KCl, pH 7.3
Tris-acetate-EDTA buffer (TAE)	40 mM Tris 1 mM $Na_2EDTA{\cdot}2H_2O$ 20 mM Acetic acid 99%, pH 8.0
SDS-PAGE running buffer (10x) (Reducing)	250 mM Tris, pH 8.5 1.9 M Glycine

	1% SDS
SDS-PAGE sample preparation RIPA I (Reducing)	50 mM Tris-HCl, pH 7.5 150 mM NaCl 1% Triton X-100 1% Na-desoxycholate 0.1% SDS
SDS-PAGE sample preparation RIPA II	RIPA I + 1mM EDTA
SDS sample buffer (2x) (Non-reducing)	62.5 mM Tris-HCl pH 6.8 25% Glycerol 1% Bromophenol Blue
SDS running buffer (Non-reducing)	25 mM Tris 192 mM Glycine pH 8.3
Buffer P1 (Resuspension buffer)	50 mM Tris HCL pH 8.0 10 mM EDTA 100 µg/ml RNAse
Buffer P2 (Lysis buffer)	200 mM NaOH 1% w/v SDS
Buffer P3 (Neutralization buffer)	3 M Potassium Acetate pH 5.5
Buffer TE	10 mM Tris HCl 1 mM Na_2EDTA. pH 7.4
Cell nuclei buffer	10 mM Tris-HCl 2 mM $MgCl_2$ 10% sucrose, pH 7.5
Cell permeabilization buffer	1.28 M Sucrose 20 mM $MgCl_2$ 40 mM Tris-HCl 4% Triton X-100, pH 7.5
Nuclease buffer (2x)	40 mM PIPES, pH 7.0 7% Sucrose 20 mM NaCl 2 mM $CaCl_2$, 10 mM 2-mercaptoethanol

	0.2 mM PMSF
Digestion buffer	100 mM NaCl 10 mM Tris-HCl, pH 8.0 25 mM EDTA, pH 8.0 0.5% SDS 0.1 mg/ml Proteinase K
SDS sample loading buffer (6x) (Reducing)	0.35 M Tris-HCl pH 6.8 30% glycerol 10% SDS 10% β-mercaptoethanol 0.6% bromophenol blue
Blocking buffer	3% w/v bovine serum albumin with PBS
Western blot transfer buffer	25 mM Tris 192 mM Glycine 20% v/v Methanol 1.25 M Tris-HCl, pH 6.8
Carbonate buffer	16 ml of 0.2 M Na_2CO_3 34 ml of 0.2 M $NaHCO_3$ Make volume to 200 ml with ddH_2O
Citrate buffer	40 mM citric acid 10 mM HCl 135 mM NaCl, pH 3.0
Gallati buffer	0.2 M citric acid
Stop solution for ELISA	0.16 M H_2SO_4
Karnovsky' fixative	7.5% glutaraldehyde 3% paraformaldehyde, pH 7.4

5.1.8.2 Gels

Gel type	**Composition**
1% Agarose Gel	1% w/v Agarose TAE buffer 0.5 µg/ml Ethidium bromide
Stacking gel (Reducing)	1 M Tris-HCl, pH 6.8 – 625 µl 10% SDS – 25 µl 30% Acrylamide – 325 µl 10% APS – 12.5 µl

	TEMED – 2.5 µl
	H_2O – 1.53 ml
Resolving gel (Reducing)	1.5 M Tris-HCl pH 8.8 – 2.5 ml
	10% SDS – 100 µl
	30% Acrylamide – 4.0 ml
	10% APS – 50 µl
	TEMED – 5 µl
	H_2O – 3.35 ml
Stacking gel (Non-reducing)	0.375 M Tris-HCl pH 8.8 – 4.275 ml
	30% Acrylamide – 670 µl
	10% APS – 50 µl
	TEMED – 5 µl
Resolving gel (Non-reducing)	0.375 M Tris-HCl pH 8.8 – 5.89 ml
	30% Acrylamide – 4.0 ml
	10% APS – 100 µl
	TEMED – 10 µl

5.1.8.3 Bacterial culture media

Culture medium	Composition
Luria-Bertani (LB) medium	10 g BactoTM Tryptone
	5 g BactoTM Yeast Extract
	10 g NaCl
	15 g BactoTM Agar
Super optimal broth (SOB) medium	20 g BactoTM Tryptone
	5 g BactoTM Yeast Extract
	0.584 g NaCl
	0.186 g KCl
	pH 7.0
Super optimal broth with catabolite repression (SOC) medium	SOB medium 20 mM Glucose

5.1.9 Media, cell culture supplements and composition

5.1.9.1 Media and cell culture supplements

Name	Cat. No.	Manufacturer
Dulbecco's modified Eagle's medium (DMEM)	F 0435	Biochrom AG, Berlin
Foetal bovine serum (FBS)	S 0415	Biochrom AG, Berlin
Ham's F12	F 0815	Biochrom AG, Berlin
Iscove's modified Dulbecco's medium (IMDM)	F 0465	Biochrom AG, Berlin
L-alanyl-L-Glutamine	K 0302	Biochrom AG, Berlin
Minimum essential Medium Eagle (MEM)	F 0315	Biochrom AG, Berlin
Non-essential amino acids	K 0293	Biochrom AG, Berlin
RPMI-1640 Medium	P04-17525	Pan Biotech, Aidenbach
Sodium Pyruvate	L 0473	Biochrom AG, Berlin
Trypsin	L 2103	Biochrom AG, Berlin

5.1.9.2 Cell culture medium composition

Cells	Cell culture medium composition
CrFK, MDCK II, Vero, BD, RK-13, 293T ND10 and EC	Dulbecco's modified Eagle's medium (DMEM) 10% FBS 1% Penicillin/streptomycin
ED	Iscove's modified Dulbecco's medium (IMDM) 20% FBS 1% Sodium pyruvate 1% Non-essential amino acids 1% Penicillin/streptomycin
ENL-2	1:1 mixture of IMDM (20% FBS, 1% Sodium pyruvate, 1% Non-essential amino acids and 1% Penicillin + streptomycin) and Ham's F12 (20% FBS and 1% Penicillin/streptomycin)
HrT-18G	Dulbecco's modified Eagle's medium (DMEM) 10% FBS 1% Sodium pyruvate 1% Non-essential amino acids 1% L-alanyl-L-Glutamine 1% Penicillin/streptomycin

Equine and elephant PBMC	RPMI-1640
	10% FBS
	1% L-alanyl-L-Glutamine
	1% Penicillin/streptomycin
Virus transport medium	PBS
	2% FBS
	1% Penicillin/streptomycin
	5 µg/ml Amphotercin B
Overlay medium	A: 3g of Methyl cellulose + 300 ml H_2O
	B: 4.75g of DMEM + 25 ml of FBS + 5 ml of 7.5% $NaHCO_3$
	Mix A + B +1% Penicillin/streptomycin (P-S)

5.1.10 Primers, probes and oligonucleotides

Primers, probes and oligonucleotides used in EHV-1, EHV-4 and EEHV-1A studies

Primer	Primer name	Nucleotide sequence
P1	ORF17 STOP Fwd	caaaggttggcttgctacatcaaggttatcaatcatgatgtaacagccagatagag agcccggtagggataacagggtaatcgat
P2	ORF17 STOP Rev	gcaccagacacgagtcttcaccgggctctctatctggctgttaca tcatgattgataaccttgccagtgttacaaccaattaacc
P3	ORF17 pre For	ctttatgtgaattcaccgac
P4	ORF17 post Rev	gttttatgactaatacctgg
P5	ORF17Revert Fwd	caaaggttggcttgctacatcaaggttatcaatcatgatgtacca gccagatagagagcccggtagggataacagggtaatcgat
P6	ORF17Revert Rev	gcaccagacacgagtcttcaccgggctctctatctggctggtac atcatgattgataaccttgccagtgttacaaccaattaacc
P7	ORF1 deletion Fwd	tccacctgcacctttccatctcctctccaactcgccgccaacgac tgtagtaccgcaaaaggatgacgacgataagtaggg
P8	ORF1 deletion Rev	aaaaataaatgcgattaacctttgcggtactacagtcgttggcgg cgagttggagaggagcaaccaattaaccaattctgattag
P9	ORF1 pre Fwd	ggctcctccctttggctctgg
P10	ORF1 post Rev	tctggtgctgatcggaatagtgta
P11	ORF1 BamH Fwd	attggatccatgagacccgagggagtttc
P12	ORF1 EcoRI Rev	cacgaattcttatttctccttcttgccgt
P13	ORF1 kana Fwd	atttagccttccgctcctgtctgcttacactttacacttttctgctcgtc

		atgagacccgagggagtttc
P14	ORF1 kana Rev	aggggtgtttgtgaaaataaacataatacaactgtgttgaacca cttgttttatttctccttcttgccgt
P15	ORF1 Revert Fwd	ttccactttctccacctgcacctttttccatctcctctccaactcgccg ccatgagacccgagggagtttc
P16	ORF1 Revert Rev	gagtgcatgtaaaaataaatgcgattaacctttgcggtactaca gtcgttttatttctccttcttgccgt
P17	ORF2 deletion For	aaaacgactgtagtaccgcaaaggttaatcgcatttatttgcttaa acactttggagcgaaggatgacgacgataagtaggg
P18	ORF2 deletion Rev	cgcccccataccccgcccccctcgctccaaagtgtttaagcaaat aaatgcgattaaccttcaaccaattaaccaattctgattag
P19	ORF2 pre Fwd	taacaaacggcaagaaggag
P20	ORF2 post Rev	taacgctgtagattgagttt
P21	ORF2 EcoRI Fwd	aattagaattcttacatgcactcctttccaa
P22	ORF2 Xba Rev	atatatctagaatggatccagcgtggaggag
P23	ORF2 Kan Fwd	cgcggggcggccgcactaccatcggaagtttaccaggatgac gacgataagtaggg
P24	ORF2 Kan Rev	ggtagtgcggccgccccgcggtgatttctagtaacaaccaatta accaattctgattag
P25	ORF2 Revert Fwd	aaggagaaataaaacgactgtagtaccgcaaaggttaatcgc atttatttttacatgcactcctttccaa
P26	ORF2 Revert Rev	ttcaggcatacgcccccataccccgcccccctcgctccaaagtgt ttaagcatggatccagcgtggaggag
P27	EHV-4 gB Fwd	cgcagaggatggagacttttaca
P28	EHV-4 gB Rev	catgaccgtgggggttcaa
P29	EHV-4 gB Probe	fam-ctgcccgccgcctactggatc-tamra
P30	EHV-4 gB seq Fwd	catgtctaaagactcgacat
P31	EHV-4 gB seq Rev	cgcaaaccataataccaatc
P32	EHV-4 ORF30 F1	aatctcgagtcagctttgatggggaactg
P33	EHV-4 ORF30 R1	agaactgcccagtgtgaagg
P34	EHV-4 ORF30 F2	acccccttcatgagcat
P35	EHV-4 ORF30 R2	ggagggctgtttaaggtctg
P36	EHV-4 ORF30 F3	atacaatactctcctattac
P37	EHV-4 ORF30 R3	attgcggccgcatggcggcgcacgaacagga
P38	EHV-4 ORF30 F4	agcaaaccgcgacgggtcgt
P39	EEHV-1Ter Fwd	actgcaaaygcattcttaaaagat

P40	EEHV-1Ter Rev	agaatgggattrgctaagaagct
P41	EEHV-1Ter Probe	tcaacgaggagatattaggcaccaccaaca
P42	EEHV-1 Ter Oligo	cattgacactggaatctgttagaatgggattggctaagaagctcgtgttggtggtgc ctaatatctcctcgttgaacgaatcttttaagaatgcgtttgcagttttttgatattcaaa ttaa
P43	Ele TNFα Fwd	cccatctacctgggaggagtct
P44	Ele TNFα Rev	tcgagatagtcaggcagattgatc
P45	Ele TNFα Probe	ccagctagagaagggt
P46	Ele TNFα Oligo	tgaggccaagccctggtatgagcccatctacctgggaggagtcttccagctagag aagggtgatcgactcagcgctgagatcaatctgcctgactatctcgactttgccga gtctgggcaggtca

Table 5: List of primers, probes and oligonucleotides used for PCR and qPCR analysis.

5.1.11 Quantitative (q) PCR mastermix composition and cyclic condition

	Composition
qPCR mastermix (20-µl per reaction)	10 µl of SeniFAST™ Probe Lo-ROX (2x) 0.9 µl of each forward and reverse primer (10 pmoli/µl) 0.2 µl of probe (10 pmoli/µl) 3 µl of nuclease-free water 5 µl of extracted DNA sample
Cyclic condition	2 min at 95 °C for hold 40 cycles of amplification: 3 seconds (s) at 95 °C and 30 s at 60 °C with data collection 1 min hold at 60 °C for data collection

5.2 Methods

5.2.1 Cells and viruses

5.2.1.1 Cells

Crandell–Rees feline kidney (CrFK), Madin-Darby canine kidney II (MDCK II), African green monkey kidney (Vero), bovine dermal (BD), rabbit kidney 13 (RK-13), human embryonic kidney nuclear domain 10 deletion mutant (262) (293T ND10), human rectal tumour cells (263) (HrT-18G) and equine EC (77) were propagated in Dulbecco's modified Eagle's medium (DMEM). Equine dermal (ED) (CCLV-RIE 1222, Federal Research Institute for Animal Health, Germany) cells were grown in Iscove's modified Dulbecco's medium (IMDM).

Elephant fibroblast (ENL-2) cells were grown in a 1:1 mixture of IMDM and Ham's F12 medium. PBMC were isolated from heparinised whole blood samples collected horse/elephant by Biocoll® based density gradient centrifugation as described by the manufacturer. Briefly, whole blood samples were incubated for 30 min at room temperature (RT) for plasma rich PBMC separation from whole blood. Separated PBMC rich plasma was layered over Biocoll® solution and centrifuged at 300 *xg* for 30 min. PBMC at the interphase were collected and washed twice in PBS. Isolated PBMC were cryopreserved in liquid nitrogen till use.

5.2.1.2 Viruses

The parental and mutant viruses were derived from EHV-1 strain Ab4 (179). EHV-1 DNA was cloned as an infectious bacterial artificial chromosome (BAC; pAb4). The BAC of EHV-1 Ab4 contains mini-F cassette in which the *egfp* gene is driven by human cytomegalovirus immediate early promoter (264). Viruses were reconstituted by transfection of BAC DNA into 293T cells with polyethylenimine (117). Reconstituted viruses were propagated and titrated in ED cells. Abortogenic RacL11-BAC strain of EHV-1 (158, 268), EHV-4-BAC (265) and reference EHV-4 strain T252 (266) were propagated in ED cells.

5.2.2 Engineering of EHV-1 BAC mutants and revertants

Two-step-Red-mediated recombination (*en passant*) was used for genetic manipulation of EHV-1 genome to create mutant viruses (267).The pAb4 BAC was maintained in *Escherichia coli* GS1783 cells and grown in Luria-Bertani broth supplemented with 30µg/ml chloramphenicol (146, 264). List of the primers used for generation of the mutant viruses is given in Table 5. Briefly, to create target gene deletions of ORF1, ORF2 and ORF17, a fragment flanked by homologous arms for the desired target region was PCR amplified by using a kanamycin resistance (kan^r) gene present in plasmid pEP-Kan-S2 (241). Gel extracted PCR products were digested with *Dpn1* enzyme to get rid of residual plasmid. Electro-competent GS1783 cells were electroporated with the purified PCR product and incubated at 32 ºC for 48 hrs. Kanamycin resistant colonies were screened by restriction fragment length polymorphism (RFLP) analysis and compared with the restriction digestion pattern of the parental viral BAC DNA (269, 270). Selected intermediate clones were subjected to a second step of Red-mediated recombination to induce removal of the kan^r gene from the BAC after adding 1% L(+)-arabinose. Final clones with gene deletions were confirmed by RFLP analysis and specific gene sequencing of the mutation site (LGC® sequencing service, Berlin, Germany). For virus reconstitution, 2 µg BAC DNA was transfected into 293T cells and the reconstituted viruses were subsequently propagated in

ED cells. For multiple gene deletions from the same virus, each gene was deleted successively in the BAC before final virus reconstitution. The single gene deleted mutant lacking ORF17 (147) or ORF1 or ORF2 was used for deletion of all three viral genes in combinations using primers given in Table 5 (Figure 9). Revertant BAC for the deletion mutants were constructed as described previously (72). Briefly, plasmids encoding the target gene with kan^r gene were first constructed in the beginning. Target genes were PCR amplified using primers P11-P12 and P21-P22 for ORF1 and ORF2, respectively. The PCR products were digested with appropriate restriction enzyme (RE) and inserted into pcDNA3 vector resulting in pcDNA3_ORF1 and pcDNA3_ORF2 recombinant plasmid. For construction of pcDNA3_ORF1_kan^r and pcDNA3_ORF2_kan^r, the kan^r gene was PCR amplified from pEP-kan-S2 plasmid with P13-P14 and P23-P24 primer, respectively. The resulting PCR products were digested with appropriate restriction enzymes and inserted into pcDNA3_ORF1 and pcDNA3_ORF2. Correct insertion of sequence was confirmed by nucleotide sequencing. ORF17 deletion mutant was constructed by insertion of stop codon by replacing the third codon of the ORF (TAC) with stop codon (TAA) (147). ORF17 revertant BAC was constructed by PCR amplification of kan^r genes with ORF17 homologous arm sequences using revertant primers (P5-P6). The resulting PCR product was used for a two-step-Red-mediated recombination as described above.

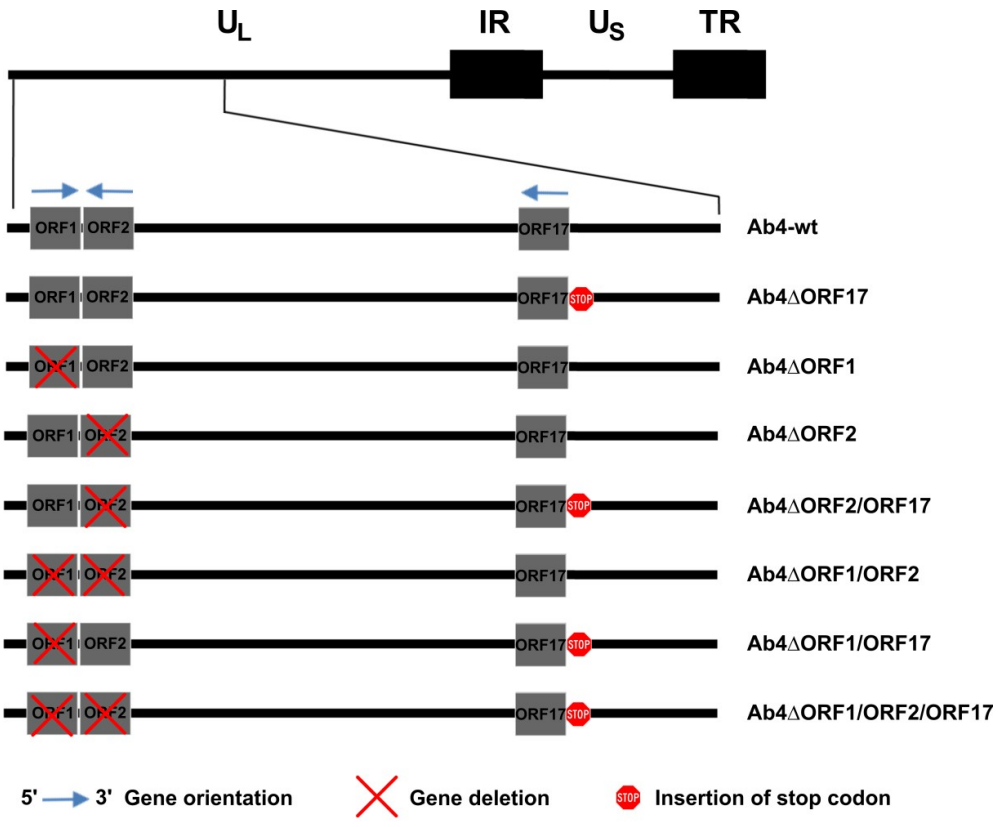

Figure 9: Schematic diagram for construction of deletion mutants of Ab4 strain of EHV-1. Mutants were constructed by either deletion of complete gene (for ORF1 and ORF2) or introduction of stop codon at 5' terminal of the gene (ORF17) in Ab4 strain of EHV-1 genome.

5.2.3 Growth kinetics and plaque size assay for Ab4-wt and mutant viruses

Influence of ORF1, ORF2 and ORF17 genes deletion in virus replication was evaluated by one-step growth kinetics. EC or ED cells were infected with wild type (Ab4-wt) virus and mutant viruses (Ab4ΔORF17, Ab4ΔORF1, Ab4ΔORF2, Ab4ΔORF17/ORF2, Ab4ΔORF1/ORF2, Ab4ΔORF1/ORF17 and Ab4ΔORF1/ORF2/ORF17) at a multiplicity of infection (MOI) of 0.1. Virus infected cells were incubated at 4 ºC for 1 hr to allow virus attachment and transferred to 37 ºC for 1 hr to permit virus entry. After incubation, cells were treated with citrate buffer for 30 seconds to inactivate cell free viruses, and washed twice with IMDM medium and PBS. Fresh medium was added and the cells were incubated at 37 ºC with 5% CO_2 supply. Supernatant and cell pellet were collected separately at 0, 6, 12, 24, 48 and 72 hrs post infection (hpi) to determine cell free and cell associated viral titer. Collected samples were titrated on confluent ED cells, over-laid with 1.5% (W/V) methyl-cellulose medium and fixed with 4% paraformaldehyde at 72 hpi. Fixed cells were stained with 0.1% (W/V) crystal violet solution, plaques were counted, and results were expressed as plaque forming units (PFU) per millilitre (ml). Data were presented from three independent and blinded experiments. To determine cell-to-cell spread, plaques induced by Ab4-wt and mutants were measured at 48 hpi on ED cells. Viral plaques were imaged using inverted fluorescence microscope. In total, 150 plaque images were processed for each virus and actual plaque diameters were measured using ImageJ® software.

5.2.4 Co-cultivation assay to evaluate cell-to-cell virus transfer under static condition

To evaluate EHV-1 transfer from infected PBMC to EC, co-cultivation assay was performed as described previously (26, 77). EC were grown to confluency on collagen IV-coated 24-well plate. PBMC were infected with either Ab4-wt or mutant viruses at MOI of 0.1 for 24 hrs. Virus infected PBMC were sorted for green fluorescent protein (GFP) expression by fluorescent-activated cell sorting (FACS) using FACSAria. Sorted PBMC (2×10^4) were treated with citrate buffer as described above and overlaid on EC monolayer "contact" in the presence of EHV-1 neutralizing antibodies (with EHV-1 antibody titer of 1:2,048 at the dilution of 1:100) for 2 hrs. Alternatively, infected PBMC were placed into a 24-well transwell tissue culture-Inserts (0.4µm pore size) in the presence of EHV-1 neutralizing antibodies without direct contact with EC "no contact". The "no contact" controls were used to assess

the efficiency of citrate buffer treatment (cell free virus inactivation) and EHV-1 neutralizing antibodies and to ensure that there was no free virus transmission. After incubation, PBMC were washed with PBS and EC were overlaid with 1.5% methyl-cellulose medium. The plates were incubated for 24 hrs and GFP-positive plaques on EC monolayer were counted under inverted fluorescent microscope. Co-cultivation assay was performed with Ab4-wt and mutant viruses. Number of virus plaques produced by Ab4-wt infected PBMC was compared with mutant viruses. Results were interpreted from three independent blinded replicates.

5.2.5 Flow chamber assay to evaluate cell-to-cell virus transfer under flow condition

Flow chamber assay was performed to evaluate virus transfer from infected PBMC to the EC under flow "dynamic" conditions as described earlier (77). EC were grown to confluency in collagen IV-coated flow chamber µ-slides. PBMC were infected with either Ab4-wt or mutant viruses at MOI of 0.1 for 24 hrs. Virus infected PBMC were FACS sorted as described above. Sorted PBMC (2×10^4) were treated with citrate buffer and re-suspended in DMEM containing EHV-1 neutralizing antibodies. EC containing flow chamber slides were connected to a perfusion system (Multi-Syringe Pump) and PBMC were allowed to flow over the EC at the mammalian physiological flow rate (0.5 mm/s) at 37 ºC (271). PBMC containing medium, flowing through chamber slide was collected as waste the on other side. Following PBMC flow, EC were washed and incubated for 24 hrs for the development of viral plaques. GFP-positive plaques on the EC monolayer were counted using inverted fluorescence microscope. The "no contact" setup was always included for each experiment. Number of plaques counted among Ab4-wt and mutants were compared to evaluate the efficiency of virus transfer between PBMC and EC under flow condition. The experiment was performed after blinding for three independent times.

5.2.6 EHV-1 infection of equine PBMC subpopulations

To determine which PBMC subpopulation (i.e. T lymphocyte, B lymphocyte and monocytes) is responsible for virus spread from infected PBMC to EC, each subpopulation was sorted and virus spread was assessed by the flow chamber assay. Briefly, PBMC were stained with (1:200 diluted) primary mouse monoclonal antibodies against equine CD3 (T lymphocyte), IgM (B lymphocyte) and CD14 (monocyte). Stained PBMC were labelled with secondary Alexa Fluor 488-conjugated goat anti-mouse IgG antibody and sorted. Sorted populations (T, B lymphocytes and monocytes; 2×10^4) were infected with Ab4-wt and mutant viruses at MOI of 0.1 for 24 hrs at 37 ºC. After incubation, cells are treated with citrate buffer, resuspended in EHV-1 neutralizing antibodies and flow chamber experiment was performed as described above. Virus transfer between each subpopulation of PBMC and EC was evaluated by

counting the number of viral plaques at 24 hpi and compared among Ab4-wt and mutant viruses. The experiment was performed after blinding for three independent times.

5.2.7 Equine epithelial cell-PBMC contact assay

Equine epithelial cell-PBMC contact assay was performed to assess virus transfer from epithelial cells to PBMC and subsequently from PBMC to the EC as described previously with modifications (222). Briefly, ED cells were seeded into a 3-µm pore size 24-well transwell insert and incubated at 37 ºC for 24 hrs. The cells were inoculated with Ab4-wt and mutant viruses at MOI of 0.1 and incubated for 1 hr. Infected cells were washed twice, treated with citrate buffer and supplemented with growth medium containing EHV-1 neutralizing antibodies. Transwell insert was inverted, and $1x10^5$ PBMC resuspended in virus neutralizing antibodies-containing medium was added and incubated at 37 ºC for 24 hrs. Epithelial cells-to-PBMC virus transfer in the presence of neutralizing antibody was assessed by counting the number of GFP-positive (EHV-1-infected) PBMC after 24 hrs. After counting GFP-positive cells, total ($1x10^5$) infected PBMC were applied over confluent EC in a flow chamber setup. The experiment was repeated three independent and blinded times.

5.2.8 Whole cell global proteomics assay for EHV-infected PBMC

5.2.8.1 Sample preparation for proteomics

Label-free quantitative (LFQ) proteomic analysis was performed to determine differentially expressed proteins in PBMC infected with EHV-1. PBMC were infected with Ab4-wt and mutant viruses at MOI of 1. At 24 hpi, 10^5 PBMC were FACS sorted. For mock-infected PBMC control, T, B lymphocytes and monocytes were mixed at percentages comparable to the population of infected PBMC (T, B lymphocytes and monocytes were mixed in the ratio of 21:13:66, respectively). After sorting, PBMC were washed twice with PBS and stored at -80 ºC until further processed. The assay was performed four independent times.

5.2.8.2 Lable-free proteomic analysis

Whole cell lysate were digested with trypsin and peptides were prepared using filter-aided sample preparation (FASP) method (272). Prepared peptides were desalted and concentrated using C18 StageTips (273).

5.2.8.3 Mass spectrometry and sequence database search

Mass spectrometry (MS) analysis was performed on a ultra-HPLC Agilent 1200 system, equipped with an in-house packed C18 column for reversed phase separation (Poroshell 120 EC-C18, 2.7 µm) and coupled online to an Orbitrap Fusion mass spectrometer. The

instrument was run in top speed mode with 3-s cycles. The RAW MS files were processed with the MaxQuant computational platform (274) using equine and equine herpesvirus type 1 sequences from the Uniprot-database with the a false discovery rate (FDR) below 1% for both peptides and proteins. Standard settings with additional options match between runs, label-free quantification (LFQ) and unique peptides for quantification were selected. Protein-group.txt table created and filtered for potential contaminants, reverse hits and only identified by site (275).

5.2.8.4 Data analysis and interpretation

PBMC protein expression data .txt file obtained using the LFQ approach from MaxQuant and was used to create a profile of expression levels with Perseus 1.6.1.3 (276). The LFQ values were log_2-transformed and missing values were imputed. Student's two-sample *t*-tests were used to assess statistical significance of differentially expressed protein abundances using a 1% permutation-based FDR (*q*-values) correction for multiple hypotheses testing with Perseus software (277). All those proteins that showed a fold-change of at least 1.5 and satisfied $p < 0.05$ were considered differentially expressed. Differentially expressed proteins were mapped to the gene ontology (GO) database, and the number of proteins at each GO term was computed. The results from label-free proteomics were used as the target list. GO and Kyoto Encyclopedia of Genes and Genomes (KEGG) annotation for each protein in the search database were retrieved from GO (http://www.geneontology.org/) and KEGG Pathway database (http://www.genome.jp/Pathway), respectively. KEGG pathway enrichment analysis of the correlation was carried out using *p* values adjusted with Benjamini correction for false discovery rate. In the GO enrichment analysis, proteins were classified by GO annotation into three categories: biological process, cellular compartment, and molecular function. For each category, a two-tailed Fisher's exact test was employed to compare the enrichment of the differentially expressed protein against all identified proteins. A corrected *p*-value < 0.05 was considered significant (278, 279).

5.2.9 Multiplex equine cytokine assay

Cytokines and chemokines released by healthy and EHV-1-infected PBMC were quantified using Milliplex® MAP equine cytokine/chemokine magnetic bead based Multiplex kit. The kits, enable simultaneous analysis of 23 cytokine and chemokine biomarkers (280). PBMC ($1x10^6$) were infected with Ab4-wt and mutant viruses as well as EHV-4 at MOI of 1. Supernatant from healthy, Ab4-wt/mutants (Ab4ΔORF17, Ab4ΔORF1, Ab4ΔORF2, Ab4ΔORF17/ORF2, Ab4ΔORF1/ORF2, Ab4ΔORF1/ORF17 and Ab4ΔORF1/ORF2/ORF17) and EHV-4 infected PBMC was collected at 3, 6 and 24 hpi. In another experiment, $1x10^6$

PBMC were infected with Ab4-wt, RacL11 or EHV-4 at MOI of 1. At 24 hpi, infected PBMC were applied over EC in a 24-well plate and incubated for 6 hrs. Supernatants were collected at 3 and 6hrs, and stored at -80 ºC until used. Cytokines/chemokines quantification in the supernatant was performed as per manufacturer's instructions using Luminex MAGPIX® system with xPONENT® software. All samples were run in duplicates.

5.2.10 EHV-4 outbreak in equine breeding stud

5.2.10.1 Premise and horses

In July 2017, an outbreak of EHV-4 occurred in an equine breeding farm in northern Germany. The affected stud farm housed Standardbred horses with three stallions, 28 pregnant mares, 13 non-pregnant mares, 18 yearlings (12 males and 6 females), 13 fillies and 12 colts at the time of outbreak. The breeding farm also houses 36 race horses in a nearby separate paddock which remained unaffected by EHV-4 during the period of disease outbreak in main farm. Mares and corresponding foals were divided in to four groups with 7 mares and foals in each group ranged by date of foaling. If a broodmare lost a foal, she will be sent to non-pregnant group mares, when tested negative for EHV-1 and EHV-4. Mares and corresponding foals remain in the same box till weaning. Horses were routinely vaccinated against EHV-1 (Prevaccinol®, MLV-vaccine), equine influenza (ProteqFlu®, canarypox vectored vaccine, H3N8) and tetanus as per manufacturer's instructions. Mares were vaccinated against EHV-1 three times during pregnancy at the 3rd, 5th and 8th months. Yearlings were vaccinated twice a year after weaning.

In 2012, the same breeding farm experienced severe EHV-1 outbreak with respiratory tract infection, neurological illness and abortion (250). In 2015, all yearlings were sick with fever and nasal discharge, started in March 21st and ended in April 14th. However, all animals were tested negative for EHV-1 and -4. Yearlings (born in 2016) started outdoor season in April 2017 (males and females). When nights were frost free, older foals and mares stayed in the grass day and night. They only brought inside for health checkups one or two times a week or when needed for other reasons. In between March and May 2017, two mares were aborted and one foal died at birth on day 319th of pregnancy; however, they tested negative for EHV-1 and -4. In June 2017, three foreign mares from two different owners (without vaccination) entered the stud farm for breeding without quarantine. Those three breeding mares were transported in transport box which has been regularly used for mares, foals and racehorses transport. Weaning of the foals started on the 5th of October 2017 and ended on the 6th of November 2017. Foals aged between 150 and 200 days old were weaned. During the outbreak, foals were along with the corresponding mares. It is noteworthy to mention that

in June and July, 2017 there was intermittent heavy rain alternated with summer at farm location.

Foals infected in the current EHV-4 outbreak have never been vaccinated against EHV-1 and EHV-4. The outbreak of EHV-4 occurred following the onset of respiratory illness in foals and mares. Infected foals showed pyrexia, cough and nasal discharge. However, few foals and most of the mares did not showed apparent clinical signs.

5.2.10.2 Sample collection during EHV-4 outbreak

On July 7th, 2017, two foals began to show signs of respiratory illness and tested positive for EHV-4 in nasal swabs. On subsequent days, several foals showed similar clinical signs. Nasal swabs were collected from mares, yearlings and foals (n = 76) showing signs of respiratory illness, including cough, nasal discharge and pyrexia at different time points as given (Table 14). In some cases, nasal swabs were collected from apparently healthy foals in contact with infected horses as many foals need to be tested for EHV-4 status before they travel to Sweden to obtain passports. Collected nasal swabs in virus transport medium were transported to the diagnostic laboratory, Institute of Virology, Freie Universität Berlin, at 4 ºC for subsequent analysis. Paired serum samples were collected from selected infected animals (n = 48; 24 mares and 24 corresponding foals) at the 2nd and 9th weeks of disease outbreak. The period of EHV-4 outbreak was between June 7th and November 17th, 2017, and lasted for 133 days.

5.2.10.3 DNA isolation and qPCR for EHV-4

Total viral DNA was extracted from (200 µl) nasal swabs using the RTP DNA-RNA virus mini kit as per manufacturer's instructions. qPCR was performed with StepOnePlus^{TM} Real-time PCR system. Primers (P27 and P28) and probes (P29) (Table 5) specific to gB gene of EHV-4 was used as described previously (180). Positive (DNA extracted from EHV-4-infected ED cell culture supernatant) and negative (nuclease free water) extractions were performed and included in every run. Nasal swab samples were considered negative for EHV-4, if the C_T values were >39.

5.2.10.4 EHV-4 isolation from clinical samples

Virus isolation was attempted for the qPCR-positive nasal swab samples using ED cells. Nasal swabs in virus transport medium were vortexed and centrifuged at 6000 x*g* for 5 min. The supernatant was collected, 2% P-S and 5 µg/ml of Amphotercin B were added, and incubated for 30 min at 4 °C. Meanwhile, ED cells were trypsinized and suspended at a

concentration of $3x10^5$ cells per ml. In 24-well plate, each 100 µl of the prepared supernatant was mixed with 400 µl of ED cell suspension and incubated at 37 ºC. Cells were examined daily till day 5 for the presence of cytopathic effect (CPE). If no CPE observed in the first passage, inoculated cells were subjected to 5 more blind passages.

5.2.10.5 Indirect immunofluorescence assay (Indirect-IF) for EHV-4

Indirect-IF was performed to detect EHV-4 specific viral antigen in cell culture. Briefly, ED cells were grown in 24-well plate and inoculated with 50 PFU of the isolated EHV-4. After 48 hpi, cells were fixed with 4% paraformaldehyde (PFA) and incubated for 30 min at room temperature (RT). Fixed cells were permeabilized with 0.1% Triton X-100 for 5 min and blocked with 3% bovine serum albumin for 1 hr. Cells were incubated overnight with primary EHV-4 anti-glycoprotein D monoclonal antibody (dilution: 1:400) at 4 ºC (72). After washing, cells were probed with goat anti-mouse IgG labeled with Alexa fluor-568 for 1 hr. Mock infected cells were stained with same dilutions of primary and secondary antibodies. Plates were analyzed using fluorescence microscope.

5.2.10.6 Virus neutralization test (VNT) to evaluate antibody titer against EHV-4 in serum

Virus neutralization test was performed, according to the OIE reference protocol (281), to evaluate the virus neutralizing antibody titer against EHV-4 in the collected serum samples. Briefly, serum samples were heat inactivated at 56 ºC for 30 min. Reference EHV-4 strain T252 (266) propagated in ED cells was diluted in minimum essential medium to obtain 450-600 PFU/ml. In 96-well plate, 25 µl of test serum samples were serially two-fold diluted till 1:512 in MEM. Similarly, positive and negative control sera were added in respective wells. The virus (25 µl of working concentration; 45-65 PFU/4 wells) was added to each well and the plates were incubated at 37 ºC for 1 hr. Trypsinized ED cells (50 µl; $3x10^5$ cells/ml) were added to each well and incubated at 37 ºC for 1 hr. Finally, 100 µl of methyl cellulose overlay medium was added to all wells and incubated at 37 ºC. After 72 hrs, cells were fixed and stained with 0.5% crystal violet. Virus neutralizing antibody titer was calculated by determining the reciprocal of the highest serum dilution which caused 50% of plaque number reduction. Antibody titre of ≤1:4 is considered as negative, between 1:8 and 1:32 is positive but non-protective, and ≥1:64 antibody titre is protective against infection. Further, 4-fold increase in titre between paired sera is considered as seroconversion.

5.2.10.7 Peptide ELISA for EHV-4

EHV-4 gG based peptide enzyme linked immunesorbent assay (ELISA) was performed to assess serum antibody response against EHV-4 during and after the disease outbreak. The assay was performed as described before (282). The assay was repeated three independent times for each serum sample. The average optical density (OD) values of ≥ 0.118 are considered positive, OD values between 0.100 and 0.118 are considered questionable, and OD values of < 0.100 is considered as negative.

5.2.10.8 RFLP analysis for EHV-4 genomic DNA

RFLP analysis was performed for genomic characterization of EHV-4 isolates. Viral DNA was extracted from the four EHV-4 isolates and the reference EHV-4 laboratory strain (T252) using Sinzger method (283). Briefly, EHV-4 full-infected ED cells were incubated with cell permeabilization buffer on ice for 10 min and centrifuged at 1300 x *g* for 15 min at 4 ºC. The pellet was re-suspended in equal volumes of cell nuclei buffer and 2x nuclease buffer with 2000 Gel U micrococcal nuclease and incubated for 30 min at 37 ºC. Digestion buffer with 0.2 mol/l EDTA was added and the lysate was incubated overnight at 50 ºC. Viral DNA was extracted by phenol/choloroform/isoamyl alcohol. A total of 0.5 volume of 7.5 M ammonium acetate and 2 volume of absolute ethanol were added to the aqueous phase. DNA pellets were washed with 70% ethanol and re-suspended in Tris-EDTA buffer. The obtained DNA was stored at 4 ºC till use. For RFLP, 1.5 µg of viral DNA was digested with *Bam*H1 for 4 hrs at 37 ºC and separated on 0.8% agarose gel.

5.2.10.9 Genome sequencing and phylogenetic analysis for EHV-4 isolates

For clustering of EHV-4 isolates, sequencing of partial gB gene and complete ORF30 (DNA polymerase) gene was performed for all four isolates using specific primer sets; gB: P30 and P31; ORF30: P32-P38 (Table 5). PCR products were purified and sequenced. EHV-4 gG gene sequences obtained from whole genome sequencing analysis was also used for phylogenetic analysis. Maximum-likelihood phylogenetic tree was constructed by aligning the nucleotide sequences of ORF30, gB and gG of my isolates and reference sequences retrieved from Genbank using MEGA7.0.26 software. One thousand bootstrap replicates were used to assess the significance of the tree topology.

5.2.11 Fatal EEHV-1 infection in young Asian elephants

5.2.11.1 EEHV-1 case history

The sudden death of a male Asian elephant “Kanja” (two years and five months of age) at Tierpark Hagenbeck was reported on 6 June 2018 after a short period of illness. “Kanja” was housed in the zoo along with nine other Asian elephants and showed colic-like clinical signs, depression, and anorexia before death. Two days later, the in-contact female elephant “Anjuli” (two years and 11 months old) showed an elevated body temperature without clinical signs. Immediately, before viral infection was diagnosed, Anjuli was treated with virostatic drug - Famvir 500 mg [Famciclovir,15 mg/kg TID (three times a day]) orally for three days; she was then tablets rectally for two days when she was sedated, as recommended by the zoo veterinarian and previous reports (284). The infected elephant developed clinical signs, failed to recover, and eventually died on 13 June 2018. In both cases, none of the elephants had a previous history of illness, but had not been previously tested for EEHVs. After the death of the two young elephants, as a precautionary measure, blood samples and trunk washes were collected from the other eight apparently healthy in-contact elephants and tested for EEHV-1A infection.

5.2.11.2 Samples collection from elephants

Whole blood was collected from both elephants immediately before and after death. Complete necropsy was performed immediately after death and tissue samples were collected. All methods were carried out in accordance with the relevant guidelines and regulations according to the National Animal Protection Act (Behörde für Gesundheit und Verbraucherschutz, Fachbereich Veterinärwesen; approval number AFF012–EWG, 30 September 2009) .Tissues and blood samples for virological diagnostics were collected and shipped to laboratory at Institut für Virologie, Freie Universität Berlin, in virus transport medium at 4 °C. Tissue samples for transmission electron microscopy (TEM) were collected in 10% phosphate-buffered formalin and re-fixed in Karnovsky’ fixative. PBMC were isolated from heparinised whole blood samples collected from infected elephant by Biocoll® based density gradient centrifugation as described earlier.

5.2.11.3 DNA isolation and qPCR analysis for elephant tissue and cell culture samples

DNA was isolated from PBMC (10^5 cells), tissue samples (200 µg) (*viz*. mammary gland, muscle, bone marrow, adrenal gland, kidneys, spleen, pancreas, urinary bladder, liver, gall bladder, lymph nodes, blood vessels, lung, trunk, thyroid, temporal gland, cerebrum,

cerebellum, stomach, small intestine, colon, uterus, tonsil, salivary gland, aorta, thymus, spinal cord, and heart), and infected cell cultures using innuPREP virus DNA/RNA kit®. DNA was extracted from whole blood using innuPREP blood DNA mini kit®. qPCR was performed using the StepOnePlus™ real-time PCR system (Applied Biosystems. Primers (P39 and P40) and probes (P41) specific to EEHV-1 were used as described previously and as seen in Table 5 (285, 286). Standard curves were created using a synthetic 123-base pair length oligonucleotide of EEHV-1 terminase gene (P42) (GenBank Accession number: KC618527.1) and quantified by measuring the absorbance at 260/280 nm using Nanodrop and an online application for calculating DNA copy numbers (http://www.sciencelauncher.com/mwcalc.html). Amplification efficiency (E > 90%) was calculated from the slope of the standard curve (with a correlation coefficient: $R^2 > 0.98$) generated from 10-fold serial dilutions of the terminase gene oligonucleotide. EEHV-1 genome copies in the samples were compared with the generated standard curves. Positive DNA previously extracted from positive samples (286)) and negative (PBS) controls were used and included in every run. All samples were run in duplicates and samples were considered negative if the C_T value was >39. Viral genome copies were then normalized to a standard curve generated with host specific oligonucleotide of elephant TNFα, as seen in Table 5 (P43-P46) and as reported previously (248). EEHV-1 DNA concentration was expressed as copies per million cells given that the eukaryotic cells of each diploid elephant have two copies of the TNFα gene.

5.2.11.4 Attempts of EEHV-1A isolation in cell culture system

EEHV-1 isolation has been attempeted in various cell lines from different host species. Tissue inoculums for virus isolation was prepared as described previously (287). Briefly, tissue samples collected from the elephant “Kanja” (tongue, spleen and whole blood) were homogenized in the presence of cold PBS with 2% P-S and 2.5 µg/mL of amphotericin B, incubated on ice for 10 min, and frozen at −80 °C. Tissue homogenates clarified by centrifugation at 5000 ×*g* for 10 min were used for infecting different cells. Each cell type was grown in 24-well plates, and 200 µl of the clarified homogenate was added, incubated for 1 h at 37 °C, and 300 µl of the respective medium was added. Inoculated cultures were observed daily for the appearance of CPE for seven days. When there was no CPE, inoculated cells were blindly passaged five consecutive times. Similarly, PBMC from infected elephants were either grown separately in culture medium or co-cultured with other cell lines, including PBMC from the healthy elephant. For healthy elephant PBMC, whole blood collected from the 54-year-old healthy elephant “Tanja” from Berlin Zoologischer Garten, which had tested negative for EEHV-1, was used for PBMC isolation using Biocoll®-based

gradient centrifugation as described earlier. Blood was collected during the routine health checkup according to the National Animal Protection Act (Tierschutzgesetz; approval number D-AFF005–EWG, 30 September, 2009).

5.2.11.5 Indirect-IF assay for EEHV-1A

Immunofluorescence staining was performed to detect herpesvirus antigen in cell culture as described previously (247, 287). ENL-2, CrFK, and PBMC were incubated with 200 µl of infected tongue tissue homogenate. After 96 h, cells were washed in PBS, fixed with 4% paraformaldehyde for 30 min, and permeabilized with 0.1% Triton X-100 for 10 min. Cells were blocked with 3% bovine serum albumin in PBS for 30 min at RT, followed by incubation with primary EEHV-1 anti-gB rabbit antibodies (247) diluted 1:500 in blocking buffer at RT overnight. Secondary antibody, Alexa Fluor 488 goat anti-rabbit diluted 1:500 in blocking buffer, was incubated for 1 hr at RT. Mock-infected cells were immunostained with primary and secondary antibodies at the same dilutions. Stained plates were examined and photos were taken using fluorescent microscope.

5.2.11.6 Western blotting analysis for gB of EEHV-1A

Cell lysates prepared from infected tongue tissue homogenate (from “Kanja”) were subjected to sodium dodecyl sulfate-polyacrylamide gel electrophoresis (SDS-PAGE) analysis. Briefly, 200 mg tissue samples were snap-frozen in liquid nitrogen, subjected to homogenization using hand-held tissue homogenizer and lysis using RIPA buffer. Sample buffer was added to protein lysates. The samples were heated at 95 °C for 10 min and proteins were separated by 12% SDS-PAGE as described previously (261). Expression of gB was detected with anti-gB antibodies, which either recognize the peptide sequence located between amino acids 259 and 274 (Ab7125) or between 427 and 441 (Ab7123) of EEHV-1 gB as derived from its sequence (GenBank accession NO. AF411189) (288). Bound gB antibodies were detected with anti-rabbit IgG peroxidise conjugate. Reactive bands were visualized using enhanced chemiluminescence reagent. For non-reducing SDS-PAGE analyses, protein samples were prepared without β-mercaptoethanol as described previously (289).

5.2.11.7 Prediction of furin cleavage sites in EEHVs gB

Furin cleavage sites in EEHVs gB were predicted using the online tool ProP 1.0 Server. To predict and compare the sites in gB of different EEHVs, amino acid sequences were retrieved from Uniprot database. It is predicted that the minimal cleavage site for furin is Arg-X-X-Arg or Arg-X-Lys/Arg-Arg (290).

5.2.11.8 Illumina library preparation and sequencing of EEHV-1A genome

For NGS library preparation, DNA was extracted from tissue samples [tongue “Anjuli” and liver “Kanja”] using the innuPREP Virus DNA/RNA Kit as described above. Total DNA (5 µg) was diluted in 130 µl TE buffer and fragmented to a peak fragment size of 500 bp using the Covaris M220 focused-sonicator with appropriate settings. For size selection, the resulting DNA fragments (fragment size of 500–700 bp) were gel-purified after 1% agarose gel electrophoresis. The purified DNA was subsequently used to generate Illumina libraries using the NEBNext Ultra II Library Prep Kit for Illumina platforms according to the manufacturer’s instruction. To complete the adaptor sequences and to achieve a library yield >500 ng and complete the adaptor sequences, 8 PCR cycles were performed at the end of the protocol. The index-amplified libraries were quantified using NEBNext Library Quant Kit for Illumina and a StepOnePlus™ Instrument. Following quantification, samples were pooled to equimolar amounts to achieve a library concentration of 4 nM. The library pool was diluted further to load a final amount of 16 pM onto an Illumina MiSeq machine for DNA sequencing.

5.2.11.9 Data analysis for EEHV-1A genome sequencing

NGS read data was used for genome assembly of the viral genomes. Reads were preprocessed using Trimmomatic (291) (version 0.36) for adapter and base quality trimming, only retaining reads of a minimal length of 100 bp after trimming. Reads were filtered by mapping against a pan genome sequence (BWA-MEM (256) version0.7.17) containing all available whole genome assemblies of EEHV; only read pairs with at least one read mapping the pan genome were used for final assembly. Quality filtered reads were assembled de novo using the SPAdes (260) assembler (version 3.13.0). Resulting contigs were further corrected using Pilon (258) (version 1.23) and scaffolded against reference genome (GenBank accession NO. KC462165.1) with Ragout (259) (version 2.1.1). In addition, reads mapping the pan genome (not quality trimmed) were mapped against the reference genome KC462165.1 using the mapping assembler MIRA (257) (version 4.9.6). Wherever possible, unmapped regions in the MIRA assembly caused by high sequence variation were filled with the SPAdes assembly to obtain a consensus genome. In a final step, this consensus was then used as reference for another mapping assembly using MIRA to generate the final sequence. Phylogenetic analyses were performed on nucleotide sequences obtained from whole genome sequencing. Nucleotide sequences of the terminase and vGPCR genes were used for the analyses. Reference sequences of same genes of EEHV-1 were retrieved from GenBank. Phylogenetic analysis was performed by

maximum-likelihood method using MEGA 7.0.26 software. Branching was supported by bootstrapping with 1000 sets of data.

5.2.11.10 Transmission electron microscopy in EEHV-1 infected elephant tissue samples

Tissue samples of “Kanja’s” liver, tongue and spleen were converted from fixation by 10% formalin to fixation by Karnovsky solution as mentioned earlier, then washed in 0.1M cacodylate buffer and subsequently fixed and contrasted for 4 hr in 1% osmium tetroxide. Samples were dehydrated in an ascending series of ethanol and in intermedium propylene oxide (1.2 epoxypropane), and afterwards embedded in a mixture of agar 100 (epoxy resin), dodecenylsuccinic anhydride (plasticizer), methylnadic anhydride (hardener), and DMP 30 (catalyst). Polymerization took place at 45 °C and 55 °C for 24 h. Semi- and ultrathin sections were cut at an ultra-microtome Reichert Ultracut S. Semi-thin sections (0.5 µm) were stained with modified Richardson solution (292) for 45 s on an electric hotplate adjusted to 80 °C. The semi-thin sections were checked by light microscopy Olympus CX 21 (Fa. Olympus; Stuttgart, Germany), and areas for ultra-thin sections were selected where the presence of the viruses in the cells was suspected. Ultrathin (80 nm) sections were mounted on Nickel-grids and examined with an electron microscope. The digital photos were edited with Adobe Photoshop Program.

5.2.12 Statistical analysis

Statistical analyses for various assays described above were performed using GraphPad PRISM® 8.02 software. Normally distributed group samples were analyzed with one-way ANOVA test followed by multiple comparisons test. For all analyses, a ‘*p*’ value of less than 0.05 was considered as statistically significant. All results of qPCR, plaque reduction, and ELISA assays were performed in triplicates and results were interpreted as average values ± standard deviation. Differences in rate of infection among stallions, mares and foals were analyzed using Fisher’s exact test.

6 Results

6.1 Molecular mechanisms of EHV-1 pathogenesis

6.1.1 ORF1, ORF2 and ORF17 genes are dispensable of EHV-1 replication

EHV-1 BAC mutants lacking ORF1, ORF2 and ORF17 genes as single, double or triple gene deletions were successfully generated using *en passant* mutagenesis. Specific gene deletion in EHV-1 BAC was confirmed by sequencing and RFLP (Figure 10A-E) and all mutant viruses (Ab4ΔORF17, Ab4ΔORF1, Ab4ΔORF2, Ab4ΔORF17/ORF2, Ab4ΔORF1/ORF2, Ab4ΔORF1/ORF17 and Ab4ΔORF1/ORF2/ORF17) were successfully reconstituted. Three independent growth kinetic experiments were performed to evaluate replicative potential of all mutant viruses in ED and EC cells. The data revealed that all mutant viruses replicate to levels comparable to Ab4-wt without any significant difference (Figure 11A, B and C). Plaque size assay was performed to assess cell-to-cell virus spread in ED cells (Figure 11D and E). Among the different gene deletion mutants, deletion of ORF17 significantly reduced plaque sizes compared to Ab4-wt ($p<0.05$). Similarly, ORF17 gene deletions in combinations with other mutations (Ab4ΔORF1/ORF17, Ab4ΔORF17/ORF2 and Ab4Δ/ORF1/ORF2/ORF17) also showed similar reduction of plaque size (13-17%).

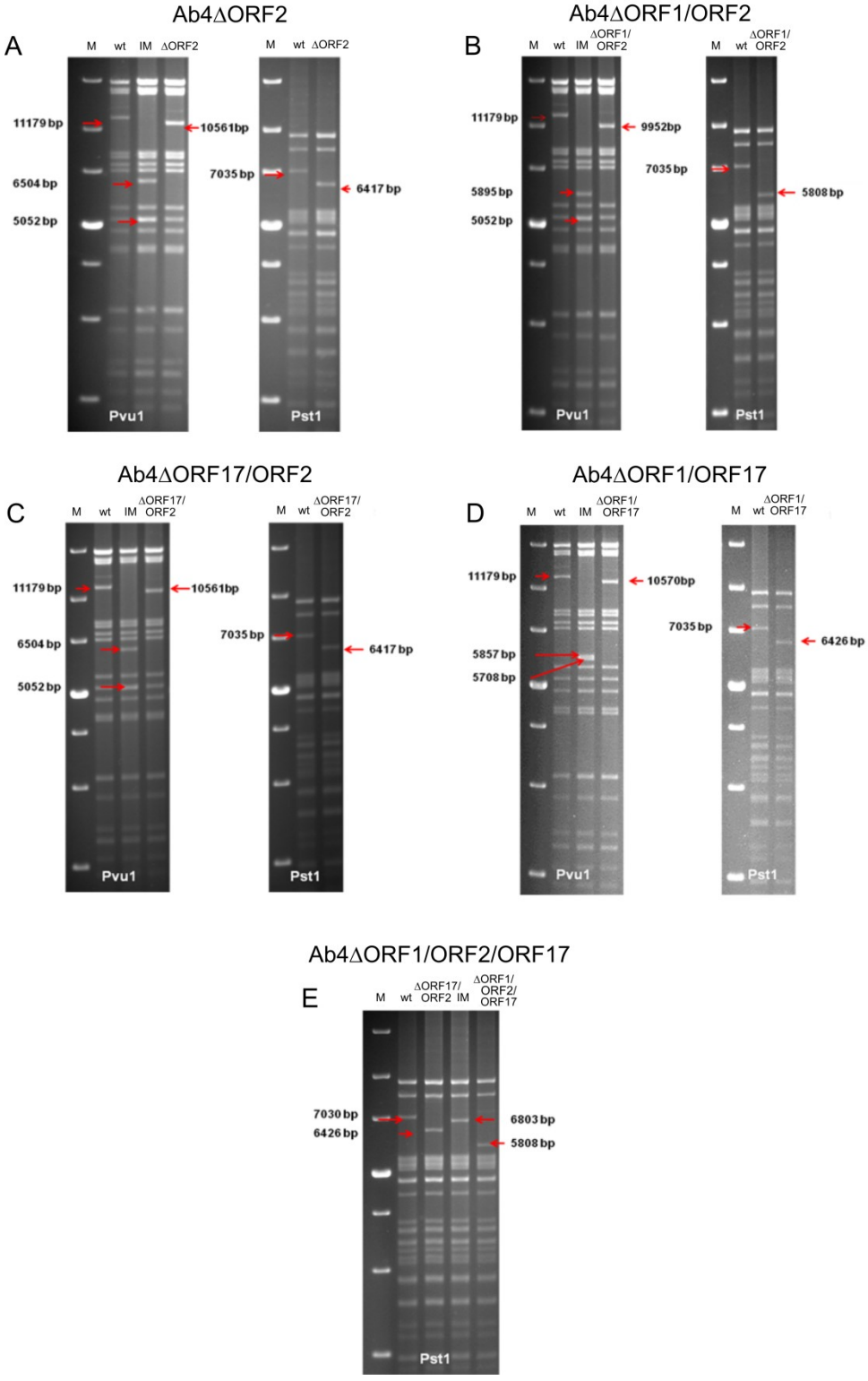

Figure 10: RFLP analysis for characterization of constructed BAC mutants. (A-E) Purified DNA from Ab4-wt, intermediate clones with kanamycin cassette and final clones with gene deletion BAC were digested with either *PstI* or *PvuI*. Fragments in the intermediate and final mutant clones that appeared as a result of kanamycin insertion or

deletion of the gene were marked by red arrows. M – 1 kb plus DNA ladder; wt – Ab4-wt; IM – intermediate BAC clone with kanamycin cassette insertion; ∆ - specific gene deletion.

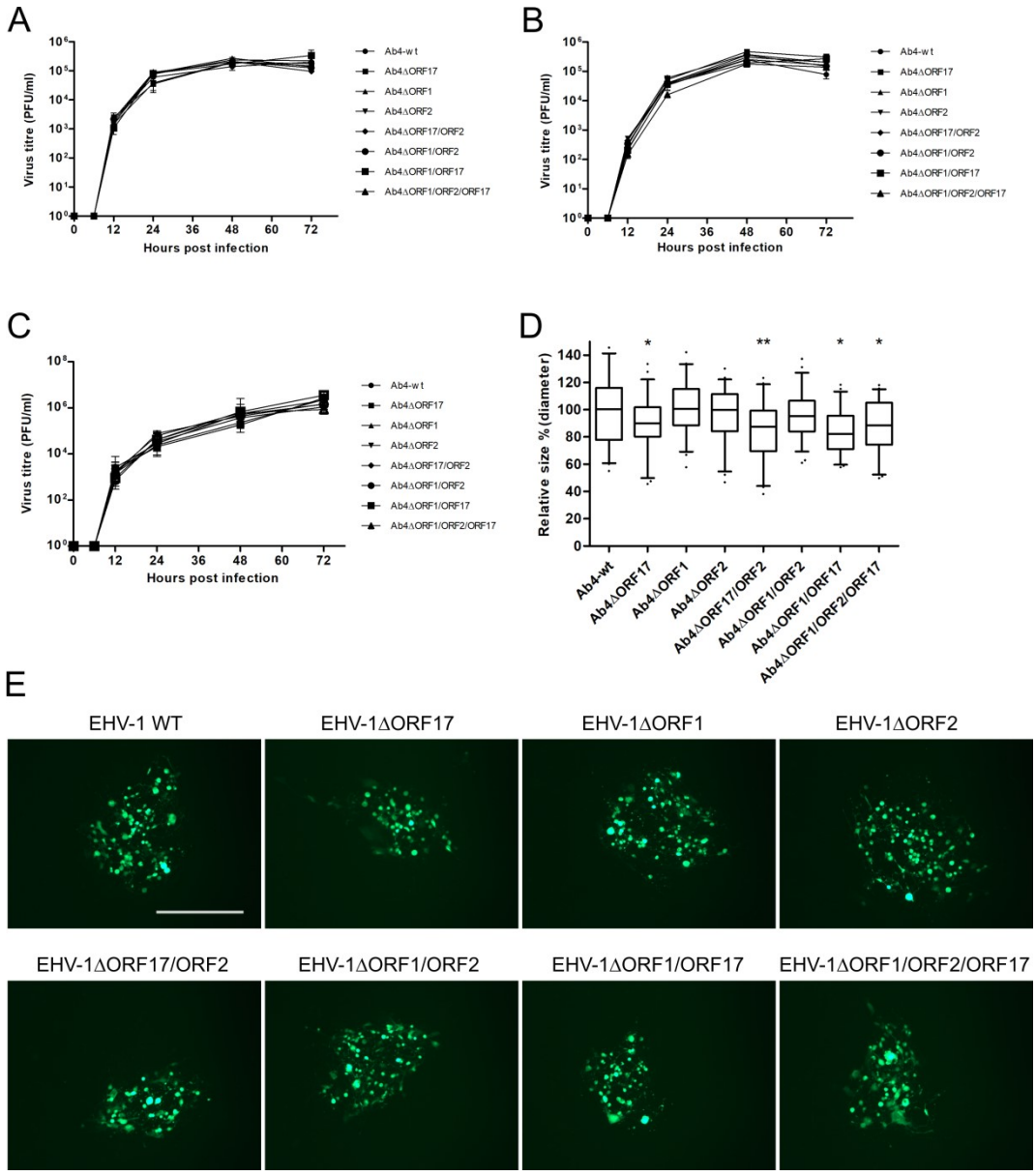

Figure 11: Characterization of Ab4-mutant viruses. (A-C) Growth kinetics assay. ED cells were infected at MOI of 0.1. (A) Infected cells and (B) supernatant were collected and virus titers were determined at different time points. (C) For EC cells, both cells and supernatants were collected together at each time point and virus titer was determined. Mean virus titer ± standard deviation were given. (D) Mean diameters of 150 plaques were measured for each virus. Plaque diameter of Ab4-wt virus was set to 100% and mean diameter ± SD were given. . (n=3; One-way ANOVA test followed by multiple comparisons test; $p<0.05$). * - $p<0.05$, ** - $p<0.01$, *** - $p<0.001$. (E) Representative figures of plaque formation of each virus on ED cells. Scale bar = 500 µm.

6.1.2 ORF2 and ORF17 genes are essential for cell-to-cell virus transfer

Co-cultivation (Figure 12A) and flow chamber (Figure 12C) assays were performed to evaluate virus transfer between infected PBMC and EC under static and dynamic conditions, respectively. Ab4-wt infected PBMC was able to transfer the virus to EC in the presence of neutralizing antibodies, under both static and flow conditions as described previously (77). No virus transfer was observed under “no contact” transwell setup, where infected PBMC was physically separated from EC (Figure 12B and 12G). Among single gene deletion mutant viruses, deletion of ORF2 and ORF17 genes of EHV-1 significantly ($p<0.05$) reduced virus spread to EC under static condition (co-cultivation), as evidenced by reduced plaque numbers. Deletion of ORF2 and ORF17 genes resulted in 65% and 52% reduction of virus transfer to EC, respectively (Figure 12D). In addition, deletions of two or three genes in the same virus (double and triple gene deletion mutants) also revealed 42-65% reduction in virus transfer (Figure 12D). No significant difference in the rate of virus transfer was seen with Ab4ΔORF1 when compared to Ab4-wt ($p>0.05$; Figure 12D). Flow chamber assay mimicked the results of co-cultivation assay in terms of virus transfer events observed for mutant viruses. Deletion of ORF17 and ORF2 genes reduced virus transfer up to 65% and 40%, respectively (Figure 12E). Deletion of two genes in combination showed up to 60-78% reduction in virus transfer (Figure 12E). In addition, deletion of all three genes (Ab4ΔORF1/ORF2/ORF17) showed 76% reduction in virus transfer (Figure 12E). Ab4ΔORF1, on the other hand, did not show a significant difference compared to parental virus. All revertant viruses (Ab4ORF17R, Ab4ORF1R, Ab4ORF2R, Ab4ORF17R/ORF2R, Ab4ORF1R/ORF2R, Ab4ORF1R/ORF17R and Ab4ORF1R/ORF2R/ORF17R) were reconstituted for each corresponding deletion mutant and flow chamber assay was performed. The revertant viruses were spread from infected PBMC to EC in rates similar to parental virus (Figure 12F). In all cases, no virus transfer was seen between infected PBMC and EC under “no contact” conditions (Figure 12G).

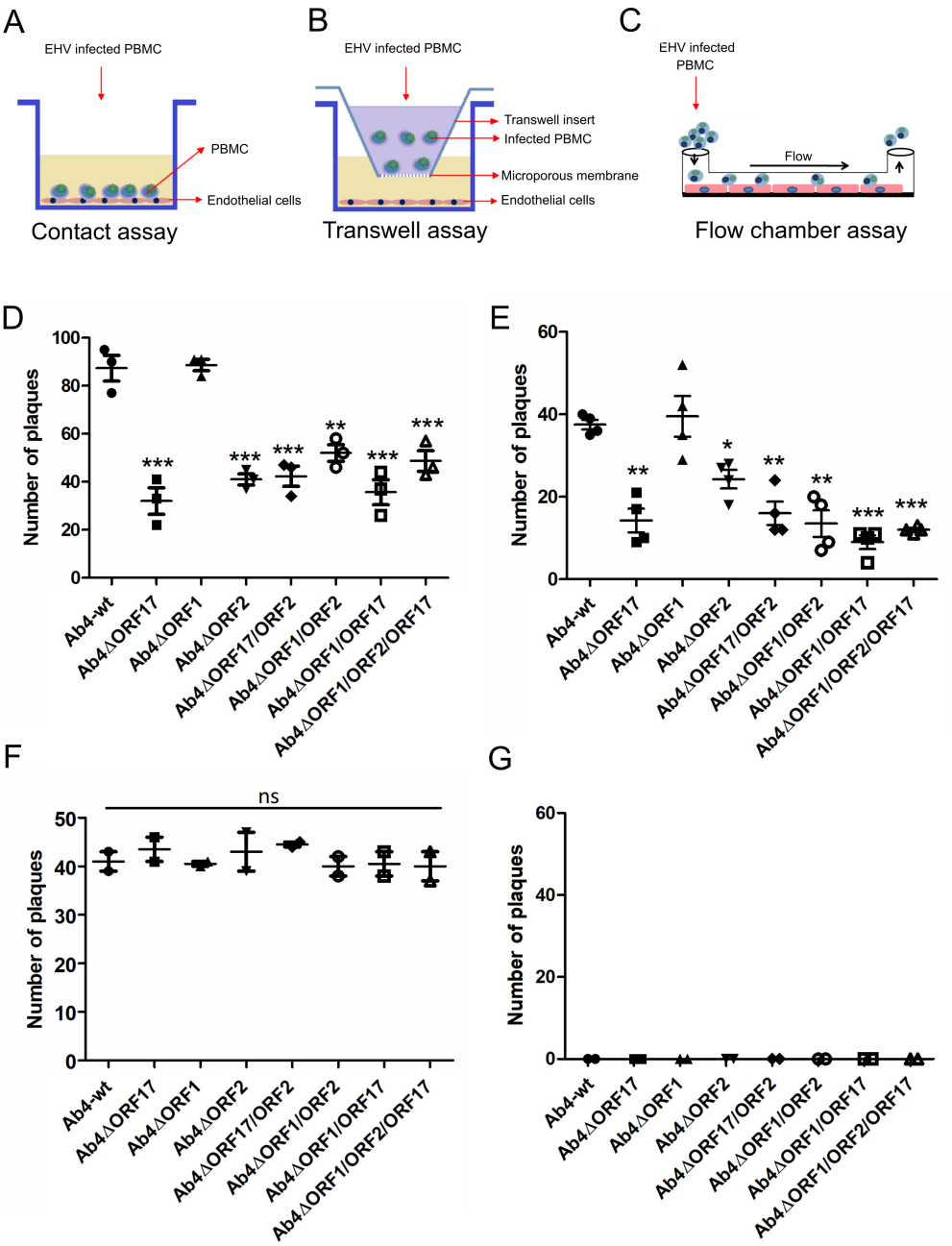

Figure 12: Virus transfer from infected PBMC to EC under static and dynamic flow conditions. Schematic diagram of (A) contact assay, (B) transwell assay and (C) flow chamber assay is depicted. (D) Contact assay and (E) flow chamber assay were performed after sorting of infected cells and viral plaques were counted after 24 hrs. (F) Flow chamber assay was performed for the corresponding revertant viruses. (G) As a control, infected PBMC were placed into a transwell insert without direct contact between PBMC and EC. Data were presented as mean plaque numbers ± SD. (n=3; One-way ANOVA test followed by multiple comparisons test; $p<0.05$). * - $p<0.05$, ** - $p<0.01$, *** - $p<0.001$.

6.1.3 PBMC subpopulations transfer virus to EC

I have isolated each PBMC subpopulations by FACS sorting after probing with specific cell marker antibodies. The cells were infected with Ab4-wt and mutant viruses and flow chamber assay was performed. Virus infection assay in PBMC showed that all three subpopulations (i.e. T, B lymphocytes and monocytes) can be infected with Ab4-wt (Table 6) (77). However, the subpopulation that is mainly responsible for virus transfer to EC is still unknown. To address this question, I have performed flow chamber assay for each infected PBMC subpopulation. Interestingly, all three subpopulations transferred the virus to EC (Figure 13A-C). Similar to the whole PBMC mixed population, individual mutant virus infected PBMC subpopulations showed significant reduction ($p<0.05$) in virus transfer to EC (Figure 13A-C). Double and triple gene deletions showed up to 45-80% reduction in virus transfer. As seen earlier, virus transfer to EC remains unaltered with Ab4ΔORF1 mutant.

Cell marker	Cell	% in PBMC	Rate of infection in %	% in infected population
CD14	Monocyte	27.1 ± 1.7	41.3 ± 2.3	66.2 ± 1.1
IgM	B lymphocyte	9.8 ± 1.1	22 ± 3.2	12.9 ± 0.8
CD3	T lymphocyte	63.2 ± 2.3	5.5 ± 0.5	20.8 ± 1.5

Table 6: Ab4-wt infection in PBMC subpopulations. The data represent the mean ± SD of three independent and blinded experiments.

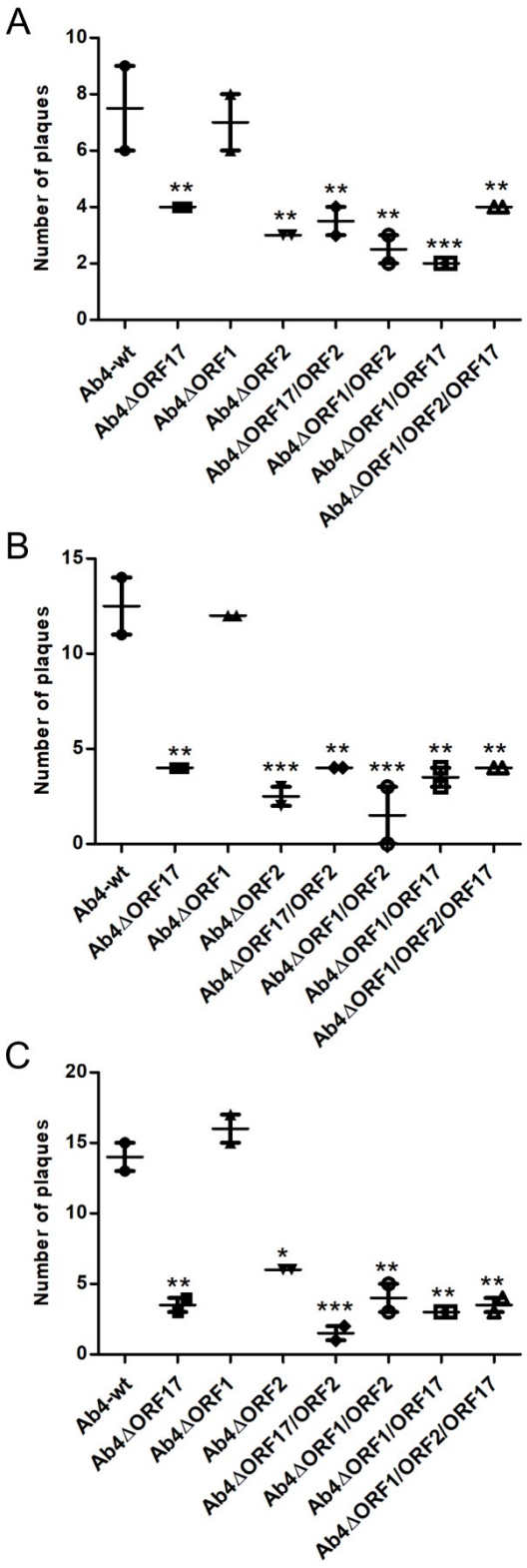

Figure 13: Virus transfer from infected PBMC subpopulations to EC under dynamic flow condition. PBMC were infected with Ab4-wt/mutant viruses at MOI of 0.1 for 24 hrs. Infected PBMC were FACS sorted for each subsets and flow chamber assay was performed for (A) T lymphocytes, (B) B lymphocytes and (C) monocytes. Viral plaques were counted at

24 hpi. The data represent the mean ± SD. (n=2; One-way ANOVA test followed by multiple comparisons test; $p<0.05$). * - $p<0.05$, ** - $p<0.01$, *** - $p<0.001$.

6.1.4 Mimicking the *in vivo* pathway of virus spread from epithelial cells to PBMC to EC

Following inhalation of EHV-1, the virus primarily replicates in respiratory tract epithelial cells, subsequently passes through basement membrane, results in cell associated viremia and, as a final station, the virus transfers to the endothelium (173). It will be interesting to mimic EHV-1 pathogenesis *in vitro* and investigate virus transfer from infected epithelial cell to PBMC and subsequently to EC. I have developed equine epithelial cell-PBMC contact assay (Figure 14A). ED cells grown on transwell membrane were infected with Ab4-wt and mutant viruses, PBMC suspended in EHV-1 neutralizing antibodies medium were added on the other side of the membrane to establish contact with ED cells. Twenty-four hrs post contact, PBMC were collected and analyzed for the rate of infection by counting GFP-positive cells. In all cases, no significant difference in rate of infection of PBMC was seen between parental and mutant viruses (Figure 14B). In contrast, when I have continued with the flow chamber experiment with the same infected PBMC, virus transfer to EC was greatly reduced, up to 35% and 65%, respectively, in case of Ab4ΔORF2 and Ab4ΔORF17 genes either in single or combination format (Figure 14C). Deletion of ORF1 did not affected virus transfer at any stage.

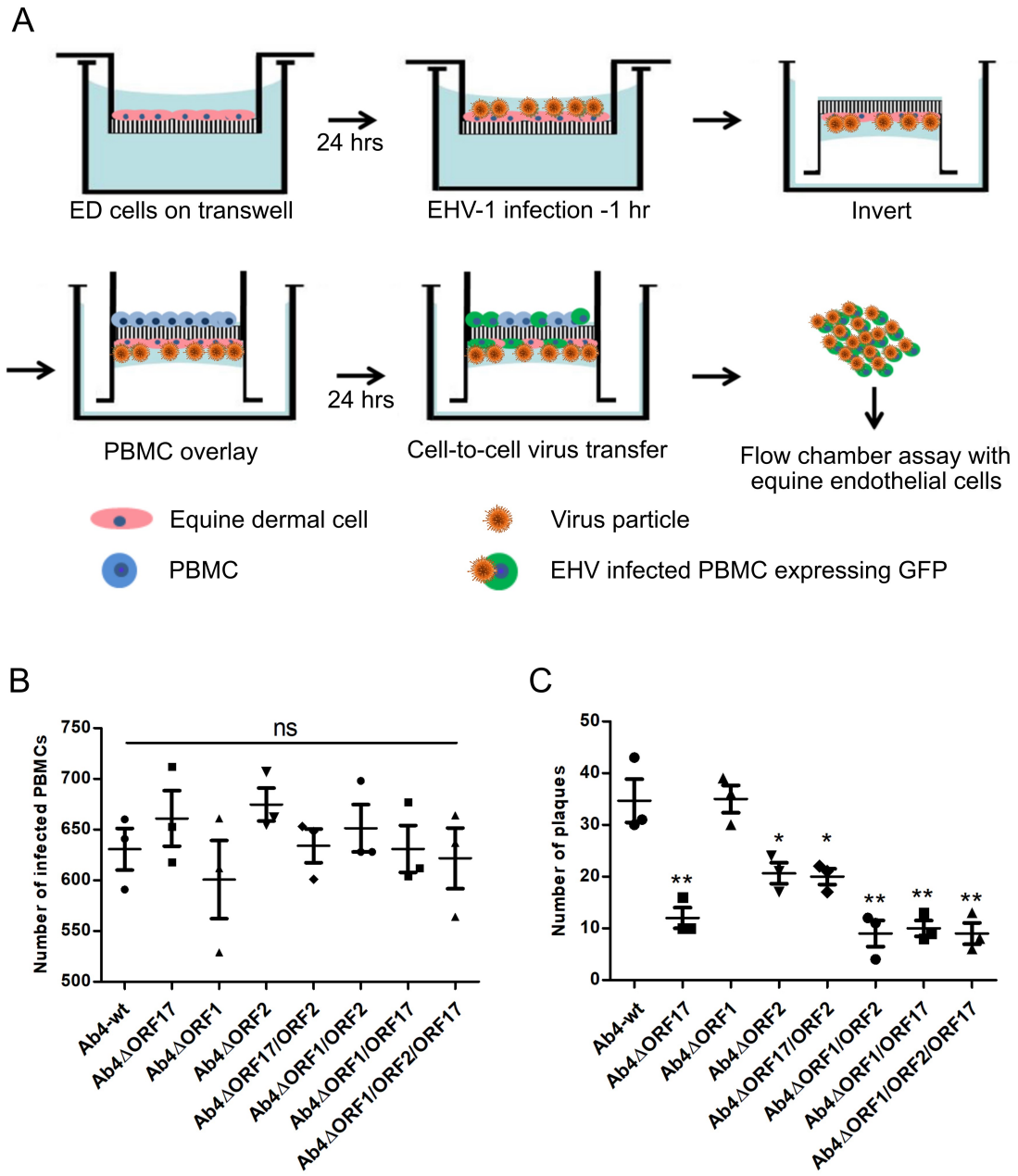

Figure 14: Cell-to-cell virus spread between epithelium to PBMC and PBMC to EC. (A) ED cells were seeded into 3-µm pore size 24-well transwell insert and incubated at 37 ºC for 24 hrs. Subsequently, ED cells were infected with Ab4-wt/mutant viruses at MOI of 0.1 for 1 hr and treated with citrate buffer. Upon infection, transwell insert was inverted, and on the other surface of the transwell insert, $1x10^5$ PBMC resuspended in virus neutralizing antibodies was added. (B) Epithelium-to-PBMC virus transfer was assessed by counting number of GFP-positive cells after 24 hrs. (C) Subsequently, infected PBMC were used for flow chamber assay. The data represent the mean ± SD. (n=3; One-way ANOVA test followed by multiple comparisons test; $p<0.05$). * - $p<0.05$, ** - $p<0.01$, *** - $p<0.001$.

6.1.5 Comparative proteomic analysis differential expression of host proteins in EHV-infected PBMC

Four replicate of PBMC were prepared from two horses and each replicate of cells were infected with Ab4-wt and mutant viruses at MOI of 0.1. At 24 hpi, infected cells were FACS-sorted and protein extracts were prepared from infected and mock-infected PBMC. Upon analysis, a total of 1300 equine cellular proteins were detected and quantified in all different samples. Among the quantified host proteins, 141 proteins displayed significant differences in expression levels between Ab4-wt -infected and uninfected PBMCs, identified by at least two high confidence (95%) peptides, with *p*-values ≤0.05, as calculated by Perseus software. In total, 63 cellular proteins were upregulated and 78 proteins were downregulated. KEGG-pathway enrichment analysis of differentially expressed proteins (p≤0.05) were calculated using Benjamini-corrected modified Fisher's exact test. In Ab4-wt infected PBMC, upregulation of several pathways including Ras signaling, platelet activation and leukocyte transendothelial migration, endocytosis, lysosome and oxidative phosphorylation pathways was detected. On the other hand, downregulation of proteins associated with herpesvirus infection, chemokine signaling, spliceosome, RNA degradation and apoptotic pathways was observed (Table 10 and 11). In total, 45 (18 non-structural, 24 structural, and 3 uncharacterized) viral proteins were detected in virus infected PBMC out of 78 ORF encoded by EHV-1 genome which includes structural and non-structural viral proteins (Figure 15 and Table 7). Function and subcellular localization of detected viral proteins in Ab4-infected PBMC were given in Table 8. No significant difference was observed in viral protein concentration in infected PBMC among EHV-wt and mutants (Table 9).

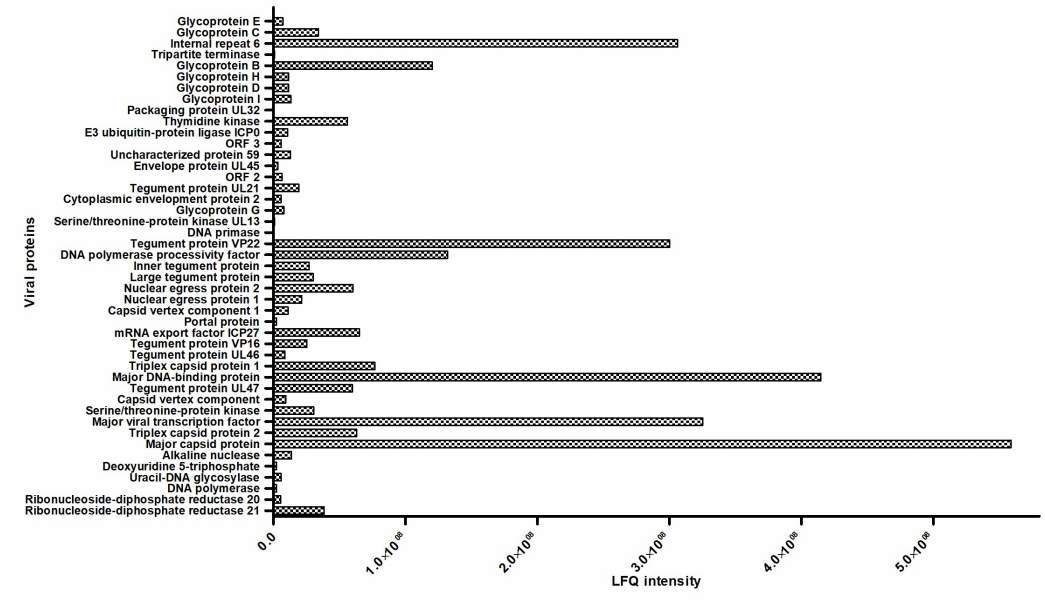

Figure 15: Quantification of Ab4-viral proteins in infected PBMC. PBMC were infected with Ab4-wt and mutant viruses, and proteomic analysis was performed at 24 hpi. Absolute viral proteins quantification in terms of LFQ values were given in X-axis (n=4).

Type	Name of viral proteins	
Nonstructural protein (18)	Ribonucleoside-diphosphate reductase R1 Ribonucleoside-diphosphate reductase R2 Uracil-DNA glycosylase Alkaline nuclease Serine/threonine-protein kinase Major DNA-binding protein mRNA export factor ICP27	Nuclear egress protein 1 Nuclear egress protein 2 DNA polymerase processivity factor DNA primase Thymidine kinase Packaging protein UL32 Tripartite terminase Deoxyuridine 5-triphosphate Internal repeat 6 DNA polymerase Major viral transcription factor
Structural protein (24)	**Tegument proteins** Tegument protein UL47 Tegument protein UL46 Tegument protein VP16 Large tegument protein Inner tegument protein Tegument protein VP22 Tegument protein UL21	 Serine/threonine-protein kinase UL13 Cytoplasmic envelopment protein 2 Envelope protein UL45 E3 ubiquitin-protein ligase ICP0
	Capsid proteins Major capsid protein Triplex capsid protein 1 Triplex capsid protein 2	 Capsid vertex component Capsid vertex component 1 Portal protein
	Envelope proteins Glycoprotein G	 Glycoprotein B Glycoprotein C

	Glycoprotein I Glycoprotein D Glycoprotein H	Glycoprotein E
Uncharacterized proteins (3)	ORF protein 2 ORF protein 59 ORF protein 3	

Table 7: Classification of Ab4 viral proteins quantified in infected PBMC at 24 hpi.

S. No	Uniprot ID	Protein names	Gene/ ORF	Function	Subcellular location
1	P28846	Ribonucleoside-diphosphate reductase large subunit (R1)	RIR1/ ORF21	Precursors necessary for viral DNA synthesis. Allows virus growth in non-dividing cells	Host membrane
2	P28847	Ribonucleoside-diphosphate reductase small subunit (R2)	RIR2/ ORF20	Precursors necessary for viral DNA synthesis. Allows virus growth in non-dividing cells	Host membrane
3	P28858	DNA polymerase catalytic subunit	ORF30	Replicates viral genomic DNA	Host nucleus, replication compartments where viral DNA replication occurs.
4	P28866	Uracil-DNA glycosylase (UDG)	ORF61	Excises uracil residues from the DNA. Reduce deleterious uracil incorporation into the viral genome, in terminally differentiated cells which lack DNA repair enzymes.	Host nucleus
5	P28892	Deoxyuridine 5'-triphosphate nucleotidohydrolase (dUTPase)	DUT / ORF9	Nucleotide metabolism - decreases the intracellular concentration of dUTP to avoid uracil incorporation into viral DANN	Host nucleus
6	P28919	Alkaline nuclease	ORF50	Role in processing non linear or branched viral DNA intermediates to promote the production of mature packaged unit-length linear progeny viral DNA molecules. Exhibits endonuclease and exonuclease activities	Host nucleus, cytoplasm
7	P28920	Major capsid protein	ORF42	Self-assembles to form an icosahedral capsid with a T=16 symmetry	Virion, Host nucleus
8	P28921	Triplex capsid protein 2	TRX2/ ORF43	Structural component of the T=16 icosahedral capsid.	Virion, Host nucleus
9	P28925	Major viral transcription factor	ORF64	This IE protein is a multifunctional protein capable of migrating to the nucleus, binding to DNA, trans-activating other viral genes, and autoregulating its own synthesis.	Host nucleus
10	P28926	Serine/threonine-protein kinase US3 homolog	ORF69	Multifunctional serine/threonine kinase, role in egress of virus particles from the nucleus, modulation of the actin cytoskeleton and inhibition of apoptosis.	Host cytoplasm, Host nucleus
11	P28928	Capsid vertex component 2	CVC2/ ORF36	Capsid vertex-specific component that plays a role during viral DNA encapsidation, assuring correct genome cleavage and presumably stabilizing capsids that contain full-	Virion, Host nucleus

				length viral genomes.	
12	P28929	Tegument protein UL47 homolog (GP10)	ORF13	Tegument protein that can bind to various RNA transcripts. Role in the attenuation of selective viral and cellular mRNA degradation by modulating the activity of host shutoff RNase UL41. Role in the primary envelopement of virions in the perinuclear space, by interacting with two nuclear egress proteins UL31 and UL34.	Virion tegument, Host nucleus, cytoplasm
13	P28932	Major DNA-binding protein (DBP)	ORF31	Crucial roles in viral infection. Participates in the opening of the viral DNA origin to initiate replication by interacting with the origin-binding protein	Host nucleus
14	P28935	Triplex capsid protein 1	TRX1/ ORF22	Structural component of the T=16 icosahedral capsid	Virion, Host nucleus
15	P28937	Tegument protein UL46 homolog	ORF14	Modulates alpha trans-inducing factor-dependent activation of alpha genes	Virion tegument, Host cell membrane
16	P28938	Tegument protein VP16 homolog (Alpha trans-inducing protein)	ORF12	Transcriptional activator of IE gene products. Key activator of lytic infection by initiating the lytic program through the assembly of the transcriptional regulatory VP16-induced complex composed of VP16 and two cellular factors, HCFC1 and POU2F1. VP16-induced complex represents a regulatory switch: when it is on, it promotes IE-gene expression and thus lytic infection, and when it is off, it limits IE-gene transcription favoring latent infection.	Virion tegument, Host nucleus
17	P28939	mRNA export factor ICP27 homolog (Transcriptional regulator IE63 homolog)	ORF5	Multifunctional regulator of the expression of viral genes that mediates nuclear export of viral intronless mRNAs. This immediate early (EI) protein promotes the nuclear export of viral intronless mRNAs by interacting with mRNAs and host NXF1/TAP	Host cytoplasm, nucleus
18	P28944	Portal protein	ORF56	Forms a portal in the viral capsid through which viral DNA is translocated during DNA packaging. Assembles as a dodecamer at a single fivefold axe of the T=16 icosahedric capsid. Binds to the molecular motor that translocates the viral DNA, termed terminase.	Virion, Host nucleus
19	P28950	Capsid vertex component 1	CVC1/ ORF45	Role during viral DNA encapsidation, assuring correct genome cleavage and presumably stabilizing capsids that contain full-length viral genomes	Virion, Host nucleus
20	P28951	Nuclear egress protein 1	NEC1/ ORF29	Essential role in virion nuclear egress, the first step of virion release from infected cell	Host nucleus inner membrane through interaction with NEC2
21	P28954	Nuclear egress protein 2	NEC2/ ORF26	Essential role in virion nuclear egress, the first step of virion release from infected cell	Host nucleus inner membrane
22	P28955	Large tegument protein deneddylase	ORF24	Large tegument protein that plays multiple roles in the viral cycle	Virion tegument, cytoplasm, nucleus. Associated with capsid
23	P28956	Inner tegument protein	ORF23	Essential role in cytoplasmic secondary envelopment during viral	Virion tegument, cytoplasm,

				egress.	nucleus, golgi apparatus
24	P28958	DNA-binding Polymerase accessory protein	ORF18	Essential role in viral DNA replication by acting as the polymerase accessory subunit	Host nucleus
25	P28960	Tegument protein VP22	ORF11	Tegument protein that plays different roles during the time course of infection. Participates in both the accumulation of viral mRNAs and viral protein translation at late time of infection.	Virion tegument, Host cytoplasm, nucleus, Golgi apparatus
26	P28962	DNA primase	ORF7	Essential component of the helicase/primase complex. Unwinds the DNA at the replication forks and generates single-stranded DNA for both leading and lagging strand synthesis	Host nucleus
27	P28966	Serine/threonine-protein kinase UL13 homolog	ORF49	Multifunctional serine/threonine kinase, role in egress of virus particles from the nucleus, modulation of the actin cytoskeleton and regulation of viral and cellular gene expression. Regulates the nuclear localization of viral envelopment factors UL34 and UL31 homologs, by phosphorylating the US3 kinase homolog, indicating a role in nuclear egress. Disrupts host nuclear lamins, including LMNA and LMNB1. Phosphorylates the viral Fc receptor composed of glycoproteins E (gE) and I (gI).	Virion tegument, Host nucleus
28	P28967	Envelope glycoprotein G (gG)	gG/ ORF70	Chemokine-binding protein that inhibits neutrophils' chemotaxis.	Virion membrane, Single-pass membrane protein
29	P28970	Cytoplasmic envelopment protein 2	ORF46	Plays a critical role in cytoplasmic virus egress. Participates in the final step of tegumentation and envelope acquisition within the host cytoplasm by directly interacting with the capsid. Upon virion binding to target cell, a signaling cascade is triggered to disrupt the interaction with the capsid, thereby preparing capsid uncoating.	Virion tegument, Host cytoplasm, nucleus
30	P28972	Tegument protein UL21 homolog	ORF40	May participate in DNA packaging/capsid maturation events. Promotes efficient incorporation of tegument proteins UL46, UL49, and US3 homologs into virions. May also play a role in capsid transport to the trans-Golgi network.	Virion tegument, Host cytoplasm, nucleus
31	P28979	Gene 2 protein	ORF2	Immunomodulatory protein	
32	P28981	Envelope protein UL45 homolog	ORF15	Uncharacterized	Virion membrane, Single-pass type II membrane protein
33	P28983	Uncharacterized gene 59 protein	ORF59	Uncharacterized	
34	P28988	Gene 3 protein	ORF3	Uncharacterized	
35	P28990	E3 ubiquitin-protein ligase ICP0	ORF63	Evades nuclear antiviral defenses triggered by dsDNA viruses. Acts during the initial stages of lytic infection and the reactivation of latent viral genome. Prevents the antiviral effect of nuclear bodies by degrading host PML and SP100	Virion tegument, Host cytoplasm
36	P69185	Thymidine kinase	TK/ ORF38	Catalyzes the transfer of the gamma-phospho group of ATP to thymidine to generate dTMP in the salvage pathway	Host nucleus

				of pyrimidine synthesis. The dTMP - substrate for DNA polymerase in viral DNA replication. Allows virus to be reactivated and to grow in non-proliferative cells lacking a high concentration of phosphorylated nucleic acid precursors.	
37	P69329	Packaging protein UL32 homolog	ORF28	Role in efficient localization of neo-synthesized capsids to nuclear replication compartments, thereby controlling cleavage and packaging of virus genomic DNA.	Host cytoplasm, nucleus
38	Q6DLD8	Envelope glycoprotein I (gI)	gI/ ORF73	In epithelial cells, the heterodimer gE/gI is required for the cell-to-cell spread of the virus, by sorting nascent virions to cell junctions	Virion membrane, Host cell membrane, cell junction, Golgi apparatus membrane
39	Q6DLD9	Envelope glycoprotein D (gD) (Glycoprotein 17/18)	gD/ ORF72	Envelope glycoprotein that binds to host cell entry receptors. May trigger fusion with host membrane, by recruiting the fusion machinery composed of gB and gH/gL	Virion membrane, endosomes and trans-Golgi
40	Q6DLH1	Envelope glycoprotein H (gH)	gH/ ORF39	The heterodimer glycoprotein H-glycoprotein L is required for the fusion of viral and plasma membranes leading to virus entry into the host cell.	Virion membrane, Host cell membrane, endosome membrane
41	Q6DLH8	Envelope glycoprotein B (gB)	gB/ ORF33	Envelope glycoprotein that forms spikes at the surface of virion envelope	Virion membrane, Host cell membrane, endosome membrane, Golgi
42	Q6DLH9	Tripartite terminase subunit 1	TRM1/ ORF32	Component of the molecular motor that translocates viral genomic DNA in empty capsid during DNA packaging. Forms a tripartite terminase complex with TRM2 and TRM3 in the cytoplasm. The complex reaches the host nucleus and interacts with capsid portal vertex. This portal forms a ring in which genomic DNA is translocated into the capsid. Role for the cleavage of concatemeric viral DNA into unit length genomes.	Host nucleus. Seen external surface of the viral capsid during assembly and DNA packaging, but absent in extracellular mature virions.
43	Q6LAQ8	Uncharacterized gene 67 protein (IR6 protein)	IR6/ ORF67	Determinant of EHV-1 virulence and play role in virus maturation and/or egress	Host cytoplasm
44	Q6S6Q5	Envelope glycoprotein C (gC) (Glycoprotein 13)	gC GP13/ ORF16	Essential for the initial attachment to heparan sulfate moities of the host cell surface proteoglycans. Plays also a role in host immune evasion by inhibiting the host complement cascade activation	Virion membrane
46	Q6S6V7	Envelope glycoprotein E (gE)	gE/ ORF74	In epithelial cells, the heterodimer gE/gI is required for the cell-to-cell spread of the virus, by sorting nascent virions to cell junctions	Virion membrane, Host cell membrane, cell junction, Golgi, endosome membrane

Table 8: Function and subcellular localization Ab4-viral proteins quantified in infected PBMC. PBMC were infected with Ab4-wt and mutant viruses, and proteomic analysis was performed at 24 hpi. (n=4). Data regarding function of viral proteins were from uniprot database.

S. No:	Viral protein Name	LFQ intensity					
		ORF	Ab4-wt	Ab4Δ ORF17	Ab4Δ ORF1	Ab4Δ ORF2	Ab4ΔORF1/ ORF2/ORF17
1	Ribonucleoside-diphosphate reductase	21	38457000	42760000	28937000	34619000	31547000
2	Ribonucleoside-diphosphate reductase	20	5598100	5476500	5585500	5649700	6021400
3	DNA polymerase	30	2382500	3150200	3580700	3538800	3046200
4	Uracil-DNA glycosylase	61	5891500	5534200	8313800	7703800	6132800
5	Deoxyuridine 5-triphosphate	9	2214900	1760400	2349300	2203100	2709400
6	Alkaline nuclease	50	13880000	15983000	13770000	15895000	15346000
7	Major capsid protein	42	5.59E+08	7.13E+08	4.05E+08	3.15E+08	4.34E+08
8	Triplex capsid protein 2	43	62978000	95072000	60136000	87828000	64373000
9	Major viral transcription factor	64	3.25E+08	82903000	6.86E+08	5.72E+08	82162000
10	Serine/threonine-protein kinase	69	30570000	40562000	42719000	37277000	32926000
11	Capsid vertex component	36	9458300	10320000	5259200	12150000	8031600
12	Tegument protein UL47	13	59701000	95905000	48184000	74667000	82758000
13	Major DNA-binding protein	31	4.15E+08	4.22E+08	4.44E+08	3.27E+08	4.39E+08
14	Triplex capsid protein 1	22	76925000	80867000	49053000	85817000	74079000
15	Tegument protein UL46	14	8763400	11152000	8561200	12463000	9024200
16	Tegument protein VP16	12	25461000	29828000	24032000	32303000	33741000
17	mRNA export factor ICP27	5	65052000	45830000	48386000	41274000	62247000
18	Portal protein	56	2174600	3901800	3018400	3896100	3299100
19	Capsid vertex component 1	45	10922000	15555000	9218600	13059000	11478000

20	Nuclear egress protein 1	29	21609000	15946000	11739000	12550000	16998000
21	Nuclear egress protein 2	26	60217000	96829000	64970000	82555000	70709000
22	Large tegument protein	24	30209000	38959000	22967000	26724000	31338000
23	Inner tegument protein	23	27162000	31615000	23699000	30601000	26773000
24	DNA polymerase processivity factor	18	1.32E+08	1.45E+08	1.33E+08	1.53E+08	1.22E+08
25	Tegument protein VP22	11	3E+08	1.05E+08	72235000	1.11E+08	77521000
26	DNA primase	7	0	403560	0	416120	445360
27	Serine/threonine-protein kinase UL13	49	1029400	1267500	0	992370	1066300
28	Glycoprotein G	70	7763200	10651000	6170100	5697000	5825100
29	Cytoplasmic envelopment protein 2	46	5710100	6904300	5807900	5667900	5820700
30	Tegument protein UL21	40	19523000	13215000	10426000	10602000	40850000
31	ORF protein 2	2	6509700	13405000	2613700	0	0
32	Envelope protein UL45	15	3423900	6110500	2451900	4253500	4048600
33	ORF protein 59	59	12931000	10356000	10649000	10223000	10612000
34	ORF protein 3	3	5969100	8898100	7535900	3729600	0
35	E3 ubiquitin-protein ligase ICP0	63	10721000	11200000	9420800	12522000	15578000
36	Thymidine kinase	38	56063000	72649000	44132000	67118000	64495000
37	Packaging protein UL32	28	0	0	799790	0	1261800
38	Glycoprotein I	73	13318000	14348000	10520000	12638000	13165000
39	Glycoprotein D	72	11519000	17086000	0	9276600	9266900
40	Glycoprotein H	39	11487000	24548000	10290000	16199000	12927000
41	Glycoprotein B	33	1.2E+08	2.15E+08	74321000	1.46E+08	1.4E+08
42	Tripartite terminase	32	747020	797000	725740	813340	755250
43	Internal repeat 6	67	3.06E+08	6.6E+08	4.3E+08	5.31E+08	2.38E+08

44	Glycoprotein C	16	34061000	82703000	20409000	58136000	46296000
45	Glycoprotein E	74	7132200	13009000	7924400	8334700	8958100

Table 9: LFQ intensity of each viral protiens detected in PBMC infected with Ab4-wt and mutants. Proteomic analysis was performed in infected PBMC at 24 hpi. Protein quantification for viral proteins were given interms of LFQ intensity. (n=4)

While comparing the host proteomic profile of Ab4-wt and mutant viruses infected PBMC, differential expression of more than 100 proteins was observed. Details of pathways differentially modulated are shown in Table 10 and 11. Ab4ΔORF17 upregulated proteins associated with herpesvirus infection (CD58/lymphocyte function-associated antigen 3[LFA-3], TNFRSF1A associated via death domain [TRADD], Recombination signal binding protein for immunoglobulin kappa J region [RBPJ] I, RBPJ like, Proteasome 26S subunit, non-ATPase 12) and downregulated chemokine signaling (MAPK kinase 1, Ras-related protein Rap-1A, stress induced phosphoprotein 1, RAP1A – RAS ongogene family protein) and MAPK (MAPK kinase 1, Protein phosphatase 5 catalytic subunit, Ras-related protein Rap-1A, RAP1A – RAS ongogene family protein) signaling pathways. Proteins like CD58, RPBJ, RPBJL (herpesvirus infection pathways) involved in cytokine release, leukocyte migration, cell-to-cell adhesion and signaling receptor pathways. Ab4ΔORF1 infection resulted in upregulation of mTOR signaling, focal adhesion and chemokine signaling pathway. Ab4ΔORF2 showed upregulation of herpesvirus infection and chemokine signaling pathways, and downregulated MAPK signaling pathways. Finally, the triple gene deletion mutant upregulated herpesvirus infection, T-cell signaling and chemokine signaling pathways, and downregulated MAPK signaling and RNA degradation pathways. Proteomic analysis of Ab4-mutant viruses infected PBMC revealed significant alteration in proteins associated with herpesvirus infection, chemokine and MAPK signaling pathways (Table 10). From these findings, it can be predicted that all these three viral genes plays an essential role in modulating several host pathways in addition to release and regulation of cytokines and chemokines from infected PBMCs. Complete details of differentially expressed proteins involved in various pathways listed above given in supplementary Table 11.

Infected population	Pathways upregulated	Pathways downregulated
PBMC	Lysosome	Herpesvirus infection
Vs	cAMP signalling	Spliceosome
Ab4-wt	Ras signalling pathway	Chemokine signalling pathway

	Endocytosis	RNA degradation
	Platelet activation and leukocyte transendothelial migration	Apoptosis
	Oxidative phosphorylation	
	Fatty acid elongation	
PBMC	Lysosome	Chemokine signalling pathway
Vs	Herpesvirus infection	MAPK signalling pathway
Ab4ΔORF17	Oxidative phosphorylation	Spliceosome
	Protein processing in endoplasmic reticulum	RNA trnasport
	Fc epsilon RI signalling	
	Metabolic pathways	
PBMC	mTOR signalling pathway	Spliceosome
Vs	Endocytosis	RNA degradation
Ab4ΔORF1	Lysosome	Metabolic pathways
	Focal adhesion	Aminoacyl-tRNA biosynthesis
	Ras signalling pathway	
	Herpesvirus infection	
	Chemokine signalling pathway	
	Leukocyte transendothelial migration	
	Platelet activation	
PBMC	Herpesvirus infection	Spliceosome
Vs	mTOR signalling pathway	RNA degradation
Ab4ΔORF 2	Regulation of actin cytoskeleton	MAPK signalling pathway
	Chemokine signalling pathway	
PBMC	Endocytosis	Spliceosome
Vs	Lysosome	RNA degradation
Ab4ΔORF 1/ORF2/ORF17	Herpesvirus infection	MAPK signalling pathway
	T cell signalling	
	Chemokine signalling pathway	

Table 10: Pathways differentially regulated in Ab4-wt and mutant viruses infected PBMC. PBMC were infected with Ab4-wt and mutants at MOI of 1. At 24 hpi, infected PBMC were sorted and proteomic analysis was performed. Pathways significantly upregulated and

downregulated (based on *p*-value and Benjamini-corrected modified Fisher's exact test value) in infected PBMC in comparison healthy PBMC were given (n=4).

Infected population	Pathways upregulated		Pathways downregulated	
	Pathways	**Genes**	**Pathways**	**Genes**
PBMC Vs Ab4-wt	**Lysosome**	ATPase H+ transporting V0 subunit d1 Adaptor related protein complex 3 mu 1 subunit Adaptor related protein complex 3 mu 2 subunit Scavenger receptor class B member 2	**Herpesvirus infection**	CD58 molecule Proteasome 26S subunit, non-ATPase 2 recombination signal binding protein for immunoglobulin kappa J region like recombination signal binding protein for immunoglobulin kappa J region
	Ras signaling pathway	RAP1A, member of RAS oncogene family Phosphoinositide-3-kinase regulatory subunit 1 Ras-related protein Rap-1A		
	Endocytosis	EH domain containing 1 EH domain containing 3 RAB35, member RAS oncogene family RAB5A, member RAS oncogene family	**Spliceosome**	LSM6 homolog, U6 small nuclear RNA and mRNA degradation associated RNA binding motif protein 22 Cell division cycle 40
	Platelet activation	RAP1A, member of RAS oncogene family Phosphoinositide-3-kinase regulatory subunit 1		Squamous cell carcinoma antigen recognized by T-cells 1
	Leukocyte transendothelial migration	Ras-related protein Rap-1A	**Chemokine signaling pathway**	RAP1A, member of RAS oncogene family Mitogen-activated protein kinase kinase 1 Stress induced phosphoprotein 1
	Oxidative phosphorylation	ATP synthase, H+ transporting, mitochondrial F1 complex, alpha subunit 1 ATPase H+ transporting V0 subunit d1 NADH:ubiquinone oxidoreductase core subunit V1	**RNA degradation**	TNFRSF1A associated via death domain Chromodomain helicase DNA binding protein 4 LSM6 homolog, U6 small nuclear RNA and mRNA degradation associated RNA binding motif protein 22
	Fatty acid elongation	Hydroxysteroid 17-beta dehydrogenase 12 Mitochondrial trans-2-enoyl-CoA reductase	**Apoptosis**	Apoptosis inducing factor, mitochondria associated 1 Caspase 1, apoptosis-related cysteine peptidase Caspase 10 MALT1 paracaspase
PBMC Vs Ab4ΔORF17	**Herpesvirus infection**	CD58 molecule TNFRSF1A associated via death domain Proteasome 26S subunit, non-ATPase 12 Recombination signal binding protein for immunoglobulin kappa J region like Recombination signal binding protein for immunoglobulin kappa J region l	**Chemokine signaling pathway**	RAP1A, member of RAS oncogene family Mitogen-activated protein kinase kinase 1 Ras-related protein Rap-1A Stress induced phosphoprotein 1
	Lysosome	ATPase H+ transporting V0 subunit d1 Adaptor related protein complex 3 mu 1 subunit Adaptor related protein complex 3 mu 2 subunit Scavenger receptor class B member 2	**MAPK signaling pathway**	Protein phosphatase 5 catalytic subunit RAP1A, member of RAS oncogene family Mitogen-activated protein kinase kinase 1 Ras-related protein Rap-1A
	Oxidative	ATP synthase, H+ transporting, mitochondrial F1		

	phosphorylation	complex, alpha subunit 1 ATPase H+ transporting V0 subunit d1 NADH:ubiquinone oxidoreductase core subunit V1	**RNA transport**	RNA binding motif protein 22 Pre-mRNA processing factor 3 NOP2/Sun RNA methyltransferase family member 2 Ribosomal RNA processing 1B
	Protein processing in endoplasmic reticulum and Fc epsilon RI signaling	ER membrane protein complex subunit 1 Endoplasmic reticulum lectin 1 Serine/threonine-protein phosphatise 6 catalytic subunit Receptor-type tyrosine-protein phosphatase epsilon	**Spliceosome**	LSM6 homolog, U6 small nuclear RNA and mRNA degradation associated RNA binding motif protein 22 Cell division cycle 40 Squamous cell carcinoma antigen recognized by T-cells 1
	Metabolic pathways	24-dehydrocholesterol reductase T-cell immune regulator 1, ATPase H+ transporting V0 subunit a3 Acetyl-CoA acetyltransferase 2 Acyl-CoA synthetase long-chain family member 3 Adenosylhomocysteinase like 1 Adenosylhomocysteinase like 2 Branched chain amino acid transaminase 2 Ceramide synthase 2 Inositol polyphosphate-1-phosphatase Methylcrotonoyl-CoA carboxylase 1 Methylcrotonoyl-CoA carboxylase 2 Phosphatidylinositol glycan anchor biosynthesis class U Phospholipase B1 Pyruvate dehydrogenase complex component X		
PBMC Vs Ab4ΔORF1	**mTOR signaling pathway**	3-phosphoinositide dependent protein kinase 1 Ras related GTP binding C Ras related GTP binding D Phosphatidylinositol-4,5-bisphosphate 3-kinase catalytic subunit gamma	**Metabolic pathways**	ATP synthase, H+ transporting, mitochondrial F1 complex, epsilon subunit(ATP5E) ATPase H+ transporting V0 subunit a1 NADH:ubiquinone oxidoreductase core subunit V1 Aconitase 1 Fucokinase Galactosidase beta 1 Hydroxysteroid 17-beta dehydrogenase 12 Mannosidase alpha class 2A member 1
	Herpesvirus infection	CD58 molecule Phosphatidylinositol-4,5-bisphosphate 3-kinase catalytic subunit gamma Proteasome 26S subunit, non-ATPase 12		

	Lysosome	ATPase H+ transporting V0 subunit d1 Adaptor related protein complex 3 mu 1 subunit Adaptor related protein complex 3 mu 2 subunit Scavenger receptor class B member 2		Thymidine phosphorylase
	Chemokine signaling pathway	RAP1A, member of RAS oncogene family Mitogen-activated protein kinase kinase 1 Ras-related protein Rap-1A Stress induced phosphoprotein 1	**Spliceosome**	LSM6 homolog, U6 small nuclear RNA and mRNA degradation associated RNA binding motif protein 22 Cell division cycle 40 Squamous cell carcinoma antigen recognized by T-cells 1
	Platelet activation **Leukocyte transendothelial migration**	RAP1A, member of RAS oncogene family Phosphoinositide-3-kinase regulatory subunit 1 Ras-related protein Rap-1A CD58 molecule	**RNA degradation**	TNFRSF1A associated via death domain Chromodomain helicase DNA binding protein 4 LSM6 homolog, U6 small nuclear RNA and mRNA degradation associated RNA binding motif protein 22
	Focal adhesion and Ras signaling pathway	RAP1A, member of RAS oncogene family Phosphoinositide-3-kinase regulatory subunit 1 Ras-related protein Rap-1A	**Aminoacyl-tRNA biosynthesis**	Histidyl-tRNA synthetase 2, mitochondrial Histidyl-tRNA synthetase phenylalanyl-tRNA synthetase beta subunit
	Endocytosis	EH domain containing 1 EH domain containing 3 RAB35, member RAS oncogene family RAB5A, member RAS oncogene family		
PBMC Vs Ab4ΔORF2	**Herpesvirus infection**	CD58 molecule proteasome 26S subunit, non-ATPase 12 proteasome 26S subunit, non-ATPase 2	**Spliceosome**	LSM6 homolog, U6 small nuclear RNA and mRNA degradation associated RNA binding motif protein 22 Cell division cycle 40 Squamous cell carcinoma antigen recognized by T-cells 1
	mTOR signaling	3-phosphoinositide dependent protein kinase 1 Ras related GTP binding C Ras related GTP binding D Phosphatidylinositol-4,5-bisphosphate 3-kinase catalytic subunit gamma		
	Regulation of actin cytoskeleton	FYVE, RhoGEF and PH domain containing 3 Integrin subunit beta Phosphatidylinositol-4,5-bisphosphate 3-kinase catalytic subunit gamma Phosphatidylinositol-5-phosphate 4-kinase type 2 gamma Protein phosphatase 1 regulatory subunit 12A	**RNA degradation**	TNFRSF1A associated via death domain Chromodomain helicase DNA binding protein 4 LSM6 homolog, U6 small nuclear RNA and mRNA degradation associated RNA binding motif protein 22

	Chemokine signaling pathway	RAP1A, member of RAS oncogene family Mitogen-activated protein kinase kinase 1 Ras-related protein Rap-1A Stress induced phosphoprotein 1	**MAPK signaling pathway**	RAP1A, member of RAS oncogene family Interleukin 1 alpha Protein phosphatase 5 catalytic subunit Ras-related protein Rap-1A Ribosomal protein S6 kinase A5
PBMC Vs Ab4ΔORF1/ ORF2/ORF17	**Endocytosis**	EH domain containing 1 EH domain containing 3 RAB35, member RAS oncogene family RAB5A, member RAS oncogene family	**Spliceosome**	LSM6 homolog, U6 small nuclear RNA and mRNA degradation associated RNA binding motif protein 22 Cell division cycle 40 Squamous cell carcinoma antigen recognized by T-cells 1
	Herpesvirus infection	CD58 molecule proteasome 26S subunit, non-ATPase 12 proteasome 26S subunit, non-ATPase 2		
	Lysosome	ATPase H+ transporting V0 subunit d1 Adaptor related protein complex 3 mu 1 subunit Adaptor related protein complex 3 mu 2 subunit Scavenger receptor class B member 2	**MAPK signaling pathway**	RAP1A, member of RAS oncogene family Interleukin 1 alpha Protein phosphatase 5 catalytic subunit Ras-related protein Rap-1A Ribosomal protein S6 kinase A5
	Chemokine signaling pathway	RAP1A, member of RAS oncogene family Mitogen-activated protein kinase kinase 1 Ras-related protein Rap-1A Stress induced phosphoprotein 1	**RNA degradation**	TNFRSF1A associated via death domain Chromodomain helicase DNA binding protein 4 LSM6 homolog, U6 small nuclear RNA and mRNA degradation associated RNA binding motif protein 22
	T cell signaling	T-cell immune regulator 1, ATPase H+ transporting V0 subunit a3 Squamous cell carcinoma antigen recognized by T-cells 1 Phosphatidylinositol-4,5-bisphosphate 3-kinase catalytic subunit gamma Phosphatidylinositol-5-phosphate 4-kinase type 2 gamma		

Table 11: Complete list of proteins differentially regulated in corresponding pathways in Ab4-wt and mutant viruses infected PBMC. PBMC were infected with Ab4-wt and mutants at MOI of 1. At 24 hpi, infected PBMC were sorted and proteomic analysis was performed. Pathways significantly upregulated and downregulated (based on *p*-value and Benjamini-corrected modified Fisher's exact test value) in infected PBMC in comparison healthy PBMC were given (n=4).

6.1.6 EHV-1 infection modulates cytokine and chemokine profiles of PBMC

Equine PBMC were infected with Ab4-wt and mutant viruses at 1 MOI of 1. Supernatants from infected PBMC were collected at 3, 6, and 24 hpi and the secreted cytokines/chemokines were quantified with luminex-based multiplex detection system. I have detected 12 cytokines in total, expressed by PBMCs (healthy and or EHV infected) out of 23 cytokines tested in the panel. All standards and quality controls were within the specified range. In general, release of most cytokines/chemokines was strongly inhibited upon Ab4-wt infection in PBMC. Only FGF-2 was expressed in infected PBMC at 6 hpi (Figure 16A and B; Table 12). In contrast, infecting PBMC with Ab4-mutant viruses restored cytokine/chemokine expression partially or completely, and showed expression of G-CSF, IL-1α, IL-1β, IL-8 and TNFα.

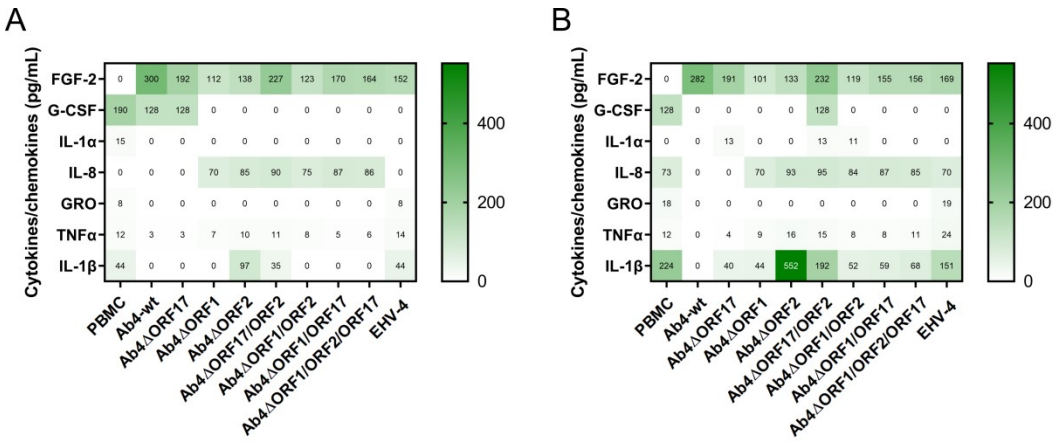

Figure 16: PBMC cytokine/chemokine profile at 3 and 6 hpi. Equine PBMC were infected with either Ab4-wt or mutant viruses or EHV-4 at MOI of 1. (A) At 3 and (B) 6 hpi supernatants were collected, cytokines and chemokines were quantified with luminex-based multiplex equine cytokine detection system. Mean concentration of cytokines/chemokines were given in picogram (pg) per ml (n=2).

At 24 hr, healthy PBMC released nine cytokine/chemokine, but Ab4-wt and Ab4ΔORF17 mutant infected PBMC released only four cytokine/chemokine (FGF-2, IL-8, TNFα and IL-1β) (Figure 17A; Table 12). Ab4ΔORF1 and Ab4ΔORF2 mutant infection restored release of several cytokines. Especially, ORF2 single deletion mutant showed release of more cytokines in higher quantity including IL-10, IL-8 and IL-1β. However, deletion of ORF17 together with ORF2 reduced the expression of cytokines (Table 12). All mutants with ORF1 deletion showed expression of more cytokines (Figure 17A). IFNγ levels was higher in all ORF1 deletion mutants. It is worthy to mention that FGF-2 expression was only observed in

infected PBMC and the that its concentration was always high in case of Ab4-wt, followed by ORF17/ORF2 and ORF17 deletion mutants at different time points.

We were interested in studying cytokine release profile of EHV-infected PBMC in the presence of EC. PBMC ($1x10^6$) were infected with EHV-1 (Ab4 or RacL11) or EHV-4 at MOI of 1. At 24 hpi, infected PBMC were applied over EC and supernatants were collected at 3 and 6 hr for cytokine estimation. In PBMC-EC co-culture, healthy PBMC released more cytokine than virus infected PBMC. Among virus infected PBMC, number of cytokines detected was the lowest for Ab4-wt (Fig. 17B). Furthermore, a difference in cytokine profile was observed when PBMC infected with different strains of EHV-1 (Ab4-wt vs RacL11), where RacL11-infected PBMC showed release of IP-10. In both PBMC infection and PBMC-EC co-culture, EHV-4 infected PBMC released more cytokines in higher concentration than EHV-1-infected PBMC. Overview of cytokine produced, cell source, targets and functions were given in Table 13.

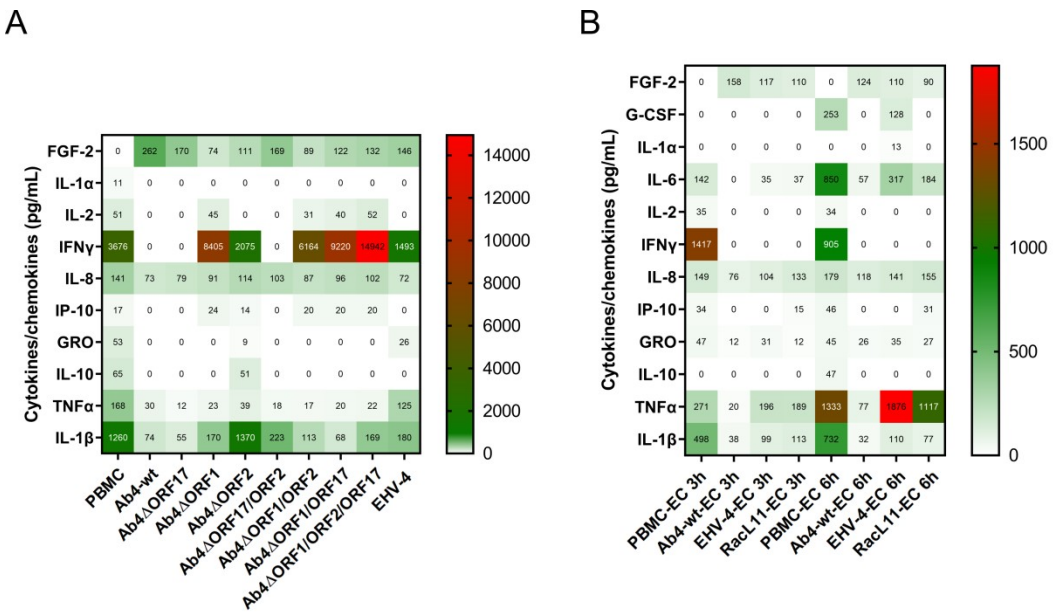

Figure 17: PBMC cytokine/chemokine profile at 24 hpi and PBMC-EC co-culture at 3 and 6 hr. (A) Equine PBMC were infected with Ab4-wt, mutant viruses, or EHV-4 at MOI of 1. At 24 hpi supernatants were collected and cytokines and chemokines were quantified with luminex-based multiplex equine cytokine detection system. (B) Equine PBMC were infected with Ab4-wt, RacL11, or EHV-4 at MOI of 1. Infected PBMC were collected and co-cultivated with EC, incubated for 3 and 6 hrs, supernatants were collected and cytokines/chemokines concentrations were measured. Mean concentration of cytokines and chemokines were given in pg per ml (n=2).

PBMC samples	Number of detected cytokines			Co-culture samples	Number of detected cytokines	
	3 hpi	6 hpi	12 hpi		3 hpi	6 hpi
PBMC	5	5	9	PBMC-EC	8	10
Ab4-wt	3	1	4	Ab4-wt-EC	5	6
Ab4ΔORF17	3	4	4	EHV-4-EC	6	8
Ab4ΔORF1	3	4	7	RacL11-EC	7	7
Ab4ΔORF2	4	4	8			
Ab4ΔORF17/ORF2	4	6	4			
Ab4ΔORF1/ORF2	3	5	7			
Ab4ΔORF1/ORF17	3	4	7			
Ab4ΔORF1/ORF2/ORF17	3	4	7			
EHV-4	4	5	6			

Table 12: Compiled cytokines/chemokines profiles.

Taken together, infection of PBMCs with Ab4-wt mostly downregulates cytokine expression and deletion of different viral genes (ORF1, ORF2 and ORF17) clearly altered the cytokine expression profile and restored cytokine expression partially at different time points. When compared with Ab4-wt, EHV-4 infected PBMCs expressed more cytokines. ORF2 gene deletion expressed higher level of IL-1β cytokine (proinflammatory) at all three time points.

Cytokine	Cell source	Targets	Functions	Reference
G-CSF	Monocytes, endothelial cells, fibroblasts	Stem cells in bone marrow	Granulocyte production	(293, 294)
IL-1α and IL-1β	Macrophages, B cells and dendritic cells	T and B cells, NK cells	Proinflammatory proliferation and differentiation, pyrogenic	(295, 296)
IL-2	$CD4^+$ and $CD8^+$ activated T cells, dendritic cells, NK cells	$CD4^+$ and $CD8^+$ T cells, B and NK cells	Proliferation of effector T and B cells, development of Treg cells, B and NK cells stimulation, proliferation and cytokine production in innate lymphoid cells	(297, 298)
IL-6	T and B cells, EC, monocytes, macrophages, granulocytes	Leukocytes, T and B cells, haematopoietic cells	Leukocyte trafficking and activation; T and B cell differentiation, activation and survival;	(299)
IL-8	Monocytes, macrophages, neutrophils, lymphocytes, EC, fibroblasts	T cells, neutrophils, NK cells, monocytes, endothelial cells,	Chemoattractant for T cells, neutrophils, NK cells, basophils, eosinophils, mobilization of haemotopoietic stem cells, angiogenesis	(300)

		eosinphils, mast cells		
IL-10	T and B cells, monocytes, macrophages and dendritic cells	Macrophages, monocytes, T and B cells, NK cells, DC	Immunosuppressive effect through antigen presenting cells,	(301)
TNFα	Activated macrophages, monocytes, CD^+ T cells, B cells, NK cells, neutrophils	Nucleated cells	Host defense, dual role as proinflammatory and immunosuppressive mediator	(302)
IFNγ	Macrophages, cytotoxic T lymphocytes, B cells, NK cells	Epithelial cells, macrophages, dendritic cells, NK cells, T and B cells	Antiviral properties, promotion of cytotoxic activity, T_H1 differentiation, upregulation of MHC class I and II, inhibition of cell proliferation, proapoptotic effects	(303)
GRO (growth related oncogene) CXCL1	Macrophages, neutrophils, epithelial cells	Leukocytes	Chemotaxis, inflammation, angiogenesis, tumor cell transformation, wound healing	(304, 305)
IP-10 (IFNγ-inducible protein) CXCL10	T and B cells, monocytes, EC, neutrophils, epithelium	Activated T and B cells, NK cells, dendritic cells, macrophages	Chemotaxis, proinflammatory, modulate angiogenesis and wound healing	(306-308)
FGF2	Cells of inflammation and immunity, T cells, mononuclear phagocytes, and EC	Autocrine action, EC, variety of tissues	Inflammation, neovascularisation, angiogenesis, wound healing	(309-312)

Table 13: Overview of cytokine produced, their cell source, targets and functions.

6.2 EHV-4 outbreak: Virological, molecular and serological investigations

6.2.1 The outbreak of EHV-4

During July 2017, an outbreak of a respiratory illness was reported in a group of foals and mares at a breeding farm in northern Germany. The outbreak was initiated upon intake of three breeding mares with unknown history of EHV-1 and EHV-4 status into the farm; however, this could be just a co-incidence. During the first week of the outbreak, 12 foals in a group of 25 foals showed clinical signs of mild to moderate respiratory illness. Molecular investigation by qPCR revealed EHV-4 infection in 11 out of the 12 foals. At the same time, two corresponding mares housed with the foals had mild respiratory signs and were tested also positive for EHV-4. Clinical signs in foals were largely restricted to the upper respiratory

tract, characterized by pyrexia, cough, nasal discharge and anorexia. The disease course in infected foals last for 7 to 14 days. Immediately after diagnosis, biosecurity measures were taken and management practices were implemented. Biosecurity measures to curtain the outbreak included movement restriction, different personnel for handing sick animals, and the use of disinfectant foot baths and hand sanitizers. Further, healthy animals that are already contacted the sick animals were monitored daily for clinical signs. However, EHV-4 infected horses have not been separated from healthy horses due to insufficient space to keep all infected horses in isolation pen. Infected and healthy horses shared common housing and feeding facilities in the farm throughout the period of disease outbreak Nasal swabs were regularly collected from infected and contact animals to identify any new infected animals and to study the outbreak pattern. In spite of strict biosecurity measures, during the second and third weeks after initial outbreak, the disease spreads to a nearby barn and several foals and mares showed mild to moderate respiratory illness and were confirmed EHV-4-positive. Disease outbreak was peaked between 2 to 8 weeks after initiation and lasts for 17 weeks (Figure 18; Table 14). Some apparently healthy mares also tested EHV-4 positive by qPCR and shed viruses through nostrils continuously for up to 8 weeks. It was surprising that some mares/stallions shed viruses through nostrils for long time (i.e. Mare_3, Stallion_6; Table 14) without any clinical signs in spite that mares were vaccinated against EHV-1 during 3rd, 5th and 8th months of pregnancy in addition to regular annual vaccination for mares and stallions. None of the unweaned foals were vaccinated before or at the time of outbreak. In total, nasal swabs were collected from 76 animals including 25 foals, 15 stallions, 34 mares and 2 geldings at different intervals (Table 14). Infected individuals (foals, mares and stallions) were tested maximum at five time points and minimum at two time points before they were tested negative for EHV-4 (Table 14). Ages of infected foals were ranged between 85 and 209 days with average of 125.5±32 days (Table 14). Among infected mares, 73% (8 out of 11) of mares and corresponding foals shedded virus at the same time. Most of the infected foals were in a physical contact with other foals, mares, and/or stallions, as groups were built for social contact very early (2-3 weeks after birth), which suggests direct contact as the mode of virus transmission during later phase of disease outbreak.

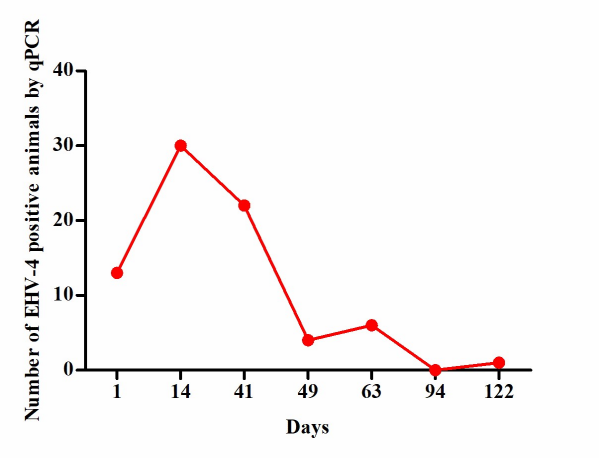

Figure 18: EHV-4 disease outbreak pattern in the equine stud. The number of EHV-4 qPCR positive animals during the period of the outbreak is shown.

S. No	Animal	Sex	Date of birth	Day 1	Day 3	Day 8	Day 10	Day 15	Day 22	Day 42	Day 46	Day 60	Day 95	Day 116
1.	Mare_1	Mare	02.04.2005	+	n/a	n/a	n/a	n/a	n/a	+	n/a	n/a	(-)	(-)
2.	Foal_1	Stallion	08.03.2017	++	n/a	n/a	n/a	++	n/a	(-)	n/a	+++	n/a	(-)
3.	Foal_2	Stallion	16.05.2017	+++	n/a	n/a	n/a	+	n/a	+	n/a	n/a	n/a	(-)
4.	Foal_3	Mare	26.05.2017	+	n/a	n/a	n/a	+	n/a	(-)	n/a	n/a	n/a	n/a
5.	Foal_4	Stallion	15.04.2017	+++ [a]	n/a	n/a	n/a	+	n/a	+	n/a	n/a	n/a	(-)
6.	Mare_2	Mare	17.01.2005	+	n/a	n/a	n/a	n/a	n/a	+	n/a	n/a	(-)	n/a
7.	Foal_5	Mare	18.03.2017	+++	n/a	n/a	n/a	++	n/a	++	n/a	n/a	n/a	(-)
8.	Foal_6	Stallion	20.04.2017	++	n/a	n/a	n/a	+	n/a	+	n/a	n/a	n/a	(-)
9.	Foal_7	Mare	24.05.2017	+	n/a	n/a	n/a	+	n/a	(-)	n/a	n/a	n/a	n/a
10.	Foal_8	Mare	16.05.2017	+	n/a	n/a	n/a	n/a	n/a	+	n/a	n/a	n/a	(-)
11.	Foal_9	Stallion	24.05.2017	+	n/a	n/a	n/a	+	n/a	(-)	n/a	n/a	n/a	n/a
12.	Foal_10	Mare	12.05.2017	(-)	n/a	n/a	n/a	n/a	n/a	(-)	(-)	n/a	n/a	n/a
13.	Foal_11	Mare	05.05.2017	++++ [a]	n/a	n/a	n/a	++	n/a	(-)	n/a	n/a	n/a	n/a
14.	Foal_12	Mare	21.04.2017	+++	n/a	n/a	n/a	+	n/a	(-)	n/a	n/a	n/a	n/a
15.	Mare_3	Mare	24.04.2016	n/a	+	+	n/a	++	+	n/a	+	+	n/a	(-)
16.	Stallion_1	Stallion	24.03.2013	n/a	(-)	n/a	n/a	n/a	n/a	n/a	n/a	n/a	n/a	n/a
17.	Gelding_1	Gelding	02.04.2012	n/a	(-)	n/a	n/a	n/a	n/a	n/a	n/a	n/a	n/a	n/a
18.	Gelding_2	Gelding	26.05.2012	n/a	(-)	n/a	n/a	n/a	n/a	n/a	n/a	n/a	n/a	n/a
19.	Mare_4	Mare	26.05.2015	n/a	(-)	n/a	n/a	n/a	n/a	n/a	n/a	n/a	n/a	n/a
20.	Mare_5	Mare	31.05.2014	n/a	(-)	n/a	n/a	n/a	n/a	n/a	n/a	n/a	n/a	n/a
21.	Stallion_2	Stallion	14.05.2014	n/a	(-)	n/a	n/a	n/a	n/a	n/a	n/a	n/a	n/a	n/a

22.	Mare_6	Mare	21.04.2014	n/a	(-)	n/a	n/a	n/a	n/a	n/a	n/a	n/a	n/a	n/a
23.	Stallion_3	Stallion	02.05.2014	n/a	(-)	n/a	n/a	n/a	n/a	n/a	n/a	n/a	n/a	n/a
24.	Stallion_4	Stallion	31.03.2016	n/a	n/a	+	n/a	n/a	(-)	n/a	(-)	(-)	n/a	n/a
25.	Stallion_5	Stallion	08.04.2016	n/a	n/a	+	n/a	n/a	(-)	n/a	(-)	(-)	n/a	n/a
26.	Stallion_6	Stallion	06.05.2016	n/a	n/a	++++[a]	n/a	n/a	+	n/a	+	+	(-)	n/a
27.	Stallion_7	Stallion	09.05.2016	n/a	n/a	+	n/a	n/a	+	n/a	(-)	(-)	n/a	n/a
28.	Stallion_8	Stallion	10.05.2016	n/a	n/a	+	n/a	n/a	(-)	n/a	n/a	n/a	n/a	n/a
29.	Stallion_9	Stallion	17.05.2016	n/a	n/a	++++	n/a	n/a	(-)	+	(-)	n/a	n/a	n/a
30.	Stallion_10	Stallion	23.05.2016	n/a	n/a	++++	n/a	n/a	+	(-)	n/a	n/a	n/a	n/a
31.	Stallion_11	Stallion	25.05.2016	n/a	n/a	+	n/a	n/a	(-)	(-)	(-)	(-)	n/a	n/a
32.	Stallion_12	Stallion	02.06.2016	n/a	n/a	+++	n/a	n/a	(-)	n/a	n/a	n/a	n/a	n/a
33.	Stallion_13	Stallion	10.06.2016	n/a	n/a	++++	n/a	n/a	(-)	n/a	(-)	(-)	n/a	n/a
34.	Mare_7	Mare	03.05.2016	n/a	n/a	(-)	n/a	n/a	(-)	n/a	n/a	n/a	n/a	n/a
35.	Mare_8	Mare	02.05.2016	n/a	n/a	(-)	n/a	n/a	(-)	n/a	n/a	n/a	n/a	n/a
36.	Mare_9	Mare	24.04.2016	n/a	n/a	(-)	n/a	n/a	(-)	n/a	n/a	n/a	n/a	n/a
37.	Mare_10	Mare	10.04.2016	n/a	n/a	(-)	n/a	n/a	(-)	n/a	n/a	n/a	n/a	n/a
38.	Mare_11	Mare	03.05.2016	n/a	n/a	(-)	n/a	n/a	(-)	n/a	n/a	n/a	n/a	n/a
39.	Foal_13	Stallion	27.04.2017	n/a	n/a	n/a	++++[a]	n/a	n/a	(-)	n/a	n/a	(-)	(-)
40.	Foal_14	Mare	06.06.2017	n/a	n/a	n/a	(-)	(-)	n/a	(-)	n/a	(-)	n/a	n/a
41.	Foal_15	Stallion	25.03.2017	n/a	n/a	n/a	n/a	+	n/a	+	n/a	++	n/a	(-)
42.	Foal_16	Stallion	11.03.2017	n/a	n/a	n/a	n/a	+	n/a	+	n/a	(-)	n/a	n/a
43.	Foal_17	Stallion	02.02.2017	n/a	n/a	n/a	n/a	+++	n/a	+	n/a	+	n/a	(-)
44.	Foal_18	Stallion	24.05.2017	n/a	n/a	n/a	n/a	++	n/a	(-)	n/a	n/a	n/a	n/a
45.	Foal_19	Mare	16.05.2017	n/a	n/a	n/a	n/a	+	n/a	n/a	n/a	n/a	n/a	(-)

46.	Foal_20	Stallion	12.05.2017	n/a	n/a	n/a	n/a	++	n/a	+	n/a	n/a	n/a	(-)
47.	Foal_21	Stallion	11.05.2017	n/a	n/a	n/a	n/a	+	n/a	(-)	n/a	n/a	n/a	n/a
48.	Mare_12	Mare	17.03.2005	n/a	n/a	n/a	n/a	n/a	n/a	+	n/a	n/a	(-)	(-)
49.	Mare_13	Mare	24.03.2006	n/a	n/a	n/a	n/a	n/a	n/a	(-)	n/a	n/a	(-)	(-)
50.	Mare_14	Mare	02.04.1999	n/a	n/a	n/a	n/a	n/a	n/a	+	n/a	n/a	(-)	(-)
51.	Mare_15	Mare	05.05.2004	n/a	n/a	n/a	n/a	n/a	n/a	+	n/a	n/a	(-)	+
52.	Mare_16	Mare	08.02.2006	n/a	n/a	n/a	n/a	n/a	n/a	(-)	n/a	n/a	(-)	(-)
53.	Mare_17	Mare	25.05.2010	n/a	n/a	n/a	n/a	n/a	n/a	(-)	n/a	n/a	(-)	(-)
54.	Mare_18	Mare	19.05.2011	n/a	n/a	n/a	n/a	n/a	n/a	(-)	n/a	n/a	(-)	(-)
55.	Mare_19	Mare	16.05.2002	n/a	n/a	n/a	n/a	n/a	n/a	(-)	n/a	n/a	(-)	(-)
56.	Mare_20	Mare	16.05.2007	n/a	n/a	n/a	n/a	n/a	n/a	(-)	n/a	n/a	(-)	(-)
57.	Mare_21	Mare	08.04.2012	n/a	n/a	n/a	n/a	n/a	n/a	(-)	n/a	n/a	(-)	(-)
58.	Mare_22	Mare	26.04.2010	n/a	n/a	n/a	n/a	n/a	n/a	+	n/a	n/a	(-)	(-)
59.	Mare_23	Mare	21.03.2009	n/a	n/a	n/a	n/a	n/a	n/a	+	n/a	n/a	(-)	n/a
60.	Mare_24	Mare	06.05.2004	n/a	n/a	n/a	n/a	n/a	n/a	+	n/a	n/a	(-)	(-)
61.	Mare_25	Mare	10.06.2011	n/a	n/a	n/a	n/a	n/a	n/a	+	n/a	n/a	(-)	n/a
62.	Mare_26	Mare	07.03.2012	n/a	n/a	n/a	n/a	n/a	n/a	(-)	n/a	n/a	(-)	n/a
63.	Mare_27	Mare	03.03.2004	n/a	n/a	n/a	n/a	n/a	n/a	(-)	n/a	n/a	n/a	n/a
64.	Mare_28	Mare	11.05.2007	n/a	n/a	n/a	n/a	n/a	n/a	+	n/a	n/a	(-)	n/a
65.	Mare_29	Mare	28.04.2007	n/a	n/a	n/a	n/a	n/a	n/a	(-)	n/a	n/a	(-)	n/a
66.	Mare_30	Mare	30.05.2008	n/a	n/a	n/a	n/a	n/a	n/a	(-)	n/a	n/a	(-)	n/a
67.	Mare_31	Mare	04.06.2006	n/a	n/a	n/a	n/a	n/a	n/a	(-)	n/a	(-)	(-)	n/a
68.	Mare_32	Mare	05.03.2010	n/a	n/a	n/a	n/a	n/a	n/a	(-)	n/a	n/a	(-)	n/a
69.	Mare_33	Mare	03.04.2001	n/a	n/a	n/a	n/a	n/a	n/a	+	n/a	(-)	(-)	n/a

70.	Foal_22	Mare	18.03.2017	n/a	n/a	n/a	n/a	n/a	n/a	(-)	n/a	n/a	n/a	n/a
71.	Foal_23	Mare	08.05.2017	n/a	n/a	n/a	n/a	n/a	n/a	(-)	n/a	n/a	n/a	n/a
72.	Foal_24	Mare	11.05.2017	n/a	n/a	n/a	n/a	n/a	n/a	+	n/a	n/a	(-)	n/a
73.	Foal_25	Mare	06.06.2017	n/a	n/a	n/a	n/a	n/a	n/a	(-)	n/a	(-)	n/a	n/a
74.	Stallion_14	Stallion	06.05.2003	n/a	n/a	n/a	n/a	n/a	n/a	(-)	n/a	n/a	n/a	n/a
75.	Stallion_15	Stallion	24.02.1998	n/a	n/a	n/a	n/a	n/a	n/a	(-)	n/a	n/a	n/a	(-)
76.	Mare_34	Mare	30.04.2013	n/a	n/a	n/a	n/a	n/a	n/a	(-)	n/a	n/a	(-)	n/a

Interpretation of C_T values: C_T < 20 = ++++; C_T 20.1-25 = +++; C_T 25.1-30 = ++; C_T 30.1 - 39 = +; C_T > 39 = Negative (-)

[a] Nasal swab samples from which EHV-4 virus have been isolated

n/a Not tested

Table 14: Summary of nasal swab sample collection and EHV-4 qPCR analysis. PCR was performed on DNA extracted from nasal swab samples collected from horses at different time points. Detail of individual animals and qPCR results for EHV-4 in nasal swab samples collected were interpreted.

6.2.2 Shedding of EHV-4 in infected animals

Nasal swabs were collected from foals, stallions and mares throughout the course of disease outbreak at different time points (Table 14). Virus shedding through nostril was investigated using qPCR. A C_T value of ≤ 39 was considered as positive for EHV-4 shedding. In total, 80% (20 out of 25) foals, 67% (10 out of 15) stallions and 32% (11 out of 34) mares were tested positive for virus shedding. Out of EHV-4 positive animals, 54% (22 out of 41) of horses shed viruses through nostrils (in nasal swabs) at more than one time point during the outbreak. Remaining 46% of animals showed virus shedding once and no EHV-4 viral DNA could be detected nasal swabs in later time points (Table 14). Fisher's exact test showed significant ($p<0.05$) higher rates of infection and virus shedding in foals and yearling stallions in comparison to mares. In addition, 75% infected foals showed virus shedding for 14 days on an average with typical course of EHV-4 infection, initially shed high virus load (low C_T values) followed by low virus load (high C_T values) and then the animal becomes negative for EHV-4 nucleic acids. However, some foals shed the virus for 6 to 9 weeks. In general, foals and mares with low C_T values shed viruses for long duration than those with high C_T values. Differences in clinical signs among those animals could not be correlated based on C_T values. Few foals (e.g. Foal_1, Table 14) became completely negative for virus shedding in 2 weeks after initial infection, but 6 weeks later showed secondary virus shedding with low C_T values (C_T = 23.9; 26.2) without any clinical signs.

6.2.3 Virus isolation

Virus isolation from infected animals (mares, stallions and foals) has been attempted on ED cells. Nasal swabs with low C_T values (< 25; n = 12; from 7 foals, 4 stallions and 1 mare) and low C_T values (25-30; n = 4; from 2 foals and 2 mares) were selected. In total, EHV-4 was isolated from 4 animals including one stallion (Stallion_6: EHV-4_DE17_1) and 3 foals (Foal_11: EHV-4_DE17_2; Foal_13: EHV-4_DE17_3; Foal_4: EHV-4_DE17_4). In all four cases, cytopathic effect characterized by rounding of the cells, syncytia formation and detachment begin to appear 48 hr post inoculation in passage 1 (Figure 19A, B and C). It is noteworthy to mention that virus isolation was successful from the four nasal swabs which had low C_T values (high virus titer) (Table 14). The virus could not be isolated from nasal swabs with high C_T values (C_T ≥ 25) even after five blind passages on ED cells. Indirect IF confirmed EHV-4 specific gD expression in infected cells in cell culture (Figure 19D).

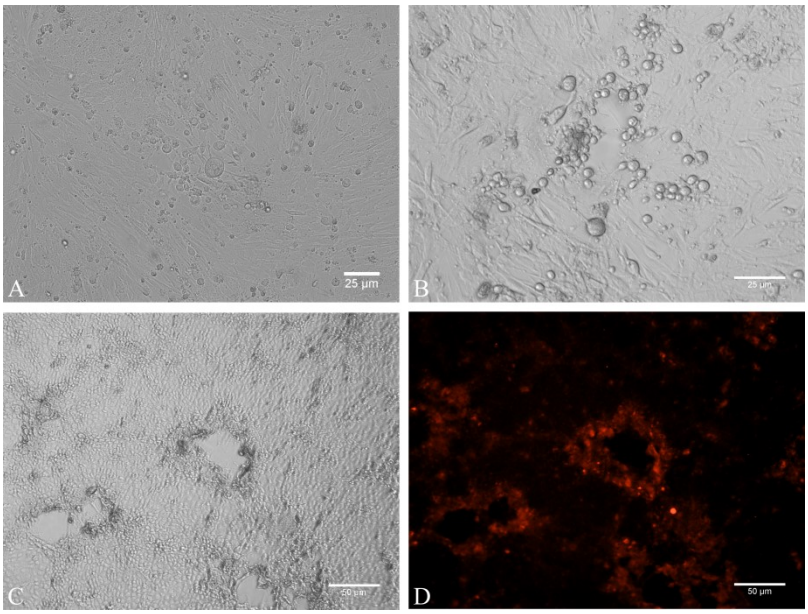

Figure 19: EHV-4 isolation in ED cells. (A-C) CPE caused by EHV-4 on ED cells characterized by rounding of cells and syncytia formation at 24 hrs post infection. (D) Indirect immunofluorescence staining of EHV-4-infected cells from (C) to detect gD expression in EHV- at 24 hpi. Red: gD stained with primary anti-gD antibodies and secondary Alex Fluor-568 antibody.

6.2.4 Serology

VNT and EHV-4 gG-peptide based-ELISA were performed on paired serum samples collected from 24 mares and the corresponding 24 foals. VNT revealed that none of the foals had neutralizing antibodies against EHV-4 at the time of outbreak (2nd week), and only 3 foals (12.5%) were subsequently sero-converted at 9th week (with non-protective antibody titre, <1:64) (Figure 20A and B; Table 15). In contrast, all mares had neutralizing antibodies at the time of outbreak (antibody titre of >1:8), and 58.33% of mares had protective antibody titre (≥1:64) against EHV-4. None of the mares were sero-converted at the end of the outbreak. Peptide ELISA showed that all tested foals and corresponding mares had specific antibody against gG of EHV-4 at the time of outbreak (Figure 21A and B; Table 15) and persisted till the end of disease outbreak without major change. Serological response to EHV-4 infection determined using gG peptide ELISA results were compared with standard virus neutralization test. Mares already had EHV-4 specific neutralizing antibodies in serum which might be due to previous infection and or vaccination. All foals had detectable EHV-4 specific antibodies in serum and only few foal had antibodies with virus neutralizing titre which could be due to delayed onset of neutralizing antibody production and/ or interference of maternally derived antibodies.

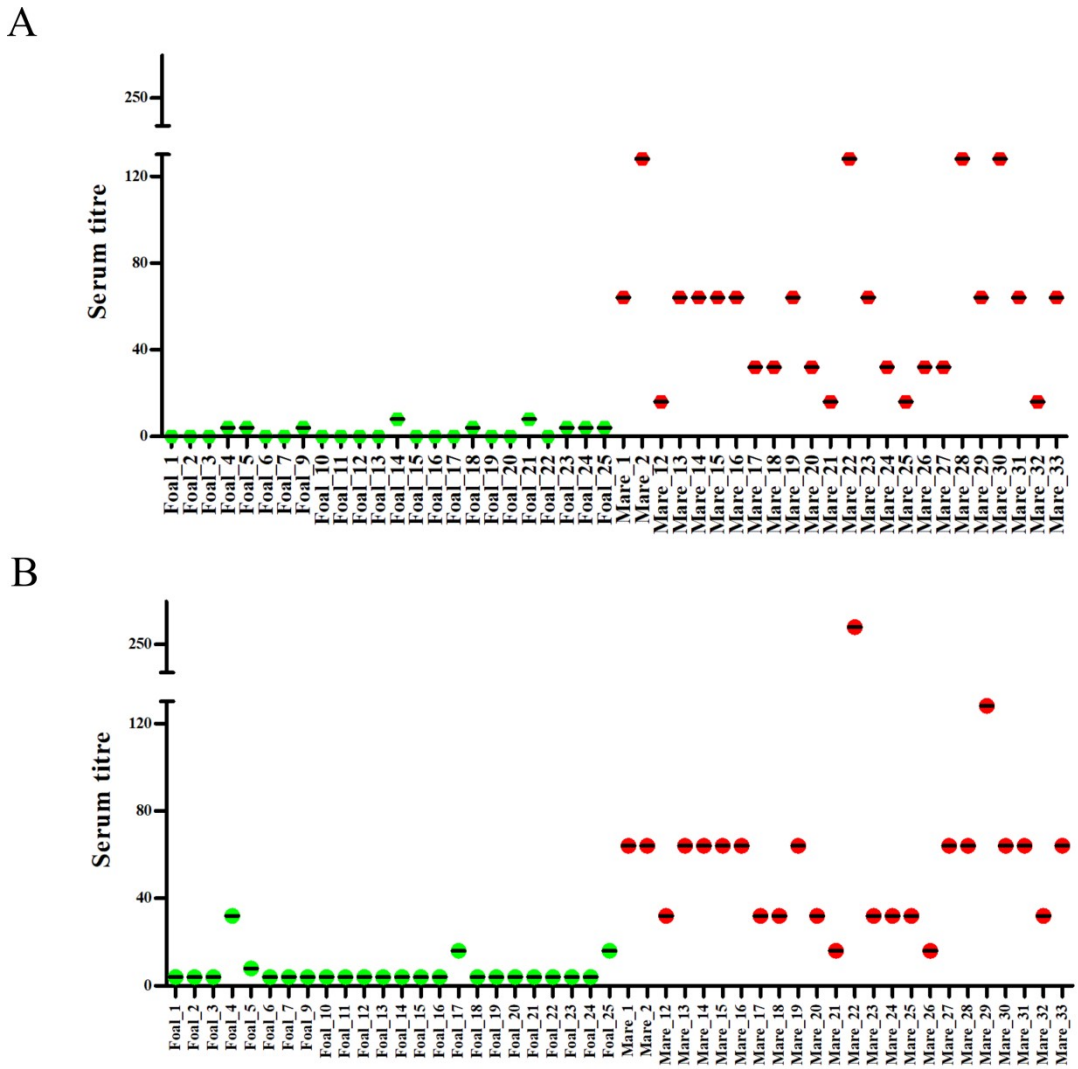

Figure 20: Virus neutralization assay in paried equine serum samples. Serum antibody titre against EHV-4 at the time of outbreak [Second week] (A) and after the outbreak period [Ninth week] (B). Green: Foals and Red: Mares.

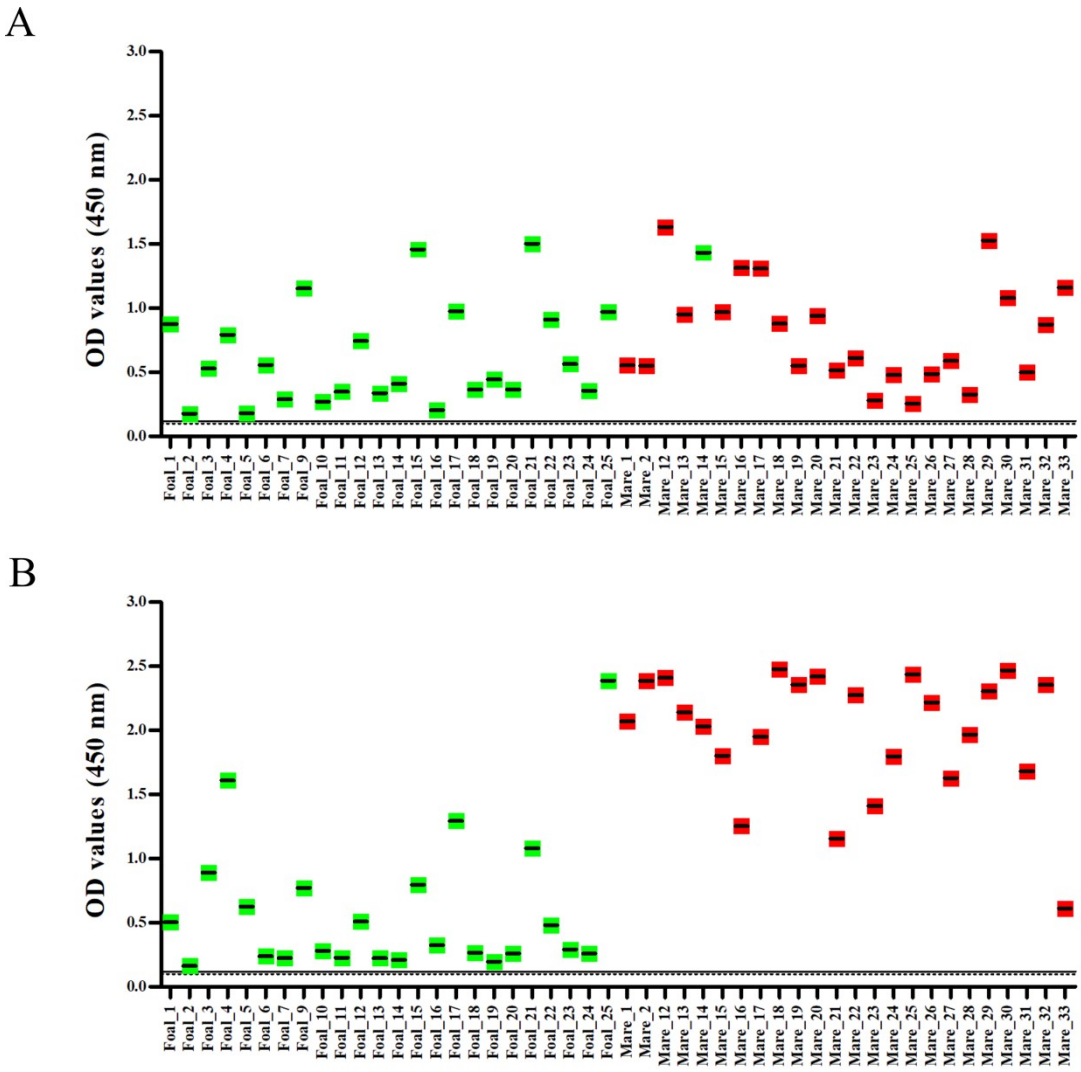

Figure 21: EHV-4 gG-peptide based-ELISA in paried equine serum samples. Average OD values of serum antibody against gG of EHV-4 at the time of outbreak [Second week] (A) and post outbreak period [Ninth week] (B). Green: Foals and Red: Mares. Continuous line and dotted lines are cut off for questionable and negative for EHV-4 antibodies, respectively.

Animals	Number of samples	VNT				ELISA			
		2nd week		9th week		2nd week		9th week	
		Positive	Negative	Positive	Negative	Positive	Negative	Positive	Negative
Foals	24	0	24	3	21	24	0	24	0
Mares	24	24	0	24	0	24	0	24	0
Total	48	24	24	27	21	48	0	48	0

Table 15: Summary of VNT and gG peptide ELISA results in paired equine serum samples. Serum samples were collected at and after EHV-4 disease outbreak. VNT and

ELISA were performed, and result summary in terms of number of animals positive and negative for each assay was given

6.2.5 RFLP analysis for EHV-4 genomic DNA

The *Bam*H1 digestion of genomic DNA from the four isolates of EHV-4 (DE17_1-4) revealed four different restriction patterns. By comparing the restriction profiles obtained in this study, including the reference isolate (T252), I could able to conclude that all four isolates were distinct from each other's (Figure 22). The digestion profiles of the isolates were different from those of the reference strain due to the presence of different size fragments approximately between 8 and 9 kb. Isolate 1 (DE17_1) had a fragment at 8.5 kb, isolate 2 (DE17_2) had at 8 kb, isolate 3 (DE17_3) had at 9 kb and isolate 4 (DE17_4) had two bands at 8.5 and 9 kb positions. RFLP prediction with the available whole EHV-4 genome (Genbank accession: KT324742.1[virus isolate from Australia] and NC_001844.1[virus isolate from United Kingdom]) revealed that the fragment of the 8.5 kb size is between genome sequences of 42,867 and 51,555 bp size, which code, partially, very large tegument protein (ORF24: 36,006 bp - 46,610 bp), Capsid protein (ORF25: 47,068 bp – 46,610 bp), Membrane associated phosphoprotein (ORF26: 47,980 bp – 47,156 bp), DNA packaging proteins (ORF27 and 28: 48,543 bp – 50,365 bp), uncharacterized protein (ORF29: 50358 bp – 51,338 bp) and, partially, DNA polymerase protein (ORF30: 54,924 bp – 51,262 bp). Differences in restriction profile reflects changes in the sequence of genes listed above, however, correlation between changes in RFLP pattern and its implication in viral protein production needs to be studied. Further, none of the four isolates had a fragment of approximately 18 kb, which was only observed with the reference virus strain (T252).

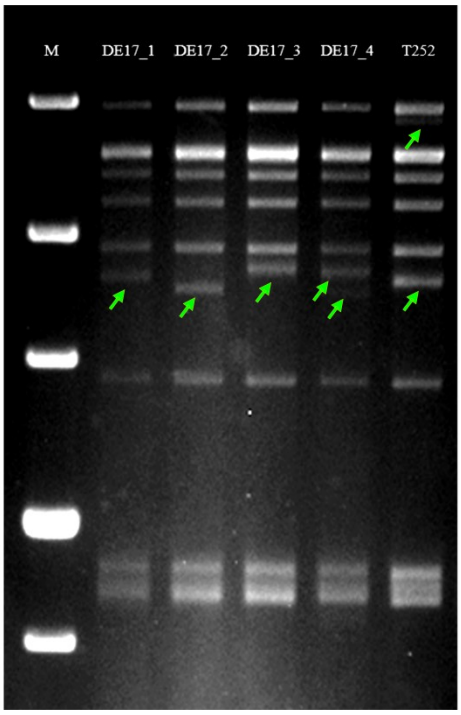

Figure 22: RFLP analysis for EHV-4 isolates. The *Bam*H1 digestion of genomic DNA from the four isolate of EHV-4 (DE17_1-4) and reference isolate (T252). For RFLP, 1.5 µg of viral DNA was digested with *Bam*H1 for 4 hrs at 37 ºC and separated on 0.8% agarose gel by electrophoresis at 60 Volt for 16 hr. M – marker (1 kb plus DNA ladder). Green arrow – differences in DNA fragments size.

6.2.6 Phylogenetic analysis of EHV-4 isolates

Whole ORF30 gene and partial gB gene of EHV-4 isolates were successfully PCR amplified. By sequencing of ORF30 and gB genes, all four of my isolates possessed the same nucleotide sequence. All sequence obtained for ORF30 and gB showed almost 99% similarity with EHV-4 sequences published in Genbank. Phylogenetic analysis for ORF30 was performed on total of 22 isolates and strains of EHV-4 including the four German isolates from the current study, 10 isolates from Australia, 6 isolates from Japan, and one each from USA and Ireland. They clustered into 2 groups, I and II (Figure 23A). The genome sequences of the 23 isolates and strains appeared to be very similar, especially in group II. My four German isolates clustered into group I. My isolates were closely related to viruses from Australia and Japan. The structure of the gB tree was constructed on total of 19 isolates [4 German isolates (from current study), 2 Ireland isolates, 1 USA isolate, 6 Australian isolates and 6 Japanese isolates). The gB tree clustered all four German isolates into group II and the remaining all 15 isolates into group I (Figure 23B). All 15 isolate sequences available in online as mentioned earlier had the same gB sequence, but, my four

isolates had a single nucleotide change at position 624 (61280 of genome) from T to C. However, biological relevance and significance of this point mutation in surface glycoprotein need to studied in future. In addition, phylogenetic analysis for gG was performed on total of 20 isolates and strains of EHV-4 including the four German isolates from the current study, 7 isolates from Australia, 6 isolates from Japan, and one each from USA, United Kingdom and Ireland. My four isolates clustered into viruses from Ireland, Japan and Australia (Group I; Figure 23C).

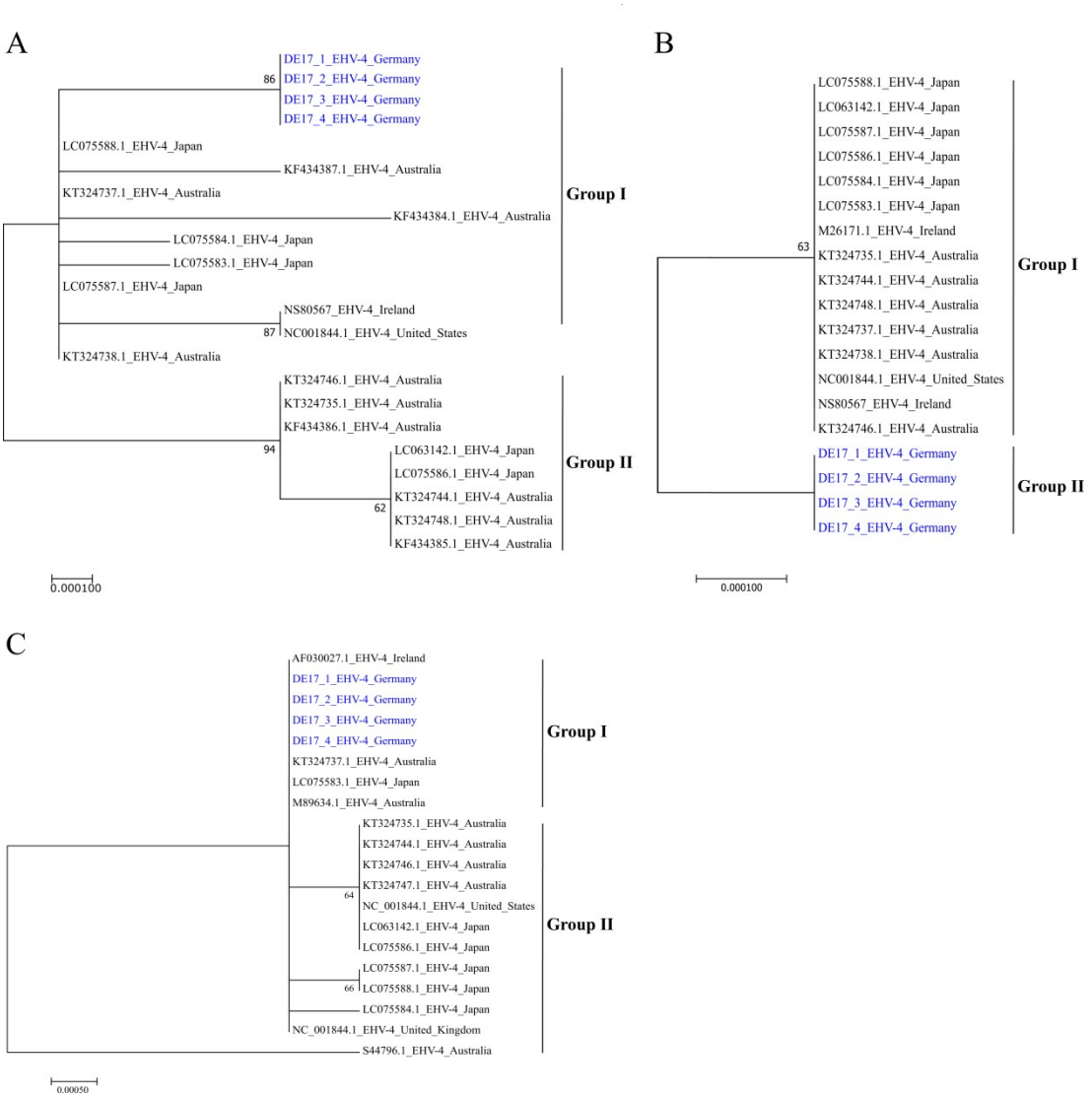

Figure 23: Phylogenetic analysis of EHV-4 isolates isolated from infected equines. Phylogenetic tree constructed by the maximum-likelihood method using full ORF30 gene (A), partial gB gene (B) and gG gene (C) sequence of EHV-4. GenBank accession numbers are indicated with country of origin. EHV-4 sequences from current study were indicated in blue.

6.3 Fatal EEHV-1 infection in two young Asian elephants: Virological and molecular investigations

6.3.1 Hemorrhagic lesions in all organs

Necropsy was performed immediately after death of both elephants and post-mortem lesions were recored. At necropsy, gross examination revealed severe vascular lesions in all organs, as seen in Figure 24A–F. Prominent pathological changes were extensive haemorrhages in heart, skeletal muscles, small and large intestines, and lung. The heart showed severe and generalized endocardial and myocardial congestion, as seen in Figure 24A and B. Abdominal cavity revealed ascites with sero-sanguineous fluid accumulation (about five liters). Hemorrhages in skeletal muscles, congestion of mucosal surface of trunk, pharynx, larynx and lung, subcutaneous edema, and cyanosis of tongue were important findings, as seen in Figure 24C–F. In addition to pericardial effusion, diffuse petechial hemorrhages were observed on the serosal surfaces of stomach, intestine, mesentery, omentum, urinary bladder, and abdominal wall. Small and large intestine mucosal surfaces were edematous, hemorrhagic, and congested. Post-mortem lesions were very similar in both deceased elephants.

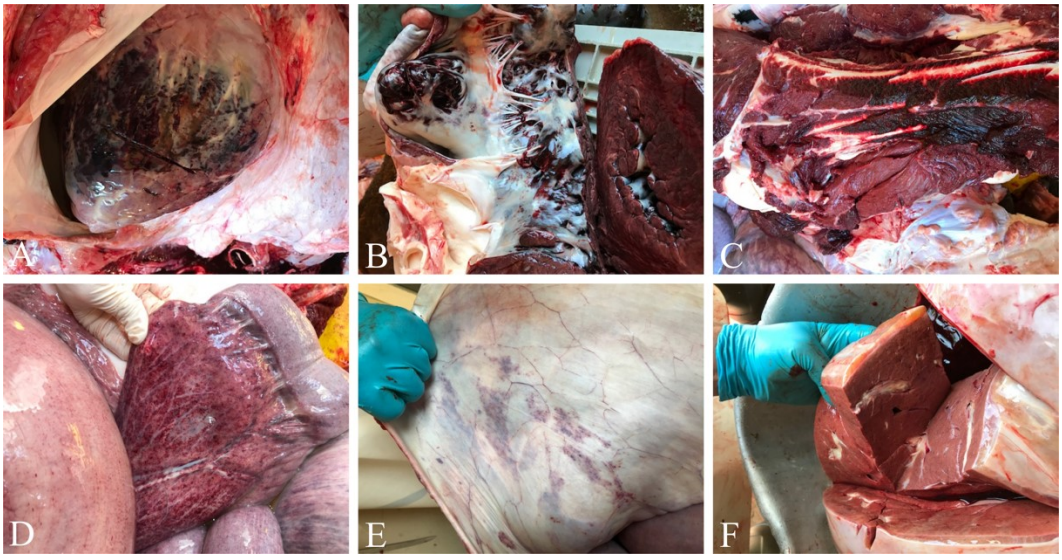

Figure 24: Gross pathology of EEHV-1 infected elephants. Necropsy of elephant endotheliotropic herpesvirus (EEHV-1A)-infected elephants. Post-mortem examination revealed severe petechial hemorrhages on the epicardial and endocardial surface of the heart with accumulations of sero-sanguinous fluid in the pericardium (A and B). Intermuscular hemorrhages in skeletal muscles (C), petechial hemorrhages in the mesentery (D) and thoracic wall (E), and peri-hepatic gelatinization of fat (F) were common findings. Picture was taken from publication (313).

6.3.2 Extensive distribution of virus in all organs

DNA was extracted from all collected tissues and blood, and qPCR analysis was performed. Because the virus is endotheliotropic in nature and viremia is the common finding during infection, it was expected that all tissues would be positive for EEHV-1. However, I have surmised that quantification of viral genome copies in each tissue might help in understanding predilection sites for virus replication. Thirty-eight samples were collected from the infected elephants “Kanja” and “Anjuli” and qPCR analysis was performed. All tissues were positive for EEHV-1 and most of tissues had virus genome copies in the range of 10^6–10^8 copies per million cells, as seen in Table 16. Viral DNA load was very high in bone marrow, heart, liver, urinary bladder, trunk, axillar lymph node (LN), tongue, and muscle with a range of $3.17 \times 10^8 - 5.11 \times 10^7$ copies per million cells. All remaining samples had virus genome copies between 4×10^7–1.5×10^6 per million cells. Inguinal LN, gall bladder, cerebellum, and prescapular LN had the lowest range of viral genome copies ($5.25 \times 10^3 - 8.72 \times 10^4$ copies per million cells). Viral DNA load in tissues from “Kanja” was almost similar and within a comparable range without much difference.

Tissues	Normalized viral genome copies	Tissues	Normalized viral genome copies
Bone marrow	3.17×10^8	Lung	1.19×10^7
Heart	2.25×10^8	Temporal gland	1.15×10^7
Liver	1.65×10^8	Colon	1.00×10^6
Urinary bladder	9.49×10^7	Adrenal gland (left)	7.00×10^5
Trunk	6.79×10^7	Uterus	5.62×10^5
Axillar LN	6.71×10^7	Mesenteric LN	5.55×10^5
Tongue	5.36×10^7	Adrenal gland (right)	5.25×10^5
Muscle	5.11×10^7	Thymus	3.81×10^5
PBMC	4.04×10^7	Thyroid	3.46×10^5
Cervical LN	3.98×10^7	Cerebrum	3.44×10^5
Tonsils	3.04×10^7	Small intestine	3.17×10^5
Mammary gland	2.97×10^7	Kidney	2.68×10^5
Stomach	2.89×10^7	Pancreas	2.37×10^5
Trunk mucosa	2.88×10^7	Spinal cord	2.50×10^5
Spleen	2.87×10^7	Salivary gland	1.53×10^5
Mandibular LN	2.34×10^7	Prescapular LN	8.72×10^4
Aorta	1.69×10^7	Cerebellum	7.79×10^4
Blood vessel	1.46×10^7	Gall bladder	7.05×10^4

Blood	1.37×10^7	Inguinal LN	5.25×10^3

Table 16: qPCR of the terminase gene of EEHV-1 in collected tissue samples. Normalized viral genome copies in various tissue samples collected from the infected elephant “Anjuli” at necropsy were given. Mean values of viral genome copies were calculated from two replicates for each sample.

6.3.3. Trials of virus isolation in cell culture revealed limited virus replication

Attempts has been made to isolate EEHV-1A in cell culture. For which, tissue (tongue, spleen, and whole blood; “Kanja”) homogenates and infected PBMC from “Kanja” and “Anjuli” were inoculated into 10 different cell lines and the PBMC collected from the healthy elephant “Tanja”. Upon inoculation, cells were observed daily for the presence of CPE. As no CPE was observed, cells were blindly passaged continuously five times. qPCR analysis and indirect IF were performed to assess the infectivity and replication of the virus. qPCR analysis revealed limited replication of EEHV-1 in ENL-2 (elephant) cells, endothelial (equine) cells, CrFK (feline) cells, and 293T (ND10-knocked down, human) cells until passage 3, as seen in Tables 17 and 18. Interestingly, elephant fibroblast cells (ENL-2) supported virus replication and maintained viral nucleic acids until passage 4 when co-cultured with infected PBMC (from both “Kanja” and “Anjuli”). Indirect IF results confirmed expression of EEHV-1 gB in cell cultures. The positive immunofluorescence signals in ENL-2 cells, CrFK cells, and elephant PBMCs at 96 h post-infection revealed that these cells were infected by the virus and further supported virus replication and late protein expression to some extent, as seen in Figure 25A–J. Although the virus infected these cells, no clear CPE was observed at any passage, and the cells did not support virus replication beyond passage 4. On the other hand, tissue samples inoculated on MDCK II, Vero, ED, RK-13, BD, HrT-18G cells did not support EEHV-1 replication after the first passage as all inoculated samples tested negative for EEHV-1 DNA in qPCR.

Tissue	Cell Line	Pass 1		Pass 2		Pass 3		Pass 4		Pass 5	
		Cell	Sup	Cell	Sup	Cell	Sup	Cell	Sup	Cell	Sup
Tongue “Kanja”	ENL-2	12775	136614	2018	5128	-	212	-	-	-	-
PBMC “Kanja”	ENL-2	1944	4233	110	301	-	-	-	56	-	-
PBMC “Anjuli”	ENL-2	36011	27753	-	604	91	1279	-	538	-	-
	PBMC	19873	15322	976	392	-	-	-	-	-	-

Table 17: qPCR of the terminase gene of EEHV-1 in infected ENL-2 and elephant PBMC co-culture. qPCR was performed on DNA extracted from cell cultures (cells and supernatant separately) after inoculation with tissue samples from infected elephants from passage 1 to passage 5. Mean values of viral genome copies for each sample were calculated from two replicates. Pass: Passage; Cell: cell pellet; Sup: supernatant; -: negative.

Tissue	Cell Line	Pass 1		Pass 2		Pass 3		Pass 4		Pass 5	
		Cell	Sup	Cell	Sup	Cell	Sup	Cell	Sup	Cell	Sup
Tongue "Kanja"	CrFK	30	25	37	32	-	-	-	-	-	-
	MDCK II	32	25	-	37	-	-	-	-	-	-
	Vero	29	23	-	34	-	-	-	-	-	-
	BD	32	28	-	32	-	-	-	-	-	-
	RK-13	31	25	-	37	-	-	-	-	-	-
	293T	31	26	37	33	-	38	-	-	-	-
	ED	30	24	-	32	-	-	-	-	-	-
	EC	29	24	36	31	-	37	-	-	-	-
PBMC "Kanja"	CrFK	33	31	-	37	-	-	-	-	-	-
	MDCK II	34	31	-	38	-	-	-	-	-	-
	Vero	31	31	-	-	-	-	-	-	-	-
	BD	35	36	-	37	-	-	-	-	-	-
	RK-13	34	31	37	-	-	-	-	-	-	-
	293T	34	32	-	-	-	-	-	-	-	-
	ED	36	34	37	36	-	-	-	-	-	-
	EC	32	31	35	35	-	37	-	-	-	-
Blood "Kanja"	CrFK	38	29	-	-	-	-	-	-	-	-
	MDCK II	-	30	-	-	-	-	-	-	-	-
	Vero	38	29	-	-	-	-	-	-	-	-
	BD	38	35	-	38	-	-	-	-	-	-
	RK-13	-	30	-	-	-	-	-	-	-	-
	293T	38	30	-	38	-	-	-	-	-	-
	ED	-	29	-	-	-	-	-	-	-	-
	EC	33	29	-	35	-	-	-	-	-	-
Spleen "Kanja"	CRFK	32	25	-	33	-	-	-	-	-	-
	MDCK II	34	26	-	35	-	-	-	-	-	-
	Vero	33	26	-	36	-	-	-	-	-	-
	BD	33	28	-	33	-	-	-	-	-	-
	RK-13	31	25	-	36	-	-	-	-	-	-
	293T	32	26	-	34	-	-	-	-	-	-
	NBL-6	34	25	-	34	-	-	-	-	-	-
	EC	37	25	-	36	-	-	-	-	-	-

PBMC "Anjuli"	HrT-18G	29	29	38	38	-	-	-	-	-	-

Table 18: qPCR of the terminase gene of EEHV-1 in infected cultures. qPCR was performed on DNA extracted from cell cultures (cells and supernatant separately) after inoculation with tissue samples from infected elephants from passage 1 to passage 5 and C_T values were given. Pass: Passage; Cell: cell pellet; Sup: supernatant; -: negative.

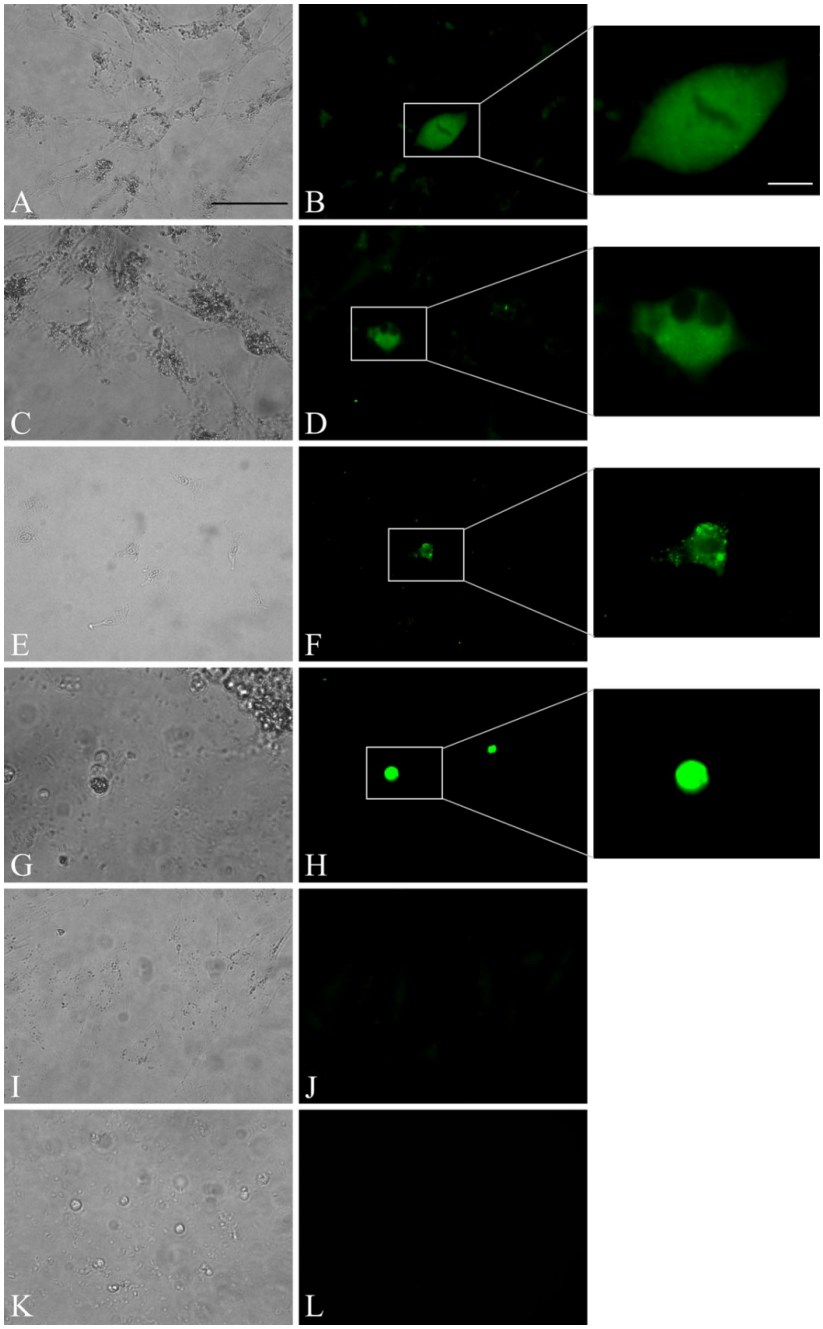

Figure 25: Indirect-IF for EEHV-1 infected staining of EEHV-1 gB 96 hpi. Indirect IF revealed expression of gB of EEHV-1 in ENL-2, CrFK, PBMC inoculated with tongue

homogenate. (A, C, E and G) Bright green IF-staining of cytoplasm of the EEHV-1 infected ENL-2 (A and C), CrFK (E), and PBMC (G). (B, D, F and H) Corresponding bright-field images for A, C, E and G. (I and K) Uninfected negative control staining shows no IF signals for ENL-2 (I) and healthy PBMC (K). (J and L) Corresponding bright-field images for I and K. Scale bar is 50 µm. Inserts: magnification of corresponding positive immunofluorescence signals. Insert scale bar is 10 µm. Picture was taken from publication (313).

6.3.4. Expression and cleavage of gB

SDS-PAGE was performed for protein lysates obtained from frozen tongue tissues of EEHV-1 infected elephant “Kanja”. A signal of the band corresponding to the predicted gB protein size of 100 kDa was observed using Ab7123 antibodies (recognizing the peptide sequence located between amino acids (aa) 427 and 441 of gB), as seen in Figure 26A. A second band of 55 kDa was observed when Ab7125 antibodies (recognizing the peptide sequence located between aa 259 and 274 of gB) were used, as seen in Figure 26B. The predicted size of the EEHV-1 gB gene is 2553 bp, which encodes a 97 kDa protein (850 aa). However, when I have performed WB from infected tissue homogenates using two different antibodies raised against different regions of gB (aa259–274 and aa427–441), I have observed two bands with different sizes. I have performed a prediction (ProP v.1.0b ProPeptide Cleavage Site Prediction) for the presence of possible protease cleavage sites, which revealed the presence of a furin recognition motif (^{433}RRKR^{436}) recognized by cellular propeptide protease and can lead to the cleavage of gB into two subunits of 50.5 and 46.5 kDa, as seen in Figure 27. Further analysis of available gB sequences of other EEHVs from GenBank revealed the presence of one or two furin cleavage sites in a similar fashion: one motif in EEHV-1B (^{429}RRKR^{432}), EEHV-5 (^{416}RKKR^{420}), and EEHV-6 (^{429}RRKR^{432}) and two motifs in EEHV-4 (^{26}RGVR^{29} and ^{447}RTKR^{450}). The Ab7125 antibodies were raised against the peptide sequence ^{259}EPSTKFKVYKDYERLQ^{274}, whereas Ab7123 antibodies were raised against the peptide sequence ^{427}ANVTSRRRKRDANTA^{441} covering the furin cleavage site in gB of EEHV-1 (Uniprot: Q8JTJ0). Hence, Ab7125 antibodies detected the cleaved *N*-terminal part of gB while Ab7123 antibodies detected uncleaved gB, as evidenced by the 55 kDa and 100 kDa bands, respectively. Further, non-denaturing native SDS-PAGE yielded gB-specific bands of around 60 kDa and 120 kDa with both Ab7123, as seen in Figure 26C, and Ab7125, as seen in Figure 26D.

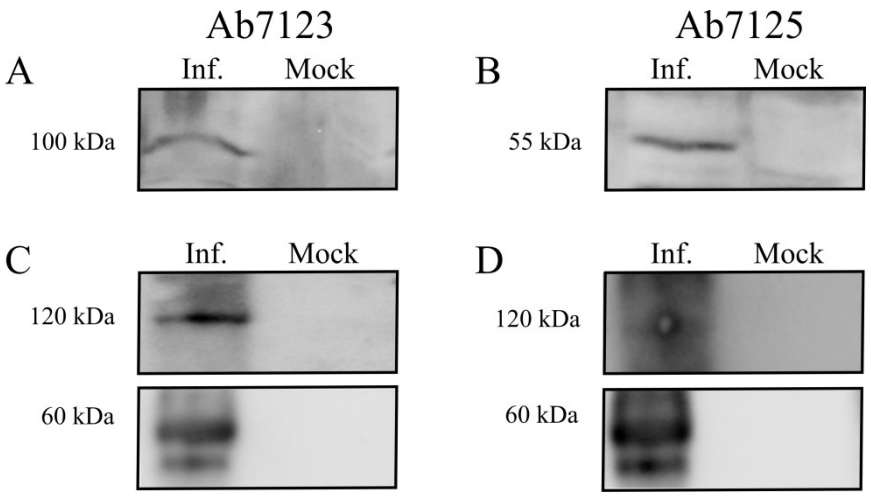

Figure 26: Western blot analysis for EEHV-1 infected tissues. (A and B) Western blot analysis was performed under reducing conditions using antibodies raised against EEHV-1 gB (Ab7123 and Ab7125). Ab7123 (A) reacted with a band of 100 kDa (uncleaved gB) while Ab7125 (B) detected cleaved gB with a size of 55 kDa. (C and D) Western blot under non-reducing conditions, in which both Ab7123 and Ab7125 reacted with proteins of 120 kDa and 60 kDa size. Cropped western blot images given in C and D were from the same gel and probed with Ab7123 and Ab7125, respectively. Inf. – infected tissue, Mock – healthy tissue. Picture was taken from publication (313).

```
                                  10         20         30         40         50
EEHV-1A gB_Liver     MSFTDQTYTR SCMHTCITHD PR-------- ----AYHIGF VLLMLLLNNN
EEHV-1A gB_Q77JN0    MSFTDQTYTR SCMHTCITRD HR-------- ----LYGIVI ISLLLLLDN-
EEHV-1B gB_G3FDU8    MSFTDQTYTR SCMHTCITRD HR-------- ----LYGIVI ISLLLLLDN-
EEHV-5  gB_N0D279    --------TR SCMRTCITRR PR-------- ----RVTVLF FTIVIFSDL-
EEHV-6  gB_G3FDV0    MSFMDPIYTQ SCMRTCMTRD CH-------- ----ICRFTF LLLTLLLN--
EEHV-4  gB_A0S1TP73  MWCTGRTCTR SCTRTCLTSR RSGSRRGVRA VVLSRYWLAI MTTTACVLTN

                                460        470        480        490        500
EEHV-1A gB_Liver     TSRRRKRDTN AANAASAKGI YDLYADLNVA QVQFAFNTLR TYINQALMSI
EEHV-1A gB_Q77JN0    TKHRRKRETS SSASS--KGI YDLYGDLNVA QVQFAFNTLK SYINQALMSI
EEHV-1B gB_G3FDU8    TKHRRKRETS SSASS--KGI YDLYGDLNVA QVQFAFNTLK SYINQALMSI
EEHV-5  gB_N0D279    TNIRKKREAK QSSAS-NKGI YDLYGDLNVA QVQYAFNTLR TYINQALTSI
EEHV-6  gB_G3FDV0    TKQRRKRDVS NTNPN-AKGI YDLYGDLNVA QVQFAFNTLR AYINHALMSI
EEHV-4  gB_A0S1TP73  TS-RTKRDTS QSVTR--GDL YDQFLDLSVA QVQFAYDTIR SYINQALTNI
```

Figure 27: Furin cleavage site prediction among other gBs of EEHVs. Red boxes mark the predicted furin cleavage sites. EEHV-1A gB_Liver: gB sequence obtained from the current study. Picture was taken from publication (313).

6.3.5. Transmission electron microscopy (TEM) revealed intranuclear and intracytoplasmic viral particles

For the detection of EEHV-1 virions, liver, tongue, and spleen tissues were ultrastructurally examined. Within hepatic endothelial cells, cytoplasmic and intranuclear virus particles were detected, as seen in Figure 28A. Intranuclear virus particles (empty and DNA-containing nucleocapsids) were found at the marginal zone of the endothelial nucleus. In addition, a large number of virus particles was accumulated within and around an electron-dense cytoplasmic matrix, which was located in close proximity to the cell nucleus, as seen in Figure 28B. The electron-dense cytoplasmic matrix contained nucleocapsids with electron-dense and electron-lucent cores. The capsids measured approximately 80 nm and the cores 60 nm in diameter. At the periphery of the electron-dense cytoplasmic body, tegument formation was visualized around the nucleocapsids and the empty capsids, as seen in Figure 28C–F. Virus particles with tegument had a diameter of approximately 120 nm. Tongue and spleen tissues also showed ultra-structural lesions along with virus like particles in the cytoplasm of endothelial cells.

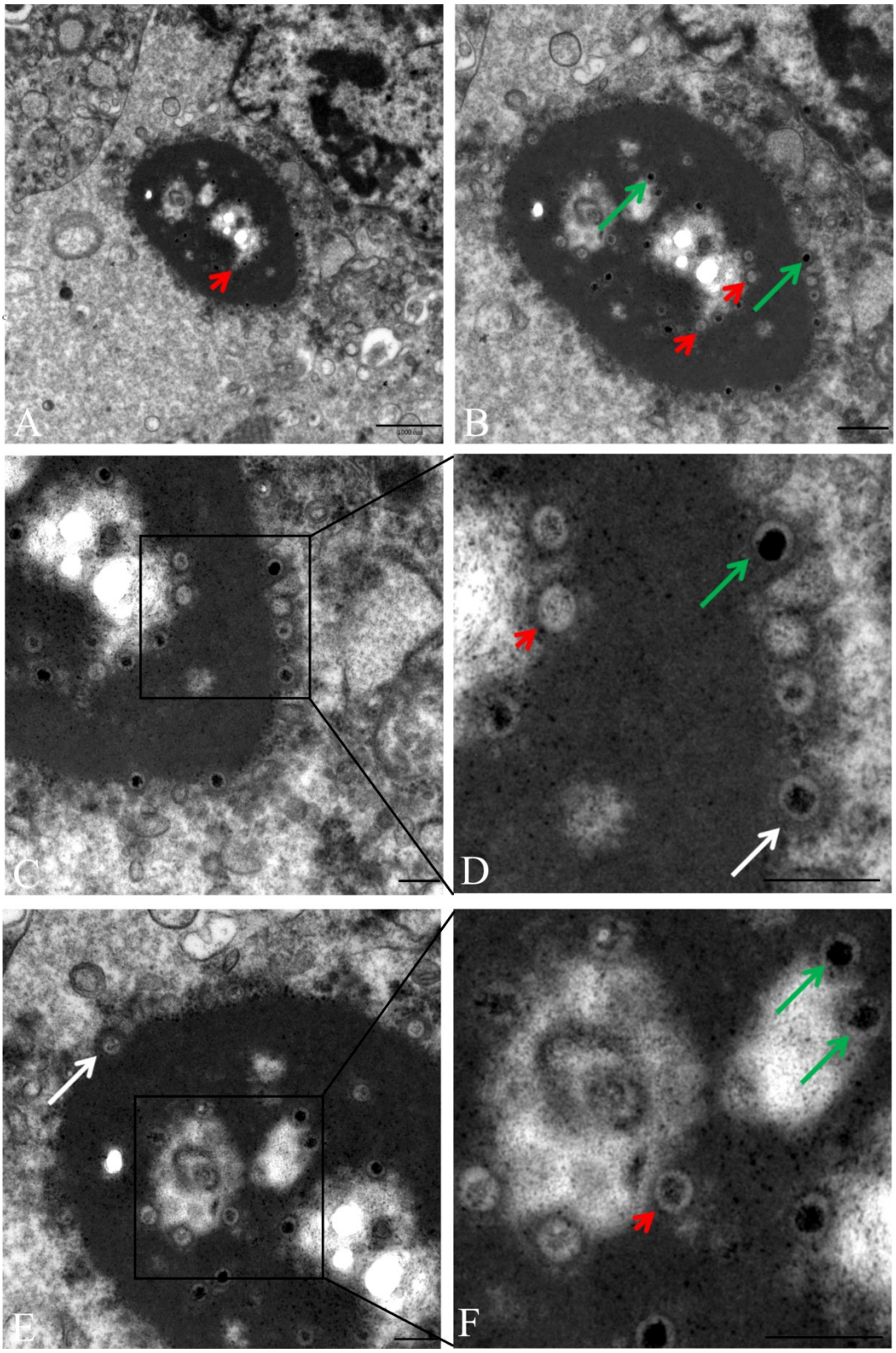

Figure 28: Transmission electron microscopy analysis for tissue samples collected from EEHV-1 infected elephant. (A) Hepatic endothelial cells contained cytoplasmic and intranuclear viral particles (scale bar 1000 nm). (B) Viral particles are accumulated in perinuclear cytoplasmic electron-dense bodies (scale bar 500 nm). (C and E) Electron-dense

cytoplasmic matrix contained nucleocapsids with electron dense cores and capsids with electron lucent cores. Tegument formation was visualized around the nucleocapsids (scale bar 250 nm). D and F are magnification of C and E, respectively (scale bar 250 nm). Green arrow - nucleocapsids with electron dense core; white arrow – nucleocapsids and capsids, surrounded by a tegument; Red arrowhead – capsid with electro-lucent cores. Picture was taken from publication (313).

6.3.6. Whole genome sequencing of EEHV-1A

The datasets for the liver and tongue samples comprised a total of ~12.5 and ~8.4 million paired-end reads with ~6.9 and ~6.0 million pairs passing quality filtering. Removing read pairs not mapping the pan-genome produced a set of ~43,000 read pairs for liver but only ~9000 read pairs for tongue. The reads of the tongue sample were not sufficient to produce a high-quality assembly of the virus genome and was excluded from further analysis. For the liver sample “Kanja”, the reference-based scaffolding of SPAdes contigs using Ragout created a scaffold of length ~169.5 kbp containing the two longest contigs with ~161.4 kbp and ~8.2 kbp (average coverage of ~18.8 and ~15). The initial mapping assembly with MIRA against the ~180 kbp reference genome KC462165.1 contained 426 ambiguous and 7422 uncovered bases. After using the SPAdes de novo assembly to fill gaps in the MIRA consensus and to run MIRA again with this augmented consensus, the numbers were reduced to 295 and 4919, respectively. The complete viral DNA genome of EEHV-1A has been determined and annotated from liver sample “Kanja” as described earlier and has 98.52% identity with the available EEHV-1A sequences from the GenBank. The obtained sequence of EEHV-1A genome was deposited in GenBank under accession number MN067515.

Genetic relatedness of the current EEHV-1A was further determined by phylogenetic analysis of the terminase and vGPCR genes. At the nucleotide level, terminase gene sequence obtained from “Kanja” was clustered with several EEHV-1A isolates from North America, Europe, and Asia (Figure 29A). On the other hand, the vGPCR gene sequence, although clustering with other EEHV-1A isolates, formed a separate clade (Figure 29B).

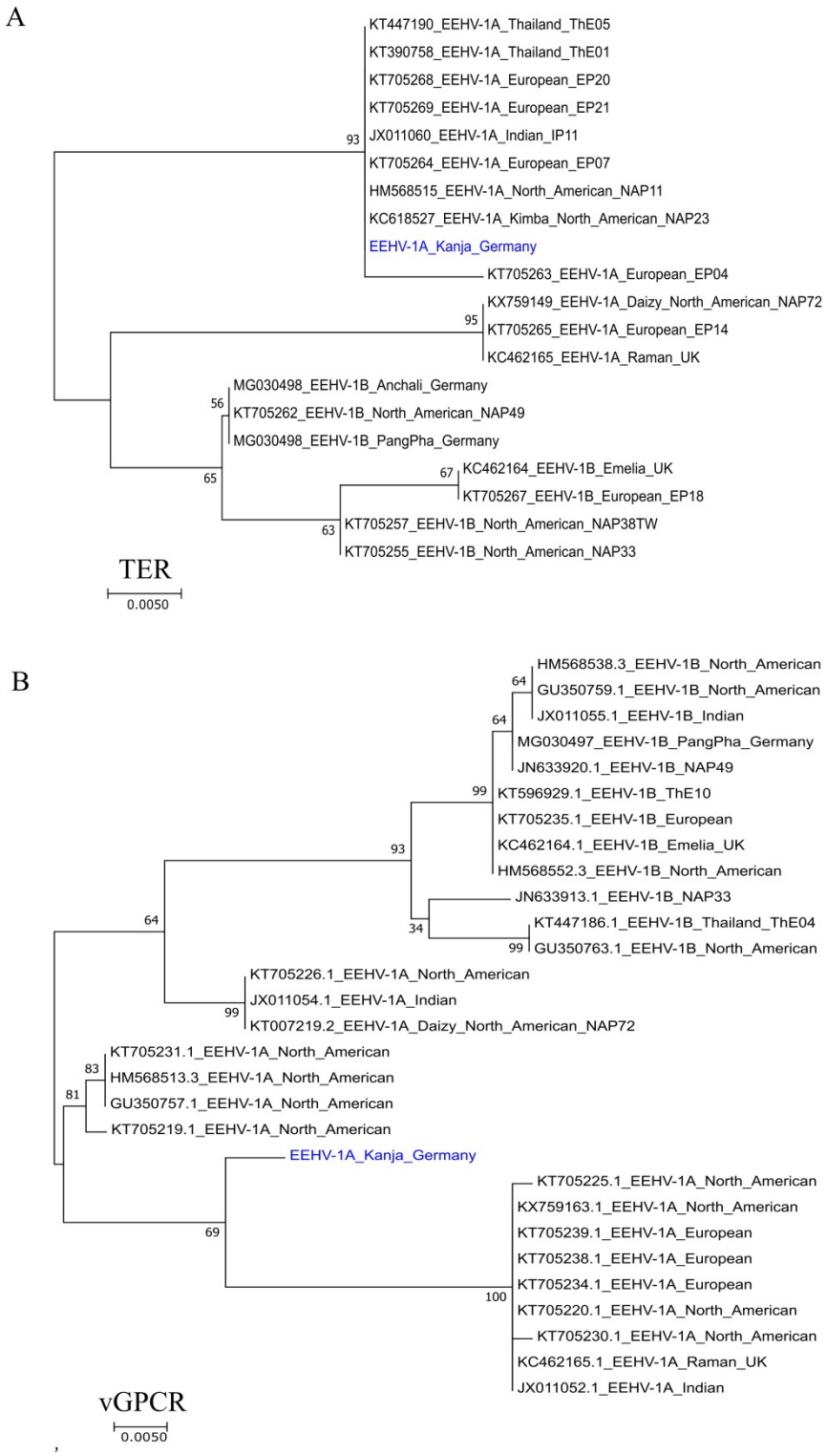

Figure 29: Phylogenetic tree of EEHV-1 DNA. Maximum-likelihood trees are shown for the terminase (A) and vGPCR (B) genes of EEHV-1. EEHV-1A “Kanja” sequence from current study was indicated in blue. Reference sequences obtained from GenBank are represented by their accession numbers. Bootstrap values above 50% are shown. The scale bar indicates nucleotide substitution per site. Picture was taken from publication (313).

7 Discussion

7.1 Molecular mechanisms of EHV-1 pathogenesis

EHV-1 infection of PBMC is a critical step in deciding EHV-1 pathogenesis; thereby the virus can spread from infected PBMC to EC without being captured by the host immune system. As described earlier, the process of virus transfer is complex, requires coordinated action of viral proteins, adhesion molecules expressed by both cells, and cytokines and chemokines for facilitating inter-cellular adhesion, intra-cellular trafficking and cellular polarity (192, 193). Several viral proteins are involved in mediating such process. Our previous studies revealed that gD, gB and US3 proteins play an essential role in PBMC and EC infection as well as virus transfer between the two compartments (72, 77). Cell-to-cell virus transfer considered to be a mechanism of immune evasion and immunomodulation properties of herpesviruses (196). Earlier studies revealed that EHV-1 can evade host immune response by modulating MHC-I expression on the surface of the infected cells (314) with the help of Ab4-viral proteins UL49.5, ORF1 and ORF17 (146-148, 151, 315). Further, ORF1 and ORF2 deletion mutants showed significantly reduced virus shedding, shorter course of pyrexia and modulated cytokine response with attenuation of virulence in comparison to Ab4-wt in *in vivo* studies in ponies (152). Experimental infection with ORF1 and ORF71 deletion mutants revealed brief period of pyrexia, low virus shedding and decreased cytokine response (IFNα, IL-10 and soluble CD14); however, had comparable viremia like Ab4-wt (153). In another study, ORF2 deletion mutant was attenuated, however, had a strong immunogenicity without altering viremia in Icelandic horses (160, 161). Failure to induce T-cell response was suggested as a reason of viremia in both Ab4-wt and mutant viruses infected horses (152, 153, 160). As animal experiments were performed in non-pregnant horses and no distinct neurological signs were observed following infection with Ab4-wt and mutant viruses, it is unclear that cell-associated viremia with mutant viruses can result in subsequent endothelial infection or not. With this background, I have hypothesized that EHV-1 immunomodulating proteins (ORF1, ORF2 and ORF17) are essential for virus pathogenesis and play an important role in virus spread from PBMC to EC.

ORF1, ORF2 and ORF17 genes of EHV-1 are dispensable for virus replication in equine cells as confirmed by growth kinetics and plaques size assay. Double and triple gene deletion mutant also replicated normally like parental virus. Only ORF17 deletion mutant showed a significant, but slight, reduction in plaque size ranged between 10-15%. Albeit the plaque size reductions were less, similar plaque size reductions of UL43 (ORF17 homolog) deletion mutant were observed in HSV-1 and PrV (165, 316). Despite of the non-essential

character, the conservation of UL43 homologs function in relation to plaque size within the alphaherpesviruses is striking.

I show here that PBMC can be infected, to similar levels, with all mutant viruses without any significant differences. Co-cultivation and flow chamber assays with parental EHV-1 virus showed efficient virus spread from infected PBMC to EC as reported previously (77). However, deletion of ORF17 and ORF2 significantly reduced virus transfer between PBMC and EC under static and flow conditions. Furthermore, ORF17 and ORF2 mutants (single and double gene deletions) also reduced the virus transfer to EC. Double and triple gene deletions showed additive reduction in virus transfer to EC in flow condition than in static condition which can be attributed to an synergetic effect on the functional dynamic rolling of infected PBMC over EC. Flow chamber system creates a homogenous fluid shear stress in endothelium similar to that observed in the blood vessel environment *in vivo*. Fluid flow over the endothelium results in ranges of ion fluxes, modulation of several pathways including biochemical, gene and protein expression in both *in vitro* and *in vivo*. Specifically, shear forces modulates cell surface transmembrane adhesion molecule via cytoskeleton by integrin-dependent activation of MAP kinases via Ras GTPase and RhoA activation (317). Furthermore, rolling of PBMC over the endothelium provides kinetics of cell-to-cell adhesion and increase the binding strength of interaction between the two cells (318), which was the advantage of flow chamber system rather than static condition. As it will be discussed later, ORF2 and ORF17 modulated the MAP kinase and Ras GTPase pathways, which might explain the reduction of virus spread.

In the epithelium-PBMC contact assay, all mutant viruses transferred from infected epithelial cells to PBMC similar to parental virus. However, subsequent flow chamber assay with infected PBMC, showed reduced virus transfer to EC. It is very clear that gene deletions affected only the virus transfer step to EC, but not from the epithelium to the PBMC. The process of cell-to-cell virus transfer from infected epithelial cells to PBMC is relatively simple. Dendritic cells can capture the virus after being released from the infected epithelial cells; EHV-1 has full replication cycles in the epithelium (214, 319, 320). Since the mutant viruses can replicate to levels comparable to parental viruses (Figure 11), it was not surprising to see no effect on virus spread between epithelial cells and PBMC. On the hand, virus replication in PBMC with subsequent egress is not fully identified. In addition, virus transfer between PBMC to EC is very complex and require the interplay of several viral and cellular molecules (77, 81, 194). I assume that these viral proteins (ORF2, and ORF17) are involved in modulating several pathways in PBMC, including cell signaling, adhesion and immune pathways, thereby ORF2 and ORF17 gene deletions results in reduced virus transfer to EC.

My findings clearly correlates with previous *in vivo* findings where ORF2, ORF1/ORF71 and ORF1/ORF2 deletion mutants showed respiratory infection, comparable viremia, but no noticeable endothelial cell infection in four different experimental studies in horses (152, 153, 160, 161).

It was shown before that all three PBMC subpopulations can be infected with EHV-1 (64, 66, 76, 191), however identification of which subpopulation transfers the virus to EC is not known. My flow chamber assay showed that all three subpopulations of PBMC (T, B lymphocytes and monocytes) could transfer the virus to EC. Gene deletions affected virus transfer from each PBMC subpopulation to levels comparable to the whole PBMC populations. I have surmised that these viral proteins might target the same mechanisms in each subpopulations of PBMC.

EHV-1 undergo limited virus replication in PBMC (76, 77), but details regarding expression of viral proteins, virus induced changes in host pathways were limited (321). Although several proteomic approaches have been reported for other herpesviruses, data regarding EHV-1 induced widespread changes in the host cell proteome is lacking (322, 323). In my proteomic analysis, I have quantified the expression of 45 viral proteins in infected PBMC that includes structural and nonstructural proteins belonging to immediate early, early and late expression kinetics. Expression of ORF2, but not ORF1 and ORF17 protein was observed in parental EHV-1-infected PBMC. Our previous study revealed that in cell culture, expression of ORF17 and ORF1 was detectable from 2 and 4 hrs post infection, but decreased after 8 and 16 hrs post infection, respectively (146, 147). This can be correlated with absence of ORF17 and ORF1 in infected PBMC at 24 hpi. ORF2 protein was not detected in PBMC infected with Ab4ΔORF2 and Ab4ΔORF1/ORF2/ORF17 deletion mutant.

Parental EHV-1 infection upregulated several pathways including MAPK, Ras signaling, endocytosis, oxidative phosphorylation, lysosomal pathways but downregulated herpesvirus and spliceosome pathways. MAPK pathway is involved in the manipulation of cellular functions like signal transduction, cell adhesion, virus replication in target cells and cell survival (324, 325). Ras signaling pathway implicated in sequential phosphorylation of at least 20downstream molecules which transduce the signals from cell surface to nucleus including MAPK, c-Jun amino-terminal kinases (JNK) which is essential for cell survival from apoptosis (326). Endocytosis pathway plays an essential role in regulating levels of many essential surface proteins like G-protein coupled receptors, receptor tyrosine kinases and adhesion molecules, and transporters (327). Herpesvirus infection pathway is mediated by numerous host and viral proteins which includes several pathways like toll-like receptor signaling, pro-inflammatory cytokines, inhibition of apoptosis, antigen processing and

presentation, JAK-STAT, calcium signaling, nuclear factor-kappa B (NF-κB) and B cell receptor signaling pathways (78, 328, 329). Similar findings have been reported for other herpesviruses like HSV, human cytomegalomegalievirus virus, Kaposi's sarcoma-associated herpesvirus (326, 330-334). Upregulation of endocytosis, MAPK and Ras signaling pathways following EHV-1 infection have been reported before (78, 184, 185, 335).

While comparing proteomic profile of Ab4-wt and mutants infected PBMC, ORF1, ORF2 and ORF17 gene deletions have modulated several pathways, mainly chemokine signaling, MAPK, herpesvirus infection and oxidative phosphorylation pathways. Ab4-wt infection downregulated herpesvirus infection pathway, while Ab4ΔORF1/ORF2/ORF17 mutant virus upregulated this pathway. Similar to the single gene deletion (Ab4ΔORF1 and Ab4ΔORF2), triple gene deletions modulated several pathways including chemokine signaling pathways. A previous *in vitro* study showed the upregulation of MAPK pathway in EHV-1-infected PBMC. Inhibition of this pathway with chemical inhibitor reduced virus transfer from infected monocytes to EC (78). In my study, ORF17 and ORF2 gene deletions downregulated the MAPK pathway and showed reduced virus transfer to EC. I surmise that ORF17 and ORF2 viral proteins are involved in upregulating the MAPK pathway thereby facilitating virus transfer to EC. As described earlier, MAPK is essentially involved in transmitting various extracellular signals that induce cellular proliferation, differentiation and survival (336). It has been reported that herpesvirus infection alters MAPK signaling to promote virus internalization, dysregulate the cell cycle, regulate viral replication and prevent host-cell death (337, 338). However, exact mechanisms of how viral proteins modulating host pathways is less understood. I assume that, these TM viral proteins may involved in sorting and trafficking of various host proteins within different compartment of cytoplasm and plasma membrane by modulation of vesicle/endosomal transport. Futher, modulation at transcription, translation level for various host proteins also a possible alternate hypothesis. Studying the underlying mechanism and role ORF17 and ORF2 in modulating MAPK will be the scope of our future studies.

Parental EHV-1 infection greatly reduced cytokine and chemokine release. Higher level of FGF-2 in Ab4-wt infected PBMC can be correlated with activation of MAPK pathway as confirmed by proteomic analysis. FGF-2 results in the activation of Ras-MAPK pathway, which is essential for virus spread (339, 340). Previous *in vivo* studies following experimental infection with Ab4-wt (neuropathogenic) strain showed release of fewer cytokines/chemokines at low concentration (IL-10, CCL2, CCL3) in comparison to RacL11 and NY03 strains (abortigenic strains) (199, 341). As expected from proteomic analysis, cytokine/chemokine estimation assay confirmed deletion of viral genes in altering

cytokine/chemokine response. ORF1 deletion showed release of more cytokine in infected PBMC. Similar findings of release of more cytokines by ORF1 deletion mutant in infected PBMC were confirmed by mRNA expression, cytokine quantification and migration assay (151). Further, IFNγ levels were higher in all ORF1 deletion mutants. IFNγ is produced by antigen-activated leukocytes. Secreted IFNγ activates antigen specific immunity, innate-cell mediated immunity and cytokines/chemokines release (342). Ab4-wt infection blocks IFNγ release from PBMC and deleting ORF1 gene resulted in release of more cytokines/chemokines which shows the immune modulating potential of ORF1 in Ab4 strain. ORF2 gene deletion also showed release of more cytokines in both *in vitro* and *in vivo* (160, 161). Specially, ORF2 gene deletion expressed higher level of IL-1β cytokine. Increase in level of this pro-inflammatory cytokine is considered as a host defense to virus infection. It was a well-known immune evasion strategy employed by HSV-1 to retain IL-1β in the intracellular space of infected macrophage without being released to extracellular space by blocking the function of caspase-1, which blocks the pro-inflammatory activity of IL-1β (343, 344). We presume that ORF2 of EHV-1 also may have similar function, thereby Ab4-wt infection in PBMC results in decreased release of IL-1β, while ORF2 deletion restores expression. Role of ORF2 in modulating of IL-1β secretion could be the potential area for future investigation. ORF17 gene deletion did not restore cytokine/chemokine release completely, however, released more cytokines than parental EHV-1. Infected PBMC in the presence of EC released more cytokines, which declares that PBMC-EC interaction is necessary and the interaction can stimulate the release of more cytokines. Differences in cytokine release were observed between Ab4 (neuropathogenic) and RacL-11 (abortogenic) strains of EHV-1. Strain dependent cytokine release by PBMC has been reported previously (199, 341) and the difference in cytokine secretion could be attributed to differences in the genetic makeup of both strains. RacL11 strain naturally lacks ORF1 and ORF2 in its genome in comparison to Ab4-wt, which is poorly spread to EC (data not shown) and showed release of more cytokines upon infecting PBMC (341). Similarly, deletion of ORF1 and ORF2 genes in Ab4 restored expression of more cytokines, which clearly demonstrate that ORF1 and ORF2 have major role in cytokine production Although EHV-4 infected PBMC did not transfer the virus to EC, they showed release of more cytokines (345). Taken together, I have identified and confirmed immune evading and cytokine modulating properties of different viral proteins of herpesviruses. Based on my flow chamber, proteomics and cytokine/chemokine assay, all three targeted genes in the study were multifunctional in nature. Nevertheless, these viral proteins are involved in more than one pathway in PBMC. I presume that ORF1 probably plays major role in Ras-signaling, chemokine signaling and cell adhesion pathways. ORF2 and ORF17 are implicated in chemokine signaling and MAPK

signaling pathways thereby facilitating cell-to-cell virus spread. Furthermore, ORF1, ORF2 and ORF17 deletion mutants (alone and in combinations) were capable of stimulating strong cytokine response *in vitro*. These genes could be potential targets for the development of live attenuated vaccine therapeutics against EHV-1 infection in equines. In addition, identifying possible interaction and finding interaction partners for ORF1, ORF2 and ORF17 proteins including viral and cellular proteins are the potential area of future studies.

7.2 EHV-4 outbreak: Virological, molecular and serological investigations

In the present study I have reported a large outbreak of respiratory infection caused by EHV-4 in foals and corresponding mares, and stallions in a breeding stud farm in northern Germany. Three main factors may have initiated the outbreak including, introducing three breeding mares with unknown history of EHV-1 or EHV-4 status to the farm, seasonal changes, and weaning. During the first week of July 2017, a group of foals and mares begin to show signs of respiratory infection. Immediate qPCR analysis of nasal swabs confirmed EHV-4 infection in almost all foals with respiratory signs. All foals were tested negative for EHV-1. Clinical signs were mild to moderate in foals and almost in-apparent in mares and stallions with few exceptions where pyrexia, dyspnea and nasal discharge was observed. This is in agreement with previous reports (346), where most of the clinically infected horses were less than three years of age and majority of affected horses were foals and weanlings, and nearly all EHV-4 positive aged horses were healthy. Though strict biosecurity measures were implemented subsequently; however, it did not mitigate the outbreak and more horses get infected and experienced respiratory illness and shed virus during the second and third weeks of the outbreak. This could be because of the fact that most of the foals in the farm already contracted the infection from corresponding mares or from silent shedders (mares and stallions) and begin to show clinical signs during the second and third weeks. However, this does not exclude that the biosecurity measures prevented the spread of infection outside the stud and helped other animals not to contract the infection.

One interesting finding of the study was the different restriction digestion (RFLP) pattern of the four isolates that might indicate that more than one virus was circulating in the farm at the time of the outbreak. Differences in restriction profile reflects changes in the sequence of genes of very large tegument protein, capsid protein, membrane associated phosphoprotein and DNA packaging protein of EHV-4. Further, the gene sequence of current virus isolates were related to currently circulating EHV-4 (347). It was a well-known fact that EHV-4 is highly stable genetically in comparison to EHV-1 (348), so the concept of possible mutations

during the outbreak can be excluded. Further, it suggests that there were no single animal source (index cases) for disease outbreak.

Generally, foals are kept with corresponding mares till weaning. Most of the EHV-4 positive foals in the current study were either unweaned or weaned recently. Further, foals from which the virus was isolated were unweaned during the outbreak. In addition, most of the foals and their corresponding mares were tested positive for EHV-4. It is possible that EHV-4 was reactivated from a latent stage in mares due to the above mentioned stressful factors and resulted in infection of their corresponding foals and other foals from negative mares or stallions in contact. Although mares were positive for EHV-4 by qPCR, C_T values were very low, indicating virus shedding at very low level. My virus isolation trials also raise the concern about C_T values, as virus was successfully isolated from nasal swabs with C_T values of less than 25. No virus was isolated from samples with C_T values more than 25 even after 5 blind passages. Animals with low C_T values shed viruses through nostrils for extended period of time (up to 9 weeks) in comparison to animals with high C_T values. Few mares shed viruses at few early time points and became negative for few weeks and again begin to shed the virus, which indicates the occurrence of intermittent reactivation in silent shedders, and necessitate long isolation period of infected animals, and frequent sample collection and testing before declaring the animal is EHV-4 negative. Significance of this very low virus shedding for long periods and its role in disease outbreak would be very interesting aspect to study in the future. In addition, regular virological surveillance for EHV-4 in mares during gestation and till few weeks after weaning would give a clear picture about EHV-4 reactivation and transmission cycle from mare to foals and may be helpful in indentifying and formulating suitable intervention strategies to prevent disease spread.

Horses are considered as long day seasonal breeders. Period of foaling will be restricted to few weeks in the year and most of the foals will be of same age on an average. During the time of weaning, most of the foals may not have maternally derived antibodies and weaning stress will make the foals susceptible to infection. In my case, weaning was coincided with seasonal changes (severe rain in summer). Meanwhile, yearlings in stud were already broken which were housed closely with broodmares and foals. Limited number feeding spaces for horses in paddock is also a factor attributed to stress. Horses in different stages were routinely conglomerate with each other during routine farm activities. In stressed mares and stallions, EHV-4 virus might have been reactivated and spread to foals by direct and indirect means. This shows the importance of stress in disease outbreak and necessitates exercising stress-alleviating measures. Previous reports suggested that EHV-4 infection may

happen throughout the year (74), however, the current study indicates the impact of season in inducing stress and subsequent disease outbreak.

Mostly, EHV-4 causes in-apparent infections even in foals as reported previously (349). But in my study, I have observed distinct clinical signs in most of the infected foals and in some mares. This could be because of differences in the virus strains and/or regular carefully monitoring and surveillance of the animals in the farm for presence of any clinical signs. Although EHV-4 can infect PBMCs and endothelial cells *in vitro* (77) and abortions have been reported to be caused by EHV-4 in mares (350-352), no abortions and mortalities were observed in any of the infected animals during the outbreak.

As reported early, it is clear from my study that foals were infected in early age without distinct sero-conversion as evidenced by serological assays. The average age of infected foals was 125.5±32 days and ranged between 85 and 209 days. Few foals had low level of EHV-4 neutralizing antibodies (titre of 1:4 - 1:8) and gG specific antibodies at the time of outbreak. This could be maternally derived antibodies as most of the foals were unweaned. Foals did not have protective neutralizing antibodies in serum against EHV-4 at the time of disease outbreak, which indicates that foals are highly susceptible to EHV-4 infection around the weaning time as maternally derived antibody levels in serum goes down. In contrast, all mares had EHV-4 neutralizing antibodies in the serum due to prior infection and/or immunization. Only 12.5% of infected foals were sero-converted at the end of the outbreak. None of the mares were sero-converted which shows that mares with protective antibody titre can develop in-apparent infection and shed the virus without sero-conversion. As mentioned earlier few foals had low level of antibodies against EHV-4 without sero-conversion; this could be because of residual maternally derived antibodies as reported earlier (353, 354). Although foals were tested negative for neutralizing antibodies in VNT, still EHV-4 gG specific antibodies can be detected through peptide ELISA. So, peptide ELISA can be used as an effective tool for detecting antibodies against EHV-4 during early infection and VNT for late infection in foals.

All four EHV-4 isolate had similar ORF30, gG and gB gene sequence and different RFLP pattern. Virus strains isolated were different from previously reported existing strain. ORF-30 and gG sequence from my study mostly clustered with EHV-4 isolated from Australia and Japan. Sequence analysis of gB gene revealed unique point mutation in position T624 to C624, which clustered my four isolates in to separate group and rest of all reported isolates in Genbank in to another group. Importance of this point mutation in gB and their role in virus biology need to be studied.

In conclusion, mares/stallions of origin from different places, harbored different EHV-4 viruses in latency as evidenced by RFLP and whole genome sequencing, reactivated almost at same time due to stress and resulted in EHV-4 outbreak among foals, mares and stallions.

7.3 Fatal EEHV-1 infection in two young Asian elephants: Virological and molecular investigations

Elephants are facing a serious infection threat since EEHVs became one of the main causes of death of young elephants in captivity in the last three decades. The viruses, which were described to cause skin nodules and local infections in the 1970s, have caused severe fatal hemorrhagic disease outbreaks since the late 1980s (52, 244, 355-357). Today, EEHVs are considered ubiquitous in Asian elephant populations in captivity and in free range throughout the world (53, 246, 358). Like other herpesviruses, EEHVs seem to have successfully co-evolved with their hosts and established a well-balanced adaptation. However, incidence of peracute disease in young elephants remains peculiar as this contradicts the herpesvirus survival strategy exclusively adapted for long-term persistence in the host (359).

In the present study, I have identified that EEHV-1A was the cause of the death of two young elephants consecutively in Tierpark, Hagenbeck. In each case, the elephant showed clinical signs just before death for a brief period of time, did not respond to treatment, and eventually died. Lesions of haemorrhagic nature were observed in most of the visceral organs and tissues including heart, liver, lung, intestine, mesentery, tongue, and pharynx. Similar findings of acute onset of illness and sudden death due to haemorrhagic disease in EEHV-1A-infected juvenile elephants has been described previously as the virus infects epithelial and endothelial cells (38, 244, 247, 358). I have detected EEHV-1A DNA in various organs and tissues of the infected elephants, as was reported earlier (359). Widespread distribution of viral nucleic acid might be attributed to the extensive virus replication, at least in the endothelial lining, of all tissues. However, the portal of virus entry, target sites, receptors involved, and the primary site of virus replication remain unclear.

Electron microscopy revealed non-enveloped viral particles of about 120 nm in diameter accumulated within and associated to perinuclear cytoplasmic electron-dense bodies in hepatic endothelial cells. Aggregation of fully formed enveloped virus particles at the proximity within cytoplasmic dense bodies have been reported twice (52, 360). In all cases, cytoplasmic dense bodies were observed only in the liver. Capillary endothelial cells of the liver showing basophilic intracytoplasmic viral inclusion bodies in histopathology were reported previously (361). This finding can be correlated with the perinuclear electron-dense

bodies in the cytoplasm observed by electron microscope. The reason of cytoplasmic dense bodies' formation specifically in the endothelium of the liver and its role in virus replication is not yet understood. It can be surmised that the liver supports virus replication better than other organs, as viral nucleic acid load is very high in liver tissues in comparison to other tissues. Virus particles in different steps of virus replication were also observed in endothelial cells of tongue and spleen tissues, which confirmed that virus replication always occurs in endothelial cells of different tissues and contributes to high viral load in different organs. Similarly, the presence of virus particles in endothelial cells of spleen (60) and heart (244, 357) has been previously shown.

It was previously reported that EEHV-1 could not be isolated on cell culture system (52). Here, I have attempted to isolate the virus on different cell cultures, and Iobserved limited virus replication for few passages. I have used different cell lines originating from different species including elephant, human, equine, bovine, canine, rabbit, feline, and monkey. Among the different cells used, only elephant fibroblast cells (ENL-2) showed limited virus replication for up to four passages (28 days) when inoculated with infected tongue tissue homogenate and co-cultured with infected elephant PBMC. This finding lead to the assumption that elephant cells are a potential platform for virus replication in vitro. However, after the fourth passage, no viral DNA was detected in infected ENL-2 cells, which again limits the use of these cells. Equine endothelial cells and 293T (with ND10 knockdown) human cells showed persistence of viral genomes up to three passages. As reported earlier (52), virus replication was not supported in other cell lines tested. One can argue that the reduction of DNA copies in cells was mainly due to a dilution effect. However, this was not the case with all cell lines. The DNA disappeared completely from some cell cultures after the first passage but continued in others until the fourth passage, as seen in Tables 16 and 17. Moreover, the viral genome copies fluctuated between low and high with ENL-2 cells when co-cultured with infected PBMC. I propose that (i) EEHV-1 preferentially replicates in cells derived from its natural host, i.e., elephant; (ii) endothelial cells may support virus replication longer than other cells from different hosts; and (iii) deletion of host restriction factors (such as ND10) that block virus replication may help in supporting EEHV-1 replication. Another possible reason for the overall less efficient virus replication in cell culture is the lack of suitable tissue complexity required for virus replication as provided in the natural host.

In addition to qPCR, indirect IF demonstrated the expression of viral proteins (gB) in infected cells (ENL-2, CrFK and PBMC) at 96 hrs post infection, which was not shown before. Although expression of viral protein (gB) was observed in both ENL-2 and CrFK cells, only

ENL-2 cells supported virus replication as shown in qPCR results. Herpesvirus gBs are highly conserved, homologous among other members, and essential for virus replication (362-365). Across the members of the *Herpesviridae*, gB possesses a conserved cleavage site Arg-X-Lys/Arg-Arg targeted by the cellular protease furin. Here, I show that EEHV-1 gB has also a furin cleavage site like other members (261). gB of EEHV-1A has a conserved furin cleavage motif ^{433}RRKR^{436}, which cleaves gB in the middle. In western blotting, antibodies raised against two different peptides of gB detected both cleaved and uncleaved forms of gB. This may point to the importance of gB cleavage for the protein to be functionalized. Furthermore, I have conducted a prediction analysis for gB sequence of other EEHVs available online, which revealed that all available EEHVs (EEHV-1A, 1B, 4, 5, and 6) also have at least one furin cleavage site. As no information is available regarding the function of any protein of EEHV-1, this study makes the initial step in describing the similarity of gB among different EEHVs in terms of furin cleavage, which was highly conserved across the family of herpesviruses. I therefore assume that gB plays an important role in virus entry and egress from target cells, as it is described for other herpesviruses (116, 366, 367).

I have determined the whole 180 kb genome sequence of EEHV-1A in liver tissue by next-generation sequencing and de novo assembly. EEHV-1A genome analysis of my current study confirms the relatedness of the virus to other reported whole genome sequences of EEHV-1A. The phylogenetic analysis of terminase and vGPCR genes showed clustering of EEHV-1A sequences (of the current study) with other isolates of EEHV_1A of other countries in North America, Europe, and Asia. The complete EEHV-1A genome sequence will provide a basis for better understanding of epidemiology, host-pathogen interaction, and evolution of EEHV-1 virulence.

Taken together, I have examined two fatal cases of EEHV-1A in young Asian elephants in captivity. I have studied the pathology of the virus in both elephant calves, demonstrated viral particles in liver endothelium, and showed widespread viral distribution in host tissues. My attempt to isolate EEHV-1A in established cell lines showed interesting results as cells derived from elephants supported virus replication for four passages. Additionally, I found that gB of EEHV-1 possesses a conserved cleavage site targeted by cellular furin protease. This pattern is also known for other members of the *Herpesviridae* and this cleavage is required to generate a functional glycoprotein. Finally, the whole EEHV-1A DNA genome was sequenced from one of the cases: “Kanja”. The findings and facts of this study will be helpful for the development of suitable cell culture system and further characterization of EEHVs with respect to developing prophylactic strategies and implementing control measures in future.

8 Summary

Herpesviruses are important viral pathogens infecting human and animal populations worldwide. In the current study, we have investigated molecular mechanisms of equine herpesvirus type 1 (EHV-1) pathogenesis and characterized EHV-4 and elephant endotheliotropic herpesvirus type 1A (EEHV-1A) following disease outbreak in horses and elephants, respectively. To evaluate the role of viral proteins in cell-to-cell virus transfer between peripheral blood mononuclear cells (PBMC) and endothelium, we have constructed EHV-1 (Ab4 strain) mutants after deleting open reading frame 1 (ORF1), ORF2 and ORF17 genes, either as single gene deletions or in combinations. Ab4 deletion mutants were analysed for replication properties, PBMC infection, cell-to-cell virus transfer between epithelium-PBMC and PBMC-endothelium, virus induced changes in PBMC proteome and cytokine/chemokine expression profiles. All deletion mutants were successfully reconstituted. ORF1, ORF2 and ORF17 genes are not essential for virus replication, and ORF17 deletion containing mutants showed significant reduction in plaque size. ORF2 and ORF17 were implicated in virus spread to the endothelium as evaluated by contact and flow chamber models; however, virus transfer from epithelial cells to PBMCs was not affected. Interestingly, all PBMC subpopulations including B lymphocytes, T lymphocytes and monocytes were able to transfer EHV-1 to EC. Ab4 infection in PBMC upregulated host proteins associated with endocytosis, Ras signaling, oxidative phosphorylation, platelet activation and leukocyte transendothelial migration, and downregulated chemokine signaling, herpesvirus infection, ribonucleic acid degradation and apoptotic pathways. Deletion of ORF1, ORF2 and ORF17 modulated chemokine signalling, mitogen activated protein kinase (MAPK) and herpesvirus infection pathways in infected PBMC. We presume that reduction in virus transfer from PBMC to endothelium may be attributed to modulation of host signaling and immune pathways. MAPK pathway is implicated in signal transduction, cell adhesion, cell survival and virus replication; Herpesvirus pathway is mediating receptor signaling, pro-inflammatory cytokine release, inhibition of apoptosis, nuclear factor-kappa B and antigen processing and presentation; Chemokine signaling is essential for activation of various immune pathways. Proteomic results were further confirmed by chemokine assay where Ab4 infection completely reduced the cytokine/chemokine release in infected PBMC and deletion of ORF1, ORF2 and ORF17 genes restored expression. Collectively, ORF2 and ORF17 genes essentially involved in virus spread to endothelium and along with ORF1 could stimulate strong cytokine/chemokine response. Therefore, these gene deletion mutants could be the potential target for development of live attenuated-vaccine.

EHV-4 is enzootic in equine population. We have investigated a large outbreak of respiratory infection occurred in a group of in-housed foals and mares, at a Standardbred horse

breeding farm in northern Germany. Virological assay revealed the involvement of EHV-4 in all the cases of respiratory illness as confirmed by virus isolation, quantitative-polymerase chain reaction and serological follow-up in paired serum sample using virus neutralization test and peptide-specific enzyme linked immunosorbent assay. Different restriction fragment length polymorphism profiles of the four isolates suggested the involvement of more than one animal as an index case of infection either due to primary infection or reactivation from latency. Epidemiological investigation revealed multifactorial causation as stress caused by seasonal changes, management practices, routine equestrian activities and exercise contributed in EHV-4 outbreak. Our study necessitates the stress alleviating measures and management practices in stud farm in order to avoid immuosuppression and disease outbreak.

EEHV causes fatal hemorrhagic disease in young Asian elephants. Our investigation on two young Asian elephants died due to acute hemorrhagic disease revealed the involvement of EEHV-1A as a cause of the death. Widespread distribution of EEHV-1A was observed in various organs and tissues of the infected elephants. In hepatic endothelial cells, enveloped viral particles were accumulated within and around cytoplasmic electron-dense bodies. Virus isolation study in different cell cultures showed only limited virus replication; however, late viral protein expression was detected in infected cells. We have further demonstrated that glycoprotein B of EEHV-1A possesses a conserved cleavage site Arginine-X-Lysine/Arginine-Arginine that is targeted by the cellular protease furin, as like other members of the *Herpesviridae*. Through next-generation sequencing, we have determined the complete 180 kilobase pair genome sequence of EEHV-1A isolated from the liver. Though our virus isolation was unsuccessful, only little information is available regarding virus culture and the function of viral proteins. We have attempted to take an initial step in the development of appropriate cell culture system and virus characterization. Further, the complete genome sequence of EEHV-1A from our investigation will facilitate future studies on the epidemiology and diagnosis of EEHV infection in elephants. Taken together, our findings provide new insights into EHV-1 pathogenesis, especially molecular mechanisms of virus spread between PBMC and endothelium. Further our study with EHV-4 and EEHV-1A makes a significant contribution to existing knowledge and offers an important resource on herpesvirology.

9 Zusammenfassung

Molekulare Charakterisierung und Pathogenese von Pferde- und Elefanten-Herpesviren

Herpesviren sind wichtige virale Pathogene die sowohl Menschen als auch Tierpopulationen weltweit infizieren. In dieser Arbeit haben wir molekulare Mechanismen in der Equinen Herpesvirus Typ 1 (EHV-1) Pathogenese untersucht und EHV-4 und Elephant Endotheliotropic Herpes Virus Typ 1A (EEHV-1A) nach Krankheitsausbrüchen in Pferden bzw. Elefanten charakterisiert. Um die Rolle von viralen Proteinen im Virustransfer zwischen PBMC (Peripheral Blood Mononuclear Cells; dt.: ‚mononukleäre Zellen des peripheren Blutes') und Endothel zu untersuchen, haben wir EHV-1 Mutanten(Stamm Ab4) mit Deletionen der Gene Open Reading Frame 1 (ORF1), ORF2 und ORF17 konstruiert, entweder als Einzelgen-Deletionsmutanten oder in Kombinationen. Die Ab4 Deletionsmutanten wurden auf Replikationsfähigkeit, PBMC-Infektivität, Zell-zu-Zell Transfer zwischen Epithel und PBMC bzw. PBMC und Endothel, virusinduzierte Veränderungen im PBMC-Proteom und die Zytokin/Chemokin Expressionsprofile hin untersucht. Alle Deletionsmutanten konnten erfolgreich rekonstituiert werden. Die Gene ORF1, ORF2 und ORF17 sind für die Virusreplikation nicht essenziellund die ORF17 Deletionsmutanten wiesen eine statistisch signifikante Reduktion der Plaque-Größen auf. ORF2 und ORF17 sind in der Virusverbreitung ins Endothel involviert, was durch Kontakt- und Durchflusskammer Modelle gezeigt werden konnte. Allerdings war die Virusverbreitung von Epithelzellen zu PBMC nicht beeinträchtigt. Interessanterweise waren alle PBMC Subpopulationen inkl. B- und T-Lymphozyten und Monozyten im Stande, EHV-1 auf Endothelzellen zu übertragen. Ab4 Infektionen von PBMC führte zur Hochregulierung von Wirtsproteinen welche mit Endozytose, der Ras Signalkaskade, oxidativer Phosphorylierung, Thrombozytenaktivierung und der transendothelialen Migration von Leukozyten assoziiert sind. Herunterreguliert wurde die Chemokin-Signalkaskade, Herpesvirusinfektion, Ribonukleinsäure Degradation und apoptotische Reaktionswege. Die Deletion von ORF1, ORF2 und ORF17 beeinflusste die Chemokin-Signalkaskade, MAP-Kinasen (MAPK; MAP, engl.: mitogen-activated protein) und Herpesvirusinfektions-Reaktionswege in infizierten PBMC. Wir vermuten, dass die Reduktion der Virusausbreitung von PBMC zum Endothel mit der Regulation von Wirtszell-Signalkaskaden und immunologischen Reaktionswegen zusammenhängt. Der MAPK-Reaktionsweg ist in Signaltransduktion, Zell-Adhäsion, Überleben von Zellen und Virusreplikation involviert. Der Herpesvirus-Reaktionsweg mediiert Rezeptor-Signalkaskaden, proinflammatorische Zytokinausschüttung, die Unterdrückung von Apoptose, sowie NF-κB und Antigenverarbeitung und -präsentation. Die Chemokin-Signalkaskade ist für die Aktivierung von zahlreichen immunologischen Reaktionswegen

essenziell. Die Proteom-Ergebnisse wurden mittels Chemokin-Assays bestätigt, in denen Ab4 Infektionen die Zytokin-/Chemokinausschüttung in infizierten PBMC reduzierte, wobei die Deletion von ORF1, ORF2 und ORF17 die Genexpression wiederherstellte. Zusammenfassend sind die ORF2 und ORF17 Gene essenziell in die Virusausbreitung ins Endothel involviert und können zusammen mit ORF1 eine starke Zytokin-/Chemokinausschüttung stimulieren. Deswegen stellen diese Deletionsmutanten potenzielle Kandidaten für die Entwicklung von attenuierten Lebendimpfstoffen dar.

EHV-4 ist in Pferdepopulationen endemisch. Wir haben einen großen Ausbruch von Infektionen des Respirationstraktes untersucht, der in einer Gruppe von Fohlen und Stuten auf einemGestüt in Norddeutschland aufgetreten ist. Virologische Untersuchungen zeigten die Beteiligung von EHV-4 in allen Fällen von Erkrankungen des Respirationstraktes, verifiziert durch Virusisolation, quantitative Polymerase-Kettenreaktion (qPCR) und serologische *follow-up*-Untersuchungen per Virusneutralisationstest und peptidspezifischem Enzyme-linked Immunosorbent Assay. Verschiedene Restriktionsfragmentlängenpolymorphismus-Profile von vier Isolaten lassen darauf schließen, dass mehr als ein Tier als Indexfall der Infektion verantwortlich sein könnten – entweder durch Primärinfektion oder Reaktivierung aus der Latenz. Epidemiologische Studien legten eine multifaktorielle Kausalität aus saisonbedingtem Stress und Stress durch Management, Routinebewegung und Training offen, die zum EHV-4-Ausbruch führte. Unsere Studie bestärkt die Wichtigkeit stresslindernder Maßnahmen und Managementpraktiken in Gestüten, um Immunsuppression und Krankheitsausbrüche zu vermeiden.

EEHV ruft eine tödliche hämorrhagische Erkrankung in jungen asiatischen Elefanten hervor. Unsere Untersuchungen zweier asiatischer Elefanten, die an einer akut verlaufenden hämorrhagischen Krankheit verstorben sind, deckten EEHV-1A als Todesursache auf. Wir konnten eine weitverbreitete EEHV-1A-Infektion in verschiedene Organe und Gewebe der infizierten Elefanten beobachten. In Endothelzellen der Leber akkumulierten behüllte Viruspartikel, umgeben von zytoplasmatischen elektronendichten Einschlusskörperchen. Virusisolationen in verschiedenen Zellkulturen zeigte eine nur schwache Virusreplikation. Allerdings wurde die Expression von späten Virusproteinen in infizierten Zellen detektiert. Weiterhin konnten wir zeigen, dass Glykoprotein B (gB) von EEHV-1A eine konservierte Schnittstelle Arginin-X-Lysin/Arginin-Arginin besitzt die durch die zelluläre Protease Furin gespalten werden kann – wie andere Mitglieder der *Herpesviridae*. Mittels Next Generation Sequencing haben wir das komplette 180 Kilobasenpaare-Genom von aus der Leber isoliertem EEHV-1A bestimmt. Obwohl die Virusisolation nicht erfolgreich war ist zur Viruskultivierung und den Funktionen der viralen Proteine nur sehr wenig Information

verfügbar. Wir haben versucht, einen initialen Schritt in der Entwicklung von geeigneten Zellkultursystemen und der Viruscharakterisierung zu gehen. Außerdem wird die komplette Genomsequenz eines EEHV-1A unserer Untersuchungen weitere Studien zur Epidemiologie und Diagnose von EEHV-1A -Infektionen in Elefanten erleichtern. Zusammenfassend bieten unsere Ergebnisse neue Einsichten in EHV-1 Pathogenese, speziell zu molekularen Mechanismen der Virusausbreitung von PBMC und Endothel. Des Weiterensind unsere Studien zu EHV-4 und EEHV-1A signifikante Beiträge zu bereits existierendem Wissen und bieten eine wichtige Ressource für die Herpesvirologie.

10 References

1. Popgeorgiev N, Boyer M, Fancello L, Monteil S, Robert C, Rivet R, et al. Marseillevirus-like virus recovered from blood donated by asymptomatic humans. J Infect Dis. 2013;208(7):1042-50.
2. Qin J, Li R, Raes J, Arumugam M, Burgdorf KS, Manichanh C, et al. A human gut microbial gene catalogue established by metagenomic sequencing. Nature. 2010;464(7285):59-65.
3. Garcia-Lopez R, Perez-Brocal V, Moya A. Beyond cells - The virome in the human holobiont. Microb Cell. 2019;6(9):373-96.
4. Wylie KM, Mihindukulasuriya KA, Zhou Y, Sodergren E, Storch GA, Weinstock GM. Metagenomic analysis of double-stranded DNA viruses in healthy adults. BMC Biol. 2014;12:71.
5. Virgin HW, Wherry EJ, Ahmed R. Redefining chronic viral infection. Cell. 2009;138(1):30-50.
6. Grinde B. Herpesviruses: latency and reactivation - viral strategies and host response. J Oral Microbiol. 2013;5.
7. McGeoch DJ, Cook S. Molecular phylogeny of the alphaherpesvirinae subfamily and a proposed evolutionary timescale. J Mol Biol. 1994;238(1):9-22.
8. McGeoch DJ, Cook S, Dolan A, Jamieson FE, Telford EA. Molecular phylogeny and evolutionary timescale for the family of mammalian herpesviruses. J Mol Biol. 1995;247(3):443-58.
9. Adler B, Sattler C, Adler H. Herpesviruses and Their Host Cells: A Successful Liaison. Trends Microbiol. 2017;25(3):229-41.
10. Cohrs RJ, Gilden DH. Human herpesvirus latency. Brain Pathol. 2001;11(4):465-74.
11. Pusterla N, Mapes S, Wilson WD. Prevalence of equine herpesvirus type 1 in trigeminal ganglia and submandibular lymph nodes of equids examined postmortem. Vet Rec. 2010;167(10):376-8.
12. Goodrum F, Caviness K, Zagallo P. Human cytomegalovirus persistence. Cell Microbiol. 2012;14(5):644-55.
13. Bloom DC. Alphaherpesvirus Latency: A Dynamic State of Transcription and Reactivation. Adv Virus Res. 2016;94:53-80.
14. Jones C. Herpes simplex virus type 1 and bovine herpesvirus 1 latency. Clin Microbiol Rev. 2003;16(1):79-95.
15. Welch HM, Bridges CG, Lyon AM, Griffiths L, Edington N. Latent equid herpesviruses 1 and 4: detection and distinction using the polymerase chain reaction and co-cultivation from lymphoid tissues. J Gen Virol. 1992;73 (Pt 2):261-8.

16. Flano E, Jia Q, Moore J, Woodland DL, Sun R, Blackman MA. Early establishment of gamma-herpesvirus latency: implications for immune control. J Immunol. 2005;174(8):4972-8.

17. Lippe R. Deciphering novel host-herpesvirus interactions by virion proteomics. Front Microbiol. 2012;3:181.

18. Lyman MG, Enquist LW. Herpesvirus interactions with the host cytoskeleton. J Virol. 2009;83(5):2058-66.

19. Davison AJ, Eberle R, Ehlers B, Hayward GS, McGeoch DJ, Minson AC, et al. The order Herpesvirales. Arch Virol. 2009;154(1):171-7.

20. Davison AJ. Channel catfish virus: a new type of herpesvirus. Virology. 1992;186(1):9-14.

21. Davison AJ, Cunningham C, Sauerbier W, McKinnell RG. Genome sequences of two frog herpesviruses. J Gen Virol. 2006;87(Pt 12):3509-14.

22. Davison AJ. The genome of salmonid herpesvirus 1. J Virol. 1998;72(3):1974-82.

23. Waltzek TB, Kelley GO, Stone DM, Way K, Hanson L, Fukuda H, et al. Koi herpesvirus represents a third cyprinid herpesvirus (CyHV-3) in the family Herpesviridae. J Gen Virol. 2005;86(Pt 6):1659-67.

24. Freitas JT, Subramaniam K, Kelley KL, Marcquenski S, Groff J, Waltzek TB. Genetic characterization of esocid herpesvirus 1 (EsHV1). Diseases of aquatic organisms. 2016;122(1):1-11.

25. Burge CA, Griffin FJ, Friedman CS. Mortality and herpesvirus infections of the Pacific oyster Crassostrea gigas in Tomales Bay, California, USA. Diseases of aquatic organisms. 2006;72(1):31-43.

26. Image Processing and Analysis in Java [http://rsb.info.nih.gov/ij/].

27. Roizman B, Carmichael LE, Deinhardt F, de-The G, Nahmias AJ, Plowright W, et al. Herpesviridae. Definition, provisional nomenclature, and taxonomy. The Herpesvirus Study Group, the International Committee on Taxonomy of Viruses. Intervirology. 1981;16(4):201-17.

28. Roizman B, Baines J. The diversity and unity of Herpesviridae. Comp Immunol Microbiol Infect Dis. 1991;14(2):63-79.

29. Sterz H, Ludwig H, Rott R. Immunologic and genetic relationship between herpes simplex virus and bovine herpes mammillitis virus. Intervirology. 1974;2(1):1-13.

30. Pellett PE, Biggin MD, Barrell B, Roizman B. Epstein-Barr virus genome may encode a protein showing significant amino acid and predicted secondary structure homology with glycoprotein B of herpes simplex virus 1. J Virol. 1985;56(3):807-13.

31. Gompels UA, Craxton MA, Honess RW. Conservation of glycoprotein H (gH) in herpesviruses: nucleotide sequence of the gH gene from herpesvirus saimiri. J Gen Virol. 1988;69 (Pt 11):2819-29.

32. Cameron KR, Stamminger T, Craxton M, Bodemer W, Honess RW, Fleckenstein B. The 160,000-Mr virion protein encoded at the right end of the herpesvirus saimiri genome is homologous to the 140,000-Mr membrane antigen encoded at the left end of the Epstein-Barr virus genome. J Virol. 1987;61(7):2063-70.

33. Allen GP, Bryans JT. Molecular epizootiology, pathogenesis, and prophylaxis of equine herpesvirus-1 infections. Prog Vet Microbiol Immunol. 1986;2:78-144.

34. Borchers K, Wiik H, Frolich K, Ludwig H, East ML. Antibodies against equine herpesviruses and equine arteritis virus in Burchell's zebras (Equus burchelli) from the Serengeti ecosystem. J Wildl Dis. 2005;41(1):80-6.

35. Borchers K, Frolich K, Ludwig H. Detection of equine herpesvirus types 2 and 5 (EHV-2 and EHV-5) in Przewalski's wild horses. Arch Virol. 1999;144(4):771-80.

36. Kydd JH, Slater J, Osterrieder N, Lunn DP, Antczak DF, Azab W, et al. Third International Havemeyer Workshop on Equine Herpesvirus type 1. Equine Vet J. 2012;44(5):513-7.

37. Azab W, Damiani AM, Ochs A, Osterrieder N. Subclinical infection of a young captive Asian elephant with elephant endotheliotropic herpesvirus 1. Arch Virol. 2017.

38. Long SY, Latimer EM, Hayward GS. Review of Elephant Endotheliotropic Herpesviruses and Acute Hemorrhagic Disease. ILAR J. 2016;56(3):283-96.

39. Whitwell KE, Blunden AS. Pathological findings in horses dying during an outbreak of the paralytic form of Equid herpesvirus type 1 (EHV-1) infection. Equine Vet J. 1992;24(1):13-9.

40. Craig MI, Barrandeguy ME, Fernandez FM. Equine herpesvirus 2 (EHV-2) infection in thoroughbred horses in Argentina. BMC Vet Res. 2005;1:9.

41. Galosi CM, de la Paz VC, Fernandez LC, Martinez JP, Craig MI, Barrandeguy M, et al. Isolation of equine herpesvirus-2 from the lung of an aborted fetus. J Vet Diagn Invest. 2005;17(5):500-2.

42. Barrandeguy M, Thiry E. Equine coital exanthema and its potential economic implications for the equine industry. Vet J. 2012;191(1):35-40.

43. Crabb BS, Studdert MJ. Equine herpesviruses 4 (equine rhinopneumonitis virus) and 1 (equine abortion virus). Adv Virus Res. 1995;45:153-90.

44. Williams KJ, Maes R, Del Piero F, Lim A, Wise A, Bolin DC, et al. Equine multinodular pulmonary fibrosis: a newly recognized herpesvirus-associated fibrotic lung disease. Vet Pathol. 2007;44(6):849-62.

45. Marenzoni ML, Stefanetti V, Danzetta ML, Timoney PJ. Gammaherpesvirus infections in equids: a review. Vet Med (Auckl). 2015;6:91-101.

46. Ehlers B, Dural G, Yasmum N, Lembo T, de Thoisy B, Ryser-Degiorgis MP, et al. Novel mammalian herpesviruses and lineages within the Gammaherpesvirinae: cospeciation and interspecies transfer. J Virol. 2008;82(7):3509-16.

47. Ehlers B, Borchers K, Grund C, Frolich K, Ludwig H, Buhk HJ. Detection of new DNA polymerase genes of known and potentially novel herpesviruses by PCR with degenerate and deoxyinosine-substituted primers. Virus Genes. 1999;18(3):211-20.

48. Garvey M, Suarez NM, Kerr K, Hector R, Moloney-Quinn L, Arkins S, et al. Equid herpesvirus 8: Complete genome sequence and association with abortion in mares. PLoS One. 2018;13(2):e0192301.

49. Fukushi H, Tomita T, Taniguchi A, Ochiai Y, Kirisawa R, Matsumura T, et al. Gazelle herpesvirus 1: a new neurotropic herpesvirus immunologically related to equine herpesvirus 1. Virology. 1997;227(1):34-44.

50. Yanai T, Sakai T, Fukushi H, Hirai K, Narita M, Sakai H, et al. Neuropathological study of gazelle herpesvirus 1 (equine herpesvirus 9) infection in Thomson's gazelles (Gazella thomsoni). J Comp Pathol. 1998;119(2):159-68.

51. Abdelgawad A, Damiani A, Ho SY, Strauss G, Szentiks CA, East ML, et al. Zebra Alphaherpesviruses (EHV-1 and EHV-9): Genetic Diversity, Latency and Co-Infections. Viruses. 2016;8(9).

52. Ossent P, Guscetti F, Metzler AE, Lang EM, Rubel A, Hauser B. Acute and fatal herpesvirus infection in a young Asian elephant (Elephas maximus). Vet Pathol. 1990;27(2):131-3.

53. Richman LK, Zong JC, Latimer EM, Lock J, Fleischer RC, Heaggans SY, et al. Elephant endotheliotropic herpesviruses EEHV1A, EEHV1B, and EEHV2 from cases of hemorrhagic disease are highly diverged from other mammalian herpesviruses and may form a new subfamily. J Virol. 2014;88(23):13523-46.

54. Ortega J, Corpa JM, Orden JA, Blanco J, Carbonell MD, Gerique AC, et al. Acute death associated with Citrobacter freundii infection in an African elephant (Loxodonta africana). J Vet Diagn Invest. 2015;27(5):632-6.

55. Latimer E, Zong JC, Heaggans SY, Richman LK, Hayward GS. Detection and evaluation of novel herpesviruses in routine and pathological samples from Asian and African elephants: identification of two new probosciviruses (EEHV5 and EEHV6) and two new gammaherpesviruses (EGHV3B and EGHV5). Vet Microbiol. 2011;147(1-2):28-41.

56. Ling PD, Long SY, Fuery A, Peng RS, Heaggans SY, Qin X, et al. Complete Genome Sequence of Elephant Endotheliotropic Herpesvirus 4, the First Example of a GC-Rich Branch Proboscivirus. mSphere. 2016;1(3).

57. Fuery A, Browning GR, Tan J, Long S, Hayward GS, Cox SK, et al. Clinical Infection of Captive Asian Elephants (Elephas Maximus) with Elephant Endotheliotropic Herpesvirus 4. J Zoo Wildl Med. 2016;47(1):311-8.

58. Wilkie GS, Davison AJ, Kerr K, Stidworthy MF, Redrobe S, Steinbach F, et al. First fatality associated with elephant endotheliotropic herpesvirus 5 in an Asian elephant: pathological findings and complete viral genome sequence. Sci Rep. 2014;4:6299.

59. Atkins L, Zong JC, Tan J, Mejia A, Heaggans SY, Nofs SA, et al. Elephant endotheliotropic herpesvirus 5, a newly recognized elephant herpesvirus associated with clinical and subclinical infections in captive Asian elephants (Elephas maximus). J Zoo Wildl Med. 2013;44(1):136-43.

60. Garner MM, Helmick K, Ochsenreiter J, Richman LK, Latimer E, Wise AG, et al. Clinico-pathologic features of fatal disease attributed to new variants of endotheliotropic herpesviruses in two Asian elephants (Elephas maximus). Vet Pathol. 2009;46(1):97-104.

61. Reed SM, Toribio RE. Equine herpesvirus 1 and 4. Vet Clin North Am Equine Pract. 2004;20(3):631-42.

62. Baghi HB, Nauwynck HJ. Impact of equine herpesvirus type 1 (EHV-1) infection on the migration of monocytic cells through equine nasal mucosa. Comp Immunol Microbiol Infect Dis. 2014;37(5-6):321-9.

63. Kydd JH, Smith KC, Hannant D, Livesay GJ, Mumford JA. Distribution of equid herpesvirus-1 (EHV-1) in respiratory tract associated lymphoid tissue: implications for cellular immunity. Equine Vet J. 1994;26(6):470-3.

64. Scott JC, Dutta SK, Myrup AC. In vivo harboring of equine herpesvirus-1 in leukocyte populations and subpopulations and their quantitation from experimentally infected ponies. Am J Vet Res. 1983;44(7):1344-8.

65. Hussey SB, Clark R, Lunn KF, Breathnach C, Soboll G, Whalley JM, et al. Detection and quantification of equine herpesvirus-1 viremia and nasal shedding by real-time polymerase chain reaction. J Vet Diagn Invest. 2006;18(4):335-42.

66. Wilsterman S, Soboll-Hussey G, Lunn DP, Ashton LV, Callan RJ, Hussey SB, et al. Equine herpesvirus-1 infected peripheral blood mononuclear cell subpopulations during viremia. Vet Microbiol. 2011;149(1-2):40-7.

67. Goehring LS, Hussey GS, Ashton LV, Schenkel AR, Lunn DP. Infection of central nervous system endothelial cells by cell-associated EHV-1. Vet Microbiol. 2011;148(2-4):389-95.

68. van der Meulen KM, Nauwynck HJ, Pensaert MB. Increased susceptibility of peripheral blood mononuclear cells to equine herpes virus type 1 infection upon mitogen stimulation: a role of the cell cycle and of cell-to-cell transmission of the virus. Vet Microbiol. 2002;86(1-2):157-63.

69. Nauwynck HJ, Pensaert MB. Virus production and viral antigen expression in porcine blood monocytes inoculated with pseudorabies virus. Arch Virol. 1994;137(1-2):69-79.

70. Mainka C, Fuss B, Geiger H, Hofelmayr H, Wolff MH. Characterization of viremia at different stages of varicella-zoster virus infection. J Med Virol. 1998;56(1):91-8.

71. Patel JR, Heldens J. Equine herpesviruses 1 (EHV-1) and 4 (EHV-4)--epidemiology, disease and immunoprophylaxis: a brief review. Vet J. 2005;170(1):14-23.

72. Azab W, Osterrieder N. Glycoproteins D of equine herpesvirus type 1 (EHV-1) and EHV-4 determine cellular tropism independently of integrins. J Virol. 2012;86(4):2031-44.

73. Vandekerckhove AP, Glorieux S, Gryspeerdt AC, Steukers L, Van Doorsselaere J, Osterrieder N, et al. Equine alphaherpesviruses (EHV-1 and EHV-4) differ in their efficiency to infect mononuclear cells during early steps of infection in nasal mucosal explants. Vet Microbiol. 2011;152(1-2):21-8.

74. Matsumura T, Sugiura T, Imagawa H, Fukunaga Y, Kamada M. Epizootiological aspects of type 1 and type 4 equine herpesvirus infections among horse populations. J Vet Med Sci. 1992;54(2):207-11.

75. Patel JR, Foldi J, Bateman H, Williams J, Didlick S, Stark R. Equid herpesvirus (EHV-1) live vaccine strain C147: efficacy against respiratory diseases following EHV types 1 and 4 challenges. Vet Microbiol. 2003;92(1-2):1-17.

76. van Der Meulen KM, Nauwynck HJ, Buddaert W, Pensaert MB. Replication of equine herpesvirus type 1 in freshly isolated equine peripheral blood mononuclear cells and changes in susceptibility following mitogen stimulation. J Gen Virol. 2000;81(Pt 1):21-5.

77. Spiesschaert B, Goldenbogen B, Taferner S, Schade M, Mahmoud M, Klipp E, et al. Role of gB and pUS3 in Equine Herpesvirus 1 Transfer between Peripheral Blood Mononuclear Cells and Endothelial Cells: a Dynamic In Vitro Model. J Virol. 2015;89(23):11899-908.

78. Laval K, Favoreel HW, Poelaert KC, Van Cleemput J, Nauwynck HJ. Equine Herpesvirus Type 1 Enhances Viral Replication in CD172a+ Monocytic Cells upon Adhesion to Endothelial Cells. J Virol. 2015;89(21):10912-23.

79. Poelaert KCK, Van Cleemput J, Laval K, Favoreel HW, Couck L, Van den Broeck W, et al. Equine Herpesvirus 1 Bridles T Lymphocytes To Reach Its Target Organs. J Virol. 2019;93(7).

80. Hogg N, Landis RC. Adhesion molecules in cell interactions. Curr Opin Immunol. 1993;5(3):383-90.

81. Smith D, Hamblin A, Edington N. Equid herpesvirus 1 infection of endothelial cells requires activation of putative adhesion molecules: an in vitro model. Clin Exp Immunol. 2002;129(2):281-7.

82. Baxi MK, Efstathiou S, Lawrence G, Whalley JM, Slater JD, Field HJ. The detection of latency-associated transcripts of equine herpesvirus 1 in ganglionic neurons. J Gen Virol. 1995;76 (Pt 12):3113-8.

83. Chesters PM, Allsop R, Purewal A, Edington N. Detection of latency-associated transcripts of equid herpesvirus 1 in equine leukocytes but not in trigeminal ganglia. J Virol. 1997;71(5):3437-43.

84. Borchers K, Wolfinger U, Ludwig H. Latency-associated transcripts of equine herpesvirus type 4 in trigeminal ganglia of naturally infected horses. J Gen Virol. 1999;80 (Pt 8):2165-71.

85. Pronost S, Cook RF, Fortier G, Timoney PJ, Balasuriya UB. Relationship between equine herpesvirus-1 myeloencephalopathy and viral genotype. Equine Vet J. 2010;42(8):672-4.

86. Greenwood AD, Tsangaras K, Ho SY, Szentiks CA, Nikolin VM, Ma G, et al. A potentially fatal mix of herpes in zoos. Curr Biol. 2012;22(18):1727-31.

87. Blunden AS, Smith KC, Whitwell KE, Dunn KA. Systemic infection by equid herpesvirus-1 in a Grevy's zebra stallion (Equus grevyi) with particular reference to genital pathology. J Comp Pathol. 1998;119(4):485-93.

88. Montali RJ, Allen GP, Bryans JT, Phillips LG, Bush M. Equine herpesvirus type 1 abortion in an onager and suspected herpesvirus myelitis in a zebra. J Am Vet Med Assoc. 1985;187(11):1248-9.

89. Wolff PL, Meehan TP, Basgall EJ, Allen GP, Sundberg JP. Abortion and perinatal foal mortality associated with equine herpesvirus type 1 in a herd of Grevy's zebra. J Am Vet Med Assoc. 1986;189(9):1185-6.

90. Guo X, Izume S, Okada A, Ohya K, Kimura T, Fukushi H. Full genome sequences of zebra-borne equine herpesvirus type 1 isolated from zebra, onager and Thomson's gazelle. J Vet Med Sci. 2014;76(9):1309-12.

91. Rebhun WC, Jenkins DH, Riis RC, Dill SG, Dubovi EJ, Torres A. An epizootic of blindness and encephalitis associated with a herpesvirus indistinguishable from equine herpesvirus I in a herd of alpacas and llamas. J Am Vet Med Assoc. 1988;192(7):953-6.

92. Crandell RA, Ichimura H, Kit S. Isolation and comparative restriction endonuclease DNA fingerprinting of equine herpesvirus-1 from cattle. Am J Vet Res. 1988;49(11):1807-13.

93. Chowdhury SI, Ludwig H, Buhk HJ. Molecular biological characterization of equine herpesvirus type 1 (EHV-1) isolates from ruminant hosts. Virus Res. 1988;11(2):127-39.
94. Pagamjav O, Yamada S, Ibrahim el SM, Crandell RA, Matsumura T, Yamaguchi T, et al. Molecular characterization of equine herpesvirus 1 (EHV-1) isolated from cattle indicating no specific mutations associated with the interspecies transmission. Microbiol Immunol. 2007;51(3):313-9.
95. Abdelgawad A, Hermes R, Damiani A, Lamglait B, Czirjak GA, East M, et al. Comprehensive Serology Based on a Peptide ELISA to Assess the Prevalence of Closely Related Equine Herpesviruses in Zoo and Wild Animals. PLoS One. 2015;10(9):e0138370.
96. Dimock WWaE, P. R. Is there a filterable virus of abortion in

mares? In: Bulletin KAES, editor. 1933. p. 297-301.
97. Jackson T, Kendrick JW. Paralysis of horses associated with equine herpesvirus 1 infection. J Am Vet Med Assoc. 1971;158(8):1351-7.
98. Saxegaard F. Isolation and identification of equine rhinopneumonitis virus (equine abortion virus) from cases of abortion and paralysis. Nordic Veterinary Medicine (Baltimore). 1966;18:504-10.
99. Doll ER, McCollum WH, Wallace ME, Bryans JT, Richards MG. Complement-fixation reactions in equine virus abortion. Am J Vet Res. 1953;14(50):40-5.
100. Kawakami Y, Kaji T, Sugimura K, Ishitani R, Shimizu T, Matumoto M. Histopathological study of aborted fetuses naturally infected with equine abortion virus with some epidemiological findings. Jpn J Exp Med. 1959;29:635-41.
101. Kawakami Y, Kaji T, Sugimura K, Shimizu T, Matumoto M. A preliminary survey for equine abortion virus infection by complement fixation test in Hokkaido, Japan. Jpn J Exp Med. 1959;29:203-11.
102. Shimizu T, Ishizaki R, Ishii S, Kawakami Y, Kaji T, Sugimura K, et al. Isolation of equine abortion virus from natural cases of equine abortion in horse kidney cell culture. Jpn J Exp Med. 1959;29:643-9.
103. Studdert MJ, Simpson T, Roizman B. Differentiation of respiratory and abortigenic isolates of equine herpesvirus 1 by restriction endonucleases. Science. 1981;214(4520):562-4.
104. Roizmann B, Desrosiers RC, Fleckenstein B, Lopez C, Minson AC, Studdert MJ. The family Herpesviridae: an update. The Herpesvirus Study Group of the International Committee on Taxonomy of Viruses. Arch Virol. 1992;123(3-4):425-49.
105. Ruyechan WT, Dauenhauer SA, O'Callaghan DJ. Electron microscopic study of equine herpesvirus type 1 DNA. J Virol. 1982;42(1):297-300.

106. Turtinen LW, Allen GP. Identification of the envelope surface glycoproteins of equine herpesvirus type 1. J Gen Virol. 1982;63(2):481-5.
107. Ma G, Azab W, Osterrieder N. Equine herpesviruses type 1 (EHV-1) and 4 (EHV-4)--masters of co-evolution and a constant threat to equids and beyond. Vet Microbiol. 2013;167(1-2):123-34.
108. Shakya AK, O'Callaghan DJ, Kim SK. Comparative Genomic Sequencing and Pathogenic Properties of Equine Herpesvirus 1 KyA and RacL11. Front Vet Sci. 2017;4:211.
109. Telford EA, Watson MS, McBride K, Davison AJ. The DNA sequence of equine herpesvirus-1. Virology. 1992;189(1):304-16.
110. Telford EA, Watson MS, Perry J, Cullinane AA, Davison AJ. The DNA sequence of equine herpesvirus-4. J Gen Virol. 1998;79 1197-203.
111. Perdue ML, Kemp MC, Randall CC, O'Callaghan DJ. Studies of the molecular anatomy of the L-M cell strain of equine herpes virus type 1: proteins of the nucleocapsid and intact virion. Virology. 1974;59(1):201-16.
112. Purewal AS, Allsopp R, Riggio M, Telford EA, Azam S, Davison AJ, et al. Equid herpesviruses 1 and 4 encode functional homologs of the herpes simplex virus type 1 virion transactivator protein, VP16. Virology. 1994;198(1):385-9.
113. McLauchlan J, Rixon FJ. Characterization of enveloped tegument structures (L particles) produced by alphaherpesviruses: integrity of the tegument does not depend on the presence of capsid or envelope. J Gen Virol. 1992;73 (Pt 2):269-76.
114. Kim SK, Ahn BC, Albrecht RA, O'Callaghan DJ. The unique IR2 protein of equine herpesvirus 1 negatively regulates viral gene expression. J Virol. 2006;80(10):5041-9.
115. Wellington JE, Love DN, Whalley JM. Evidence for involvement of equine herpesvirus 1 glycoprotein B in cell-cell fusion. Arch Virol. 1996;141(1):167-75.
116. Neubauer A, Braun B, Brandmuller C, Kaaden OR, Osterrieder N. Analysis of the contributions of the equine herpesvirus 1 glycoprotein gB homolog to virus entry and direct cell-to-cell spread. Virology. 1997;227(2):281-94.
117. Spiesschaert B, Osterrieder N, Azab W. Comparative analysis of glycoprotein B (gB) of equine herpesvirus type 1 and type 4 (EHV-1 and EHV-4) in cellular tropism and cell-to-cell transmission. Viruses. 2015;7(2):522-42.
118. Osterrieder N. Construction and characterization of an equine herpesvirus 1 glycoprotein C negative mutant. Virus research. 1999;59(2):165-77.
119. Azab W, Tsujimura K, Maeda K, Kobayashi K, Mohamed YM, Kato K, et al. Glycoprotein C of equine herpesvirus 4 plays a role in viral binding to cell surface heparan sulfate. Virus Res. 2010;151(1):1-9.

120. Huemer HP, Nowotny N, Crabb BS, Meyer H, Hubert PH. gp13 (EHV-gC): a complement receptor induced by equine herpesviruses. Virus Res. 1995;37(2):113-26.
121. Elton DM, Halliburton IW, Killington RA, Meredith DM, Bonass WA. Identification of the equine herpesvirus type 1 glycoprotein 17/18 as a homologue of herpes simplex virus glycoprotein D. J Gen Virol. 1992;73 (Pt 5):1227-33.
122. Whittaker GR, Taylor LA, Elton DM, Giles LE, Bonass WA, Halliburton IW, et al. Glycoprotein 60 of equine herpesvirus type 1 is a homologue of herpes simplex virus glycoprotein D and plays a major role in penetration of cells. J Gen Virol. 1992;73 (Pt 4):801-9.
123. Kurtz BM, Singletary LB, Kelly SD, Frampton AR, Jr. Equus caballus major histocompatibility complex class I is an entry receptor for equine herpesvirus type 1. J Virol. 2010;84(18):9027-34.
124. Favoreel HW, Nauwynck HJ, Pensaert MB. Role of the cytoplasmic tail of gE in antibody-induced redistribution of viral glycoproteins expressed on pseudorabies-virus-infected cells. Virology. 1999;259(1):141-7.
125. Matsumura T, Kondo T, Sugita S, Damiani AM, O'Callaghan DJ, Imagawa H. An equine herpesvirus type 1 recombinant with a deletion in the gE and gI genes is avirulent in young horses. Virology. 1998;242(1):68-79.
126. Thormann N, Van de Walle GR, Azab W, Osterrieder N. The role of secreted glycoprotein G of equine herpesvirus type 1 and type 4 (EHV-1 and EHV-4) in immune modulation and virulence. Virus Res. 2012;169(1):203-11.
127. Van de Walle GR, May ML, Sukhumavasi W, von Einem J, Osterrieder N. Herpesvirus chemokine-binding glycoprotein G (gG) efficiently inhibits neutrophil chemotaxis in vitro and in vivo. J Immunol. 2007;179(6):4161-9.
128. Bryant NA, Davis-Poynter N, Vanderplasschen A, Alcami A. Glycoprotein G isoforms from some alphaherpesviruses function as broad-spectrum chemokine binding proteins. The EMBO journal. 2003;22(4):833-46.
129. Azab W, Lehmann MJ, Osterrieder N. Glycoprotein H and alpha4beta1 Integrins Determine the Entry Pathway of Alphaherpesviruses. J Virol. 2013;87(10):5937-48.
130. Chowdary TK, Cairns TM, Atanasiu D, Cohen GH, Eisenberg RJ, Heldwein EE. Crystal structure of the conserved herpesvirus fusion regulator complex gH-gL. Nat Struct Mol Biol. 2010;17(7):882-8.
131. Azab W, Zajic L, Osterrieder N. The role of glycoprotein H of equine herpesviruses 1 and 4 (EHV-1 and EHV-4) in cellular host range and integrin binding. Vet Res. 2012;43(1):61.

132. Tsujimura K, Yamanaka T, Kondo T, Fukushi H, Matsumura T. Pathogenicity and immunogenicity of equine herpesvirus type 1 mutants defective in either gI or gE gene in murine and hamster models. J Vet Med Sci. 2006;68(10):1029-38.

133. Neubauer A, Osterrieder N. Equine herpesvirus type 1 (EHV-1) glycoprotein K is required for efficient cell-to-cell spread and virus egress. Virology. 2004;329(1):18-32.

134. Kim SK, Bowles DE, O'Callaghan D J. The gamma2 late glycoprotein K promoter of equine herpesvirus 1 is differentially regulated by the IE and EICP0 proteins. Virology. 1999;256(2):173-9.

135. Azab W, El-Sheikh A. The role of equine herpesvirus type 4 glycoprotein k in virus replication. Viruses. 2012;4(8):1258-63.

136. Stokes A, Alber DG, Greensill J, Amellal B, Carvalho R, Taylor LA, et al. The expression of the proteins of equine herpesvirus 1 which share homology with herpes simplex virus 1 glycoproteins H and L. Virus Res. 1996;40(1):91-107.

137. Spear PG. Herpes simplex virus: receptors and ligands for cell entry. Cell Microbiol. 2004;6(5):401-10.

138. Spear PG, Longnecker R. Herpesvirus entry: an update. J Virol. 2003;77(19):10179-85.

139. Osterrieder N, Neubauer A, Brandmuller C, Braun B, Kaaden OR, Baines JD. The equine herpesvirus 1 glycoprotein gp21/22a, the herpes simplex virus type 1 gM homolog, is involved in virus penetration and cell-to-cell spread of virions. J Virol. 1996;70(6):4110-5.

140. Osterrieder N, Neubauer A, Fakler B, Brandmuller C, Seyboldt C, Kaaden OR, et al. Synthesis and processing of the equine herpesvirus 1 glycoprotein M. Virology. 1997;232(1):230-9.

141. Rudolph J, Osterrieder N. Equine herpesvirus type 1 devoid of gM and gp2 is severely impaired in virus egress but not direct cell-to-cell spread. Virology. 2002;293(2):356-67.

142. Seyboldt C, Granzow H, Osterrieder N. Equine herpesvirus 1 (EHV-1) glycoprotein M: effect of deletions of transmembrane domains. Virology. 2000;278(2):477-89.

143. Rudolph J, Seyboldt C, Granzow H, Osterrieder N. The gene 10 (UL49.5) product of equine herpesvirus 1 is necessary and sufficient for functional processing of glycoprotein M. J Virol. 2002;76(6):2952-63.

144. Verweij MC, Ressing ME, Knetsch W, Quinten E, Halenius A, van Bel N, et al. Inhibition of mouse TAP by immune evasion molecules encoded by non-murine herpesviruses. Molecular immunology. 2011;48(6-7):835-45.

145. Smith PM, Kahan SM, Rorex CB, von Einem J, Osterrieder N, O'Callaghan DJ. Expression of the full-length form of gp2 of equine herpesvirus 1 (EHV-1) completely

restores respiratory virulence to the attenuated EHV-1 strain KyA in CBA mice. J Virol. 2005;79(8):5105-15.

146. Ma G, Feineis S, Osterrieder N, Van de Walle GR. Identification and characterization of equine herpesvirus type 1 pUL56 and its role in virus-induced downregulation of major histocompatibility complex class I. J Virol. 2012;86(7):3554-63.

147. Huang T, Ma G, Osterrieder N. Equine Herpesvirus 1 Multiply Inserted Transmembrane Protein pUL43 Cooperates with pUL56 in Downregulation of Cell Surface Major Histocompatibility Complex Class I. J Virol. 2015;89(12):6251-63.

148. Huang T, Lehmann MJ, Said A, Ma G, Osterrieder N. Major histocompatibility complex class I downregulation induced by equine herpesvirus type 1 pUL56 is through dynamin-dependent endocytosis. J Virol. 2014;88(21):12802-15.

149. Cardone J, Le Friec G, Kemper C. CD46 in innate and adaptive immunity: an update. Clin Exp Immunol. 2011;164(3):301-11.

150. Pols MS, Klumperman J. Trafficking and function of the tetraspanin CD63. Exp Cell Res. 2009;315(9):1584-92.

151. Soboll Hussey G, Ashton LV, Quintana AM, Van de Walle GR, Osterrieder N, Lunn DP. Equine herpesvirus type 1 pUL56 modulates innate responses of airway epithelial cells. Virology. 2014;464-465:76-86.

152. Soboll Hussey G, Hussey SB, Wagner B, Horohov DW, Van de Walle GR, Osterrieder N, et al. Evaluation of immune responses following infection of ponies with an EHV-1 ORF1/2 deletion mutant. Vet Res. 2011;42:23.

153. Wimer CL, Schnabel CL, Perkins G, Babasyan S, Freer H, Stout AE, et al. The deletion of the ORF1 and ORF71 genes reduces virulence of the neuropathogenic EHV-1 strain Ab4 without compromising host immunity in horses. PLoS One. 2018;13(11):e0206679.

154. Perkins G, Babasyan S, Stout AE, Freer H, Rollins A, Wimer CL, et al. Intranasal IgG4/7 antibody responses protect horses against equid herpesvirus-1 (EHV-1) infection including nasal virus shedding and cell-associated viremia. Virology. 2019;531:219-32.

155. Ushijima Y, Goshima F, Kimura H, Nishiyama Y. Herpes simplex virus type 2 tegument protein UL56 relocalizes ubiquitin ligase Nedd4 and has a role in transport and/or release of virions. Virol J. 2009;6:168.

156. Koshizuka T, Kawaguchi Y, Goshima F, Mori I, Nishiyama Y. Association of two membrane proteins encoded by herpes simplex virus type 2, UL11 and UL56. Virus Genes. 2006;32(2):153-63.

157. Berkowitz C, Moyal M, Rosen-Wolff A, Darai G, Becker Y. Herpes simplex virus type 1 (HSV-1) UL56 gene is involved in viral intraperitoneal pathogenicity to immunocompetent mice. Arch Virol. 1994;134(1-2):73-83.

158. Hubert PH, Birkenmaier S, Rziha HJ, Osterrieder N. Alterations in the equine herpesvirus type-1 (EHV-1) strain RacH during attenuation. Zentralbl Veterinarmed B. 1996;43(1):1-14.

159. Yalamanchili RR, Raengsakulrach B, O'Callaghan DJ. Equine herpesvirus 1 sequence near the left terminus codes for two open reading frames. Virus Res. 1991;18(2-3):109-16.

160. Schnabel CL, Wimer CL, Perkins G, Babasyan S, Freer H, Watts C, et al. Deletion of the ORF2 gene of the neuropathogenic equine herpesvirus type 1 strain Ab4 reduces virulence while maintaining strong immunogenicity. BMC Vet Res. 2018;14(1):245.

161. Schnabel CL, Babasyan S, Rollins A, Freer H, Wimer CL, Perkins GA, et al. An equine herpesvirus type 1 (EHV-1) Ab4 open reading frame (ORF)2 deletion mutant provides immunity and protection from EHV-1 infection and disease. J Virol. 2019.

162. Goodman LB, Wagner B, Flaminio MJ, Sussman KH, Metzger SM, Holland R, et al. Comparison of the efficacy of inactivated combination and modified-live virus vaccines against challenge infection with neuropathogenic equine herpesvirus type 1 (EHV-1). Vaccine. 2006;24(17):3636-45.

163. Kim SK, Shakya AK, O'Callaghan DJ. Immunization with Attenuated Equine Herpesvirus 1 Strain KyA Induces Innate Immune Responses That Protect Mice from Lethal Challenge. J Virol. 2016;90(18):8090-104.

164. MacLean CA, Efstathiou S, Elliott ML, Jamieson FE, McGeoch DJ. Investigation of herpes simplex virus type 1 genes encoding multiply inserted membrane proteins. J Gen Virol. 1991;72 (Pt 4):897-906.

165. Klupp BG, Altenschmidt J, Granzow H, Fuchs W, Mettenleiter TC. Identification and characterization of the pseudorabies virus UL43 protein. Virology. 2005;334(2):224-33.

166. Edington N, Welch HM, Griffiths L. The prevalence of latent Equid herpesviruses in the tissues of 40 abattoir horses. Equine Vet J. 1994;26(2):140-2.

167. Doll ER, Mc CW, Bryans JT, Crowe ME. Effect of physical and chemical environment on the viability of equine rhinopneumonitis virus propagated in hamsters. Cornell Vet. 1959;49(1):75-81.

168. Dayaram A, Franz M, Schattschneider A, Damiani AM, Bischofberger S, Osterrieder N, et al. Long term stability and infectivity of herpesviruses in water. Sci Rep. 2017;7:46559.

169. Ataseven VS, Dagalp SB, Guzel M, Basaran Z, Tan MT, Geraghty B. Prevalence of equine herpesvirus-1 and equine herpesvirus-4 infections in equidae species in Turkey as determined by ELISA and multiplex nested PCR. Res Vet Sci. 2009;86(2):339-44.
170. Gilkerson JR, Love DN, Drummer HE, Studdert MJ, Whalley JM. Seroprevalence of equine herpesvirus 1 in thoroughbred foals before and after weaning. Aust Vet J. 1998;76(10):677-82.
171. Gilkerson JR, Love DN, Whalley JM. Epidemiology of equine herpesvirus abortion: searching for clues to the future. Aust Vet J. 1998;76(10):675-6.
172. Foote CE, Love DN, Gilkerson JR, Whalley JM. Detection of EHV-1 and EHV-4 DNA in unweaned Thoroughbred foals from vaccinated mares on a large stud farm. Equine Vet J. 2004;36(4):341-5.
173. Slater J. Chapter 14 - Equine Herpesviruses. In: Sellon DC, Long MT, editors. Equine Infectious Diseases (Second Edition). St. Louis: W.B. Saunders; 2014. p. 151-68.e8.
174. Gibson JS, Slater JD, Awan AR, Field HJ. Pathogenesis of equine herpesvirus-1 in specific pathogen-free foals: primary and secondary infections and reactivation. Arch Virol. 1992;123(3-4):351-66.
175. Stokes A, Corteyn AH, Murray PK. Clinical signs and humoral immune response in horses following equine herpesvirus type-1 infection and their susceptibility to equine herpesvirus type-4 challenge. Res Vet Sci. 1991;51(2):141-8.
176. Slater JD, Borchers K, Thackray AM, Field HJ. The trigeminal ganglion is a location for equine herpesvirus 1 latency and reactivation in the horse. J Gen Virol. 1994;75 (Pt 8):2007-16.
177. McCulloch J, Williamson SA, Powis SJ, Edington N. The effect of EHV-1 infection upon circulating leucocyte populations in the natural equine host. Vet Microbiol. 1993;37(1-2):147-61.
178. Allen GP, Breathnach CC. Quantification by real-time PCR of the magnitude and duration of leucocyte-associated viraemia in horses infected with neuropathogenic vs. non-neuropathogenic strains of EHV-1. Equine Vet J. 2006;38(3):252-7.
179. Edington N, Bridges CG, Patel JR. Endothelial cell infection and thrombosis in paralysis caused by equid herpesvirus-1: equine stroke. Arch Virol. 1986;90(1-2):111-24.
180. Pusterla N, Leutenegger CM, Wilson WD, Watson JL, Ferraro GL, Madigan JE. Equine herpesvirus-4 kinetics in peripheral blood leukocytes and nasopharyngeal secretions in foals using quantitative real-time TaqMan PCR. J Vet Diagn Invest. 2005;17(6):578-81.
181. Borchers K, Wolfinger U, Lawrenz B, Schellenbach A, Ludwig H. Equine herpesvirus 4 DNA in trigeminal ganglia of naturally infected horses detected by direct in situ PCR. J Gen Virol. 1997;78 (Pt 5):1109-14.

182. Banfield BW, Leduc Y, Esford L, Visalli RJ, Brandt CR, Tufaro F. Evidence for an interaction of herpes simplex virus with chondroitin sulfate proteoglycans during infection. Virology. 1995;208(2):531-9.

183. Sasaki M, Hasebe R, Makino Y, Suzuki T, Fukushi H, Okamoto M, et al. Equine major histocompatibility complex class I molecules act as entry receptors that bind to equine herpesvirus-1 glycoprotein D. Genes Cells. 2011;16(4):343-57.

184. Hasebe R, Sasaki M, Sawa H, Wada R, Umemura T, Kimura T. Infectious entry of equine herpesvirus-1 into host cells through different endocytic pathways. Virology. 2009;393(2):198-209.

185. Frampton AR, Jr., Uchida H, von Einem J, Goins WF, Grandi P, Cohen JB, et al. Equine herpesvirus type 1 (EHV-1) utilizes microtubules, dynein, and ROCK1 to productively infect cells. Vet Microbiol. 2010;141(1-2):12-21.

186. Caughman GB, Staczek J, O'Callaghan DJ. Equine herpesvirus type 1 infected cell polypeptides: evidence for immediate early/early/late regulation of viral gene expression. Virology. 1985;145(1):49-61.

187. Lewis JB, Thompson YG, Caughman GB. Transcriptional control of the equine herpesvirus 1 immediate early gene. Virology. 1993;197(2):788-92.

188. Weller SK, Coen DM. Herpes simplex viruses: mechanisms of DNA replication. Cold Spring Harb Perspect Biol. 2012;4(9):a013011.

189. Azab W, Osterrieder K. Initial Contact: The First Steps in Herpesvirus Entry. In: Osterrieder K, editor. Cell Biology of Herpes Viruses. Cham: Springer International Publishing; 2017. p. 1-27.

190. Gleeson LJ, Coggins L. Response of pregnant mares to equine herpesvirus 1 (EHV1). Cornell Vet. 1980;70(4):391-400.

191. Paillot R, Daly JM, Juillard V, Minke JM, Hannant D, Kydd JH. Equine interferon gamma synthesis in lymphocytes after in vivo infection and in vitro stimulation with EHV-1. Vaccine. 2005;23(36):4541-51.

192. Mothes W, Sherer NM, Jin J, Zhong P. Virus cell-to-cell transmission. J Virol. 2010;84(17):8360-8.

193. Johnson DC, Huber MT. Directed egress of animal viruses promotes cell-to-cell spread. J Virol. 2002;76(1):1-8.

194. Leick M, Azcutia V, Newton G, Luscinskas FW. Leukocyte recruitment in inflammation: basic concepts and new mechanistic insights based on new models and microscopic imaging technologies. Cell Tissue Res. 2014;355(3):647-56.

195. Proft A, Spiesschaert B, Izume S, Taferner S, Lehmann MJ, Azab W. The Role of the Equine Herpesvirus Type 1 (EHV-1) US3-Encoded Protein Kinase in Actin Reorganization and Nuclear Egress. Viruses. 2016;8(10).

196. Zhong P, Agosto LM, Munro JB, Mothes W. Cell-to-cell transmission of viruses. Curr Opin Virol. 2013;3(1):44-50.

197. Smith KC, Borchers K. A study of the pathogenesis of equid herpesvirus-1 (EHV-1) abortion by DNA in-situ hybridization. J Comp Pathol. 2001;125(4):304-10.

198. Lunn DP, Davis-Poynter N, Flaminio MJ, Horohov DW, Osterrieder K, Pusterla N, et al. Equine herpesvirus-1 consensus statement. J Vet Intern Med. 2009;23(3):450-61.

199. Wagner B, Wimer C, Freer H, Osterrieder N, Erb HN. Infection of peripheral blood mononuclear cells with neuropathogenic equine herpesvirus type-1 strain Ab4 reveals intact interferon-alpha induction and induces suppression of anti-inflammatory interleukin-10 responses in comparison to other viral strains. Vet Immunol Immunopathol. 2011;143(1-2):116-24.

200. Griffin BD, Verweij MC, Wiertz EJ. Herpesviruses and immunity: the art of evasion. Vet Microbiol. 2010;143(1):89-100.

201. York IA. Immune evasion strategies of the herpesviruses. Chem Biol. 1996;3(5):331-5.

202. Awan AR, Chong YC, Field HJ. The pathogenesis of equine herpesvirus type 1 in the mouse: a new model for studying host responses to the infection. J Gen Virol. 1990;71 (Pt 5):1131-40.

203. Field HJ, Awan AR. Effective chemotherapy of equine herpesvirus 1 by phosphonylmethoxyalkyl derivatives of adenine demonstrated in a novel murine model for the disease. Antimicrob Agents Chemother. 1990;34(5):709-17.

204. Awan AR, Gibson JS, Field HJ. A murine model for studying EHV-1-induced abortion. Res Vet Sci. 1991;51(1):94-9.

205. Osterrieder N, Wagner R, Brandmuller C, Schmidt P, Wolf H, Kaaden OR. Protection against EHV-1 challenge infection in the murine model after vaccination with various formulations of recombinant glycoprotein gp14 (gB). Virology. 1995;208(2):500-10.

206. Mori CM, Mori E, Favaro LL, Santos CR, Lara MC, Villalobos EM, et al. Equid herpesvirus type-1 exhibits neurotropism and neurovirulence in a mouse model. J Comp Pathol. 2012;146(2-3):202-10.

207. Walker C, Perotti VM, Love DN, Whalley JM. Infection with equine herpesvirus 1 (EHV-1) strain HVS25A in pregnant mice. J Comp Pathol. 1999;120(1):15-27.

208. Yu MH, Kasem SG, Tsujimura K, Matsumura T, Yanai T, Yamaguchi T, et al. Diverse pathogenicity of equine herpesvirus 1 (EHV-1) isolates in CBA mouse model. J Vet Med Sci. 2010;72(3):301-6.

209. Csellner H, Whalley JM, Love DN. Equine herpesvirus 1 HVS25A isolated from an aborted foetus produces disease in balb/C mice. Aust Vet J. 1995;72(2):68-9.

210. van Woensel PA, Goovaerts D, Markx D, Visser N. A mouse model for testing the pathogenicity of equine herpes virus-1 strains. J Virol Methods. 1995;54(1):39-49.

211. Vandekerckhove A, Glorieux S, Broeck WV, Gryspeerdt A, van der Meulen KM, Nauwynck HJ. In vitro culture of equine respiratory mucosa explants. Vet J. 2009;181(3):280-7.

212. Baghi HB, Nauwynck HJ. Effect of equine herpesvirus type 1 (EHV-1) infection of nasal mucosa epithelial cells on integrin alpha 6 and on different components of the basement membrane. Arch Virol. 2016;161(1):103-10.

213. Van Cleemput J, Poelaert KCK, Laval K, Maes R, Hussey GS, Van den Broeck W, et al. Access to a main alphaherpesvirus receptor, located basolaterally in the respiratory epithelium, is masked by intercellular junctions. Sci Rep-Uk. 2017;7.

214. Vandekerckhove AP, Glorieux S, Gryspeerdt AC, Steukers L, Duchateau L, Osterrieder N, et al. Replication kinetics of neurovirulent versus non-neurovirulent equine herpesvirus type 1 strains in equine nasal mucosal explants. J Gen Virol. 2010;91(Pt 8):2019-28.

215. Vandekerckhove AP, Glorieux S, Gryspeerdt AC, Steukers L, Van Doorsselaere J, Osterrieder N, et al. Equine alphaherpesviruses (EHV-1 and EHV-4) differ in their efficiency to infect mononuclear cells during early steps of infection in nasal mucosal explants. Vet Microbiol. 2011.

216. Negussie H, Li Y, Tessema TS, Nauwynck HJ. Replication characteristics of equine herpesvirus 1 and equine herpesvirus 3: comparative analysis using ex vivo tissue cultures. Vet Res. 2016;47:19.

217. Vonbonsdorff CH, Fuller SD, Simons K. Apical and Basolateral Endocytosis in Madin-Darby Canine Kidney (Mdck) Cells Grown on Nitrocellulose Filters. Embo Journal. 1985;4(11):2781-92.

218. Handler JS, Preston AS, Steele RE. Factors affecting the differentiation of epithelial transport and responsiveness to hormones. Fed Proc. 1984;43(8):2221-4.

219. Rousset M. The human colon carcinoma cell lines HT-29 and Caco-2: two in vitro models for the study of intestinal differentiation. Biochimie. 1986;68(9):1035-40.

220. Poelaert KCK, Van Cleemput J, Laval K, Favoreel HW, Hussey GS, Maes RK, et al. Abortigenic but Not Neurotropic Equine Herpes Virus 1 Modulates the Interferon Antiviral Defense. Front Cell Infect Mi. 2018;8.

221. Quintana AM, Landolt GA, Annis KM, Hussey GS. Immunological characterization of the equine airway epithelium and of a primary equine airway epithelial cell culture model. Vet Immunol Immunopathol. 2011;140(3-4):226-36.

222. Soboll Hussey G, Ashton LV, Quintana AM, Lunn DP, Goehring LS, Annis K, et al. Innate immune responses of airway epithelial cells to infection with equine herpesvirus-1. Vet Microbiol. 2014;170(1-2):28-38.

223. Stokol T, Serpa PBS, Zahid MN, Brooks MB. Unfractionated and Low-Molecular-Weight Heparin and the Phosphodiesterase Inhibitors, IBMX and Cilostazol, Block Ex Vivo Equid Herpesvirus Type-1-Induced Platelet Activation. Front Vet Sci. 2016;3:99.

224. Stokol T, Yeo WM, Burnett D, DeAngelis N, Huang T, Osterrieder N, et al. Equid herpesvirus type 1 activates platelets. PLoS One. 2015;10(4):e0122640.

225. Edmondson R, Broglie JJ, Adcock AF, Yang LJ. Three-Dimensional Cell Culture Systems and Their Applications in Drug Discovery and Cell-Based Biosensors. Assay Drug Dev Techn. 2014;12(4):207-18.

226. Gupta N, Liu JR, Patel B, Solomon DE, Vaidya B, Gupta V. Microfluidics-based 3D cell culture models: Utility in novel drug discovery and delivery research. Bioeng Transl Med. 2016;1(1):63-81.

227. Li XJ, Valadez AV, Zuo P, Nie Z. Microfluidic 3D cell culture: potential application for tissue-based bioassays. Bioanalysis. 2012;4(12):1509-25.

228. Huh D, Kim HJ, Fraser JP, Shea DE, Khan M, Bahinski A, et al. Microfabrication of human organs-on-chips. Nat Protoc. 2013;8(11):2135-57.

229. Huh D, Matthews BD, Mammoto A, Montoya-Zavala M, Hsin HY, Ingber DE. Reconstituting organ-level lung functions on a chip. Science. 2010;328(5986):1662-8.

230. Toh YC, Zhang C, Zhang J, Khong YM, Chang S, Samper VD, et al. A novel 3D mammalian cell perfusion-culture system in microfluidic channels. Lab Chip. 2007;7(3):302-9.

231. Doll ER, Bryans JT. Immunization of young horses against viral rhinopneumonitis. Cornell Vet. 1963;53:24-41.

232. Heldens JG, Pouwels HG, van Loon AA. Efficacy and duration of immunity of a combined equine influenza and equine herpesvirus vaccine against challenge with an American-like equine influenza virus (A/equi-2/Kentucky/95). Vet J. 2004;167(2):150-7.

233. Burki F, Rossmanith W, Nowotny N, Pallan C, Mostl K, Lussy H. Viraemia and abortions are not prevented by two commercial equine herpesvirus-1 vaccines after experimental challenge of horses. Vet Q. 1990;12(2):80-6.
234. Goehring LS, Wagner B, Bigbie R, Hussey SB, Rao S, Morley PS, et al. Control of EHV-1 viremia and nasal shedding by commercial vaccines. Vaccine. 2010;28(32):5203-11.
235. Bresgen C, Lammer M, Wagner B, Osterrieder N, Damiani AM. Serological responses and clinical outcome after vaccination of mares and foals with equine herpesvirus type 1 and 4 (EHV-1 and EHV-4) vaccines. Vet Microbiol. 2012;160(1-2):9-16.
236. Matsumura T, O'Callaghan DJ, Kondo T, Kamada M. Lack of virulence of the murine fibroblast adapted strain, Kentucky A (KyA), of equine herpesvirus type 1 (EHV-1) in young horses. Vet Microbiol. 1996;48(3-4):353-65.
237. Colle CF, 3rd, Tarbet EB, Grafton WD, Jennings SR, O'Callaghan DJ. Equine herpesvirus-1 strain KyA, a candidate vaccine strain, reduces viral titers in mice challenged with a pathogenic strain, RacL. Virus Res. 1996;43(2):111-24.
238. Minke JM, Fischer L, Baudu P, Guigal PM, Sindle T, Mumford JA, et al. Use of DNA and recombinant canarypox viral (ALVAC) vectors for equine herpes virus vaccination. Vet Immunol Immunopathol. 2006;111(1-2):47-57.
239. Foote CE, Love DN, Gilkerson JR, Rota J, Trevor-Jones P, Ruitenberg KM, et al. Serum antibody responses to equine herpesvirus 1 glycoprotein D in horses, pregnant mares and young foals. Vet Immunol Immunopathol. 2005;105(1-2):47-57.
240. Cook RF, O'Neill T, Strachan E, Sundquist B, Mumford JA. Protection against lethal equine herpes virus type 1 (subtype 1) infection in hamsters by immune stimulating complexes (ISCOMs) containing the major viral glycoproteins. Vaccine. 1990;8(5):491-6.
241. Tischer BK, Smith GA, Osterrieder N. En passant mutagenesis: a two step markerless red recombination system. Methods Mol Biol. 2010;634:421-30.
242. Hofmann-Sieber H, Wild J, Fiedler N, Tischer K, von Einem J, Osterrieder N, et al. Impact of ETIF deletion on safety and immunogenicity of equine herpesvirus type 1-vectored vaccines. J Virol. 2010;84(22):11602-13.
243. Van de Walle GR, May MA, Peters ST, Metzger SM, Rosas CT, Osterrieder N. A vectored equine herpesvirus type 1 (EHV-1) vaccine elicits protective immune responses against EHV-1 and H3N8 equine influenza virus. Vaccine. 2010;28(4):1048-55.
244. Richman LK, Montali RJ, Garber RL, Kennedy MA, Lehnhardt J, Hildebrandt T, et al. Novel endotheliotropic herpesviruses fatal for Asian and African elephants. Science. 1999;283(5405):1171-6.

245. Fickel J, Richman LK, Montali R, Schaftenaar W, Goritz F, Hildebrandt TB, et al. A variant of the endotheliotropic herpesvirus in Asian elephants (Elephas maximus) in European zoos. Vet Microbiol. 2001;82(2):103-9.

246. Zong JC, Latimer EM, Long SY, Richman LK, Heaggans SY, Hayward GS. Comparative genome analysis of four elephant endotheliotropic herpesviruses, EEHV3, EEHV4, EEHV5, and EEHV6, from cases of hemorrhagic disease or viremia. J Virol. 2014;88(23):13547-69.

247. Kochagul V, Srivorakul S, Boonsri K, Somgird C, Sthitmatee N, Thitaram C, et al. Production of antibody against elephant endotheliotropic herpesvirus (EEHV) unveils tissue tropisms and routes of viral transmission in EEHV-infected Asian elephants. Sci Rep. 2018;8(1):4675.

248. Ackermann M, Hatt JM, Schetle N, Steinmetz H. Identification of shedders of elephant endotheliotropic herpesviruses among Asian elephants (Elephas maximus) in Switzerland. PLoS One. 2017;12(5):e0176891.

249. Said A, Azab W, Damiani A, Osterrieder N. Equine herpesvirus type 4 UL56 and UL49.5 proteins downregulate cell surface major histocompatibility complex class I expression independently of each other. J Virol. 2012;86(15):8059-71.

250. Damiani AM, de Vries M, Reimers G, Winkler S, Osterrieder N. A severe equine herpesvirus type 1 (EHV-1) abortion outbreak caused by a neuropathogenic strain at a breeding farm in northern Germany. Vet Microbiol. 2014;172(3-4):555-62.

251. Adane Mekonnen AE, Daniel Gizaw. Equine herpesvirus 1 and/or 4 in working equids: seroprevalence and risk factors in North Shewa Zone, Ethiopia. Ethiopian Veterinary Journal. 2017;21(2):28-39.

252. Ataseven VS, Bilge-Dagalp S, Oguzoglu TC, Karapinar Z, Guzel M, Tan MT. Detection and sequence analysis of equine gammaherpesviruses from horses with respiratory tract disease in Turkey. Transbound Emerg Dis. 2010;57(4):271-6.

253. Crabb BS, Studdert MJ. Equine herpesviruses 4 (equine rhinopneumonitis virus) and 1 (equine abortion virus). Adv Virus Res. 1995b;45:153-90.

254. Gilkerson JR, Whalley JM, Drummer HE, Studdert MJ, Love DN. Epidemiology of EHV-1 and EHV-4 in the mare and foal populations on a Hunter Valley stud farm: are mares the source of EHV-1 for unweaned foals. Vet Microbiol. 1999;68(1-2):27-34.

255. Yildirim Y, Yilmaz V, Kirmizigul AH. Equine herpes virus type 1 (EHV-1) and 4 (EHV-4) infections in horses and donkeys in northeastern Turkey. Iran J Vet Res. 2015;16(4):341-4.

256. Li H, Durbin R. Fast and accurate short read alignment with Burrows-Wheeler transform. Bioinformatics. 2009;25(14):1754-60.

257. Chevreux BW, T.; Suhai, S., editor Genome sequence assembly using trace signals and additional sequence information in computer science and biology. Proceedings of the German conference on bioinformatics (GCB); 1999.
258. Walker BJ, Abeel T, Shea T, Priest M, Abouelliel A, Sakthikumar S, et al. Pilon: an integrated tool for comprehensive microbial variant detection and genome assembly improvement. PLoS One. 2014;9(11):e112963.
259. Kolmogorov M, Raney B, Paten B, Pham S. Ragout-a reference-assisted assembly tool for bacterial genomes. Bioinformatics. 2014;30(12):i302-9.
260. Bankevich A, Nurk S, Antipov D, Gurevich AA, Dvorkin M, Kulikov AS, et al. SPAdes: a new genome assembly algorithm and its applications to single-cell sequencing. J Comput Biol. 2012;19(5):455-77.
261. Spiesschaert B, Stephanowitz H, Krause E, Osterrieder N, Azab W. Glycoprotein B of equine herpesvirus type 1 has two recognition sites for subtilisin-like proteases that are cleaved by furin. J Gen Virol. 2016;97(5):1218-28.
262. Sanyal A, Wallaschek N, Glass M, Flamand L, Wight DJ, Kaufer BB. The ND10 Complex Represses Lytic Human Herpesvirus 6A Replication and Promotes Silencing of the Viral Genome. Viruses. 2018;10(8).
263. Black W, Troyer RM, Coutu J, Wong K, Wolff P, Gilbert M, et al. Identification of gammaherpesvirus infection in free-ranging black bears (Ursus americanus). Virus Res. 2019;259:46-53.
264. Goodman LB, Loregian A, Perkins GA, Nugent J, Buckles EL, Mercorelli B, et al. A point mutation in a herpesvirus polymerase determines neuropathogenicity. PLoS Pathog. 2007;3(11):e160.
265. Azab W, Kato K, Arii J, Tsujimura K, Yamane D, Tohya Y, et al. Cloning of the genome of equine herpesvirus 4 strain TH20p as an infectious bacterial artificial chromosome. Arch Virol. 2009;154(5):833-42.
266. Thein PaH, P. Untersuchungen zur Stammvariabilität von Pferdeherpesviren des Typs EHV-4. Pferdeheilkunde. 2000;16(5):479–86
267. Tischer BK, von Einem J, Kaufer B, Osterrieder N. Two-step red-mediated recombination for versatile high-efficiency markerless DNA manipulation in Escherichia coli. Biotechniques. 2006;40(2):191-7.
268. Rudolph J, O'Callaghan DJ, Osterrieder N. Cloning of the genomes of equine herpesvirus type 1 (EHV-1) strains KyA and racL11 as bacterial artificial chromosomes (BAC). J Vet Med B Infect Dis Vet Public Health. 2002;49(1):31-6.
269. Sambrook J, Russell DW, editors. Molecular Cloning: a Laboratory Manual: Cold Spring Harbor, NY: Cold Spring Harbor Laboratory; 2001.

270. Birnboim HC, Doly J. A rapid alkaline extraction procedure for screening recombinant plasmid DNA. Nucleic Acids Res. 1979;7(6):1513-23.

271. Hudetz AG, Feher G, Kampine JP. Heterogeneous autoregulation of cerebrocortical capillary flow: evidence for functional thoroughfare channels? Microvasc Res. 1996;51(1):131-6.

272. Wisniewski JR, Zougman A, Nagaraj N, Mann M. Universal sample preparation method for proteome analysis. Nature methods. 2009;6(5):359-62.

273. Rappsilber J, Ishihama Y, Mann M. Stop and go extraction tips for matrix-assisted laser desorption/ionization, nanoelectrospray, and LC/MS sample pretreatment in proteomics. Anal Chem. 2003;75(3):663-70.

274. Cox J, Mann M. MaxQuant enables high peptide identification rates, individualized p.p.b.-range mass accuracies and proteome-wide protein quantification. Nat Biotechnol. 2008;26(12):1367-72.

275. van Aalderen MC, van den Biggelaar M, Remmerswaal EBM, van Alphen FPJ, Meijer AB, Ten Berge IJM, et al. Label-free Analysis of CD8(+) T Cell Subset Proteomes Supports a Progressive Differentiation Model of Human-Virus-Specific T Cells. Cell reports. 2017;19(5):1068-79.

276. Tyanova S, Temu T, Sinitcyn P, Carlson A, Hein MY, Geiger T, et al. The Perseus computational platform for comprehensive analysis of (prote)omics data. Nature methods. 2016;13(9):731-40.

277. Murugaiyan J, Eravci M, Weise C, Roesler U. Mass spectrometry data from label-free quantitative proteomic analysis of harmless and pathogenic strains of infectious microalgae, Prototheca spp. Data Brief. 2017;12:320-6.

278. Dunn J, Ferluga S, Sharma V, Futschik M, Hilton DA, Adams CL, et al. Proteomic analysis discovers the differential expression of novel proteins and phosphoproteins in meningioma including NEK9, HK2 and SET and deregulation of RNA metabolism. EBioMedicine. 2019;40:77-91.

279. Yue R, Lu C, Han X, Guo S, Yan S, Liu L, et al. Comparative proteomic analysis of maize (Zea mays L.) seedlings under rice black-streaked dwarf virus infection. BMC Plant Biol. 2018;18(1):191.

280. Martin EM, Messenger KM, Sheats MK, Jones SL. Misoprostol Inhibits Lipopolysaccharide-Induced Pro-inflammatory Cytokine Production by Equine Leukocytes. Front Vet Sci. 2017;4:160.

281. OIE. OIE Manual for Terrestial Animals, 2018. Equine Rhinopneumonitis, http://www.oie.int/standard-setting/terrestrial-manual/access-online/

2.05.09_EQUINE_RHINO.pdf (Chapter 2.5.9). 2018.

282. Lang A, de Vries M, Feineis S, Muller E, Osterrieder N, Damiani AM. Development of a peptide ELISA for discrimination between serological responses to equine herpesvirus type 1 and 4. J Virol Methods. 2013;193(2):667-73.
283. Sinzger C, Knapp J, Schmidt K, Kahl M, Jahn G. A simple and rapid method for preparation of viral DNA from cell associated cytomegalovirus. J Virol Methods. 1999;81(1-2):115-22.
284. Schmitt DL, Hardy DA, Montali RJ, Richman LK, Lindsay WA, Isaza R, et al. Use of famciclovir for the treatment of endotheliotrophic herpesvirus infections in Asian elephants (Elephas maximus). J Zoo Wildl Med. 2000;31(4):518-22.
285. Hardman K, Dastjerdi A, Gurrala R, Routh A, Banks M, Steinbach F, et al. Detection of elephant endotheliotropic herpesvirus type 1 in asymptomatic elephants using TaqMan real-time PCR. Vet Rec. 2012;170(8):205.
286. Azab W, Damiani AM, Ochs A, Osterrieder N. Subclinical infection of a young captive Asian elephant with elephant endotheliotropic herpesvirus 1. Arch Virol. 2018;163(2):495-500.
287. Dayaram A, Tsangaras K, Pavulraj S, Azab W, Groenke N, Wibbelt G, et al. Novel Divergent Polar Bear-Associated Mastadenovirus Recovered from a Deceased Juvenile Polar Bear. mSphere. 2018;3(4).
288. Fickel J, Lieckfeldt D, Richman LK, Streich WJ, Hildebrandt TB, Pitra C. Comparison of glycoprotein B (gB) variants of the elephant endotheliotropic herpesvirus (EEHV) isolated from Asian elephants (Elephas maximus). Vet Microbiol. 2003;91(1):11-21.
289. Niepmann M, Zheng J. Discontinuous native protein gel electrophoresis. Electrophoresis. 2006;27(20):3949-51.
290. Watanabe T, Nakagawa T, Ikemizu J, Nagahama M, Murakami K, Nakayama K. Sequence requirements for precursor cleavage within the constitutive secretory pathway. J Biol Chem. 1992;267(12):8270-4.
291. Bolger AM, Lohse M, Usadel B. Trimmomatic: a flexible trimmer for Illumina sequence data. Bioinformatics. 2014;30(15):2114-20.
292. Richardson KC, Jarett L, Finke EH. Embedding in epoxy resins for ultrathin sectioning in electron microscopy. Stain Technol. 1960;35:313-23.
293. Akdis M, Aab A, Altunbulakli C, Azkur K, Costa RA, Crameri R, et al. Interleukins (from IL-1 to IL-38), interferons, transforming growth factor beta, and TNF-alpha: Receptors, functions, and roles in diseases. The Journal of allergy and clinical immunology. 2016;138(4):984-1010.

294. Basu S, Hodgson G, Katz M, Dunn AR. Evaluation of role of G-CSF in the production, survival, and release of neutrophils from bone marrow into circulation. Blood. 2002;100(3):854-61.

295. Dinarello CA, Renfer L, Wolff SM. Human leukocytic pyrogen: purification and development of a radioimmunoassay. Proc Natl Acad Sci U S A. 1977;74(10):4624-7.

296. Garlanda C, Dinarello CA, Mantovani A. The interleukin-1 family: back to the future. Immunity. 2013;39(6):1003-18.

297. Morgan DA, Ruscetti FW, Gallo R. Selective in vitro growth of T lymphocytes from normal human bone marrows. Science. 1976;193(4257):1007-8.

298. Roediger B, Kyle R, Tay SS, Mitchell AJ, Bolton HA, Guy TV, et al. IL-2 is a critical regulator of group 2 innate lymphoid cell function during pulmonary inflammation. The Journal of allergy and clinical immunology. 2015;136(6):1653-63 e7.

299. Uyttenhove C, Coulie PG, Van Snick J. T cell growth and differentiation induced by interleukin-HP1/IL-6, the murine hybridoma/plasmacytoma growth factor. J Exp Med. 1988;167(4):1417-27.

300. Coelho AL, Hogaboam CM, Kunkel SL. Chemokines provide the sustained inflammatory bridge between innate and acquired immunity. Cytokine Growth Factor Rev. 2005;16(6):553-60.

301. Stanic B, van de Veen W, Wirz OF, Ruckert B, Morita H, Sollner S, et al. IL-10-overexpressing B cells regulate innate and adaptive immune responses. The Journal of allergy and clinical immunology. 2015;135(3):771-80 e8.

302. Brown SD, Brown LA, Stephenson S, Dodds JC, Douglas SL, Qu H, et al. Characterization of a high TNF-alpha phenotype in children with moderate-to-severe asthma. The Journal of allergy and clinical immunology. 2015;135(6):1651-4.

303. Akkoc T, de Koning PJ, Ruckert B, Barlan I, Akdis M, Akdis CA. Increased activation-induced cell death of high IFN-gamma-producing T(H)1 cells as a mechanism of T(H)2 predominance in atopic diseases. The Journal of allergy and clinical immunology. 2008;121(3):652-8 e1.

304. Bhat K, Sarkissyan M, Wu Y, Vadgama JV. GROalpha overexpression drives cell migration and invasion in triple negative breast cancer cells. Oncology reports. 2017;38(1):21-30.

305. Fujiwara K, Matsukawa A, Ohkawara S, Takagi K, Yoshinaga M. Functional distinction between CXC chemokines, interleukin-8 (IL-8), and growth related oncogene (GRO)alpha in neutrophil infiltration. Lab Invest. 2002;82(1):15-23.

306. Neville LF, Mathiak G, Bagasra O. The immunobiology of interferon-gamma inducible protein 10 kD (IP-10): a novel, pleiotropic member of the C-X-C chemokine superfamily. Cytokine Growth Factor Rev. 1997;8(3):207-19.

307. Liu M, Guo S, Hibbert JM, Jain V, Singh N, Wilson NO, et al. CXCL10/IP-10 in infectious diseases pathogenesis and potential therapeutic implications. Cytokine Growth Factor Rev. 2011;22(3):121-30.

308. Liu M, Guo S, Stiles JK. The emerging role of CXCL10 in cancer (Review). Oncol Lett. 2011;2(4):583-9.

309. Rusnati M, Camozzi M, Moroni E, Bottazzi B, Peri G, Indraccolo S, et al. Selective recognition of fibroblast growth factor-2 by the long pentraxin PTX3 inhibits angiogenesis. Blood. 2004;104(1):92-9.

310. Delrieu I. The high molecular weight isoforms of basic fibroblast growth factor (FGF-2): an insight into an intracrine mechanism. FEBS letters. 2000;468(1):6-10.

311. Yun YR, Won JE, Jeon E, Lee S, Kang W, Jo H, et al. Fibroblast growth factors: biology, function, and application for tissue regeneration. J Tissue Eng. 2010;2010:218142.

312. Seghezzi G, Patel S, Ren CJ, Gualandris A, Pintucci G, Robbins ES, et al. Fibroblast growth factor-2 (FGF-2) induces vascular endothelial growth factor (VEGF) expression in the endothelial cells of forming capillaries: an autocrine mechanism contributing to angiogenesis. J Cell Biol. 1998;141(7):1659-73.

313. Pavulraj S, Eschke K, Prahl A, Flugger M, Trimpert J, van den Doel PB, et al. Fatal Elephant Endotheliotropic Herpesvirus Infection of Two Young Asian Elephants. Microorganisms. 2019;7(10).

314. Rappocciolo G, Birch J, Ellis SA. Down-regulation of MHC class I expression by equine herpesvirus-1. J Gen Virol. 2003;84(Pt 2):293-300.

315. Koppers-Lalic D, Verweij MC, Lipinska AD, Wang Y, Quinten E, Reits EA, et al. Varicellovirus UL 49.5 proteins differentially affect the function of the transporter associated with antigen processing, TAP. PLoS Pathog. 2008;4(5):e1000080.

316. Zhaobing Liu JH, Qing Ding, Yan Yang and Hanxiao Sun. Analysis of contributions of herpes simplex virus type 1 UL43 protein to induction of cell-cell fusion. Tropical Journal of Pharmaceutical Research 2016;15(6):1137-44.

317. Davies PF. Hemodynamic shear stress and the endothelium in cardiovascular pathophysiology. Nat Clin Pract Cardiovasc Med. 2009;6(1):16-26.

318. Gopalan PK, Jones DA, McIntire LV, Smith CW. Cell adhesion under hydrodynamic flow conditions. Current protocols in immunology / edited by John E Coligan [et al]. 2001;Chapter 7:Unit 7 29.

319. Gryspeerdt AC, Vandekerckhove AP, Garre B, Barbe F, Van de Walle GR, Nauwynck HJ. Differences in replication kinetics and cell tropism between neurovirulent and non-neurovirulent EHV1 strains during the acute phase of infection in horses. Vet Microbiol. 2010;142(3-4):242-53.

320. Zhao J, Poelaert KCK, Van Cleemput J, Nauwynck HJ. CCL2 and CCL5 driven attraction of CD172a(+) monocytic cells during an equine herpesvirus type 1 (EHV-1) infection in equine nasal mucosa and the impact of two migration inhibitors, rosiglitazone (RSG) and quinacrine (QC). Vet Res. 2017;48(1):14.

321. van der Meulen KM, Nauwynck HJ, Pensaert MB. Absence of viral antigens on the surface of equine herpesvirus-1-infected peripheral blood mononuclear cells: a strategy to avoid complement-mediated lysis. J Gen Virol. 2003;84(Pt 1):93-7.

322. Engel EA, Song R, Koyuncu OO, Enquist LW. Investigating the biology of alpha herpesviruses with MS-based proteomics. Proteomics. 2015;15(12):1943-56.

323. Leroy B, Gillet L, Vanderplasschen A, Wattiez R. Structural Proteomics of Herpesviruses. Viruses. 2016;8(2).

324. Naranatt PP, Akula SM, Zien CA, Krishnan HH, Chandran B. Kaposi's sarcoma-associated herpesvirus induces the phosphatidylinositol 3-kinase-PKC-zeta-MEK-ERK signaling pathway in target cells early during infection: implications for infectivity. J Virol. 2003;77(2):1524-39.

325. Chang MY, Huang DY, Ho FM, Huang KC, Lin WW. PKC-dependent human monocyte adhesion requires AMPK and Syk activation. PLoS One. 2012;7(7):e40999.

326. Filippakis H, Spandidos DA, Sourvinos G. Herpesviruses: hijacking the Ras signaling pathway. Biochimica et biophysica acta. 2010;1803(7):777-85.

327. Elkin SR, Lakoduk AM, Schmid SL. Endocytic pathways and endosomal trafficking: a primer. Wien Med Wochenschr. 2016;166(7-8):196-204.

328. Young LS, Rickinson AB. Epstein-Barr virus: 40 years on. Nature reviews Cancer. 2004;4(10):757-68.

329. Qiu Y-Q. KEGG Pathway Database. In: Dubitzky W, Wolkenhauer O, Cho K-H, Yokota H, editors. Encyclopedia of Systems Biology. New York, NY: Springer New York; 2013. p. 1068-9.

330. Pan H, Xie J, Ye F, Gao SJ. Modulation of Kaposi's sarcoma-associated herpesvirus infection and replication by MEK/ERK, JNK, and p38 multiple mitogen-activated protein kinase pathways during primary infection. J Virol. 2006;80(11):5371-82.

331. Liu X, Cohen JI. The role of PI3K/Akt in human herpesvirus infection: From the bench to the bedside. Virology. 2015;479-480:568-77.

332. Nanbo A, Kachi K, Yoshiyama H, Ohba Y. Epstein-Barr virus exploits host endocytic machinery for cell-to-cell viral transmission rather than a virological synapse. J Gen Virol. 2016;97(11):2989-3006.

333. Zhu Y, Ramos da Silva S, He M, Liang Q, Lu C, Feng P, et al. An Oncogenic Virus Promotes Cell Survival and Cellular Transformation by Suppressing Glycolysis. PLoS Pathog. 2016;12(5):e1005648.

334. Cavignac Y, Esclatine A. Herpesviruses and autophagy: catch me if you can! Viruses. 2010;2(1):314-33.

335. Van de Walle GR, Peters ST, VanderVen BC, O'Callaghan DJ, Osterrieder N. Equine herpesvirus 1 entry via endocytosis is facilitated by alphaV integrins and an RSD motif in glycoprotein D. J Virol. 2008;82(23):11859-68.

336. Shaul YD, Seger R. The MEK/ERK cascade: from signaling specificity to diverse functions. Biochimica et biophysica acta. 2007;1773(8):1213-26.

337. Pleschka S. RNA viruses and the mitogenic Raf/MEK/ERK signal transduction cascade. Biol Chem. 2008;389(10):1273-82.

338. DuShane JK, Maginnis MS. Human DNA Virus Exploitation of the MAPK-ERK Cascade. Int J Mol Sci. 2019;20(14).

339. Ichise T, Yoshida N, Ichise H. FGF2-induced Ras-MAPK signalling maintains lymphatic endothelial cell identity by upregulating endothelial-cell-specific gene expression and suppressing TGFbeta signalling through Smad2. J Cell Sci. 2014;127(Pt 4):845-57.

340. Ornitz DM, Itoh N. The Fibroblast Growth Factor signaling pathway. Wiley Interdiscip Rev Dev Biol. 2015;4(3):215-66.

341. Wimer CL, Damiani A, Osterrieder N, Wagner B. Equine herpesvirus type-1 modulates CCL2, CCL3, CCL5, CXCL9, and CXCL10 chemokine expression. Vet Immunol Immunopathol. 2011;140(3-4):266-74.

342. Kang S, Brown HM, Hwang S. Direct Antiviral Mechanisms of Interferon-Gamma. Immune Netw. 2018;18(5):e33.

343. Miettinen JJ, Matikainen S, Nyman TA. Global secretome characterization of herpes simplex virus 1-infected human primary macrophages. J Virol. 2012;86(23):12770-8.

344. Milora KA, Miller SL, Sanmiguel JC, Jensen LE. Interleukin-1alpha released from HSV-1-infected keratinocytes acts as a functional alarmin in the skin. Nat Commun. 2014;5:5230.

345. Hue ES, Richard EA, Fortier CI, Fortier GD, Paillot R, Raue R, et al. Equine PBMC Cytokines Profile after In Vitro alpha- and gamma-EHV Infection: Efficacy of a Parapoxvirus Ovis Based-Immunomodulator Treatment. Vaccines (Basel). 2017;5(3).

346. Pusterla N, Kass PH, Mapes S, Johnson C, Barnett DC, Vaala W, et al. Surveillance programme for important equine infectious respiratory pathogens in the USA. Vet Rec. 2011;169(1):12.

347. Izume S, Kirisawa R, Ohya K, Ohnuma A, Kimura T, Omatsu T, et al. The full genome sequences of 8 equine herpesvirus type 4 isolates from horses in Japan. J Vet Med Sci. 2017;79(1):206-12.

348. Studdert MJ. Restriction endonuclease DNA fingerprinting of respiratory, foetal and perinatal foal isolates of equine herpesvirus type 1. Arch Virol. 1983;77(2-4):249-58.

349. Smith FL, Watson JL, Spier SJ, Kilcoyne I, Mapes S, Sonder C, et al. Frequency of shedding of respiratory pathogens in horses recently imported to the United States. J Vet Intern Med. 2018;32(4):1436-41.

350. Ahmed, F., Afify, , Basem, Ahmed M, et al. First Isolation and identification of EHV-4 during abortion outbreak among Arabian horses in Egypt reflects an alteration in pathogenic potentiality of EHV-4 Journal of Virological Sciences. 2017;2:92-101.

351. Ostlund EN. The equine herpesviruses. Vet Clin North Am Equine Pract. 1993;9(2):283-94.

352. Whitwell KE, Smith, K., Sinclair, R., Mumford, J.,, editor Fetal lesions in spontaneous 472 EHV-4 abortions in mares. Proceedings of the 473 Seventh International Conference on Equine Infectious Diseases; 1995; Newmarket: R&W Publications.

353. Kendrick JW, Stevenson W. Immunity to equine herpesvirus 1 infection in foals during the first year of life. J Reprod Fertil Suppl. 1979(27):615-8.

354. Mumford JA, Rossdale PD, Jessett DM, Gann SJ, Ousey J, Cook RF. Serological and virological investigations of an equid herpesvirus 1 (EHV-1) abortion storm on a stud farm in 1985. J Reprod Fertil Suppl. 1987;35:509-18.

355. Jacobson ER, Sundberg JP, Gaskin JM, Kollias GV, O'Banion MK. Cutaneous papillomas associated with a herpesvirus-like infection in a herd of captive African elephants. J Am Vet Med Assoc. 1986;189(9):1075-8.

356. McCully RM, Basson PA, Pienaar JG, Erasmus BJ, Young E. Herpes nodules in the lung of the African elephant (Loxodonta africana (Blumebach, 1792)). The Onderstepoort journal of veterinary research. 1971;38(4):225-35.

357. Richman LK, Montali RJ, Cambre RC, Schmitt D, Hardy D, Hildbrandt T, et al. Clinical and pathological findings of a newly recognized disease of elephants caused by endotheliotropic herpesviruses. J Wildl Dis. 2000;36(1):1-12.

358. Barman NN, Choudhury B, Kumar V, Koul M, Gogoi SM, Khatoon E, et al. Incidence of elephant endotheliotropic herpesvirus in Asian elephants in India. Vet Microbiol. 2017;208:159-63.

359. Seilern-Moy K, Darpel K, Steinbach F, Dastjerdi A. Distribution and load of elephant endotheliotropic herpesviruses in tissues from associated fatalities of Asian elephants. Virus Res. 2016;220:91-6.

360. Ehlers B, Burkhardt S, Goltz M, Bergmann V, Ochs A, Weiler H, et al. Genetic and ultrastructural characterization of a European isolate of the fatal endotheliotropic elephant herpesvirus. J Gen Virol. 2001;82(Pt 3):475-82.

361. Zachariah A, Zong JC, Long SY, Latimer EM, Heaggans SY, Richman LK, et al. Fatal herpesvirus hemorrhagic disease in wild and orphan asian elephants in southern India. J Wildl Dis. 2013;49(2):381-93.

362. Kopp A, Blewett E, Misra V, Mettenleiter TC. Proteolytic cleavage of bovine herpesvirus 1 (BHV-1) glycoprotein gB is not necessary for its function in BHV-1 or pseudorabies virus. J Virol. 1994;68(3):1667-74.

363. Oliver SL, Sommer M, Zerboni L, Rajamani J, Grose C, Arvin AM. Mutagenesis of varicella-zoster virus glycoprotein B: putative fusion loop residues are essential for viral replication, and the furin cleavage motif contributes to pathogenesis in skin tissue in vivo. J Virol. 2009;83(15):7495-506.

364. Cooper RS, Heldwein EE. Herpesvirus gB: A Finely Tuned Fusion Machine. Viruses. 2015;7(12):6552-69.

365. Borchers K, Weigelt W, Buhk HJ, Ludwig H, Mankertz J. Conserved domains of glycoprotein B (gB) of the monkey virus, simian agent 8, identified by comparison with herpesvirus gBs. J Gen Virol. 1991;72 (Pt 9):2299-304.

366. Isaacson MK, Compton T. Human cytomegalovirus glycoprotein B is required for virus entry and cell-to-cell spread but not for virion attachment, assembly, or egress. J Virol. 2009;83(8):3891-903.

367. Spear PG. Herpes simplex virus: receptors and ligands for cell entry. Cellular microbiology. 2004;6(5):401-10.

11 Publications and scientific contributions

Selected publications

1. Kamel M, **Pavulraj S**, Fauler B, Mielke T, and Azab W (2019) Herpesviruses exploit the extracellular matrix of mononuclear cells to ensure transport to target cells. Nature communications. (Under review)
2. **Pavulraj S**, Kamel M, Stephanowitz H, Liu F, Osterrieder N and Walid Azab (2019) Alphaherpesviruses modulate cytokine and chemokine profiles of mononuclear cells for efficient dissemination to target organs. In preparation.
3. **Pavulraj S**, Eschke K, Theisen J, Westhoff S, Reimers G, Osterrieder N, Azab W (2019) Equine herpesvirus type 4 (EHV-4) outbreak in Germany: virological, serological and molecular investigations. In preparation.
4. **Pavulraj S,** Eschke K, Prahl A, Flugger M, Trimpert J, van den Doel PB, Andreotti S, Kaessmeyer S, Osterrieder N and Azab W (2019). Fatal Elephant Endotheliotropic Herpesvirus Infection of Two Young Asian Elephants. **Microorganisms** 7(10). https://www.ncbi.nlm.nih.gov/pubmed/31561506
5. **Pavulraj S**, Kamel M, Osterrieder K and Azab W (2019). EHV-1 pathogenesis: Current invitro models and future perspectives. **Frontiers in Veterinary Science**. 6:251. https://www.ncbi.nlm.nih.gov/pmc/articles/PMC6684782/
6. Dayaram A, Tsangaras K, **Pavulraj S**, Azab W, Groenke N, Wibbelt G, Sicks F Osterrieder N and Greenwood A (2018). Novel Divergent Polar Bear-Associated Mastadenovirus Recovered from a Deceased Juvenile Polar Bear. **mSphere** 3(4):e00171-18. https://www.ncbi.nlm.nih.gov/pubmed/30045965
7. Anand T, Virmani N, Kumar S, Kumar Mohanty A, **Pavulraj S**, Ch Bera B, Vaid RK, Ahlawat U, Tripathi BN (2019) Phage Therapy for treatment of virulent Klebsiella pneumoniae infection in mouse model. **Journal of Global Antimicrobial Resistance**, (19)30251-6. https://www.ncbi.nlm.nih.gov/pubmed/31604128
8. **Pavulraj S**, Virmani N, Bera BC, Joshi A, Anand T, Virmani M, Singh R, Singh RK and Tripathi BN (2017). Immunogenicity and protective efficacy of inactivated equine influenza (H3N8) virus vaccine in murine model. **Veterinary Microbiology** (210): 188-196. https://www.ncbi.nlm.nih.gov/pubmed/29103691
9. **Pavulraj S**, Bera BC, Joshi A, Anand T, Virmani M, Vaid RK, Shanmugasundaram K, Gulati BR, Rajukumar K, Singh R, Misri J, Singh RK, Tripathi BN and Virmani N. (2015). Pathology of Equine Influenza virus (H3N8) in Murine Model. **PLoS ONE** 10(11): e0143094. https://www.ncbi.nlm.nih.gov/pubmed/26587990
10. Bera BC, Virmani N, Kumar N, Anand T, **Pavulraj S**, Rash A, Elton D, Rash N, Bhatia S, Sood R, Singh RK, Tripathi BN (2017). Genetic and codon usage bias analyses of

polymerase genes of equine influenza virus and its relation to evolution. **BMC genomics** 18 (1), 652.https://www.ncbi.nlm.nih.gov/pmc/articles/PMC5568313/

11. Kumar N, Bera BC, Greenbaum BD, Bhatia S, Sood R, **Pavulraj S**, Anand T, Tripathi BN, Virmani N (2016). Revelation of Influencing Factors in Overall Codon Usage Bias of Equine Influenza Viruses. **PLoS ONE** 11(4): e0154376. doi:10.1371/journal.pone.0154376. https://www.ncbi.nlm.nih.gov/pubmed/27119730
12. Virmani N, **Pavulraj S**, Bera BC, Anand T, Singh RK and Tripathi BN (2019) Equine influenza virus, in: Emerging and Transboundary Animal Viruses. Springer International Publishing, Cham, pp.1-22.
13. Mathew MK, Virmani N, Bera BC, Anand T, Kumar R, Balena V, Sansanwal R, **Pavulraj S**, Sundaram K, Virmani M and Tripathi BN (2019) Protective efficacy of inactivated reverse genetics based equine influenza 3 vaccine candidate adjuvanted with Montanide™ Pet Gel in murine model. **Journal of Veterinary Medical Science**. Accepted, in press.
14. Kumar R, Mathew MK, Virmani N, Bera BC, Anand T, Balena V, Sansanwal R, **Pavulraj S**, Sandeep B, Sood R, Kumar N, Sundaram K, Virmani M and Tripathi BN (2019) Pathologial and immunological protection induced by inactivated reverse genetics based H3N8 equine influenza vaccine candidate in murine model. **Acta virologica**. Accepted, in press.
15. Raj P, Radha K, Vijayalakshmi M, **Pavulraj S**, and Anuradha P. (2016). Study on the utilization of paneer whey as functional ingredient for papaya jam. **Italian Journal of Food Science**, 29(1).
16. Saminathan M, Rai RB, Dhama K, Ranganath GJ, Murugesan V, Kannan K, **Pavulraj S**, Gopalakrishnan, A. and Suresh, C. (2014). Histopathology and Immunohistochemical Expression of N-Methyl-N-Nitrosourea (NMU) Induced Mammary Tumours in Sprague-Dawley Rats. **Asian Journal of Animal and Veterinary Advances**, 9(10): 621 - 640.
17. **Pavulraj S**, Amsaveni S, kalaiselvi L and Ramesh S (2013). Screening of *Staphylococcus aureus* isolates from mastitis for antibacterial susceptibility pattern and betalactamase production. **Indian Journal of Veterinary and Animal Sciences Research**, 9(4): 300-309.
18. Saranya K, **Pavulraj S**, Kalaiselvi L, Amsaveni S and Ramesh S (2013). Antibacterial Susceptibility profiles of Coliforms isolated from bovine subclinical and clinical mastitis against Fluoroquinolones. **Indian Journal of Veterinary and Animal Sciences Research**, 9(4): 279-284.

Selected list of contributions in scientific meetings

1. **Pavulraj S**, Fan Liu and Walid Azab. 2019. Alphaherpesviruses Modulate Cytokine and Chemokine Profiles of Mononuclear Cells for Efficient Dissemination to Target Organs. 44th International Herpesvirus Workshop in Knoxville, Tennessee, USA.
2. **Pavulraj S**, Heike stephanowitz, Fan Liu and Walid Azab. 2019. Comparative proteomic analysis reveals the role of ORF2 and UL43 in regulating MAPK and Chemokine signalling pathways during herpesvirus infection. 27th Annual Meeting of the Society for Virology Gesellschaft für Virologie e.V. (GfV), Düsseldorf, Germany.
3. **Pavulraj S**, Nikolaus Osterrieder and Walid Azab. 2018. Equine herpesvirus type 1 and viremia: EHV-1 'hijacks' mononuclear cells for efficient dissemination to target organs. 2018 Calgary International Equine Symposium: Innovation & Discovery, Calgary, Canada.
4. **Pavulraj S** and Walid Azab. 2018. Immunomodulatory genes (ORF2 and UL43) of alphaherpesviruses play significant roles in virus pathogenesis and transfer from infected PBMC to endothelial cells. 28th Annual Meeting of the Society for Virology Gesellschaft für Virologie e.V. (GfV), Wuerzburg, Germany.

12 Acknowledgements

My thanks are due first to almighty Jesus Christ for listening to my endless prayers and showing his blessings without which I could not have achieved my target.

This thesis is the end of my journey in obtaining my PhD degree which would not have been composed and completed without the effort of many people whom I offer my most sincere and heartfelt thanks.

November, 2016, I started this journey and I had no idea where it would lead me. Fortunately, I have been extremely blessed to reach such high position. I am really excited to continue this journey and will get good name for my parents and teachers.

I was very fortunate to have Prof. Dr. Nikolaus Osterrieder, as my supervisor. I have been extremely lucky to have a supervisor who cared so much about my work, and who responded to my questions and queries so promptly. It is a great honour for me to work under his expert supervision. I would like to thank him for the patient guidance, encouragement and advice he has provided throughout my time as his student. At many stages in the course of my project I have benefited from his comments and expert advice. His guidance contributed enormously to the production of this thesis.

I would like to thank my direct supervisor Dr. Walid Azab, for giving me the opportunity to work with equine and elephant herpesviruses. He is an inspiring ideal supervisor. His positive outlook and confidence in my research motivated me and gave me confidence. I consider myself very fortunate, lucky and privileged to work with him as his student. He is one of the best researcher, good scientist and great human being, who always think for good future of his students. He always motivates, gives opportunities and freedom to me to follow my own ideas. He made my journey in PhD research as a stress-free smooth path. I would like to extend this appreciation and gratitude to Dr. Walid Azab, for all his time, patience and constant motivation.

I would like to thank Prof. Dr. Benedikt Kaufer and Prof. Dr Michael Viet for their valuable advices and support during the course of my PhD programme at FU berlin.

I want to thank Prof. Dr. Benedikt Kaufer and Prof. Dr. Robert Klopfleisch for evaluating and reviewing my thesis.

I thank Jakob Trimpert for his excellent support with next generation sequencing.

I thank Prof. Dr. Heidrun Gehlen, Horse clinic, Freie Universität Berlin, Germany and Dr Gitta Reimers, Pferde-Praxis Ahrensburg, Großhansdorf Germany for providing horse blood for

PBMC isolation. I thank Christiane Palissa and Yvonne Weber, Institute of Immunology, Freie Universität Berlin, Germany for helping with FAC sorting of PBMC. I extend my thank Friederika Ebner, institute of immunology, Freie Universität Berlin, for helping with cytokine analysis.

Luca Danilo Bertzbach gets special thanks for German translation of my thesis summary and kind help during my research work.

I would like to thank everyone in my research group, especially Oleksandr Kolyvushko, Viviane Kremling, Kathrin Eschke, Mohamed Kamel, Tobias Bergmann, Maksat, Michaela Zeitlow, Ola Bagato, Nicolar Corrales and Azza Abdelgawad for their support and help during my research work. My sincere thanks to our technicians in the institute, Ann Reum and Annett Neubert for their help. I extend my thanks to post-doc researchers Armando Damiani, Ahmed Kheimar, Dusan Kunec, Cosima, Darren, Chris, Ludwig and Susanne for all support. Thanks to all my PhD colleagues in the institute, Na Xing, Bodan Hu, Andele, Giulia, Minza, Liuba, Xuejiao, Atika, Nicole, Ibrahim, Mohamed Rasheed, Georg, Tereza and Yu You.

My sincere thanks to Katharina Malik, Kerstin Borchers, Christine Gaede and Angela Daberkow for their official and scientific help.

I feel great pleasure to acknowledge Anirban Sanyal, Pratik Khedkar, Gopinath Venugopal and Prabhanjan for their kind help for my research and for my stay in Berlin.

I take this opportunity to sincerely acknowledge Indian Council of Agricultural Research, Government of India for selecting me as an international fellow and for providing Netaji Subhas - ICAR International Fellowship during my entire PhD programme. Their excellent financial and academic support helped me in successful completion of my PhD in Germany.

I would like to thank our research funding agencies, Deutsche Forschungsgemeinschaft and Equine Herpesvirus Program at Freie Universitat Berlin for their excellent support.

I thank institute of Virology, Dahlem research school, Fachbereich Veterinärmedizin and Freie Universität Berlin for providing infrastructure and necessary facilities for course work and research work

I find no words to express my depth of gratitude to Drs. Nitin Virmani, BC Bera, Taruna Anand, BN Tripathi and RK Singh for their constant scientific and moral support from India. This also time to thank my teachers Rajendra Singh, Somvanshi, Rinku Sharma, Ramesh Srinivasan, Ezhil Velan, Sathya Moorthy, Sreekumar, Murugeswari, Jesudoss, Paul Joseph and Arokiya Raj for their support.

I feel pleasure in thanking my friends and seniors Drs. Albert Arokiyaraj, Prabakar, Saminathan U, Areshkumar, Rahamath, Mohana, Saminathan M, Karikalan, Asok kumar, Alok Joshi and Palanivel for their constant support.

I find no words to express my depth of gratitude to immortal love, blessings and never ending sacrifice of my beloved parents Selvaraj-Jesintha Selvarani, my beloved sisters Mrs Angel Mary Jansi Rani-Antony Arul Sasindran, Karolin and Stella Mary. It has been their 13-year sacrifice putting me through school and their constant belief in me that has enabled me to pursue my dreams. I will always be extremely grateful to them. I deeply acknowledge the constant encouragement. I also want to thank my cousin Dr Antan Uresh Kumar and Thommai Nicholas-Annathai for their help and guidance to choose my carrier in Veterinary Medicine.

This is the time to remember my pets Taraus and Jessy, and all my cats and hens. They are part of our family and they have greatly contributed to my happiness and well-being.

Finally, I thank my evergreen Super Star RajiniKanth for energy, inspiration and constant source of motivation in my day-to-day life since my childhood.

Thank you so much to all.

This thesis is only a beginning of my journey.

Selbständigkeitserklärung

Hiermit bestätige ich, dass ich die vorliegende Arbeit selbständig angefertigt habe. Ich versichere, dass ich ausschließlich die angegebenen Quellen und Hilfen Anspruch genommen habe.

Berlin, am 10.12.2019

Pavulraj Selvaraj